Influenza viral infection consequences on endomembrane dynamics and stress signaling

Irene Pila Castellanos

▶ **To cite this version:**

Irene Pila Castellanos. Influenza viral infection consequences on endomembrane dynamics and stress signaling. Molecular biology. Université Paris Cité, 2020. English. NNT : 2020UNIP5056 . tel-04088532

HAL Id: tel-04088532

https://theses.hal.science/tel-04088532v1

Submitted on 4 May 2023

HAL is a multi-disciplinary open access archive for the deposit and dissemination of scientific research documents, whether they are published or not. The documents may come from teaching and research institutions in France or abroad, or from public or private research centers.

L'archive ouverte pluridisciplinaire **HAL**, est destinée au dépôt et à la diffusion de documents scientifiques de niveau recherche, publiés ou non, émanant des établissements d'enseignement et de recherche français ou étrangers, des laboratoires publics ou privés.

Université de Paris

PhD defense
Irene Pila Castellanos

Influenza viral infection consequences on endomembrane dynamics and stress signaling

Ecole doctorale BIO SORBONNE PARIS CITE (BIOSPC)
UNIVERSITE DE PARIS

Institut Necker Enfant Malades (Paris)
INSERM U1151/CNRS 8253
Autophagy pathway and intracellular compartments dynamics – Director : Etienne Morel

Thesis defense in cell biology : 22 June 2020
Supervised by Etienne MOREL

Thesis committee

Pr. Florence NIEDERGANG Université de Paris	**President**
Dr. Caroline GOUJON Université de Montpellier	**Reporter**
Dr. Damien ARNOULT Université Paris-Sud	**Reporter**
Dr. Alessia RUGGIERI University of Heildelberg	**Examinator**
Dr. Mathieu COUREUIL Université de Paris	**Examinator**
Dr. Benoit de CHASSEY Enyo Pharma, Lyon	**Invited member**
Dr. Etienne MOREL Université de Paris	**Thesis director**

ACKNOWLEDGEMENTS

For me, more than a scientific adventure, this thesis has been a human adventure. It has enabled me to grow considerably as a person and has been one of the greatest learning experiences of my life. Though it has been a fairly difficult time, it has also been a rewarding one. One of the things I've learnt above it all is that it's important to not only tackle a challenge but to enjoy the journey to get there, all the while cherishing the small details of everyday life.

Many of you have accompanied me on this adventure and I want to thank you for your support. Thank you to all those who have played a role in making this journey more enjoyable: thank you for your kind words, your encouragement, your benevolence, for giving me the strength when I was lacking it, in order to accompany, support, share, advise and guide me. But as you know, there is no light without darkness and I also thank those who have challenged me, who have taken me through difficult times. It was through all these moments that I was able to learn, to appreciate life from another perspective, and to get a better grasp on that which is essential.

I'll never forget all the experiences we've shared, both good and bad. Thank you for being by my side for all the laughter, tears, jokes, disputes, the moments of hope and discouragement, the lively evenings, the moments of abandonment and loneliness but also of mutual support, periods of discontent and disarray, moments of joy and sadness, of complicity, the strokes of madness and creativity, of motivation, periods of exhaustion, of sharing and helping, the relaxing days and above all the displays of friendship .... This has been a never ending journey of emotions and events, a major learning experience that has helped me become the person who I am today, a better version of myself.

In closing, I want to pay tribute to my guardian angel, who passed over to the other side of the rainbow while I was writing this document. I miss you very much, thank you for every moment spent by your side, I will always carry you in my heart.

"We are at our most powerful the moment we no longer need to be powerful"

Eric Micha'el Leventhal

Table of contents

ABSTRACT

English version

Influenza viruses are a major public health threat considering their high rates of fatality and morbidity. Upon virus entry, host cells experience modifications in endomembranes and organelles, including those used for virus trafficking and replication. Better understanding how viral infection could alter specifically organelles morphodynamics and contribute to cell adaptation to viral replication is essential to develop innovative anti-viral therapeutics strategies. The goal of my PhD project was to investigate endomembrane alterations during influenza viral infection. Using a stress-adapted experimental framework, I show that influenza virus infection modifies mitochondria morphodynamics by promoting mitochondrial elongation and by altering endoplasmic reticulum (ER)-mitochondria tethering in host cells. My results suggest that virus induced mitochondria hyper-elongation is promoted by fission associated protein DRP1 relocalization to the cytosol, thus enhancing a pro-fusion status. Moreover, we identify a small organic molecule we named Mito-C, which is addressed to mitochondria and rapidly provokes mitochondrial network fragmentation. Biochemical analyses reveal that Mito-C targets the NEET protein family, previously reported to regulate mitochondrial iron and ROS homeostasis. One of the NEET proteins, NAF-1, is proposed for the first time to play a role in regulation of mitochondria morphodynamics. Finally, I show that altering mitochondrial hyper-fusion and restoring endoplasmic reticulum-mitochondria contact sites with Mito-C compound treatment was sufficient to dramatically reduce influenza infection (and Dengue replication, also known to cause viral-induced mitochondria elongation) and to restore mitochondrial morphodynamics in infected cells. We propose that the observed Mito-C antiviral property is directly connected with innate immunity signaling RIG-I complex at mitochondria. In conclusion, the results of my PhD project highlight the importance of mitochondrial morphodynamics, ER-mitochondria contacts sites and innate immunity machineries dialog in the context of influenza viral infection. Furthermore, NAF-1 protein could now be identified as an important therapeutic target in antiviral research and in other pathologies where altered mitochondria dynamics is part of disease etiology.

Key words: influenza, mitochondria morphodynamics, endoplasmic reticulum-mitochondria contact sites, innate immunity, antiviral drugs, NEET proteins

ABSTRACT

French version

Les virus influenza constituent une menace majeure pour la santé publique. Lors de l'entrée et de la réplication du virus, les endomembranes des cellules-hôtes sont profondément modifiées, en particulier les organelles du trafic intracellulaire et celles utilisées pour la réplication du virus. Le but de mon projet doctoral fut de comprendre l'importance des changements morphologiques endomembranaires et leur implication dans la réplication de certains virus. J'ai ainsi pu montrer que l'infection par le virus influenza modifie la morphodynamique des mitochondries en favorisant leur élongation et en altérant les contacts membranaires entre réticulum endoplasmique (RE) et mitochondries dans les cellules hôtes. L'hyper-élongation des mitochondries induite par le virus est favorisée par la relocalisation de la protéine de fission DRP1 dans le cytosol, ce qui initie un statut de pro-fusion mitochondrial. De plus, nous avons pu identifier une molécule (Mito-C) qui est adressée aux mitochondries et qui provoque rapidement la fragmentation du réseau mitochondrial. Les analyses biochimiques révèlent que Mito-C cible la famille des protéines NEET, décrites pour avoir un rôle sur l'homéostasie du fer et des ROS à la mitochondrie. L'une de ces protéines, NAF-1, est ici pour la première fois proposée pour jouer un rôle régulateur de la morphodynamique des mitochondries. Enfin, j'ai pu montrer que la réversion artificielle de l'hyperfusion mitochondriale et la restauration de sites de contact RE-mitochondrie avec le traitement Mito-C sont suffisantes pour réduire considérablement la réplication du virus influenza (et du virus de la Dengue, également connu pour provoquer une élongation de la mitochondrie) et pour restaurer la morphologie mitochondriale initiale dans les cellules infectées. Nous proposons enfin que l'effet antiviral associé à Mito-C soit directement lié à la régulation de l'immunité innée, via la voie de signalisation RIG-I. En conclusion, mon travail de thèse a permis de souligner l'importance du dialogue entre la morphodynamique mitochondriale, les sites de contact RE-mitochondrie et l'immunité innée dans le contexte de l'infection par le virus de la grippe. De plus, la protéine NAF-1 peut désormais être considérée comme une cible thérapeutique potentielle dans la recherche de molécules antivirales voire dans d'autres pathologies où l'altération de la dynamique des mitochondries fait partie de l'étiologie de la maladie.

Mots clés : influenza, morphodynamique mitochondriale, sites de contact réticulum endoplasmique- mitochondries, immunité innée, médicaments antiviraux, protéines NEET

FIGURE AND TABLE LIST

FIGURES

TABLES

ABBREVIATIONS LIST

ADP: Adenosine DiPhosphate
AP: Adaptor Protein
Apaf-1: Apoptotic Protease-Activating Factor 1
ATF2: Activating transcription factor 2
ATF4: Activating Transcription Factor 4
ATF5: Activating Transcription Factor 5
ATG: AuTophagy related Genes
ATP: Adenosine TriPhosphate
Bak: Bcl-2 homologous antagonist/killer
BCL-2: B-Cell Lymphoma 2
BCL-2-L4 (Bax): Bcl-2-Like protein 4
C1QBP: Complement component 1 Q subcomponent-Binding Protein
Ca^{2+}: Calcium
CARD: Caspase Activation and Recruitment Domains
CHOP: C/EBP Homologous Protein
CISD1: CDGSH Iron Sulfur Domain 1
CISD2: CDGSH Iron Sulfur Domain 2
CISD3: CDGSH Iron Sulfur Domain 3
CJ: Crista Junctions
CM: Cristae Membrane
COPI: COat Protein I
COPII: COat Protein II
CPSF30: Cleavage and Polyadenylation Specificity Factor 30
CRM1: ChRomosomal Maintenance 1
cRNA: complementary RNA
CTD domain: C-Terminal Domain
Cys: Cysteine
DELE1: Death Ligand Signal Enhancer 1
DENV: DENgue Virus
DRP1: Dynamin-Related Protein 1
Dyn2: Dynamin 2
EE: Early Endosomes
EEA1: Early Endosome Antigen 1
EIF2AK1 (HRI): Eukaryotic Translation Initiation Factor 2-Alpha Kinase 1
EIF2α: Eukaryotic Translation Initiation Factor 2-alpha
EMC: Endoplasmic reticulum Membrane protein Complex
ER: Endoplasmic Reticulum
ERES: Endoplasmic Reticulum Exit Sites
ERGIC: Endoplasmic Reticulum -to-Golgi Intermediate Compartment
ETC: Electron Transport Chain
$FADH_2$: Flavin Adenine Dinucleotide H (reduced form)
FDA: Food and Drug Administration
Fe: iron
Fe-S: iron-sulfur
Fis1: Fission protein 1
HA: HemAgglutinin
HBV: Hepatitis B Virus
HEF: Hemagglutinin Esterase Fusion
His: Histidine

HIV: Human Immunodeficiency Virus
HtrA2 (Omi): High temperature requirement protein A2
IAP-3 (XIAP): Inhibitor of Apoptosis Protein 3
IAV: Influenza A Virus
IBM: Inner Boundary Membrane
IBV: Influenza B Virus
ICV: Influenza C Virus
IDV: Influenza D Virus
IFN: InterFeroN
IMS: InterMembrane Space
IRF3: Interferon Regulatory Factor 3
IRP1: Iron Regulatory Protein-1
ISGs: Interferon Stimulated Genes
ISR: Integrated Stress Response
KO: Knock-Out
LAMP1: Lysosomal-Associated Membrane Protein 1
LC3-II: Light Chain 3-II protein
LE: Late Endosomes
LIR: LC3-Interacting Region
L-OPA1 : Long OPA1
M1 : Matrix protein 1
M2 : Matrix protein 2
MAVS: Mitochondrial AntiViral Signaling protein
MCSs : Membrane Contact Sites
Mff: Mitochondrial fission actor
MFN1: MitoFusiN 1
MFN2: MitoFusiN 2
MICOS: MItochondrial contact site and Cristae Organizing System
MiD49: Mitochondrial Dynamics protein 49
MiD51: Mitochondrial Dynamics protein 51
MIM: Mitochondrial Inner Membrane
MiNT: Mitochondrial inner NEET protein
MMP: Mitochondrial Membrane Potential
mNT: mitoNEET
MOM: Mitochondrial Outer Membrane
mPTP: mitochondrial Permeability Transition Pore
mRNA : messenger RNA
MT: MicroTubules
mtDNA: mitochondrial DNA
MVE/MVBs: MultiVesicular Endosomes/ MultiVesicular Bodies
NA: NeurAminidase
NADH: Nicotinamide Adenine Dinucleotide H (reduced form)
NAF-1: Nutrient-deprivation Autophagy Factor-1
NCOA7: Nuclear receptor COActivator 7
NEP: Nuclear Export Protein
NES: Nuclear Export Signals
NF-κB: nuclear factor- kappa B
NO: Nitric Oxide
NP : NucleoProtein

NS1 : Non-Structural Protein 1
NS2 : Non-Structural Protein 2
NS4B: Non- Structural protein 4B
OMA1: metallopeptidase Overlapping with the m-AAA protease1
OPA1: Optic Atrophy 1
OXPHOS: OXidative PHOSphorylation
PA: Polymerase Acidic
PACT: Protein ACTivator
PB1: Polymerase Basic Protein 1
PB1-F2: Polymerase Basic Protein 1-F2
PB2: Polymerase Basic Protein 2
PI3P: PhosphatIdylinositol-3-Phosphate
PINK1: PTEN-INduced Kinase 1
PKR: Protein Kinase R
PM: Plasma Membrane
ppp: triphosphate
PTPIP51: Protein Tyrosine Phosphatase Interacting Protein-51
RdRp: RNA-dependent RNA polymerase
RE: Recycling Endosomes
RIG-I: Retinoic acid-Inducible Gene I
RNA: RiboNucleic Acid
RNP: RiboNucleoProtein
ROS: Reactive Oxygen Species
SAMM50: Sorting and Assembly Machinery 50
Serca2b: Sarcoendoplasmic reticulum Ca^{2+} ATPase 2
SG: Secretory Granules
Smac (Diablo): Second mitochondria-derived activator of caspase
S-OPA1: Short OPA1
TGN: *Trans* - Golgi Network
TIM: Translocase of the Inner Membrane
TOM: Translocase of the Outer Membrane
TRIM25: TRIpartite Motif containing 25
VDAC: Voltage Dependent Anion-selective Channel
vRNA: viral RiboNucleic Acid
vRNP : Viral Ribonucleoprotein
WHO : World Health Organization
YME1L: ATP-dependent zinc metalloprotease
ZAPS: Zinc-finger Antiviral Protein

SCIENTIFIC ENVIRONMENT

I've completed my PhD research project within a framework of a CIFRE fellow (Industrial Agreement of Training through Research) funded by ANRT (National Association for Research and Technology). The research program is carried out via a partnership between a private company and an academic research laboratory. The aim of the CIFRE fellow is to give the PhD students the opportunity to develop a research program in two environments to enrich his/her experience and increase the chances of future career success. In parallel, the CIFRE program encourages research partnerships between the academic and business domains. Consequently, the actors composing and participating in the CIFRE program are the private company, the academic laboratory and the doctoral student.

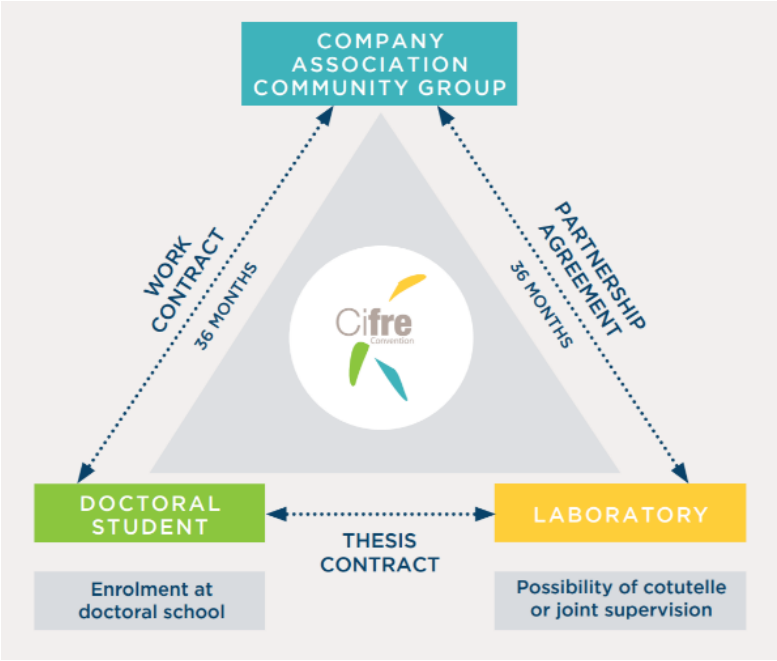

CIFRE program partnership

The company

Based in Lyon, ENYO Pharma is a biotech specialized in drug discovery by an unique approach: explore virus-host interactions to develop molecules directed against new therapeutic intracellular targets, based on virus biomimetism (see more: http://www.enyopharma.com).

The company has initiated phase 2 clinical studies with its lead compound EYP001 (a FXR agonist) in Chronic Hepatitis B and in NASH (Non Alcoholic Steatosis Hepatitis). In parallel, Enyo Pharma currently develops other research programs based on its innovative technology to develop drugs against untapped targets by the pharma industry (*i.e* mitochondrial targets). The applications can be developed for various indications like infectious diseases, metabolic diseases, oncology, etc.

The academic laboratory

Based in Paris, the Necker enfant maladies Institute (INEM) harbor Etienne's Morel team specialized in the autophagy pathway and the intracellular compartments dynamics. Etienne Morel's research team investigates the cellular and molecular mechanisms that regulate autophagic pathway during stress response and endomembranes dynamics and crosstalk in physiological and pathophysiological situations.

The doctoral student

I've leaded a transversal research project allying the proficiency in virology of Enyo Pharma and the expertise in cell biology of Etienne Morel's team. My doctoral project is thus at the interface between infectious diseases, antiviral therapy and drug mechanism of action, study of membrane dynamics and cellular trafficking in viral infection conditions.

PhD THESIS

AIMS

Influenza viruses are a public health threat considering its high rates of fatality and morbidity over the world. Current treatments and prophylaxis therapies are not absolutely effective due to the high rate of viral mutation and the continuous emergence of resistance strains to these direct-acting drugs (drugs targeting viral proteins). Moreover, organelle modifications upon influenza infection have never been fully studied. Indeed, an integrative exploration of the influenza viral infection consequences on endomembranes dynamics, morphology, trafficking and signaling can be an essential key to get a better understanding of cellular responses to viral stress. This new approach would help to identify untapped pharmaceutical targets to abrogate viral replication and spreading.

To address this problematic, the project has been divided is three main and complementary sections:

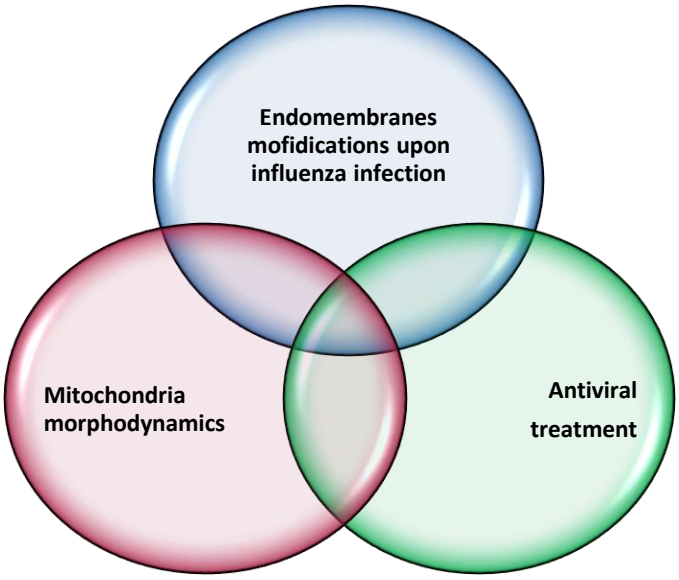

PhD project mains sections

The first aim was to understand how endomembranes and cellular trafficking machineries are modified during influenza infection in host cells. This first step should allow the identification of organelles or pathways that could become targets to treat influenza infection.

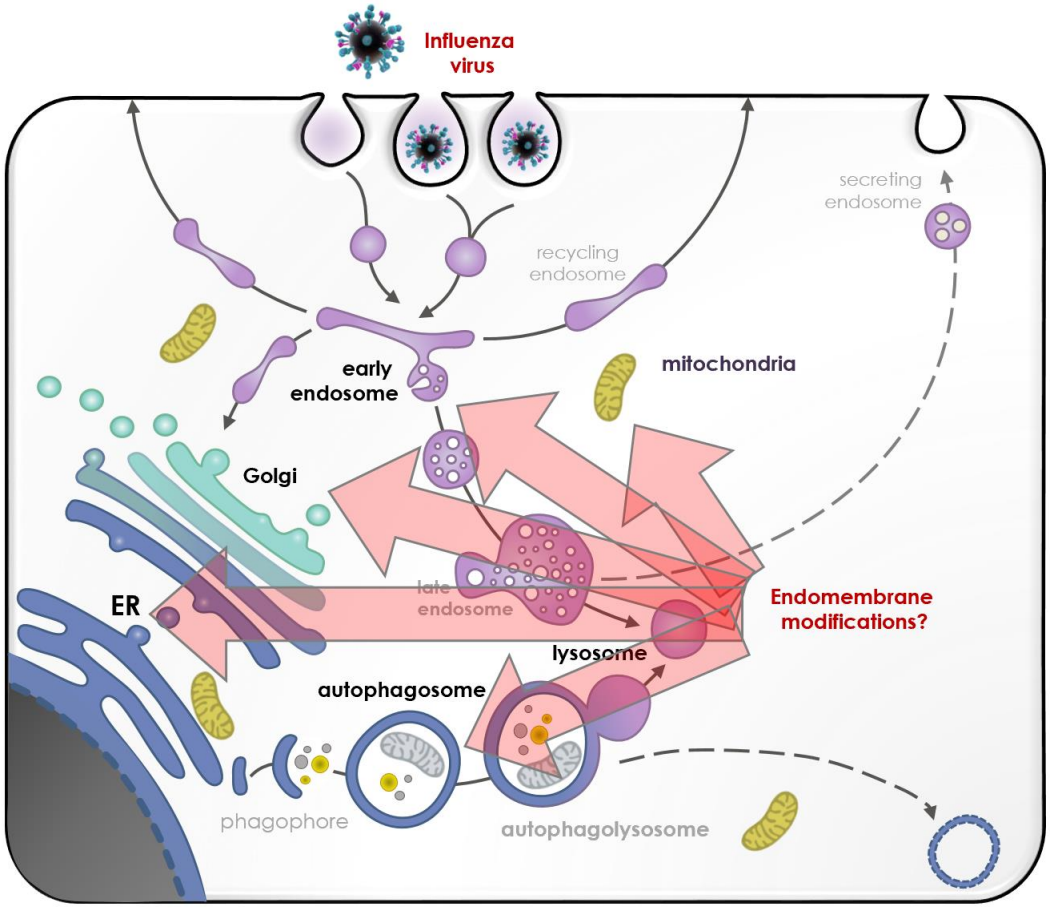

Possible organelles targeted by influenza virus

The second step was to analyze the potential antiviral impact of new indirect-acting drugs (targeting cellular host proteins) developed by Enyo Pharma. Related to the data, an in-depth study was performed focusing on mitochondria. The ultimate question was to study mitochondrial morphodynamics and the mechanism of action of new mitochondrial modulators under physiological and infectious conditions. The results obtained during this study led to the preparation of two peer-reviewed papers: the first is submitted and the second is under revision at EMBO reports.

INTRODUCTION

PART A: BIOLOGY OF INFLUENZA VIRUSES

A.1 CLASSIFICATION AND VIRAL STRUCTURE

Influenza viruses belong to the *Orthomyxoviridae* family (Dowdle et al., 1975). Four influenza viruses species have been isolated, which are divided in four genera: *Alphainfluenzavirus* (Influenza A virus (IAV)), *Betainfluenzavirus* (Influenza B virus (IBV)), *Gammainfluenzavirus* (Influenza C virus (ICV)) and *Deltainfluenzavirus* (Influenza D virus (IDV)). These four species share a common genetic ancestry that has been identified and confirmed by sequencing, but they have genetically diverged (Fig 1) (Carnell et al., 2015).

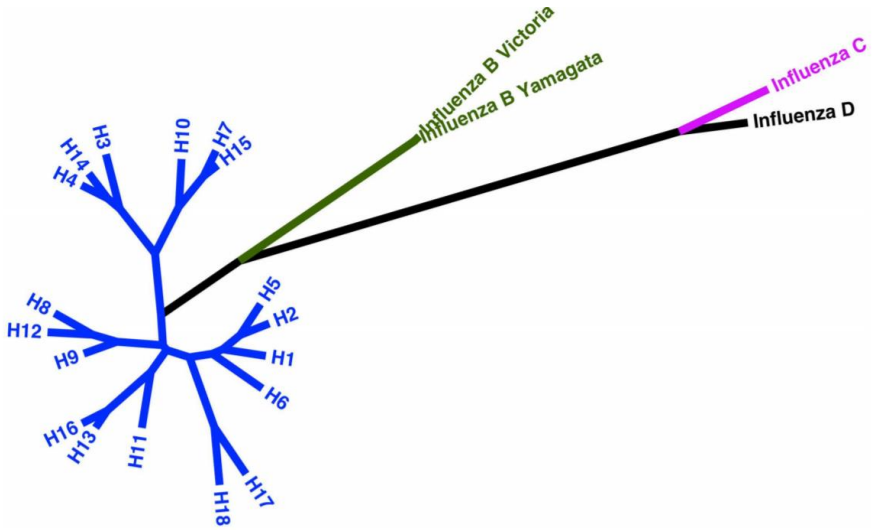

Figure 1. Phylogeny of current influenza subtypes using the hemagglutinin viral protein. Influenza viruses share a common ancestor. IAV, IBV, ICV and IDV have genetically diverged (Carnell et al., 2015).

The current system of influenza viruses nomenclature was recommended by the World Health Organization (WHO) back in 1980. It consists of two parts: first, influenza type (A, B, C or D) and second, a strain designation containing information on the antigenic type of the virus, the host of origin (when isolated from non-human sources), the geographical origin, the strain number, and the year of isolation (Memorandum, 1980; Smorodintsev et al., 1982). For IAV, the subtype of surface antigens hemagglutinin (H) and neuraminidase (N) must be also considered for proper nomenclature (Schild et al., 1980).

IAV are a major public health concern. Indeed, IAV infection attains high rates of morbidity and socio-economic loss every year. The subtypes of surface glycoproteins (hemagglutinin (HA) and neuraminidase (NA)) are the main characteristic of IAV. So far, 18 types of HA (H1-H18) and 11 types of NA (N1-N11) have been identified. IAV have a wide range of hosts (pigs, quails, bats, horses, cats, dog, marine mammals, etc.) but the waterfowl is the main reservoir (Fig 2). Species that express sialic acid α2,3-Gal and sialic acid α2,6-Gal receptors (required for virus binding to cells) have been reported to be the mixing vessels (Yoon et al., 2014). This host diversity provides to IAV a huge ability of genetic re-assortments (exchange of viral ribonucleic acid (RNA) segments between viruses), and thus the possible emergence of zoonotic strains and even pandemics that could have a serious impact on human health (Kumar et al., 2018). Importantly, reassortment occurs within each genus, but not across the viruses' types.

IBV causes also severe respiratory disease and epidemics, particularly in children and young adults (M. et al., 2016). IBV reservoirs are almost exclusively humans but a few cases have been reported in horses, seals, pigs and dogs (Fig 2). IBVs have been classified into two distinct lineages: B/Victoria/2/1987-lineages and B/Yamagata/16/1988-lineages (Rota et al., 1990). These two lineages have a different antigenic dynamic: Victoria-lineage viruses show antigenic drift of a single lineage while Yamagata-like viruses show alternating dominance between antigenic groups (Langat et al., 2017).

ICV have a relative low prevalence causing mild respiratory disease in humans, mostly infecting children (Homma et al., 1982). ICVs can also infect other species such dromedary camels, dogs and pigs and have been recently discovered to be distributed worldwide (Fig 2) (Matsuzaki et al., 2016). Multiple genetic lineages circulate at the same time (Buonagurio et al., 1986).

IDV is the newly identified genus of the Orthomyxoviridae family. They cause influenza-like illness and share around 50% genetic homology with human ICV. However, IDV are not able to reassort with ICV (S. Su et al., 2017). The major reservoir is cattle but IDV have been detected also in swine, horse, sheep, dromedaries and humans across the globe (Fig 2) (Asha & Kumar, 2019). IDV are represented by two lineages: D/swine/Oklahoma/1334/2011 (D/OK) and

D/bovine/Oklahoma/660/2013 (D/660) with distinct antigenic and genetic features (Collin et al., 2015). IDVs have a real potential of zoonotic and transmission between different species.

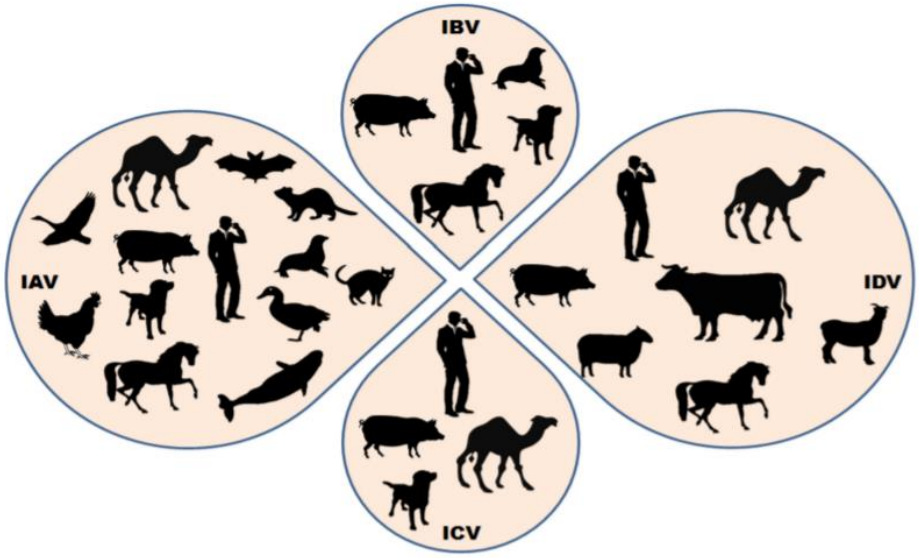

Figure 2. Summary of the wide host range of influenza viruses. Abbreviations: IAV: influenza A virus; IBV: influenza B virus; ICV: influenza C virus; IDV: influenza D virus. IAV has a wide host variety compared to IBV, ICV and IDV (Asha & Kumar, 2019)

IAV and IBV genomes (around 14 kb) are composed of eight negative-sense, single-stranded viral RNA segments (vRNA) contained in separate viral ribonucleoprotein complexes (vRNP) that are associated together with a sophisticated genome packaging mechanism into a virion of 80-120 nm in diameter. Influenza viral particles are pleomorphic, adopting spherical (Fig 3.a) or filamentous shapes (Fig 3.b) and occasionally an irregular morphology (Fig 3.c) (Dadonaite et al., 2019; Giese et al., 2016; Noda, 2012) .

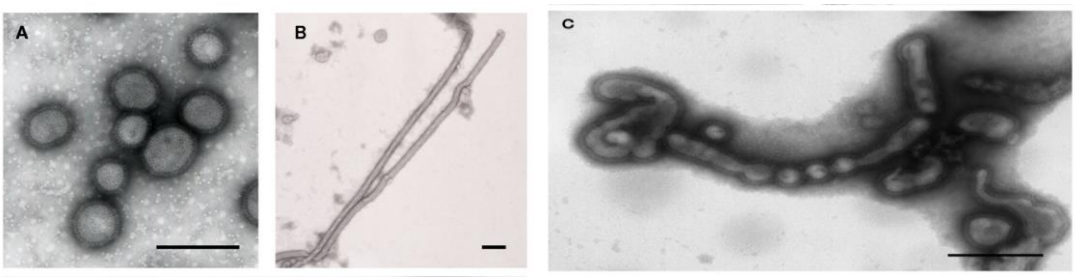

Figure 3. Influenza pleomorphism. Electron microscopy of influenza virions. A: spherical morphology of H1N1/WSN33 virus; B: filamentous shape of H3N2 virus; C: irregular virions of H1N1/Puerto Rico (Noda, 2012).

IAV virions are surrounded with lipids coming from the host cell plasma membrane and covered with spikes of hemagglutinin (HA) and neuraminidase (NA) glycoproteins (ratio 4 to 1). This lipid envelope is crossed by ion channels called matrix protein 2 (M2). Inside, the matrix protein 1 (M1) encloses the virion core, composed of the ribonucleoprotein (RNP) complexes. RNPs are viral RNA segments coated with several molecules of nucleoprotein (NP) and the RNA polymerase composed of three subunits: Polymerase Basic proteins 1 and 2 (PB1 and PB2) and Polymerase Acidic protein (PA). In addition, the virus codes for two non-structural proteins, NS1 and NS2 (also called nuclear export protein, NEP) (Fig 4) (Bouvier & Palese, 2008). Main functions of these proteins are detailed in Table 1. The function of each protein in the viral cycle will be described in more details on section B2.

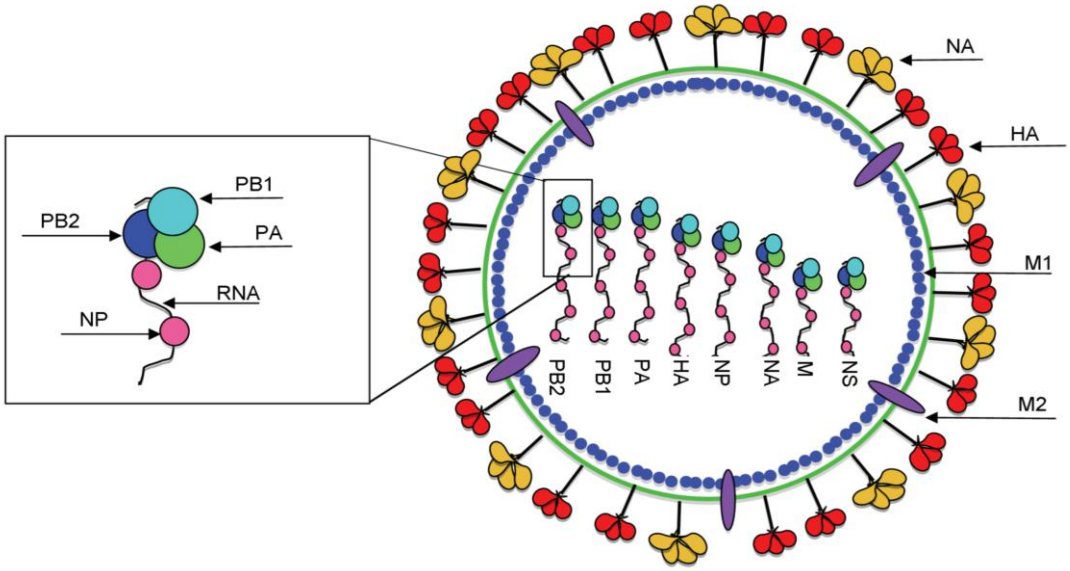

Figure 4. Structure of the influenza A virus. The viral genome is composed of 8 RNA segment coding for all the viral proteins. In the left, a representation of the ribonucleoprotein (RNP) complex which is composed of: RNA, PB1, PB2, PA and NP. Abbreviations: hemagglutinin (HA), neuraminidase (NA), matrix protein 1 (M1), matrix protein 2 (M2), nucleoprotein (NP) polymerase basic proteins 1 and 2 (PB1 and PB2) non-structural proteins (NS) (Grant et al., 2014).

The first mapping of the viral genome was made about 30 years ago and it was believed that the eight genome segments encode only for these 10 proteins. Actually, a first accessory protein, polymerase basic protein 1-F2 (PB1-F2), was discovered in 2001 (translated from the alternative open reading frame of PB1). Since then, the viral proteins PA-X, PA-N182, PB1-N40, NS3, PA-N155 and M42 have also been discovered. The wide diversity of strains and the potential alternative splicing events open new possibilities for new different influenza proteins (Vasin et al., 2014).

Segment	Segment length in nucleotides	Encoded Protein(s)	Protein length in amino acids	Protein function
1	2341	PB2	759	Polymerase subunit; mRNA cap recognition
2	2341	PB1	757	Polymerase subunit; RNA elongation
		PB1-F2	87	Pro-apoptotic activity
3	2233	PA	716	Polymerase subunit; endonuclease activity
4	1778	HA	550	Surface glycoprotein; major antigen, receptor binding and fusion activities
5	1565	NP	498	RNA binding protein; nuclear import regulation
6	1413	NA	454	Surface glycoprotein; sialidase activity, virus release
7	1027	M1	252	Matrix protein; vRNP interaction, RNA nuclear export regulation, viral budding
		M2	97	Ion channel; virus uncoating and assembly
8	890	NS1	230	Interferon antagonist protein; regulation of host gene expression
		NEP/NS2	121	Nuclear export of RNA ; regulation of Polymerase activity

Table 1. The genomic segments of influenza A/Puerto Rico/8/1934 (H1N1) and viral protein main functions
Adapted from (Bouvier & Palese, 2008)

Importantly, IBV, ICV and IDV genetic and proteomic organizations differ substantially from IAV. Indeed, IBV virions have not only two proteins in the envelope but four: HA, NA, the ion channel NB, and the proton channel BM2 (instead of M2 protein) (R. G. Paterson et al., 2003). The genome of influenza C and D viruses have only 7 segments. Moreover, IVC present one major surface glycoprotein: the hemagglutinin-esterase-fusion (HEF) protein. It bears functions of both HA and NA proteins of influenza A and B viruses. ICV also presents one minor envelope protein CM2, which functions as an ionic channel (Bouvier & Palese, 2008; M. Wang & Veit, 2016). Finally, the ICV hemagglutinin esterase is also present in IDV and displays conserved same enzymatic activity but has divergent receptor-binding sites (Hause et al., 2013).

A.2 EPIDEMIOLOGY: SEASONAL EPIDEMICS AND PANDEMICS

Influenza viruses are a public health threat for humans and animals worldwide (Fig 5). The latest estimations on the global population are of 291,243 to 645.832 seasonal influenza-associated respiratory deaths per year (4–8.8 per 100,000 individuals) (Iuliano et al., 2018). These viruses cause frequent mortality and morbidity leading to important social and economic burdens. Almost all four types of influenza viruses cause respiratory illness, but type A influenza virus is the most significant public health concern considering its highest rates of fatality and morbidity (Kumar et al., 2018).

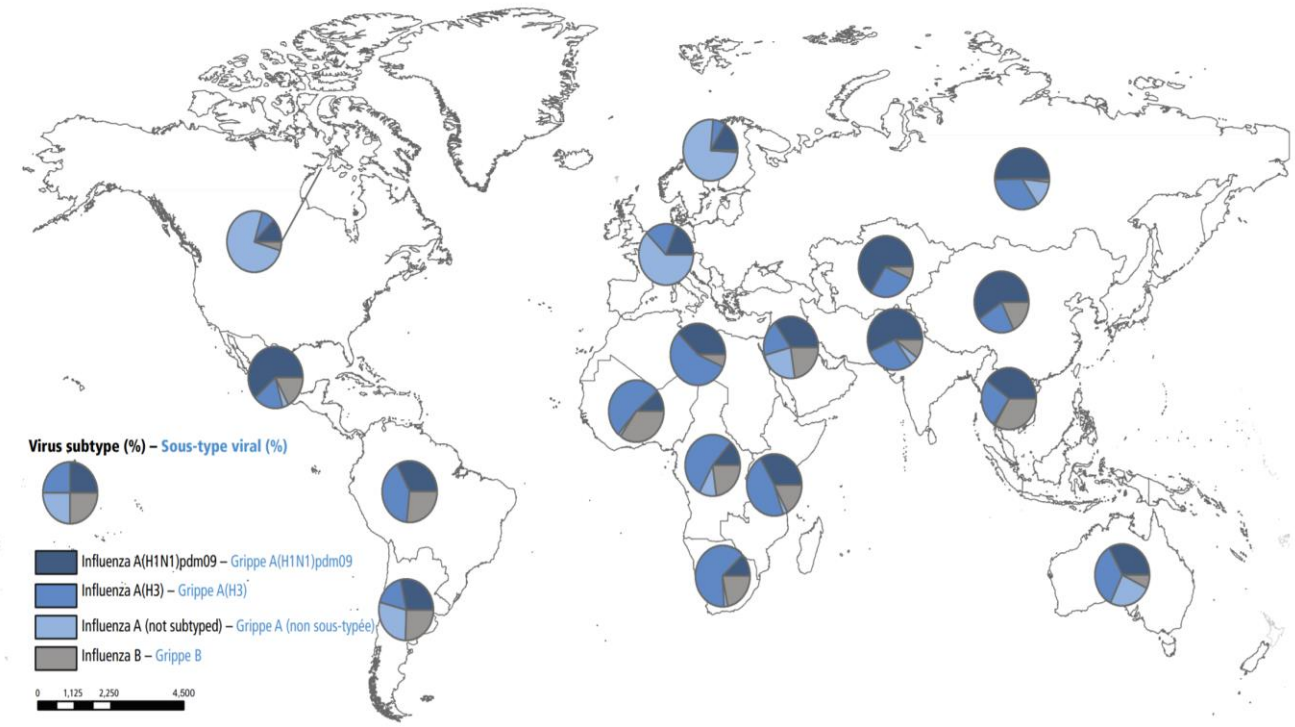

Figure 5. World distribution of influenza A and B viruses and subtypes by influenza transmission zone, October 2018 to May 2019. Influenza viruses are distributed worldwide (WHO Global Influenza program; https://who.int/influenza).

Globally two types of influenza epidemics occur: epidemics caused generally by seasonal influenza (IAV and IBV), and pandemics caused until now only by influenza A viruses. Two major events are responsible of the emerging threats due to these viruses: antigenic drift and antigenic shift.

Antigenic drift is a process that occurs continuously in both IAV and IBV. It is caused by point mutations in viral genes due to an error made by the RNA polymerase (Fig 6). When these mutations take place in genes coding for an epitope where host antibodies bind to the viral protein, the antibodies do not recognize the viral protein anymore. This strategy allows the virus to escape the adaptative immune system, previously acquired from vaccination or prior exposure. This phenomenon is responsible for influenza epidemics and that is the reason why new annual influenza vaccine composition is required. (H. Kim et al., 2018; Treanor, 2004; van der Sandt et al., 2012).

Antigenic shift is caused by a genetic re-assortment between the genes of two or more different strains infecting the same cell a same host. This event is possible due to influenza's segmented genome. This occurrence changes the genome of the virus and can result in novel combinations of the two surface glycoproteins NA and HA, resulting in an evolved virus that can escape from antibody recognition and cause pandemics (Fig 6). (H. Kim et al., 2018; Treanor, 2004; van der Sandt et al., 2012).

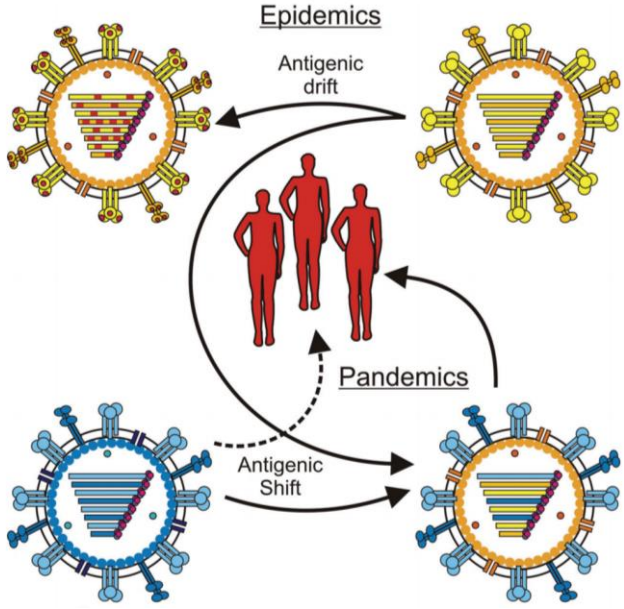

Figure 6. Antigenic drift and antigenic shift. Human epidemics are caused by point mutations (antigenic drift) while the origin of pandemics is a rearrangement of the viral genome (antigenic shift) or a virus crossing from one species to another (van der Sandt et al., 2012).

Influenza seasonal epidemics normally arise during the cold seasons in temperate regions. During this period, several atmospheric conditions are reunited to facilitate virus spreading, shedding, viability and transmission. For instance, relative humidity and temperature are suggested to be key factors for influenza transmission (Lowen et al., 2007). In addition, the virus type and host origin play an essential role in the environmental persistence of influenza viruses (Kormuth et al., 2019). The global spatiotemporal pattern of seasonal epidemics waves depends also on air traffic, epidemiological, biological and socio-demographic factors (Coletti et al., 2018; Wen et al., 2016). All these conditions are beneficial for a rapid spreading of influenza viruses and can cause annual epidemics with different severity of symptoms from common cold to severe lung injury and death.

The onset of seasonal flu is linked to IAV and/or IBV co-circulation with varying incidence each year and a different geographic distribution. Historically, IAV was in the center of influenza epidemics but since the 1940s IBV has been also detected and studied, raising the issue of vaccine matching. For both IAV and IBV, the main challenge is to predict the incidence of strains/lineages ahead of season because of the antigenic adaptation of these influenza viruses. New approaches are growing in this field to predict antigen evolution (Du et al., 2017).

Influenza pandemics represents a substantial threat to global health. Pandemics spread widely because when facing a new virus, human population is susceptible and immunologically naïve (Lowen, 2017; Taubenberger & Kash, 2010). Six main influenza pandemics have been described since the end of the XIX century: two "Russian flu" (A/H3N8 in 1889 and A/H1N1 in 1977) (Valleron et al., 2010), the deadliest in human history "Spanish flu" (A/H1N1, in 1918) (Humphreys, 2018), "Asian flu" (A/H2N2, in 1957) (Linster et al., 2019), "Hong Kong flu" (A/H3N2, in 1968) (Viboud et al., 2005) and "swine flu" (A/H1N1, in 2009) (Girard et al., 2010). Thus, authorities keep under close surveillance the new emerging strains in human population as in animal reservoirs. Even if avian influenza viruses associated human infection is quite rare, H5N1 and H7N9 avian strains have been shown to infect humans in the last decades (Lai et al., 2016; S. Su et al., 2017). These newly emerged viruses, with a high rate of mortality, are in continuous evolution and could develop mechanisms of virulence in humans, which could be a long-term concern worldwide. Therefore, it is imperative to implement the monitoring of flu viruses and reinforce surveillance and prevention strategies (de Wit & Fouchier, 2008).

A.3 CLINICAL SYMPTOMS

Influenza viruses cause acute infection of the upper respiratory tract. Infection spreads easily by aerosol transmission, droplets or direct contact from person to person. The incubation period can vary between 1 to 4 days. An infected person can be infectious from one day before the outbreak of symptoms to 5-7 days after. Viral shedding occurs during this period. In healthy individuals flu illness is usually self-limiting (some infections can be asymptomatic) with a recovery in 3-7 days (Jutel & Banister, 2013). A sudden onset of fever 24h after infection is the first characteristic of influenza-like illness. Other concomitant symptoms are myalgia, fatigue, headache, dry cough, sore

throat, sweats, chills, runny nose and nasal congestion. Gastrointestinal symptoms including nausea, vomiting and diarrhea are also common. Some complications may appear like respiratory insufficiency, renal, cardiac or even neurologic (Fig 7) (Ghebrehewet et al., 2016; Monto et al., 2000).

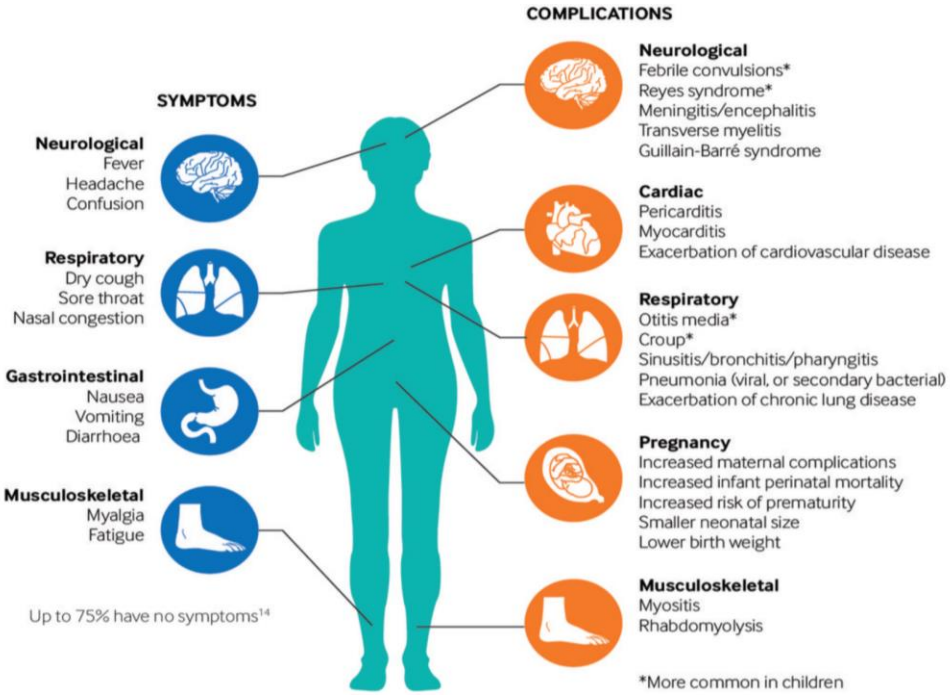

Figure 7. Symptoms and complications caused by influenza infection (Ghebrehewet et al., 2016)

A.4 VACCINES

Despite numerous efforts to produce absolutely effective vaccines or anti-influenza drugs, no such agent has been developed yet. Annual vaccination is believed to be the most efficient strategy to protect individuals from acquiring influenza infection and to prevent epidemics in population. The most common viral proteins used in vaccines production is the surface proteins HA. Indeed, currently licensed vaccines are able to induce antibody response against these viral surface proteins. Notwithstanding, the segmented genome and its error-prone RNA-dependent RNA polymerases enables these viruses to rapidly evolve through antigenic shift and drift. This evolution can result in a new influenza strain and consequently virus evasion of the adaptive immune responses previously acquired from vaccination. (Bouvier & Palese, 2008; Neirynck et al., 1999; Vemula et al., 2017). Seasonal influenza vaccines are composed of two influenza A strains (H1N1 and H3N2

subtypes) and two influenza B strains (Victoria and Yamagata lineages) recommended by the WHO every year in accord with predicted strains. In 2019 the recommendation was a tetravalent vaccine composed by an A/Brisbane/02/2018 (H1N1) pdm09- like virus, an A/Kansas/14/2017 (H3N2) - like virus, a B/Colorado/06/2017 (B/Victoria/2/87 lineage) - like virus and a B/Phuket/3073/2013 (B/Yamagata/16/88 lineage) - like virus (https://www.who.int/influenza/vaccines). WHO recommends routine annual influenza vaccination for risk groups: children aged 6-59 months, elderly, individuals with specific chronic medical conditions, health-care workers and pregnant women (https://www.who.int/influenza/vaccines/use/en/).

Despite policy recommendations, influenza vaccination remains suboptimal as a result of low uptake levels. In 2001, risk elder population was 380 million but only 250 million vaccines have been administrated worldwide (Stöhr, 2002). In 2003, the World Health Assembly asked to increase vaccination coverage to 75% among the elderly but in 2014/2015 season in Europe, only Ireland reached this recommendation (Jorgensen et al., 2018). Influenza vaccination remains a controversial subject due to the conflicting results observed in recent studies. A poor protective efficacy of 19% to 53% was reported in last five years (Biswas et al., 2019). However, a repeated vaccination every year increases the protection against influenza virus in 25% for H1N1, in 7% for H3N2 and in 18% for IBV, which demonstrate the benefits of the vaccination program (Ramsay et al., 2019). This limited protection can be linked to the difficulty of predicting next season circulating strains, causing a mismatch between the current vaccine and ongoing circulating viruses.

Several novel strategies are currently being developed to create an effective "universal" influenza vaccine to protect against both new seasonal and arising pre-pandemic strains. One approach is to study the conserved viral proteins or regions shared amongst all strains promoting an immune response to neutralize a wide spectrum of influenza virus. Furthermore, new vaccines candidates based on “stalk domains” (a conserved domain) of HA could be the used for next vaccines generation (Krammer, 2016; Sautto et al., 2018). Alternatively, the concept of proposing personalized flu vaccines depending on basal individual immune status is being explored (Biswas et al., 2019).

A.5 ANTIVIRAL DRUGS

The development of antiviral drugs against influenza virus for therapy and prophylaxis is a major public health challenge. Antivirals can be developed following two approaches; indeed, direct-acting drugs target and interact with viral proteins, while indirect-acting drugs target host cellular proteins to prevent viral replication.

Four direct-acting drugs have been approved by the FDA (USA food and drug administration) for current treatment against both IAV and IBV (FDA august 2019, https://www.fda.gov/drugs/information-drug-class/influenza-flu-antiviral-drugs-and-related-information#ApprovedDrugs). Three of these recommended drugs are peramivir (Rapivab ©), zanamivir (Relenza ©) and oseltamivir phosphate (Tamiflu ©). They target NA protein, impeding the release of newly formed virions from infected cells. (C. M. Lee et al., 2012; Mclaughlin et al., 2015; Shin et al., 2017). Baloxavir marboxil (Xofluza ©) is the last approved and recommended drug (October 2018). It is a new class of anti-influenza drugs because this compound targets the PA polymerase and prevents viral mRNA (messenger RNA) transcription of both IAV and IBV (O'Hanlon & Shaw, 2019). The administration of this drugs (oral, inhaled, intravenous) and indications (treatment or chemoprophylaxis) should be chosen following the recommendations (Table 2). Moreover, two different direct-acting drugs have been approved in other countries. Indeed, favipiravir (RNA-dependent RNA polymerase inhibitor) is used in Japan and umifenovir (Arbidol ©, targeting HA and impeding membrane fusion) is licensed in Russia and China (Leneva et al., 2019; Reina & Reina, 2017).

In 1966 and 1993 the FDA approved two molecules of the adamantame group: amantadine and rimantadine. These drugs are active for treatment and prevention of influenza A virus infection by targeting the M2 viral protein and consequently blocking its ion channel activity to avoid virus uncoating. However, adamantames are no longer recommended as a consequence of viral resistance acquired by the circulating strains (pdmH1N1 and H3N2) and because they are not effective against IBVs. Besides, recommendations are susceptible to change in case of specific virus strains emergence with sensitivity to amantadine or rimantadine (Gu et al., 2013; Wharton et al., 1994).

FDA-approved antiviral drugs for influenza

Drug class	Antiviral drug	Active against	Route	Treatment	Chemoprophylaxis	Resistance mutations
M2 ion channel inhibitors	Rimantadine	Influenza A viruses	Oral	Not Recommended	Not Recommended	S31N, L26I, V27A
	Amantadine	Influenza A viruses	Oral	Not Recommended	Not Recommended	S31N, L26I, V27A
Neuraminidase (NA) inhibitors	Oseltamivir	Influenza A and B viruses	Oral	Any age	3 months and older	H274Y, E119V
	Zanamivir	Influenza A and B viruses	Inhaled	7 years and older	5 years and older	I223R, E119V
	Peramivir	Influenza A and B viruses	Intravenous	2 years and older	Not Recommended	H274Y
Endonuclease (PA) inhibitors	Baloxavir marboxil	Influenza A and B viruses	Oral	12 years and older	Not Recommended	I38T/F/M

Table 2. Antiviral drugs for influenza treatment. The chart summarizes the approved FDA drugs, its activity, administration and indications. Moreover, it includes resistance mutations for each drug (O'Hanlon & Shaw, 2019).

A virus acquires drug resistance when the mutation of the genes encoding for its viral components causes a loss of the antiviral drug efficacy. Accordingly, resistant influenza strains have emerged to all current FDA recommended drugs (Table 2) (Dobrovolny & Beauchemin, 2017). This resistance phenomenon is common because influenza viruses possess an elevated rate of mutation, allowing the virus to rapidly evade the host immune system or obtain resistance against antiviral molecules. Indeed, hemagglutinin and neuraminidase encoding genes mutate easily. This can give them an evolutionary advantage and consequently these mutations are positively selected with a higher frequency than for other viral proteins (Shao et al., 2017; Visher et al., 2016). Finally, human influenza A viruses evolve more rapidly than influenza B viruses (Nobusawa & Sato, 2006).

In conclusion, direct-acting drugs cannot avoid the resistance phenomenon issues, leading the virus to escape the current recommended drugs. Novel insights are needed to supplement or replace existing anti-influenza therapies. In fact, the use of indirect-acting drugs to target and modulate host cellular proteins could avoid resistance formation since the virus is not attacked itself. Moreover, these drugs could keep its therapeutic activity against both circulating and new emerging influenza strains. The first evidence that influenza infection can be modulated by targeting cell proteins was discovered in 2001. Indeed, IAV infection leads to an activation of the Raf/MEK/ERK cascade implicated in cell proliferation and survival and its inhibition results in a decrease of viral replication by RNPs nuclear retention and NS2 function impairment (Pleschka et al., 2001).

Understanding virus-host cell biology is essential in the development of host-oriented antiviral therapeutics. Different approaches have been explored to identify key regulators host targets on infected cells. First, the use of genome-wide RNA interference and CRISPR/Cas9 screening allows the identification of human cells genes that have a consequence on influenza replication (Chin & Brass, 2013; Han et al., 2018; Münk et al., 2011). In 2010, 287 human genes were identified by this approach (Karlas et al., 2010). Second, the interatomics approaches aim to identify the perturbations induced in the host protein interactome upon viral infection. The analysis of this network modifications by making new connections and/or disrupting the existing ones may increase the efficiency of antiviral drug target discovery (Ackerman et al., 2019; de Chassey et al., 2014). Finally, drug repositioning and bioinformatic studies can be explored by testing existing compounds for which safety data in humans are available. Some examples of such compounds are the protein kinase C, the heat shock protein 90, the importin A5 or the proteasome (Müller et al., 2012; Rohini et al., 2019).

During the last past years, some indirect-acting drugs have used these approaches and have been tested in clinical trials showing promising results. This is notably the case for the following compounds: the MEK inhibitor Cl-1040 which has an antiviral effect over several influenza strains (Haasbach et al., 2017); the D, L-lysine-acetylsalicylate glycine, which has been shown to inhibit influenza viral replication by targeting the proapoptotic and pro-viral effects of NF-κB (nuclear factor-κB) (Scheuch et al., 2018); diltiazem, a Ca^{2+} channel blocker already used in hypertension treatments (Pizzorno et al., 2019) or nitazoxanide, initially used in treatment of diarrhea (Rossignol et al., 2009). Taken together, these data demonstrate that targeting intra-cellular signaling pathways alleviates efficiently viral influenza infection.

PART B: MEMBRANE TRAFFICKING, ORGANELLES AND VIRUS

B.1 OVERVIEW OF MAMMALIAN TRAFFICKING STATIONS

Eukaryotic cells display a sophisticated internal architecture that has evolved in a complex endomembrane system to allow communication between the cell and its environment and to regulate cellular homeostasis. Organelles are connected by two major and complex trafficking pathways: secretion pathway and endosomal pathway which comprises transit of vesicles in bidirectional fluxes in and out of the cell surface. Specifically, secretion pathway is the "way out" where intracellular vesicles fuse with the plasma membrane (PM) to release their content, while endocytosis is the "way in" where the cell can incorporate extracellular content from PM derived intracellular vesicles. These two processes directly participate in the proper functioning of specialized cellular functions, including transport of proteins and lipids, cell shape and volume regulation, organelle biogenesis homeostasis, immune defense, signaling, molecule secretion, synaptic transmission, cell migration, etc. The major membrane bound structures collaborating in this system are the PM, the endosomal-lysosomal system, the endoplasmic reticulum (ER) and the Golgi complex. A malfunction in the membrane trafficking regulation or in the specific transport can have dramatic consequences on the cell and may lead to several diseases (Bexiga & Simpson, 2013; Ivanov, 2014; Olayioye et al., 2019).

The secretory pathway

Secretion pathway trafficking is a highly specialized, responsive and dynamic process involved in many functions: biogenesis and intracellular distribution of a wide range of lipids, carbohydrates and proteins (being essential for cell signaling), formation and maintenance of intracellular compartments and release of molecules to the extracellular environment (Barlowe & Miller, 2013). Moreover, it participates in multiple transport steps including vesicular trafficking, proteins or hormones secretion, endogenous signaling cascades, response to developmental programs, synapses, chemical messengers transport, etc. The principal actors of the secretory pathway are the ER, the ER exit sites (ERES), the ER-to-Golgi intermediate compartment (ERGIC), the Golgi complex and the post-Golgi carriers (Fig 8) (Farhan & Rabouille, 2011; Thorn et al., 2016).

The ER is a large intracellular structure composed by a single continuous membrane that surrounds the nucleus and expands across all the cytoplasm towards the cell periphery. Several domains can be distinguished: the nuclear envelope, peripheral tubular ER, peripheral cisternae, and various membrane contact sites with other organelles. It is a multifunctional organelle specialized in protein and lipid synthesis, folding and secretion, exchange of molecules with other organelles and Ca^{2+} (calcium) homeostasis (English & Voeltz, 2013; Schuldiner & Weissman, 2013).

The Golgi apparatus is a complex network of stacked membrane cisternae tightly opposed one to another, located in a central cell position close to the nucleus, at the heart of the trafficking pathways. The Golgi complex has a *cis*-to-*trans* polarity due to the different repartition of enzymes and proteins over its membranes. Golgi key function is protein and lipid modification, including sulfation, glycosylation, phosphorylation, and proteolytic cleavage. Once these modifications are completed, the transformed lipids or proteins can be delivered to their final destination, which is mostly PM, but not only (*i.e*. endosomal system, lysosomes or secretory granules) (Aridor & Hannan, 2000; Bexiga & Simpson, 2013).

The secretory journey starts in the ER, where newly synthesized proteins are packaged into coat protein COPII-coated vesicles (coat protein complex) to be exported from the ERES, cross the ERGIC and are finally delivered to the Golgi complex. At the *trans* - Golgi network (TGN) these proteins are packed into clathrin-coated vesicles to be addressed to their final destination (Farhan & Rabouille, 2011; Ivanov, 2014). From this point, exocytose associated vesicles can follow two different routes: they can be directed either to the cell periphery to fuse with the PM and deliver their contents to the external milieu or they can be sent to other organelles such as lysosomes, endosomes or mitochondria. This COPII-dependent transport it also called forward or anterograde. However, membrane traffic between the ER and the Golgi is bidirectional. To ensure fidelity and the proper directionality, the retrograde transport (from Golgi to ER) is mediated by COPI-covered vesicles (Fig 8) (Brandizzi & Barlowe, 2013).

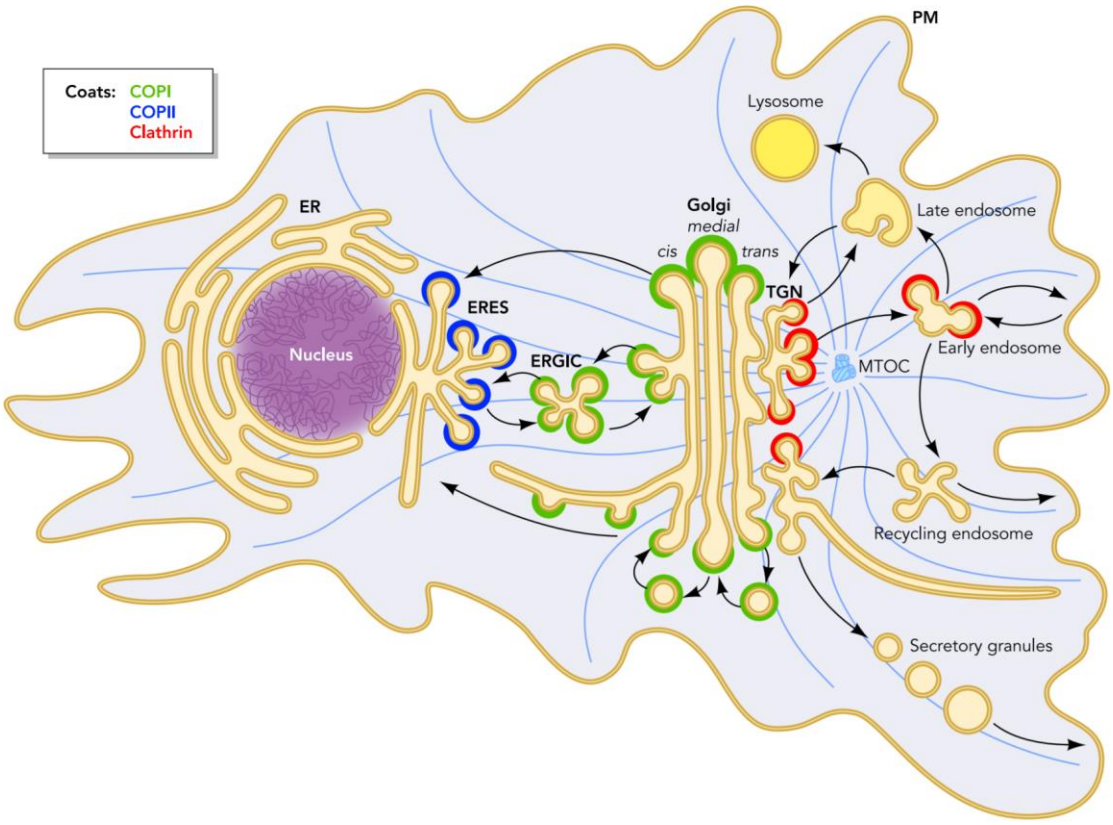

Figure 8. Secretory and endocytic pathways. Synthetized cargos in the ER exit the ERES to be addressed to the ERGIC in COPII coated vesicles to traverse the Golgi (anterograde transport). At the TGN, the vesicles are coated by clathrin and the cargos are delivered to the PM, early endosomes, late endosomes or secretory granules. COPI coated vesicles collect proteins from Golgi and ERGIC to returns them to the ER (retrograde transport) (Szul & Sztul, 2011)

Two types of exocytosis occur in cells, constitutive and regulated exocytosis. Constitutive exocytosis is associated with the "default" secretory pathway where a continuous trafficking of vesicles is present in almost every cell type and fuse with the membrane without any previous signaling in a spontaneous way. Regulated exocytosis is present in secretory specialized cells (neurons, glandular cells, intestine epithelial cells, etc.) where the cargo is stored in secretory granules (SG) to be delivered to the PM only in response triggered by a binding of a ligand with its receptor or a specific signal, like an increase of cytoplasmic calcium (Klein et al., 2018; Sebastian et al., 2006).

Through the exocytosis pathway, three major regulatory protein families are required in distinct steps. First, ARF and Sar1 family GTPases are necessary for vesicle formation, then Rab family

GTPases are needed for vesicle targeting and finally, SNARE family proteins will participate in vesicle fusion (Béraud-Dufour & Balch, 2002).

The endocytic pathway

Endocytosis is the mechanism by which eukaryotic cells internalize constituents coming from the extracellular environment through the cell surface into the internal membrane compartments, allowing cells to communicate with the outside milieu. It involves vesicles formation by PM invagination and fission, leading to a consequent internalization and fusion with intracellular endosomes. Endocytosed cargoes include a large range of incoming material like nutrients, macromolecules, receptor–ligand complexes, fluid, particles, solutes, extracellular–matrix components, lipids, cell-debris, pathogens and PM components.

Endocytosis and endosomal pathway are essential for nutrient uptake, recycling, growth, storing, endomembrane dynamics, degrading incoming substances and receptors, defense, signaling, etc. The fine-tuning regulation of several signaling pathways is notably under the control of endosomal membrane dynamics and sorting. Thus, endocytosis and consequently endosomal processes are linked to almost all key aspects of cell life and disease. (Huotari & Helenius, 2011; Ivanov, 2014; Le Roy & Wrana, 2005; Mayor & Pagano, 2007). Diverse cell entry pathways have been identified. They depend on the transported cargo and on the membrane machinery. Endocytic vesicles can be assembled via different mechanisms including phagocytosis, macropinocytosis, clathrin-dependent or clathrin-independent endocytosis.

Phagocytosis and macropinocytosis belong to a specific class of endocytic processes that internalize large particles (>1μm). These processes rely on massive actin-mediated reorganization of the PM and are preferentially associated with specialized cells such as macrophages (Fig 9) (Mayor & Pagano, 2007).

The clathrin-dependent endocytosis pathway depends on the PM recruitment of soluble cytoplasmic clathrin and specific APs (adaptor proteins). The assembly of several clathrin monomers at the PM cytoplasmic surface allows the membrane invagination and the formation of

coated pits, where the membrane will be constricted by dynamin to give rise to clathrin-coated vesicles. These clathrin-coated vesicles will be uncoated after endocytosis (Fig 9) (Mousavi et al., 2004) to allow proper fusion with endosomal stations.

Other endocytic routes can operate in a clathrin-independent manner, such as the caveolin-mediated pathway. The caveolin oligomerization at the PM leads to formation of caveolin-rich microdomains and the expansion of the caveolar invagination to form specialized endosomal structures called caveosomes (Couet et al., 2001). Moreover, in the last decades several non clathrin- and non-caveolin-dependent pathways have been discovered, but the mechanistic underlying all these endocytosis processes is not completely understood yet (Fig 9) (Le Roy & Wrana, 2005).

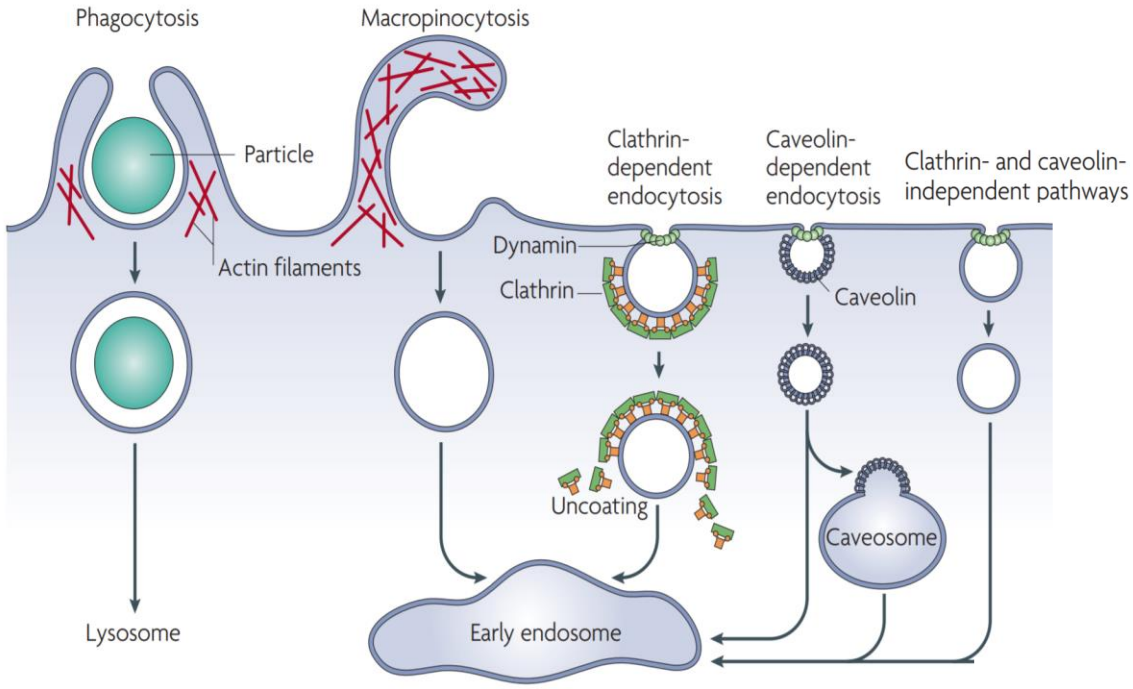

Figure 9. Viral entry pathways. Several possibilities exist to enter into cells. Phagocytosis and macropinocytosis are mediated by actin while other pathways are mediated by clathrin, caveolin or others mechanism (adapted from Mayor & Pagano, 2007)

Following endocytosis, the primary endocytic vesicles transfer their content and membranes to the early endosomes (EE). The EE possesses exclusive protein constituents such Rab5 (a master regulator of early endosome identity and functions regulation) or EEA1 (early endosome antigen

1, which binds to Rab5) and other (FYVE)-domain proteins that bind to PI3P (phosphatidylinositol-3-phosphate, a key lipid in EE membrane dynamics) which participate in EE dynamics and cargoes sorting. At this point, two routes can be followed: either the recycling circuit from where EE can be recycled back to the PM in Rab11-positive recycling endosomes (RE) or the degradative cycle where EE will be dispatched for degradation in lysosomes via a Rab7 dependent process (Zulkefli et al., 2019). For the degradation route, EE have to maturate into multivesicular endosomes/bodies (MVE/MVBs) by growing in size and acquiring intralumenal vesicles. This maturation allows the conversion of EE into late endosomes (LE). LAMP1 (lysosomal-associated membrane protein 1) and Rab7 are known markers of LE. The fusion between LE and lysosomes generates a transient hybrid organelle called the endolysosome, in which content degradation allow its maturation to a classical dense lysosome. The main partners in the process are the Golgi apparatus and the cytosol content, which provides functional proteins to all membrane compartments (Fig 10) (Huotari & Helenius, 2011; Scott et al., 2014).

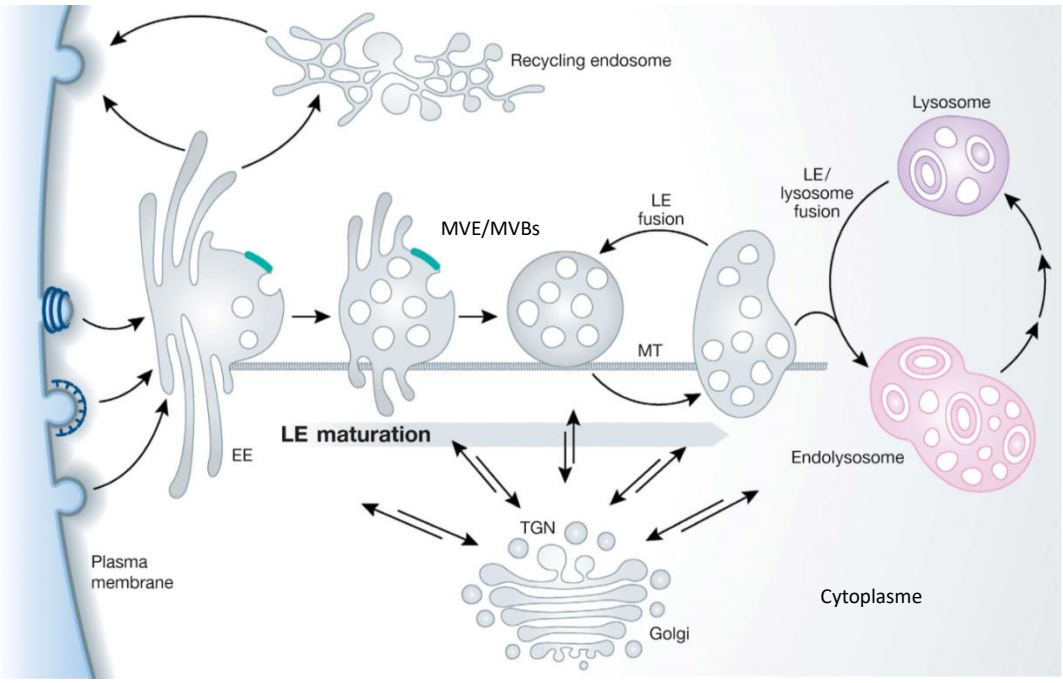

Figure 10. The endosome/lysosome system. EE can follow two distinct routes: the recycling or the degradation pathway. In the degradation pathway, EE maturates through LE to fuse with lysosome and degrade its content (adapted from Huotari & Helenius, 2011).

Most of the abovementioned pathways are bidirectional. Moreover, the main actors implicated in both pathways are able to interact together, allowing crosstalk between the endosomal and the exocytosis secretory pathways (Gagescu et al., 2000; Hariri et al., 2016; Rios & Bornens, 2003; Scott et al., 2014). To facilitate the interactions between these cellular compartments, the cytoskeletal elements (microtubules (MT) and actin filaments) and the activity of motor proteins (kinesins, dyneins, and myosins) are frequently required (Barlan et al., 2013). Finally, in parallel with classical vesicular interaction, endomembrane compartments can also communicate through membrane contact sites (MCSs), a close apposition between two or more organelles allowing the exchange of molecules, metabolites, lipids and signaling (Cohen et al., 2018).

B.2 INFLUENZA VIRAL CYCLE

Viruses are intracellular pathogens that need to enter, replicate and exit host cells to infect the adjoining cells and complete the viral cycle to survive. IAV have co-evolved over millions of years with their hosts, developing the ability to modulate or hijack cellular functions and signaling pathways, subverting the host cell machineries for its own benefit. Influenza infection cycle is composed of several stages: attachment, endocytosis and decapsulation, nuclear import, transcription and replication, mRNA nuclear export, translation, vRNP formation and nuclear export, viral assembly and budding (Samji, 2009).

Virus attachment

Influenza infection begins when the virus access the host airways. Influenza virus attach specifically to the surface of the respiratory epithelial cells in the upper respiratory tract and lungs. NA break off the protecting secretory mucins, aiding viral entry into epithelial cells (Yang et al., 2016). Host specificity and viral tropism are mostly determined by the HA receptor binding specificity to N-acetylneuraminic (sialic) acid exposed in cell surface. These surface receptors are present in various animal species like avian, primates or humans and are ubiquitous on different cell types (epithelial cells, macrophages, etc.) (Matrosovich et al., 2004). Therefore, humans can be infected by influenza viruses coming from other species, but generally avian HA favor the

binding to 2,3-linked sialic acid and human HA prefers to bind to 2,6-linked sialic acid (Leung et al., 2012).

Once the virus is bound to the sialic acid receptors, HA allows viral fusion with the host membrane. HA is a trimer composed of distinct regions: a stem region (formed by a triple-stranded coiled-coil of alpha-helices), and a globular head of antiparallel beta-sheet containing the sialic acid receptor binding site (positioned on the top of the stem) (Wilson et al., 1981). The post-translational modification of HA by host enzymes is thus critical at this stage to its activation. These enzymes are serine proteases which cleave the HA protein into HA1 and HA2 subunits (Fig. Structure of HA). HA1 contains the receptor binding and antigenic sites indispensables for HA binding to sialic acids and HA2 play a role later in the virus cycle permitting the fusion of virus envelope with host cell membranes (described in the next paragraph) (Skehel & Wiley, 2000). Moreover, NA protein has been described to play a role in viral entry by enhancing HA-mediated membrane fusion and infectivity (B. Su et al., 2009).

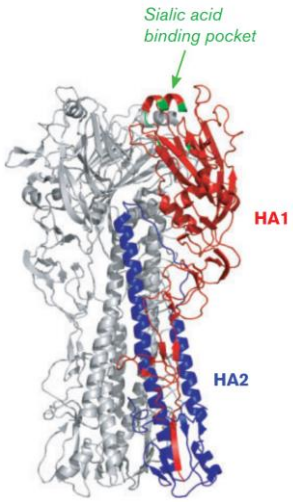

Figure 11. HA structure. HA is composed of two subunits: HA1 and HA2. The sialic acid binding pocket is localized in the HA1 subunit, being essential for viral attachment to sialic acid receptors at the cell surface (adapted from Edinger, Pohl, & Stertz, 2014).

Endocytosis, decapsulation and vRNP release into host cell cytoplasm

Following attachment, influenza viral particles are internalized into host cells. Several studies have suggested that multiple endocytic routes may allow different influenza entry pathways, including macropinocytosis, classical clathrin-mediated route or even clathrin independent pathways (Fig 12.1) (Lakadamyali et al., 2004; Sieczkarski & Whittaker, 2002; Y. Zhang & Whittaker, 2014). At this stage, M2 viral protein plays an essential role in viral decapsulation, aiming to release viral RNPs into the host cell cytoplasm.

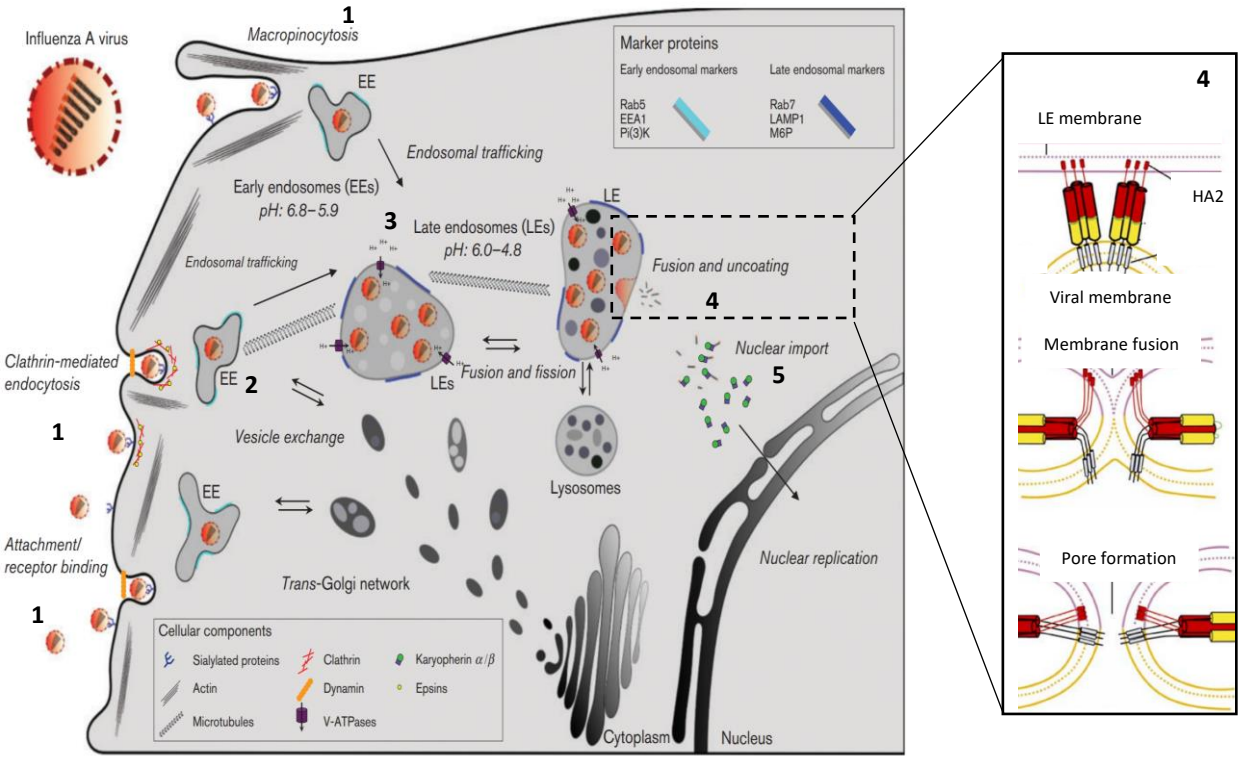

Figure 12. Schematic representation of the IAV entry. IAV can entry into the cell following different pathways: macropinocytosis, clathrin dependent or independent endocytosis (1). Influenza virus traffic through EE (2) that maturate into LE (3) where the pH drop activates viral proteins. The viral membrane fuse with the endosomal membrane to deliver its content to the cytoplasm before complete lysosomal degradation (4). Finally, vRNP are imported to the nucleus (5) (Cross et al., 2010; Edinger et al., 2014) (adapted figure)

After internalization, primary endocytic vesicles transfer viral particles to the EE (Fig 12.2), which in turn maturate into LEs (as described in section B1). At LE (Fig 12.3), the acidic environment created by cellular V-ATPases activates two viral proteins: 1) the activation of M2 transmembrane

protein (that forms pH-gated proton channels) causes an internal viral acidification leading to viral matrix dissociation. Viral protein interactions disruption allows vRNPs release from the viral matrix (Dudev et al., 2016; Helenius, 1992; Pinto et al., 1992; Pinto & Lamb, 2006; Schnell & Chou, 2008). 2) the pH drop at LE triggers a conformational change of the cleaved HA protein: HA1 subunit opens up and allow HA2 to expose a hydrophobic fusion peptide that will be inserted in the endosomal membrane where the C-terminal portion of HA2 subunit draw both membranes together. A membrane lipid mixing begins, leading lately to a complete fusion of the two membranes and a pore formation allowing vRNP release (Fig 12.4) (Cross et al., 2010; Stegmann, 2000).

Once released into the cytoplasm, vRNA is still associated with viral proteins in vRNP complexes, which cannot diffuse passively through the nuclear membrane. To reach the nucleus, vRNPs exposes import signals called nuclear localization signals, which allow vRNPs and other viral proteins to be imported into the nucleus (Fig 12.5) (Cros & Palese, 2003; Martin & Helenius, 1992).

Viral transcription, replication and translation

When vRNP reaches the nucleus, the vRNA is transcribed and replicated by the viral RNA-dependent RNA polymerase (RdRp), composed of the subunits PA, PB1, and PB2 (Stubbs & Te Velthuis, 2014). At this stage NP protein has also been shown to participate in viral RNA synthesis, being essential for RNA chains elongation (Honda et al., 1988). Viral influenza negative-sense RNA serves as a template to synthesize two different positive-sense RNA. First, the capped polyadenylated mRNA, necessary for viral proteins translation in the cytoplasm. Second, the complementary RNA (cRNA), which in turn serve as a template to the RNA polymerase to form new viral negative-sense copies (viral genome replication) (Fig 13.A) (Te Velthuis & Fodor, 2016).

Viral mRNAs possess a 5’ methylated cap and a poly(A) tail. The 5' extremity of the negative-sense vRNA is constituted of a stretch of 5 to 7 uridines representing the polyadenylation site for viral mRNA synthesis, which is transcribed by the viral polymerase into the positive sense forming the poly(A) tail (Li & Palese, 1994).

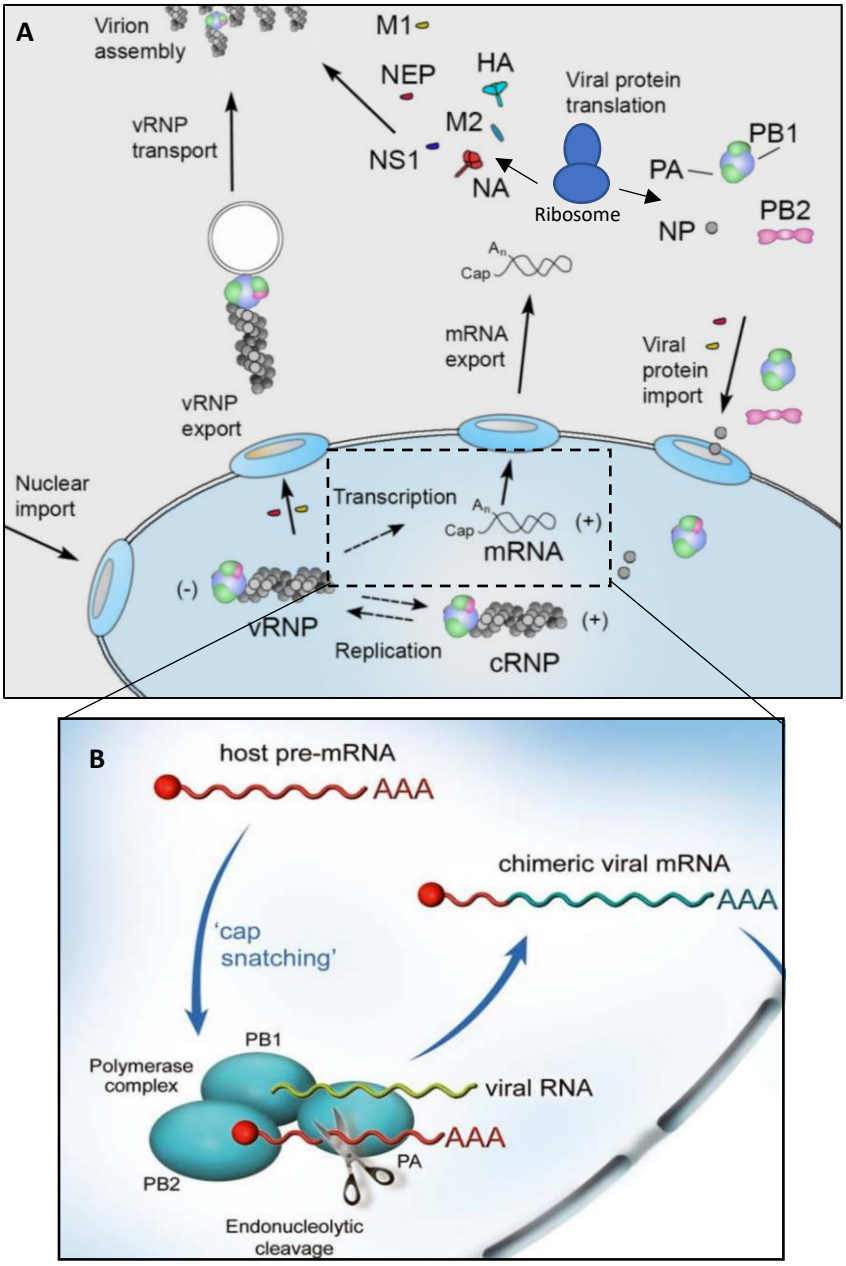

Figure 13. Influenza replication, transcription and translation. A. Negative-sense vRNA serves as a template to synthetize two positive-sense RNA (cRNA and mRNA) to complete viral replication and transcription. Then, viral translation occurs in cytosolic ribosomes. B. Cap-snatching: viral polymerase (PB1, PB2 and PA) synthesizes vRNAm using short capped primers derived from host pre-mRNA (adapted from Boivin et al., 2010; Te Velthuis & Fodor, 2016)

However, the sequence to transcribe the 5' methylated cap is not present in the viral genome (Plotch et al., 1978). Viral mRNA capping occurs by a process called "cap snatching", where the viral RdRp use short capped primers from existing cellular capped mRNA (Fig 13.B). Indeed, viral PB2 subunit recognizes and binds the 5'methylated cap of a host pre-mRNA, which is cleaved after 10

–15 nucleotides by the PA endonuclease activity. Then, PB1 use this short-capped RNA primer to initiate RNA polymerization using the negative-sense vRNA as template. The final result is a chimeric mRNA (capped and polyadenylated) (Boivin et al., 2010; Dias et al., 2009; Kerry et al., 2008).The polyadenylated and capped viral mRNA is then exported to the cytoplasm and translated just like a host mRNA in ribosomes (Fig 13.A) (De Vlugt et al., 2018). Moreover, NS1 viral protein has been described to stimulate viral translation by increasing recruitment of ribosomes on mRNAs (Panthu et al., 2017).

Viral assembly and budding

Once the viral mRNAs are translated into viral proteins and vRNA replication has finished, all the elements need to be assembled to form new virions (Jeremy S. Rossman & Lamb, 2011). This assembly process takes part in a complex and multistep process at the apical PM. Concretely, viral proteins associates to lipid rafts, specialized membrane microdomains highly enriched in sphingomyelin and cholesterol (Takeda et al., 2003).

Before being addressed to the PM for assembly, viral proteins are transported through different cellular trafficking pathways. The envelope proteins HA, NA, and M2, are folded in the ER and transported through the Golgi apparatus for specific post-translational modifications. On the other hand, once synthetized in the cytoplasm, NP, PB1, PB2 and PA proteins enter into the nucleus to assemble into vRNPs complexes (Fig 13.A). Moreover, M1 interact with other viral components like NP and vRNA and is directly addressed after its translation in ribosomes to the PM without trafficking through the ER and Golgi (Bouvier & Palese, 2008). All these proteins are then addressed to the same lipid raft domain on the cell membrane, where it has been hypothesized that they interact together to coordinate the assembly of new virus particles (Barman & Nayak, 2000; Wohlgemuth et al., 2018).

Viral RNPs are exported to the cytoplasm from the nucleus in a CRM1-dependent manner (associated with NS2 and M1) either individually or forming complexes with several vRNPs (Lakdawala et al., 2016). CRM1 (chromosomal maintenance 1) is a nuclear export receptor that binds to nuclear export signals (NESs) in numerous different cargoes (Fung et al., 2017). After

nuclear export, vRNP segments conquer the cellular endosomal recycling machinery being transported in Rab11 positive organelles guided by actin and microtubules. Then, recycling endosomes fusion allows the formation of a complex containing all eight vRNP segments. Rab11 vesicles are involved in apical trafficking of recycling endosomes (as described in B1 section) and guide the complete vRNP towards the PM assembly sites (Fig 14) (Chou et al., 2013; Lakdawala et al., 2014). For the effective formation of infectious virions, all eight RNPs must be present together once the genome packaging process is finished (Fujii et al., 2003). NP, PA, PB2, M1, NS2 and M2 proteins have been shown to be necessary during this genome-packaging process (Gao et al., 2012; D. Paterson & Fodor, 2012).

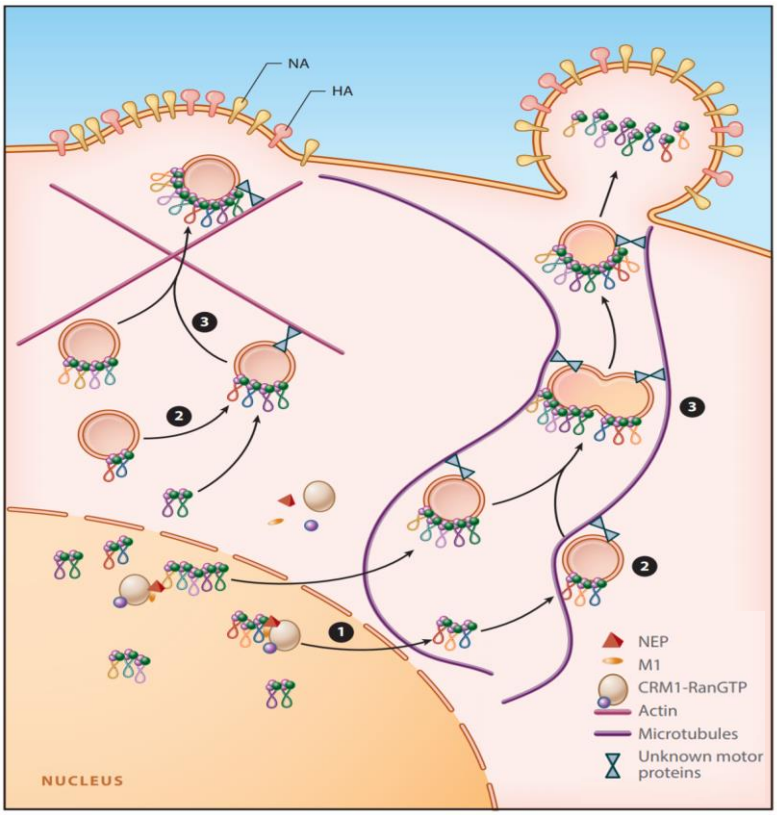

Figure 14. Influenza viral RNA nuclear export and cytoplasmic transport to the PM. 1: vRNPs are exported from the nucleus in a CRM1-dependent manner (individually or as complexes) helped by NEP and M1 proteins. 2: vRNPs are transported by Rab11 endosomes through the cytoplasm, 3: RE fusion lead to the formation of endosomes containing all 8 vRNPs (Lakdawala et al., 2016).

After the assembly process is complete, all viral proteins and the eight vRNPs are packed at the same lipid raft domain in the infected cell host membrane, where HA and NA clustering initiate a membrane deformation to start viral budding (Fig 15.A). This process allow viral formation and virion release from the infected cell (Jeremy S. Rossman & Lamb, 2011).

M1 protein plays a crucial role in the latest step of viral elements assembly, virion formation and budding. The C-terminus flexibility of M1 may be responsible for its multi-functionality, particularly to structurally organize the viral membrane to maintain shape and integrity of influenza virus (Shtykova et al., 2013). First, M1 is recruited to and accumulates at the cytoplasmic side of the lipid bilayer to bind the cytoplasmic tails of HA and NA, where it can oligomerize to begin the formation of the matrix structure of the emerging virion (Hilsch et al., 2014). Second, by interacting with viral genetic material and envelope proteins, M1 creates a docking site where vRNPs can be anchored and enclosed in the newly formed matrix. Finally, since emerging virions start to elongate by M1 polymerization (Fig 15.B), M2 is recruited in the periphery of the budding site though interaction with M1 (Nayak et al., 2004).

At this point, M2 stabilizes the budding site and alters membrane curvature at the neck of the emerging budding virion to cause membrane scission (Fig 15.C). M2 possess an amphipathic helix located in the cytoplasmic tail which may be able to binds cholesterol: the specific insertion of this amphipathic helix in the host membrane is essential for membrane scission, filament formation, stabilization of existing viral filaments and the release of the virion progeny. Because influenza is an enveloped virus, host cell PM is finally used to form new viral particles (J. S. Rossman et al., 2010). Recent results suggest that a filamentous morphology facilitates viral spread in vivo (Badham & Rossman, 2016).

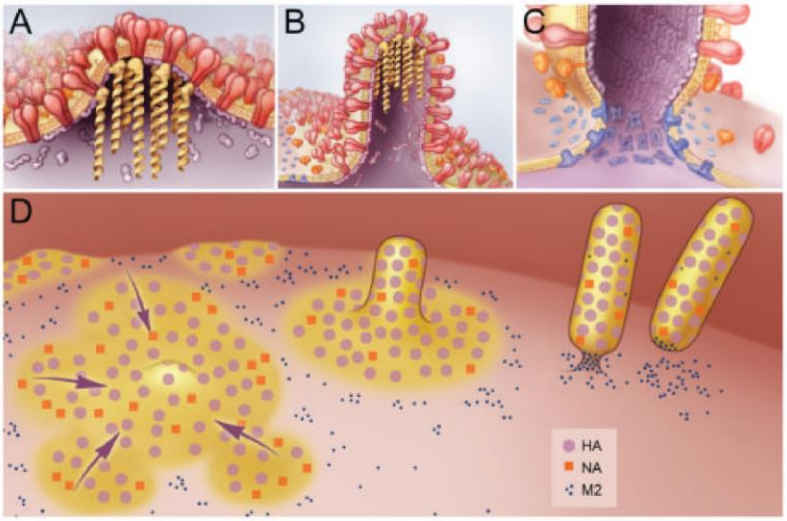

Figure 15. Model of Influenza Virus Budding. A: The initiation of virus budding caused by clustering of HA (red) and NA (orange) in lipid raft domains. M1 (purple) serves as a docking site for the vRNPs (yellow). B: Elongation of the budding virion caused by polymerization of the M1 protein. C: Membrane scission caused by M2. D: Overview of the budding of influenza viruses and lipid rafts in yellow (Jeremy S. Rossman & Lamb, 2011)

Assembly and budding need a high coordination and precise spatiotemporal regulation of its main actors: M1, M2, HA and NA (Fig 15) (Chlanda et al., 2015). Besides, others viral proteins has been described to take part in this process: NP has a role in the assembly and formation of infectious virions in a partnership with M1 (Noton et al., 2009); NS2 has been shown to recruit cellular ATPase to the cell membrane to assist the release of emerging virions (D. Paterson & Fodor, 2012).

When viral budding process is complete and when the virion is released, the HA spikes of the new virus can recognize the sialic acid present on the very same cell surface. Thus, the new sorting virus will bind to the infected cell, impeding naïve cell infection. However, the virus can get away this problem thanks to the sialidase activity of the NA viral envelope protein. Indeed, NA cleaves the terminal sialic acid residue from host cell surface glycoproteins to free new influenza virus from the host cell to go infect neighboring cells (Colman et al., 1983).

B.3 ENDOMEMBRANE MODIFICATIONS UPON INFLUENZA VIRAL INFECTION

Pathogen entry induces a stress response resulting in several consequences on endomembranes and in cell homeostasis. To turn the cellular machinery on its own benefit, influenza virus must interact with several host components, trafficking through all cellular endomembranes at different stages: endosomes, nucleus, mitochondria, endoplasmic reticulum and Golgi apparatus (as described in section B2) (Fig 16). This intracellular journey possibly mobilizes all these internal compartments and can thus modify the connections and/or crosstalk established in between them.

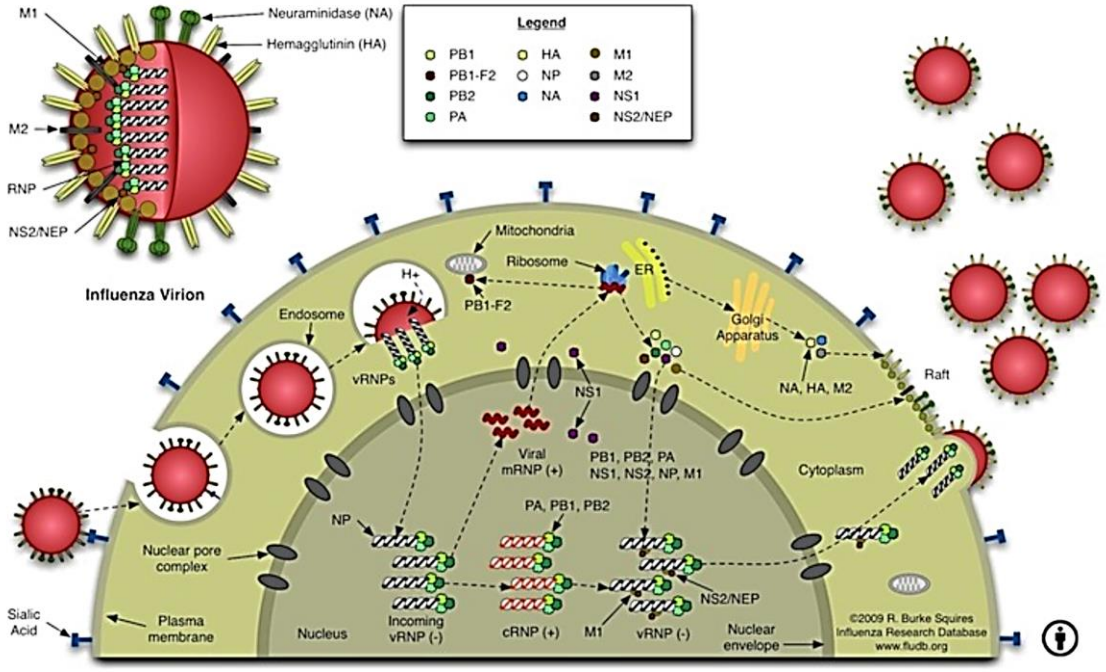

Figure 16. Influenza viral proteins trafficking. Influenza viral proteins traffic through several cellular compartments at different stages of the viral cycle: early endosomes, late endosomes, nucleus, mitochondria, endoplasmic reticulum, Golgi apparatus, cytoplasm, recycling endosomes, etc. (Wozniak, 2014).

Nucleus

The nucleus harbors viral RNA replication and transcription. Indeed, vRNP complexes enter the nucleus to this purpose, meaning that viral RNA, proteins and mRNA interact with the cellular host machinery in the nucleus (Mor et al., 2016). In 1969, electron microscopy analyses shown that in influenza infection conditions, the nucleolus was altered. Nucleolus contained dense spots at very

early stages of infection and become distended enclosing several discrete dense masses a few hours later (Compans & Dimmock, 1969). Since then, no other studies have been performed to enlighten nuclear morphology and morphodynamics upon infection.

Golgi apparatus

Golgi apparatus is the key organelle for processing influenza glycoproteins HA and NA, M2 as well as for viral particles exocytosis. Upon infection, influenza machinery tunes vesicular trafficking by disrupting the ER-Golgi intermediate compartment, then causing a progressive dispersion of the Golgi into smaller and numerous structures, resulting in the total disassembly of the Golgi ribbon structure and fragmentation (Yadav et al., 2016).

Mitochondria

Mitochondria play an important role in energy production, but they are also involved in defense-related functions like apoptosis or innate immunity (described in C5 section). For these reasons, this organelle represents a recurrent target for viruses, whose goal is to inhibit innate immune response and manipulate the infected host cell for its own benefit (Castanier & Arnoult, 2011).

Influenza virus has been described to target mitochondria. Indeed, in some influenza strains PB2 is translocated to the mitochondria where it can regulate the cellular immune response by interacting with the mitochondrial antiviral signaling protein (MAVS, described in section C5) in order to inhibit type I interferon (IFN) production (Long & Fodor, 2016). In parallel, in PB1-F2 positive influenza viral strains, PB1-F2 translocate into the mitochondrial inner membrane via Tom40 (translocase of the outer membrane 40) channels (addressed by a C-terminal polypeptide signal) leading to a reduction of mitochondrial membrane potential (MMP), resulting in a mitochondrial fragmentation. Mitochondrial-mediated innate immunity signaling is regulated in the mitochondrial membrane and depends on the MMP, consequently PB1-F2-mediated decrease of MMP impairs cellular innate immunity. The PB1-F2 C-terminal portion can also binds to MAVS protein, suppressing RIG-I (retinoic acid-inducible gene I) signaling pathway and thus inhibiting the induction of type I IFN (described in section C5) (Varga et al., 2012; Yoshizumi et al., 2014).

Furthermore, the loss of MMP induced by PB1-F2 appears to enhance virus-associated cell death in a cell type-dependent manner (Gibbs et al., 2003). Surprisingly, PB1-F2 low pathogenic viral variants (with absent C-terminal polypeptide) do not disturb mitochondrial functions (Yoshizumi et al., 2014). Altogether and importantly, these results suggest that PB2, PB1-F2 and host mitochondria associated proteins are potentials candidates for antiviral targeting.

Autophagy and autophagosomal associated membranes

Macroautophagy (or simply autophagy) is a lysosomal based catabolic process which directly participates in cellular homeostasis regulation by playing a housekeeping role in several biological functions including removing non-functional proteins and organelles. Thus, autophagy is involved in a wide range of cellular processes such as cellular differentiation, aging, nutritional starvation or defense against pathogens (Molino et al., 2017; Morel et al., 2017).

Autophagic program is associated with the formation of a double membrane bound organelle called autophagosome, aimed at transporting intracellular material to lysosome for degradation. Autophagosome assembly requires first the formation of an isolation structure termed phagophore (or isolation membrane) which originates from several membrane sources coordinated by specialized regions of ER membranes positive for PI3P and known as omegasomes (Molino et al., 2017). The phagophore thus expands and closes up to form the autophagosome, which will fuse with lysosome to deliver the trapped cargoes, forming an autolysosome. In the autolysosome, the autophagic content is degraded by lysosomal proteases and lipases, allowing the proper recycling of amino acids and other degradation products to the cytoplasm where they can be reused for biochemical reactions. The main marker to track autophagy related structures is the microtubule-associated protein light chain 3-II protein (LC3-II), present at the surface of phagophore, autophagosome and autolysosome, by a specific lipidation process which required several ATG proteins (autophagy related genes proteins) (Fig 17) (Reggiori & Ungermann, 2017).

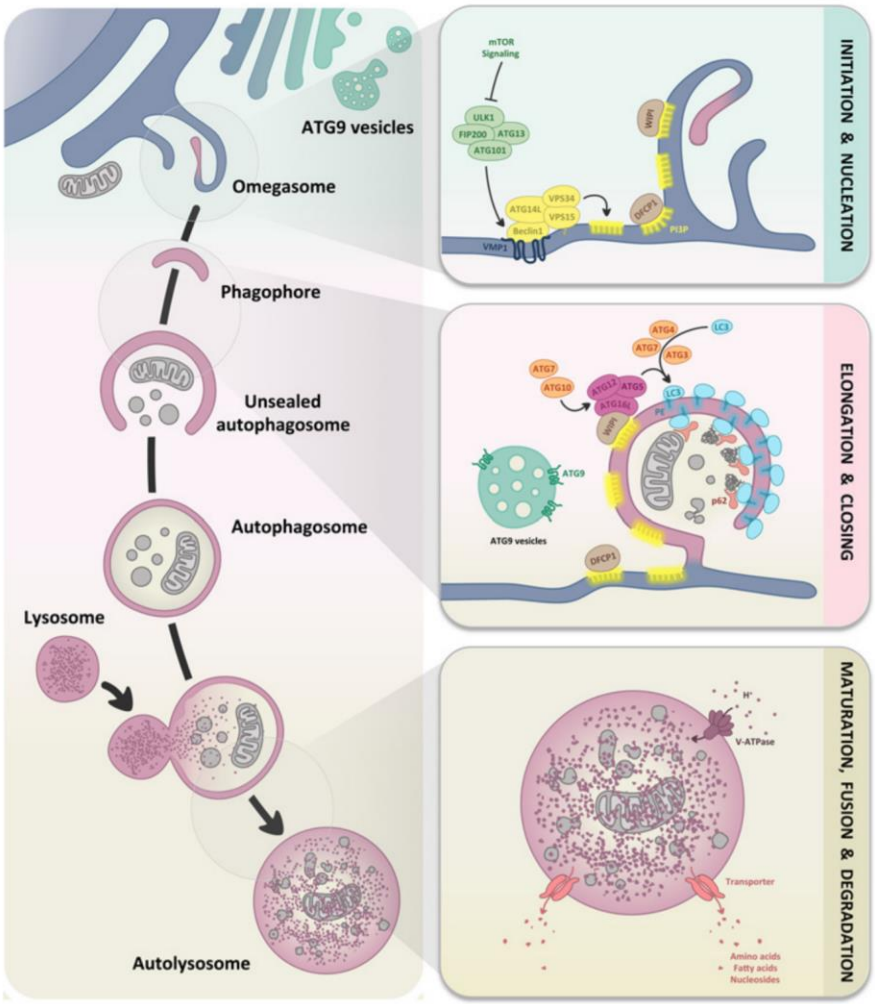

Figure 17. Autophagy pathway. The omegasome initiation and formation lead to the phagophore. The phagophore expansion traps the cargo, then it closes up and forms the autophagosome. From its fusion with the lysosome originates the autolysosome, where its content is degraded (Fenouille et al., 2017).

Autophagic pathway can be induced by influenza infection, and is considered to be necessary to obtain an optimal viral replication and accumulation of viral proteins (R. Zhang et al., 2014). In infected cells, an increase of LC3-II amount and accelerated autophagic flux (a measure of autophagic degradation activity) has been observed. This situation has been corroborated by decreased influenza titers when autophagy is pharmacologically inhibited (Zhou et al., 2009). Furthermore, besides its downregulating effect on apoptosis, NS1 viral protein seems to be involved in the upregulation of autophagic response, which artificially helps the host cell to stay alive longer while the virus is replicating (Zhirnov & Klenk, 2013).

On the contrary, influenza virus can also arrest the autophagic pathway, manifested in host cells by an autophagosome accumulation. Antiviral amantadine (an M2 inhibitor) inhibits autophagosome accumulation, which suggests that M2 may be implicated in blocking autophagosome fusion with lysosomes. Autophagy inhibition by this viral protein affects cell survival but does not alter viral replication (Gannagé et al., 2009). Moreover, the LC3-interacting region (LIR) present on the cytoplasmic tail of M2 binds directly with LC3, favoring the LC3 relocalization to the PM, which is needed for filamentous budding and results in more stable viral particles (Fig 18) (Beale et al., 2014; Münz, 2014).

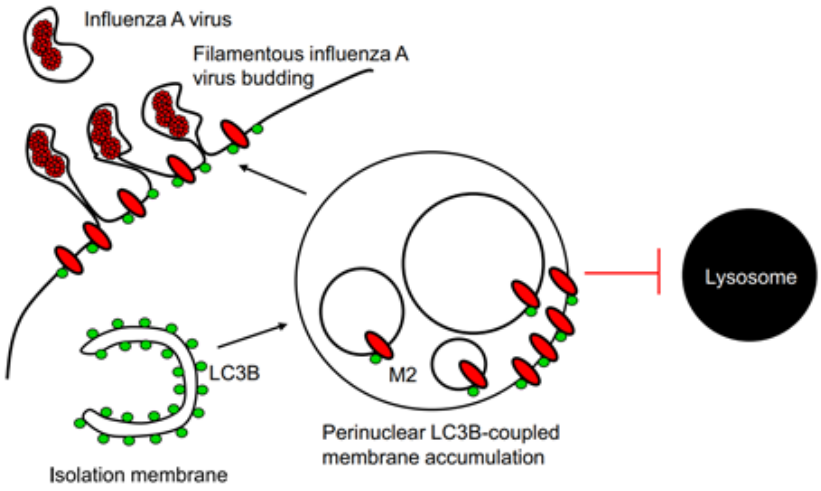

Figure 18. Influenza and autophagy. Influenza M2-LC3 interaction redirect LC3 to the PM where it participates in viral budding (Münz, 2014).

The above-mentioned examples of virus-induced endomembrane alteration give an overview of interactions between viral and host proteins and/or organelles. Surprisingly, a global quality investigation of all the intracellular membranes reorganization over the course of an infection induced by IAV has never been performed. For example, morphodynamics of the endosomal machinery or the ER have never been described to be modified upon influenza infection. Thus, a specific study of the influenza viral infection consequences on endomembranes dynamics, morphology, trafficking and signalling would help to get a better understanding of viral infectious stress associated cellular response and will facilitate identification of useful pharmaceutical targets to repeal virus replication.

PART C: MITOCHONDRIA AND CELLULAR STRESS

Mitochondria are indispensable double-membrane organelles present in the cytoplasm of most eukaryotic cells. The endosymbiotic theory postulates that two billion years ago, gram-negative aerobic bacteria were engulfed by eukaryotic cells which were unable to use oxygen by itself. These bacteria become the ancestors of present mitochondrial organelles (Roger et al., 2017). Depending on cell type, mitochondria size, shape and number can vary according to the energetic needs of the cell. Moreover, mitochondria are highly dynamic organelles, having a huge plasticity and reactivity by constant redistribution and intracellular organization. This organelle is known for being central in cellular energy production (notably via ATP (adenosine triphosphate) synthesis and release), but mitochondria accomplish polyvalent functions in cells (Van Der Bliek et al., 2017).

Despite its bacterial origin, most mitochondrial proteins are encoded by the nucleus, translated on cytosolic ribosomes and imported into the mitochondria via a targeting sequence through mitochondrial translocases in an electrochemical potential dependent manner (Friedman & Nunnari, 2014).

C.1 MITOCHONDRIA STRUCTURE

Mitochondria possess a unique architecture comprising a double membrane system: a mitochondrial outer membrane (MOM) and a mitochondrial inner membrane (MIM). The outer membrane encloses the organelle and is the gateway for exchange with the environment, playing a central role in biogenesis and mitochondria morphology. The MOM is enriched with elements of the protein import machinery, permeable to small molecules by pore-forming proteins. However, bigger molecules need other transport pathways (Milane et al., 2015). The porin named voltage dependent anion-selective channel (VDAC) gates the passage of ions and molecules across the MOM, regulating the flow of these substances depending on the transmembrane voltage (Colombini, 2016). Moreover, translocase of the outer membrane (TOM complex) constitute the principal entry site for proteins that are produced on cytosolic ribosomes (Rapaport, 2002) (Fig 19).

Between the MOM and the MIM exists a little aqueous submitochondrial compartment called the intermembrane space (IMS). This compartment allows the coordination of mitochondrial activities with other cellular processes, directly participating on molecular transport, signaling pathways and communication between the cytosol and the mitochondrial matrix (Herrmann & Riemer, 2010)

The inner membrane surface is composed of two domains: the inner boundary membrane (IBM) adjacent to the outer membrane and the cristae membrane (CM) resulting from MIM deep invaginations of different shape and size projected into the mitochondrial matrix. These two domains are connected by structures called crista junctions (CJ) (Prasai, 2017) (Fig 19). The IBM is a tight diffusion barrier, permeable only to small uncharged molecules. This membrane is enriched in translocases of the inner membrane (TIM complex) to help transport regulation of proteins and molecules across these membranes (Fig 19). The high impermeability of the IBM helps to the maintenance of the MMP (Teodoro et al., 2018). The cristae membrane increases the surface area of the inner membrane providing large areas for OXPHOS (oxidative phosphorylation) respiratory complexes and ATP synthases allowing energy production in the form of ATP (Fig 19). In cristae, the mitochondrial contact site and cristae organizing system (MICOS) connects cristae with protein components of the MOM (Fig 19) participating in the organization of mitochondrial architecture and biogenesis (van der Laan et al., 2016).

Finally, the mitochondrial matrix is the second aqueous mitochondrial compartment and it is located in the innermost part of the mitochondria (Fig 19). The difference in electric potential between IBM (positive) and the matrix (negative) allow ATP synthesis via electron transport chain (ETC) and OXPHOS in cristae membranes (Porcelli et al., 2005). This mitochondrial compartment is enriched in enzymes involved in metabolism such as fatty acid oxidation or the citric acid cycle (Prasai, 2017). Moreover, the matrix contains mitochondrial ribosomes called mitoribosomes, which synthesizes some essential proteins for biogenesis and oxidative phosphorylation (De Silva et al., 2015). The mitochondrial matrix also harbors circular mitochondrial DNA (mtDNA), being the appropriate environment for mtDNA replication and gene expression.

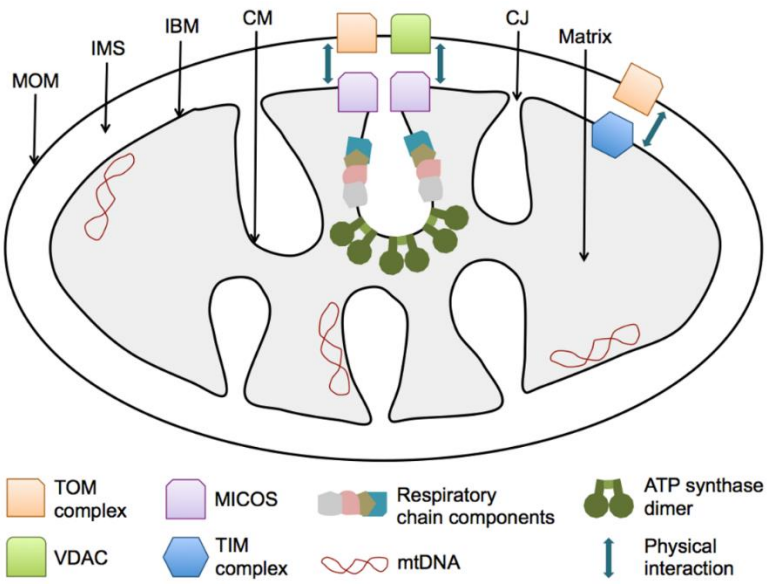

Figure 19. Mitochondria structure. CJ, crista junction; CM, cristae membrane; IBM, inner boundary membrane; IMS, intermembrane space; MICOS, mitochondrial contact site and cristae organizing system; MOM, mitochondrial outer membrane; mtDNA, mitochondrial DNA; TIM, translocase of the inner membrane; TOM, translocase of the outer membrane; VDAC, voltage-dependent anion channel (Prasai, 2017)

C.2 MITOCHONDRIAL MAIN FUNCTIONS

Mitochondria are highly interconnected organelles implicated in various metabolic pathways and signaling networks, playing a central role in several cellular functions such as bioenergetic regulation, iron homeostasis, cell death, lipid metabolism, Ca^{2+} homeostasis, thermogenesis, immunity (described in C5 section) and cellular stress response (Nunnari & Suomalainen, 2012). Importantly, mitochondria homeostasis impairment can lead to numerous diseases such as cancer (Armstrong, 2006), Alzheimer (Swerdlow, 2018), Parkinson (Barodia et al., 2019), diabetes (Sivitz & Yorek, 2010), etc.

Bioenergetic regulation and metabolism

Mitochondria are known to be the powerhouse of the cell due to their faculty of cellular energy production. The number of mitochondria per cell as well as their size and shape(s) are regulated to match the cellular bio-energetic demand (Liesa & Shirihai, 2013). Mitochondrial OXPHOS produces ATP through the cooperation of the ETC complexes and the ATP synthase situated in the mitochondria cristae.

The components of the mitochondrial respiratory complex consist of two electron carriers (coenzyme Q and cytochrome C) and five multi-protein enzyme complexes (complexes I-V): complex I (NADH-ubiquinone oxidoreductase), complex II (succinate-ubiquinone oxidoreductase), complex III (ubiquinone-cytochrome c oxidoreductase), complex IV (cytochrome c oxidase) and complex V (ATP synthase) (Signes & Fernandez-Vizarra, 2018). This complex function together with the citric acid cycle (Krebs cycle) in the matrix, that provides nicotinamide adenine dinucleotide (NADH) and flavine adenine dinucleotide ($FADH_2$) to respiratory complexes from acetyl-CoA. Redox reactions occurring in ETC are spontaneous because they take place in an increasing redox potential direction. Indeed, the passage of electrons from NADH and $FADH_2$ (-0,32V) through the ETC to O_2 (+0.81V) liberate energy at each step. This energy is used by the proton pumps complexes I, III and IV to transport protons from the matrix to the IMS. This flux establishes a proton gradient that drives the generation of ATP from ADP (adenosine diphosphate) and inorganic phosphate due to the rotation of the ATP synthase that returns the protons to the matrix (proton motive force) (Fig 20) (Bravo-Sagua et al., 2017).

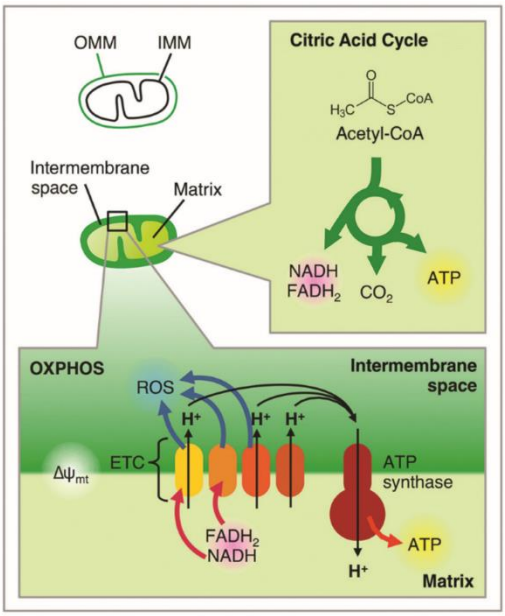

Figure 20. Mitochondrial bioenergetics. Mitochondrial OXPHOS is situated at the mitochondria cristae. The cooperation of the four ETC complexes and the ATP synthase provides ATP to the cell. The citric acid cycle occurs in the mitochondrial matrix. It provides NADH and $FADH_2$ to the respiratory chain (Bravo-Sagua et al., 2017).

In addition, mitochondria are implicated in other metabolic processes like nucleotide (L. Wang, 2016), glucose (Kwak et al., 2010), amino acids metabolisms (King, 2007) and also play a major role in detoxification and waste management (H2S, ammonia, and ROS) (Spinelli & Haigis, 2018). Indeed, reactive oxygen species (ROS) are generated in mitochondria as a consequence of OXPHOS reactions by partial reduction of oxygen following the electron transport in the respiratory chain (Fig 20). OXPHOS is thus the main source of ROS in cells and mitochondria are in charge to regulate its intracellular amount to avoid oxidative damage that could cause cell dysfunction and toxicity (Zorov et al., 2014). Several different mitochondrial systems to degrade ROS do exist, such as superoxide dismutase (Miriyala et al., 2011), glutathione peroxidase (Marí et al., 2009) or thioredoxin (Holzerova et al., 2015). Finally, mitochondrial ROS is also playing a role in the regulation of intracellular signaling for different pathways like immunity or autophagy (Dan Dunn et al., 2015).

Iron homeostasis

Mitochondria play a central role in iron metabolism. Iron is a transition metal that can accept and donate electrons, acting as an oxidant or reductant in many biochemical processes (Paul et al., 2017). In mammals, heme (required for oxygen transport) and iron-sulfur clusters (Fe-S) assembly occurs in mitochondria (Braymer & Lill, 2017; Medlock et al., 2015). Inside mitochondria, Fe-S clusters play a role in energy conversion mediating electron transfer in the ETC or being part of enzymes or cofactors. These clusters can be also exported to the cytosol, where they are involved in various functions such as genome maintenance, protein translation, ribosome biogenesis, metabolism or antiviral responses (Braymer & Lill, 2017). The mitochondrial NEET proteins play an essential role in iron homeostasis and will be largely described in section C3.

Cell death and apoptosis

Mitochondria regulate cell death through different systems, involving caspase dependent and caspase independent pathways. Numerous events can trigger cell death such as hypoxia, UV radiation, epigenetic changes, Ca^{2+} influx, p53 activation or DNA damage. The pro-apoptotic factors from the Bcl-2 family Bax (or Bcl-2-like protein 4) and Bak (Bcl-2 homologous

antagonist/killer) forms lipid pores in the MOM, leading to its permeabilization. Cytochrome c is one of the mitochondrial proteins released to the cytoplasm following this permeabilization, its binding to the caspase adaptor molecule Apaf-1 (apoptotic protease-activating factor 1) triggers a chain reaction implying several apoptosis factors such as caspases and regulatory factors. Indeed, this interaction allows conformational changes in Apaf-1 leading to its oligomerization which allow the binding to the initiator caspase procaspase-9 (forming the apoptosome). In turn procaspase-9 cleaves and activates the executioner caspases-3 and -7, leading to rapid cell death. Following MOM permeabilization, other released mitochondrial proteins can intervene in the caspase activation cascade. This the case of Smac (Second mitochondria-derived activator of caspase or Diablo) and Omi (or HtrA2, High temperature requirement protein A2) that binds to the caspase inhibitor XIAP (or IAP-3, inhibitor of apoptosis protein 3), resulting in its specific neutralization and caspase activation. Moreover, the loss of mitochondrial function can lead to a release of toxic mitochondrial proteins triggering a caspase independent cell death (Fig 21) (Bock & G Tait, 2019.; Tait & Green, 2013).

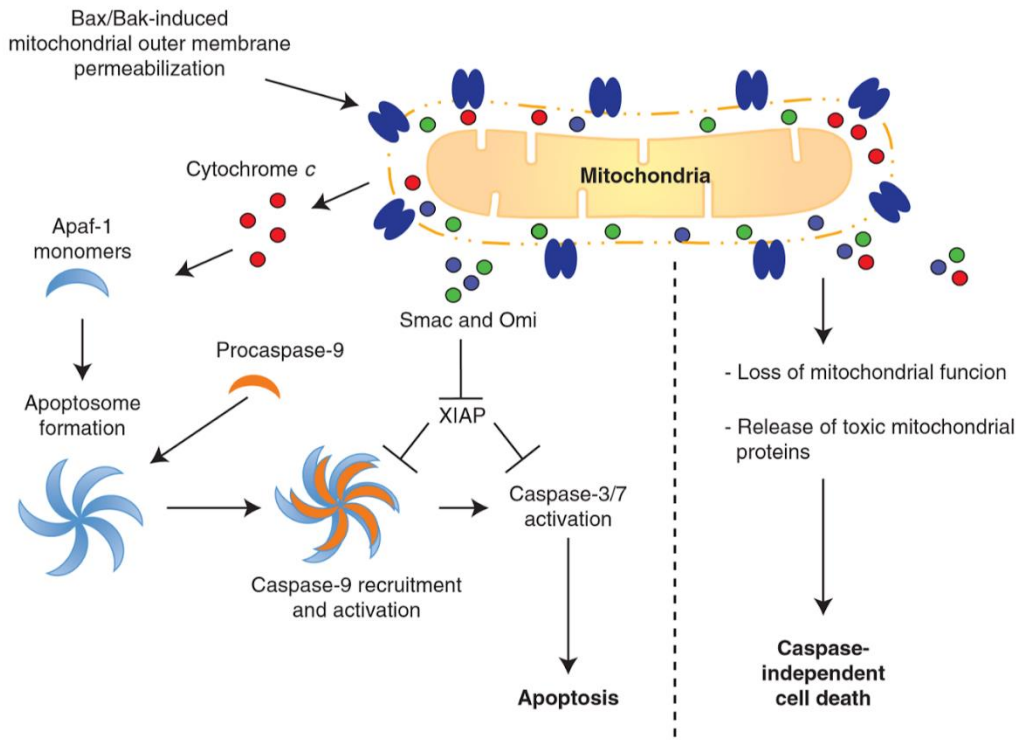

Figure 21. Mitochondria and cell death (Tait & Green, 2013). MOM permeabilization and mitochondrial dysfunction can lead to cell death in caspase dependent and caspase independent pathways.

Ca^{2+} homeostasis

Mitochondrial Ca^{2+} equilibrium plays a regulatory role both inside the mitochondria and at the whole cell level by modulating several processes such as cation homeostasis, metabolism, autophagy or even cell death (Granatiero et al., 2017). Mitochondrial fission/fusion events also respond to Ca^{2+} homeostasis (Bravo-Sagua et al., 2017). Moreover Ca^{2+} deregulation, especially when accompanied by oxidative stress, leads to abnormal function and cell damage being associated to several metabolic diseases. A mitochondrial Ca^{2+} overload can cause the sustained opening of the mitochondrial permeability transition pore (mPTP) resulting in dissipation of membrane potential, water entry and consequent matrix swelling, cristae unfolding, and MOM rupture leading to cell death (Hurst et al., 2017). Ca^{2+} homeostasis deregulation can be linked to several diseases such obesity or cancer (Bravo-Sagua et al., 2017).

Lipid metabolism

Mitochondrial MIM plays an essential role in the synthesis of several phospholipids such as phosphatidylglycerol, phosphatidylethanolamine or cardiolipin (di-phosphatidylglycerol, an exclusive lipid of mitochondria) (Dudek, 2017; Mayr, 2014; Mejia & Hatch, 2016). On the contrary, lipid degradation processes occur in mitochondria by β-oxidation of fatty acids which degradation produces acetyl-CoA molecules that feed into the Krebs cycle. Both pathways, Krebs cycle and β-oxidation itself generates NADH and FADH2, which in turn transfer electrons to the respiratory chain for energy generation (Xiong, 2018). Consequently, mitochondrial lipids are involved in various cellular functions: maintenance of membrane architecture, respiratory metabolism, mitochondrial protein homeostasis, regulation of mitophagy or cytochrome c-mediated apoptosis or fusion and fission balance (Frohman, 2015; Mårtensson et al., 2017; Mayr, 2014; Nielson & Rutter, 2018).

Stress response and signaling

Mitochondria have been recognized as mediators of cell stress, a type of response termed mitohormesis which allows cell adaptation that increments health and cell viability in stress conditions. To accomplish this function, mitochondria activate cytosolic signaling pathways to communicate their fitness to the rest of the cell and establish a coordinated dialogue with the nucleus, also named mitonuclear communication. However, high damageable stimulus can activate different pathways leading to negative cellular responses or even cell death (Bárcena et al., 2018).

The cell danger response is composed of a wide range of extrinsic and intrinsic mitochondrial perturbations of chemical, physical or biological origins that can initiate diverse cellular responses when the threat exceeds the cellular capacity for homeostasis that protects cells from severe injury. There are numerous cell stress signals like alteration of bioenergetics and metabolism, Ca^{2+} balance, metal homeostasis impairment, increase of ROS, decrease of MMP, attempts of infection, etc (Naviaux, 2014; Yun & Finkel, 2014). Mitochondria has developed various adaptive stress responses and signaling through different pathways including metabolic adaptation, mitochondrial biogenesis, metabolite release, inflammation, regulation of mitochondrial dynamics (motility and fission/fusion) and mitophagy to eliminate dysfunctional mitochondria (Chandel, 2014; Feng et al., 2017; Naviaux, 2014; Yun & Finkel, 2014).

Finally, the integrated stress response (ISR) is a cellular pathway which is activated upon stress stimuli (Pakos-Zebrucka et al., 2016). The aim of this pathway is to decrease protein synthesis and activate selective genes to promote cellular recovery. Recent studies have elucidated how the mitochondrial machinery communicates with the cytosol to trigger this pathway. Indeed, in dysfunctional mitochondria a MIM protein called OMA1 (metallopeptidase Overlapping with the m-AAA protease1) is activated and in turn cleaves DELE1 (death ligand signal enhancer 1), which is located at the IMS. A cleaved fragment of DELE1 can reach the cytosol and activate HRI (also called EIF2AK1 or eukaryotic translation initiation factor 2-alpha kinase 1), which phosphorylates EIF2α (eukaryotic translation initiation factor 2-alpha). The consequence of this phosphorylation is a reduction of protein synthesis and an increase in the production of transcription factors ATF4, ATF5 (activating transcription factors 4 and 5) and CHOP (C/EBP homologous protein).

Finally, these two events trigger the ISR (Fig 22) (Fessler et al., 2020; Guo et al., 2020; Tremblay & Haynes, 2020).

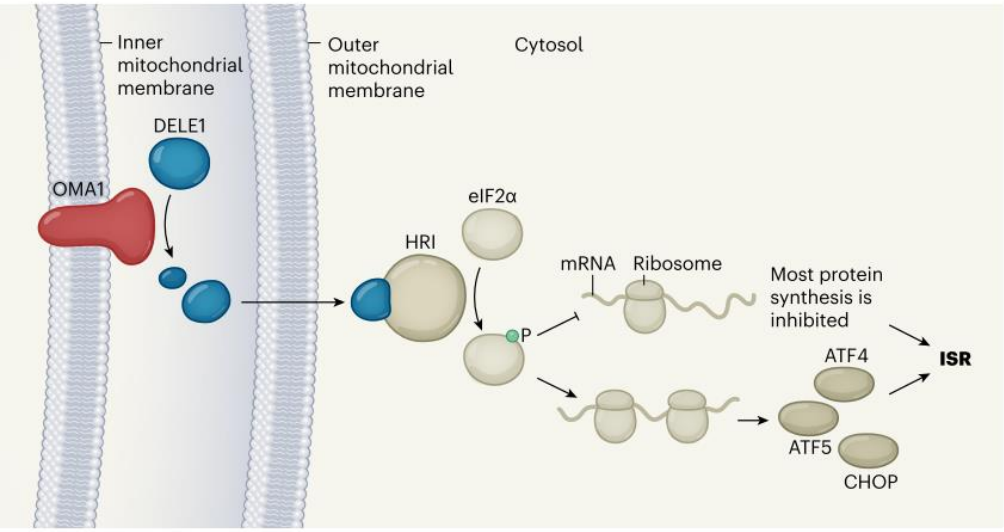

Figure 22. Mitochondria and stress response. Mitochondria communicates with the cytosol to trigger the integrated stress response to promote cellular recovery upon stress stimuli (Tremblay & Haynes, 2020)

C3. NEET PROTEINS AND MITOCHONDRIAL FUNCTIONS

As described in section C2, mitochondria play a role in iron homeostasis, which can be linked to other mitochondrial functions. A recently discovered family of proteins, the NEET proteins, belongs to a class of iron-sulfur proteins that are implicated in this specific mitochondrial process. They owe their name to their N-E-E-T motif (asparagine - glutamic acid - glutamic acid - threonine amino acid sequence). The NEET family is so far constituted of 3 proteins: MitoNEET (mNT) encoded by CISD1 gene (CDGSH iron sulfur domain 1, [**C**-X-C-X2-(S/T)-X3-P-X-C-**D**-**G**-(**S**/A/T)-**H**]), the nutrient-deprivation autophagy factor-1 (NAF-1) encoded by CISD2 gene (CDGSH iron sulfur domain 2; also called Miner 1, ERIS or Noxp70) and the mitochondrial inner NEET protein (MiNT), encoded by CISD3 gene (CDGSH iron sulfur domain 3; also called Miner2) (Inupakutika et al., 2017).

mNT (CISD1), NAF-1 (CISD2) and MiNT (CISD3) display a unique structure called the NEET-fold which is highly conserved is numerous species, indicating an important function on cell survival. All three proteins are composed of two domains: a β-cap domain and a cluster binding domain, which contains the CDGSH domain that harbors an iron-sulfur [2Fe-2S] cluster. This cluster is composed of a unique association of 3 cysteines (Cys) to 1 histidine (His) (Fig 23.D) (Tamir et al., 2015; Wiley et al., 2007).

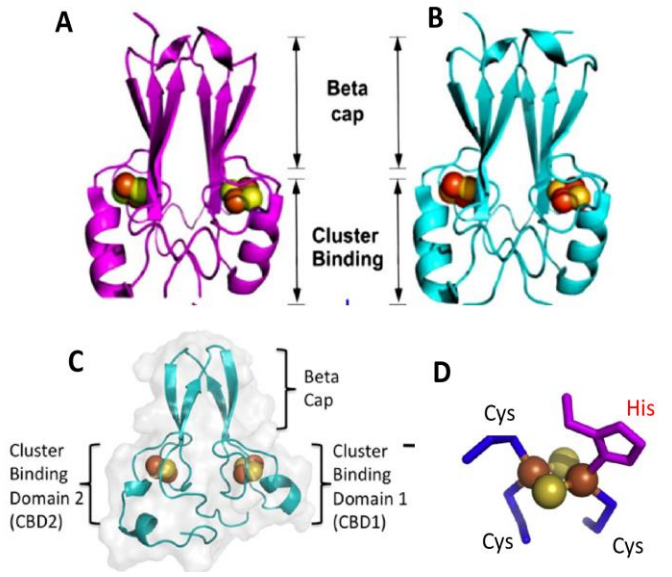

Figure 23. NEET proteins structure and [2Fe-2S] cluster A: mitoNEET, B: NAF-1, C: MiNT, D: cluster binding domain. These 3 proteins are formed by a beta cap region and a cluster binding domain containing 3Cys:1His (adapted from (Lipper et al., 2017; Tamir et al., 2015).

The [2Fe-2S] clusters of the NEET proteins have redox properties and their lability is very sensitive to the protein direct environment. When the [2Fe-2S] cluster receives a signal that induces its oxidation, it switches into an active state and the cluster can be delivered to an apo-acceptor protein. On the contrary, reduction of the cluster inhibits this transfer. The redox-sensing function of the cluster is attributed to histidine residue. These clusters can also take part in electron transfer reactions. Moreover and importantly, mNT, NAF-1 and MiNT have different subcellular localizations and possess different structures, suggesting that they have different versatile functions. (Karmi et al., 2018; Tamir et al., 2015; Wiley et al., 2007).

mitoNEET (mMT, CISD1)

mNT is a homodimer localized at the MOM, anchored to the membrane by the alpha-helix of its N-terminus (Fig 23.A) (Vernay et al., 2017; Y. Wang et al., 2017). Each monomer harbors a [2Fe-2S] in its C-terminal cytosolic domain, which can take different orientations in the cytoplasm (Wiley et al., 2007). That may allow flexibility to participate in protein–protein interactions (Zuris et al., 2011).

mNT participates in multiple mitochondria associated functions. Because of its [2Fe-2S] cluster, mNT participates in iron homeostasis and iron-sulfur cluster transport from mitochondria to cytosolic proteins like anamorsin (a protein required for iron-sulfur cluster assembly in cytosol) (Y. Wang et al., 2017), apo-ferredoxin, iron regulatory protein-1 (IRP1) (regulator of cellular iron) (Cheng et al., 2017) or aconitase (Karmi et al., 2018). Moreover, cell depletion of mNT results in an accumulation of iron and ROS in mitochondria, suggesting that this protein plays also a role in ROS homeostasis (Mittler et al., 2019). In parallel and because of its capacity to transfer electrons, mNT is involved in the energy metabolism in mitochondria by regulating electron transport and oxidative phosphorylation, as illustrated by the decrease of 30% in oxidative phosphorylation in mNT KO (knock-out) mice model (Y. Wang et al., 2017; Wiley et al., 2007). Interestingly, MitoNEET seems to participate in the control of formation of intermitochondrial junctions and can be implicated in mitochondria morphology regulation to adapt in physiological and pathological stress situations (Vernay et al., 2017).

Several diseases are related to mNT protein: 1) obesity, where mNT overexpression triggers a massive nutrient influx into the cell (Kusminski et al., 2012). 2) cystic fibrosis where a knock-down of mNT induces failure in the ETC (Tamir et al., 2015). 3) diabetes, where insulin-sensitizing drug pioglitazone inhibits iron transfer from mNT to mitochondria regulating Fe accumulation in mitochondria (Zuris et al., 2011). 4) cancer, where mNT overexpression has been demonstrated to be essential for cancer cell proliferation. (Y. Wang et al., 2017) and 5) Parkinson disease, where mitoNEET KO mice present a phenotype of early neurodegeneration (Geldenhuys et al., 2017; Mittler et al., 2019)

NAF-1 (CISD2)

NAF-1 protein is localized at the cytosolic side of the ER at the direct interface (contact sites) with mitochondria (Lipper et al., 2017). NAF-1and mNT possesses a similar structure: it is a homodimer harboring two [2Fe-2S] clusters exposed to the cytosol and also contains a transmembrane alpha-helix domain to allow membrane anchoring (Fig 23.B). Nevertheless, there is two differences between these two proteins: NAF-1 beta-cap domain allows more stability of the [2Fe-2S] clusters and NAF-1 surface charge and hydrophobicity favor specific interactions with different protein partners (Ferecatu et al., 2018; Tamir et al., 2015).

In addition to redox sensing, cluster transfer, regulation of iron and ROS metabolism functions, NAF-1 participates to other cellular tasks (Tamir et al., 2015). Indeed, NAF-1 has been described to regulate autophagy initiation by contributing to the interaction between BCL-2 (B-cell lymphoma 2) and Beclin1, which is dependent on the presence or absence of [2Fe-2S] clusters of NAF-1 (Chang et al., 2010; Karmi et al., 2018). Because NAF-1 can interact with the pro- and anti-apoptotic regions (BH3 and BH4) of BCL-2, NAF-1 is thought to have a role as well in apoptosis (Holt et al., 2016; Mittler et al., 2019). Consequently, NAF-1 seems to play a critical role in mitochondrial degeneration and aging (Y. F. Chen et al., 2009; Geldenhuys et al., 2019). Moreover, the loss of NAF-1 results in impairment of intracellular Ca2+ uptake, suggesting a role in Ca2+ homeostasis (C. H. Wang et al., 2014).

Importantly, NAF-1 has been associated with some pathological conditions in humans. The Wolfram syndrome-2 (WFS2) is an autosomal recessive disorder associated with a premature stop codon in NAF-1 transcript. The symptoms of this disorder are caused by degeneration of neurons and pancreatic b cells (Amr et al., 2007). WFS2 patients develop at early ages diabetes mellitus, sensorineural deafness, optic atrophy, dementia, diabetes insipidus, renal-tract abnormalities, bladder atony and psychiatric illnesses. Furthermore, NAF-1 has been shown to be implicated in breast, gastric, pancreatic and liver cancers and can be used as a cancer marker (Ferecatu et al., 2018; Mittler et al., 2019).

Importantly, NAF-1 has been shown to physically interact with mNT. Indeed, mNT transfers its [2Fe-2S] cluster to NAF-1, implying that these two proteins can work together to transfer [2Fe-2S] clusters from the mitochondria to the cytosol. Both proteins are known to maintain homeostasis of iron and ROS at mitochondria/ER interface and it seems that they cooperate together to accomplish this task. In addition, this interaction seems to regulate cellular proliferation and apoptosis/autophagy activation (Chang et al., 2010). Interestingly, mNT and NAF-1 have been shown to be unable to compensate for the deficiency of each other, suggesting that they may be part of the same pathway to regulate mitochondrial iron (Karmi et al., 2018; Mittler et al., 2019).

MiNT (CISD3)

The third member of the family is MiNT. MiNT structure differs from those of mNT and NAF-1. This protein is a soluble monomer residing in the mitochondrial matrix and contains two CDGSH motifs in a single polypeptide chain with distinct asymmetry (Fig 23.C). These differences lead to the idea that MiNT has different level of stability, functions and binding partners than NAF-1 and mNT. (Cheng et al., 2017; Karmi et al., 2018; Lipper et al., 2017; Vernay et al., 2017).)

Despite its peculiar structure, MiNT has been reported to also play a role in cluster transfer and iron and ROS metabolism. Indeed, MiNT transfers its [2Fe-2S] clusters to mitochondrial ferredoxins (required for iron and ROS regulation) and its downregulation decreases the level of this acceptor, leading to an inhibition of Fe-S clusters and heme production, inducing an increase on free iron levels (Lipper et al., 2017). Moreover, decreased levels of MiNT causes a MMP loss and an accumulation of mitochondrial iron and ROS. These data suggest that even if MiNT differs from mNT and NAF-1, it cooperates with them in the same functions and pathway (Lipper et al., 2017). In addition, MiNT is able to bind nitric oxide (NO), suggesting that it could have a role in NO signaling (Cheng et al., 2017). Although MiNT has been described to participate in several functions, it has only been related to cancer. Indeed, it is highly expressed in several types of cancer (lung, ependymoma, breast, liver and lymphoma) (Cheng et al., 2017; Lipper et al., 2017).

Because of their recent discovery, the knowledge of NEET proteins functions and their putative impact on other diseases is still not fully understood. Studies carried out during the past years

clearly suggest that further research is needed, especially for MiNT protein characterization. Thus, NEET proteins can become pharmaceutical targets in several kinds of cancer, diabetes, neurodegenerative diseases or other iron-related diseases.

C.4 MITOCHONDRIAL MORPHODYNAMICS: FUSION AND FISSION

Mitochondria are highly dynamic organelles able to adapt their morphology to maintain functions and cellular homeostasis. Moreover, mitochondria shape, size and distribution vary depending on several factors such as cell type, cellular needs or age. To maintain their integrity, particular architecture and functionality, these organelles form a network of elongated tubules that constantly fragment and fuse. The balance of coordinated cycles of fission and fusion maintains mitochondria characteristic shape. When this equilibrium is broken, mitochondria can show fragmented or hyperfused network (illustrated in Fig 24) (Tilokani et al., 2018).

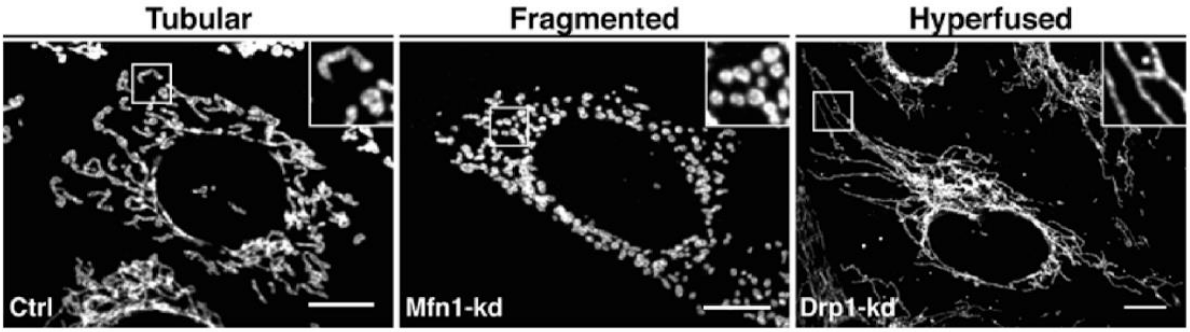

Figure 24. The mitochondrial morphology network. Control condition shows tubular mitochondria. However, MFN1 knock-down causes mitochondria fragmentation while DRP1 knock-down provokes mitochondria hyper-fusion (Tilokani et al., 2018)

Regulation of mitochondrial fusion and fission

In mammals, mitochondria fusion and fission are controlled mainly by four dynamin-related GTPases: Mitofusin 1 (MFN1), Mitofusin 2 (MFN2), Optic Atrophy 1 (OPA1) and Dynamin-related protein 1 (DRP1). These proteins are regulated by post-translational modifications and diverse protein-protein interactions (Fig 25) (Whitley et al., 2019).

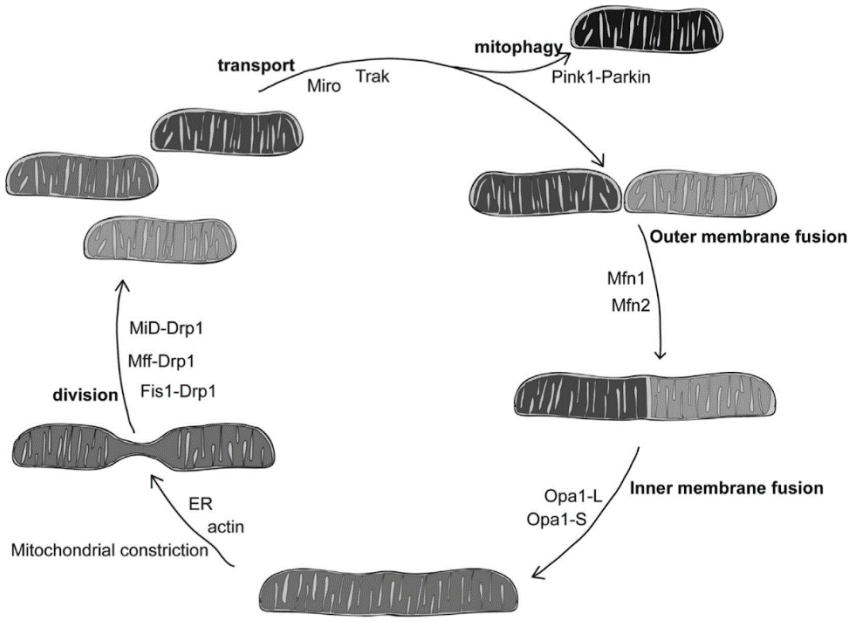

Figure 25. Mitochondrial fusion and fission cycle and main actors (Whitley et al., 2019).
Fission protein 1 homolog (Fis1), Mitochondrial Fission Factor (Mff) and Mitochondrial Dynamics (MiD) are DRP1 receptors.

Because of mitochondrial double-membrane architecture, mitochondrial fusion takes place in a two-step coordinated process that occurs sequentially (Song et al., 2009). The outer mitochondrial membrane fusion is mediated by MFN1 and MFN2 (Santel & Fuller, 2001) and is followed by inner membrane fusion ensured by OPA1 (Fig 26). Deficient cells in mitofusins present fragmented mitochondria (Fig 24), suggesting that both MFN1 and MFN2 are needed for MIM fusion (H. Chen et al., 2003).

Importantly, MOM and MIM fusion are spatially and temporally orchestrated. For MIM fusion, OPA1 requires the presence of MFN1 (Cipolat et al., 2004). OPA1 is indeed localized at the MIM and the IMS. Depleted OPA1 cells show fragmented mitochondrial and cristae disorganization membranes (Olichon et al., 2003). To regulate its activity, OPA1 is cleaved by two inner membrane proteases whose activities are modified by MMP and ATP levels (Ishihara et al., 2006). These proteases are the ATP-dependent zinc metalloprotease YME1L and the membrane potential-dependent protease OMA1 (Ehses et al., 2009). Numerous stress stimuli can activate OMA1 to cleave OPA1. Consequently, there are two distinct isoforms of OPA1: the long OPA1 (L-OPA1) and the cleaved form or short OPA1 (S-OPA1). The long form is anchored to the MIM and the

short form lacks the transmembrane domain, becoming a soluble form located at the IMS. Mitochondrial fusion depends on the balance of these two isoforms, L-OPA1 is correlated with fusion while S-OPA1 is believed to restrain fusion and facilitate fission (R. Anand et al., 2014). L-OPA1 and cardiolipin seem to be sufficient to mediate membrane fusion (Ban et al., 2017).

On the other hand, mitochondrial fission allows the division of one mitochondrion in two daughter mitochondria and ensures the removal of damaged mitochondria via mitophagy (Fig 25) (Otera & Mihara, 2011). MOM constriction is a multi-step process where the major required effector is DRP1 (Smirnova et al., 1998). Overexpression of a DRP1 dominant-negative mutant ($Drp_{K38A)}$ or DRP1 depletion results in defective mitochondrial fission and the emergence of hyperfused mitochondrial network (Fig 24) (Frank et al., 2001; Smirnova et al., 2001). Importantly, post-translational modifications of DRP1 regulates mitochondrial division: DRP1 phosphorylation at Ser637 is known to inhibit its activity, while phosphorylation at Ser616 is associated with DRP1 activation and consequent mitochondria fragmented network (Tilokani et al., 2018).

Interestingly, mitochondria fission involves a specific crosstalk between mitochondria, ER and F-actin polymerization and dynamics. This crosstalk is notably responsible for the induction of mitochondria membrane curvature and specific DRP1 recruitment at mitochondrial membrane. Indeed, ER is required to start mitochondrial division by making contact-sites with mitochondria and to initiate pre-constriction by decreasing mitochondrial diameter. This process allows DRP1 ring formation around mitochondria (Fig 26) (Friedman et al., 2011). Mitochondria-ER contact sites depend on interactions with cellular cytoskeleton (Moore & Holzbaur, 2018) and DRP1 binding to F-actin stimulates its oligomerization and GTPase activity (Hatch et al., 2016). Interestingly, MOM lipids signaling (especially based on cardiolipin lipid) also regulates assembly of DRP1 at mitochondrial constriction sites (Francy et al., 2017).

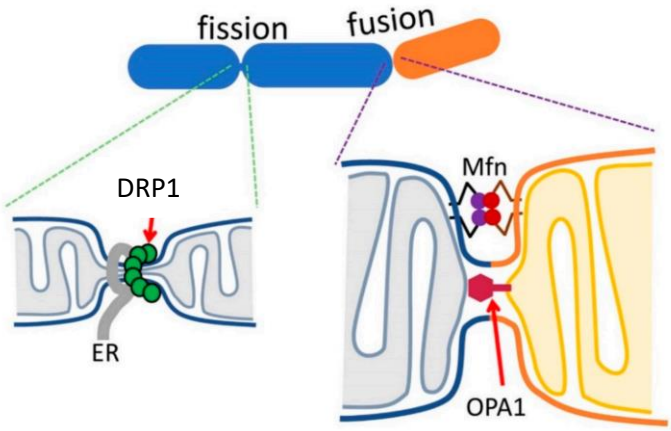

Figure 26. Fusion and fission dynamin-related proteins. ER constricts mitochondria helped by actin filaments, allowing the formation of a DRP1 ring to mediates fission. MFNs are responsible for MOM fusion while OPA1 is necessary to MIM fusion (H. Lee & Yoon, 2018)

DRP1 is a cytosolic protein that needs adaptors to be recruited to the mitochondrial outer membrane. To allow this recruitment, DRP1 binds to its identified receptors: fission protein 1 homolog (Fis1), Mitochondrial Fission Factor (Mff) and Mitochondrial Dynamics protein 49 and 51 (MiD49 and MiD51) (Fig 25). In turn, DRP1 oligomerization at constriction sites facilitates dynamin 2 (Dyn2) assembly, which complete mitochondria division (J. E. Lee et al., 2017). However, Dyn2 has been described to be dispensable for mitochondrial fission. Indeed, DRP1 activity is sufficient to constrict and sever mitochondria membrane (Kamerkar et al., 2018) .

Finally, inner mitochondrial membrane constriction occurs in an independent process regulated by calcium influx. Thus, calcium entry at mitochondria–ER contact sites induces a drop in MMP leading to the activation of OMA1 and consequent OPA1 cleavage. The increase of S-OPA1 levels disrupts MICOS complex, resulting in MIM-MOM tethering disruption and possibly constriction (Chakrabarti et al., 2018; Cho et al., 2017).

Fusion and fission balance

Mitochondria continuously undergo fusion and fission in response to cellular stimuli to maintain homeostasis and bioenergetics. Depending on the source of stress and the physiological conditions, this equilibrium may be lost and either fusion or fission could be facilitated. Fusion (and consequently a hyperfused network) is stimulated by mild stress that requires an energy demand,

resulting in an increase of respiration and ATP production to alleviate this insufficiency. On the contrary, fission favors mitochondria renewal and enables quality control. Moreover, cells under severe stress (high glucose, high fatty acids, diabetes) present fragmented mitochondria which leads to a decrease in respiration and ATP production. When stress is maintained and homeostasis is lost, the fusion and fission system cannot ensure functional mitochondria morphodynamics and damaged mitochondria are then recycled via mitophagy. If the damage perseveres and is generalized, fission can thus facilitate apoptosis (Fig 27) (Liesa & Shirihai, 2013; Westermann, 2010; Youle & Van Der Bliek, 2012; Zemirli et al., 2018).

Alterations of proteins involved in fusion and fission machinery lead to cellular dysfunction. Unbalance in mitochondrial dynamics has been reported in several diseases including severe pathologies like neurodegenerative and cardiac disorders (Liesa et al., 2009). Restoring the equilibrium in mitochondrial dynamics is a promising therapeutic tool to reduce cellular dysfunction, tissue degeneration and functional and behavioral outcomes (Whitley et al., 2019).

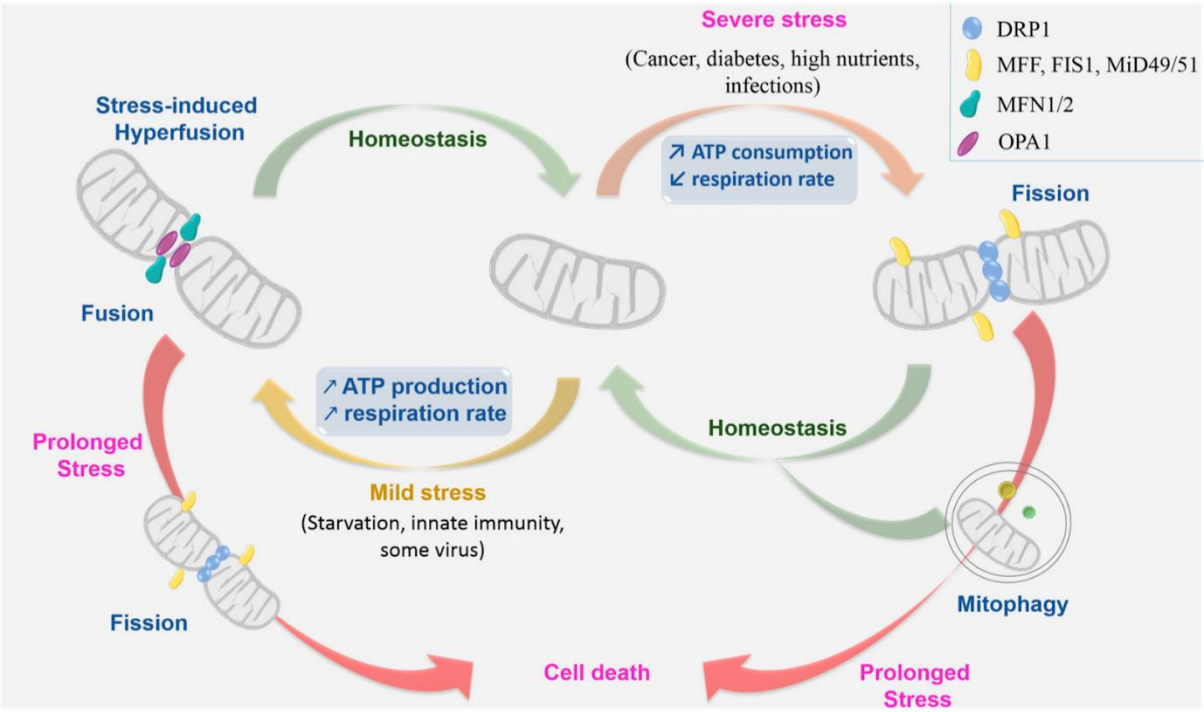

Figure 27. Mitochondria morphodynamics in stress conditions. Depending on cell context and circumstances, the equilibrium between fission and fusion could be altered. Upon mild stress, mitochondria are elongated, resist to mitophagy and increase ATP production. On the contrary, severe stress causes mitochondria fragmentation and increase of ATP consumption. Homeostasis loss results in mitophagy or apoptosis (Zemirli et al., 2018)

Fusion and fission balance in viral infection

Several viruses employ diverse strategies to either induce or inhibit distinct mitochondrial functions in a highly specific manner for prosperous replication and progeny production (S. K. Anand & Tikoo, 2013). Mitochondria morphodynamics reacts differently depending on the viruses, for instance, hepatitis B virus (HBV) causes a mitochondria fragmentation (S. J. Kim et al., 2013) while Dengue virus (DENV) provokes a mitochondria elongation (Barbier et al., 2017). HBV shifts the balance of mitochondrial morphodynamics toward fission by recruiting DRP1 (pro-fission) to the mitochondria and degrading MFN2 (pro-fusion). Then, HBV infection enhances mitophagy to deliver mitochondria to lysosomes for degradation. The goal of these two pro-viral actions it to weaken virus-induced apoptosis and to boost cell survival to enable viral persistence (S. J. Kim et al., 2013). During DENV infection, DENV nonstructural protein (NS)4B interact with mitochondria and alters its morphology inducing mitochondria elongation and increasing respiration. This shift to mitochondria fusion is due to the loss of activation of DRP1 and its phosphorylation status. As a result, the integrity of mitochondria-associated membranes and ER-mitochondria contact sites are compromised, reducing the interface for innate immune signaling and the IFN response RIG-I-dependent to promote viral infection (Barbier et al., 2017; Chatel-Chaix et al., 2016).

Other viruses are known to perturb mitochondria morphodynamics. Influenza A virus (as described in section B3), Hepatitis C virus, pseudorabies virus, human cytomegalovirus, epstein-bar virus, transmissible gastroenteritis coronavirus, porcine reproductive and respiratory syndrome virus, Venezuelan equine encephalitis virus, classical swine fever virus, new castle disease virus and human parainfluenza virus type 3 cause mitochondrial network fragmentation (Khan et al., 2015; H. Kim et al., 2018). On the contrary, SARS coronavirus, human immunodeficiency virus and sendai virus infected cells present elongated mitochondria (Khan et al., 2015; H. Kim et al., 2018).

A conflicting interpretation associated with mitochondria elongation concerning innate immunity and IFN response has recently appeared. Recent studies have shown that when mitochondria become elongated upon infection, bioenergetics and immunity are facilitated, while in fragmented mitochondria the balance turn to apoptosis and mitophagy (Fig 28) (Khan et al., 2015).

However, DENV infection has been reported to cause a mitochondria elongation associated with a reduction of the innate immune response, suggesting that the link between an immunity increase and mitochondria elongation is not a general hallmark to all viruses (Chatel-Chaix et al., 2016). Further studies are thus needed in this field to get a better understanding about the cause and effect relationship between mitochondria morphodynamics and innate immunity.

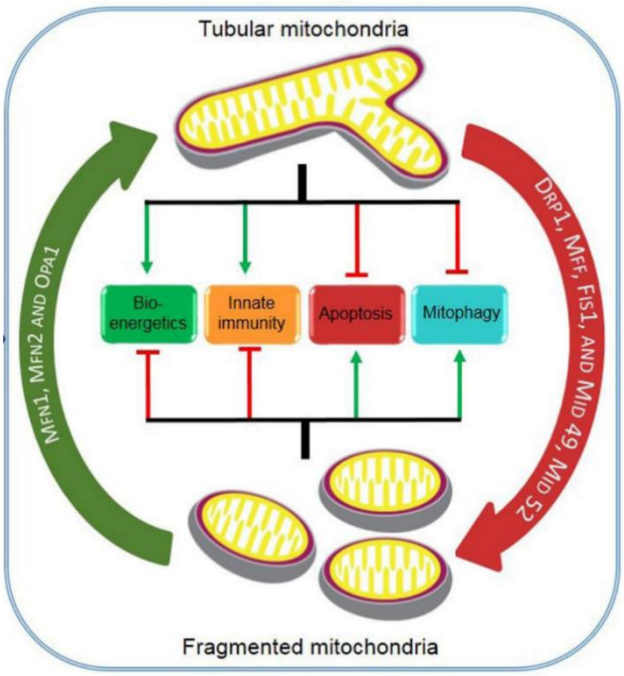

Figure 28. Mitochondrial dynamics upon infection. Elongated mitochondria favorizes bioenergetics and innate immunity while mitochondria fragmentation favorizes apoptosis and mitophagy in almost all studied virus. However, there exist some exceptions (Khan et al., 2015).

C5. MITOCHONDRIA CONTACT SITES AND IMMUNITY UPON INFLUENZA INFECTION

Among all endomembranes, mitochondria are often engaged in membrane tethering, notably through Endoplasmic Reticulum (ER) mediated contact sites. A “membrane contact site” (MCS) is defined as a membrane region where two organelles join together in physical contact and share an activity where the vesicular transport machinery is not required (Gatta & Levine, 2017). The number of contacts mitochondria set up with another organelle in the same cell can vary from a few to hundreds depending on cell needs and environmental stimuli (Lackner, 2019; Valm et al.,2017).

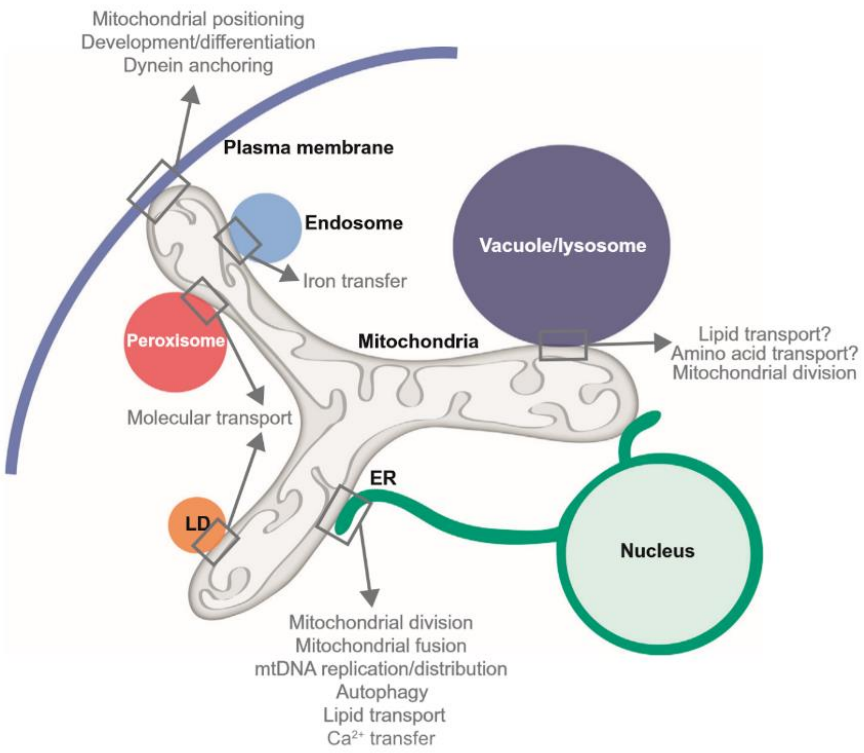

Figure 29. Mitochondria-organelle contacts and functions. Mitochondria establish contact sites with plasma membrane, endosomes, peroxisomes, vacuoles, lysosomes, lipid droplets (LD) and endoplasmic reticulum (ER) (Lackner, 2019)

Several organelles have been described to make functional contacts with mitochondria (Fig 29). For example, mitochondrial MOM has been shown to recruit two autophagosome markers (ATG5 and LC3) during starvation and to directly participate in autophagosome biogenesis (Hailey et al., 2010). Mitochondria also establish contact with lipid droplets to regulate energy homeostasis by fatty acid transfer. Perpilin 1, perpilin 5 and MFN2 are key actors in this process (Benador et al., 2018; Boutant et al., 2017; H. Wang et al., 2011). Moreover, peroxisome-mitochondria contact sites allow the transfer of β-oxidation products from peroxisomes to mitochondria (Shai et al., 2018). Besides, when the Golgi apparatus makes mitochondria contact, it benefits from ATP and calcium supply from mitochondria (Dolman et al., 2005).

Some endocytic and exocytic pathways related organelles have also been described to participate in contact sites with mitochondria. First, mitochondria–plasma membrane tethering has been reported to favor mitochondrial positioning and cellular architecture: during cell division, this contact has an impact in development and cell differentiation (Lackner, 2019; Westermann, 2015;

Wu et al., 2019). Moreover, lysosomal contacts with mitochondria seem to mark sites for mitochondria fission (Wong et al., 2018), while contacts between mitochondria and endosomes could play a specific role in iron transfer (Das et al., 2016). Besides, the vacuole and mitochondria patch (vCLAMP) has been demonstrated to play a role in metabolism processes (Hönscher et al., 2014; Peter et al., 2017).

Importantly, the contact sites that the ER forms with mitochondria are highly dynamic structures that have been described to participate in several cellular physiological processes and in adaptation to cellular needs or stresses (Csordás et al., 2018). Numerous proteins have been identified at these platforms either for physical tethering, molecule transfer or local signaling. Among others, MFN2 and the protein tyrosine phosphatase interacting protein-51 (PTPIP51) have been described to participate in ER/mitochondria membranes tethering. This specific membrane juxtaposition facilitates ER-mitochondria Ca2+ exchange (De Brito & Scorrano, 2008; Gomez-Suaga et al., 2017) which can be required for several mitochondrial functions like bioenergetics regulation, proper enzyme function, limiting cytosolic Ca2+ levels or apoptosis signaling (Helle et al., 2013). Finally, disturbing ER-mitochondria contacts by MFN2 depletion has been demonstrated to impair autophagy in starved cells (Hailey et al., 2010) and ER/mitochondria are crucial for autophagosomes formation (Hamasaki et al., 2013), confirming its implication in autophagy related processes.

ER-mitochondria contact sites are also directly implicated in mitochondrial morphodynamics because they are essential for mitochondrial fission as described in section C3. SAMM50, the core component of the Sorting and Assembly Machinery (SAM), seems to play a pivotal role in this function. Indeed, SAMM50 interacts with DRP1 at ER/mitochondria interface and its overexpression leads to a DRP1-dependent fission affecting mitochondrial morphology and function (S. Liu et al., 2016). Furthermore, SAMM50 can regulate mitophagy in a PINK1(PTEN-inducedkinase1) -Parkin-dependent manner (Fig 25) (Jian et al., 2018).

ER-mitochondria communication plays also a role in metabolite exchange and local ROS signaling at mitochondria (Csordás et al., 2018; Tubbs & Rieusset, 2017). Indeed, ER/mitochondria contact sites have been described as new hubs for nutrient signaling (insulin/glucose) (Rieusset, 2018).

These contacts also allow lipids exchange between both organelles through the tethering of the ER membrane protein complex (EMC), which is required for phospholipid synthesis, membrane biogenesis or morphology (Lahiri et al., 2014).

Importantly, contact sites at the interface between ER and mitochondria provide a platform for signaling pathways involved in immunity. Indeed, a mitochondrial protein that can be located at ER/mitochondria contact sites called Mitochondrial Anti-Viral Signaling (MAVS, also known as IPS-1, Cardif and VISA) is implicated in the innate immunity response to RNA virus infection (Horner et al., 2011). MAVS is part of the RIG-I signaling pathway.

RIG-I (also called DEAH box helicase 58, DHX58) is a cytosolic protein composed of a CTD domain (C-terminal domain), an helicase core and two N-terminal CARD domains (caspase activation and recruitment domains). In resting cells, RIG-I keep an inactive conformation where the CARD domains interact with the CTD domain to remain masked. Upon viral infection, the 5'ppp (tri-phosphate) motif of viral RNA binds to RIG-I leading to a conformational change that exposes the CARD domains (Luo et al., 2011). The interaction with PACT (protein activator), ZAPS (zinc-finger antiviral protein), TRIM25 (tripartite motif containing 25) and RIPLET/RFN125 (ring finger protein) will help in the ubiquitination process and the maintenance of the activated form of RIG-I. Then, 14-3-3ε protein allows the translocation of this complex to the ER/mitochondria contact sites, where the CARD domain of RIG-I interacts with the CARD domain of MAVS, catalyzing filament formation of MAVS to continue downstream signaling (which includes TANK and TRAF2, 3, and 6). This signaling activates TBK1 and IKK, which in turn mediates the phosphorylation of IRF3 (interferon regulatory factor) and the activation of NF-κB kinase complex. The activated forms of IRF3 and NF-κB can then translocate to the nucleus to initiate gene transcription enabling specific production of type I IFN and cytokines, which warn neighboring cells and attract immune cells to the spot of infection. Moreover, IFNs production induces numerous interferon stimulated genes (ISGs) to regulate the antiviral and immuno-modulatory response, cell growth, metabolism and cell death. The global aim of this response is to restrict viral replication and cell-to-cell spreading (Fig 30) (Cadena et al., 2019; Kell & Gale, 2015; Koshiba, 2013).

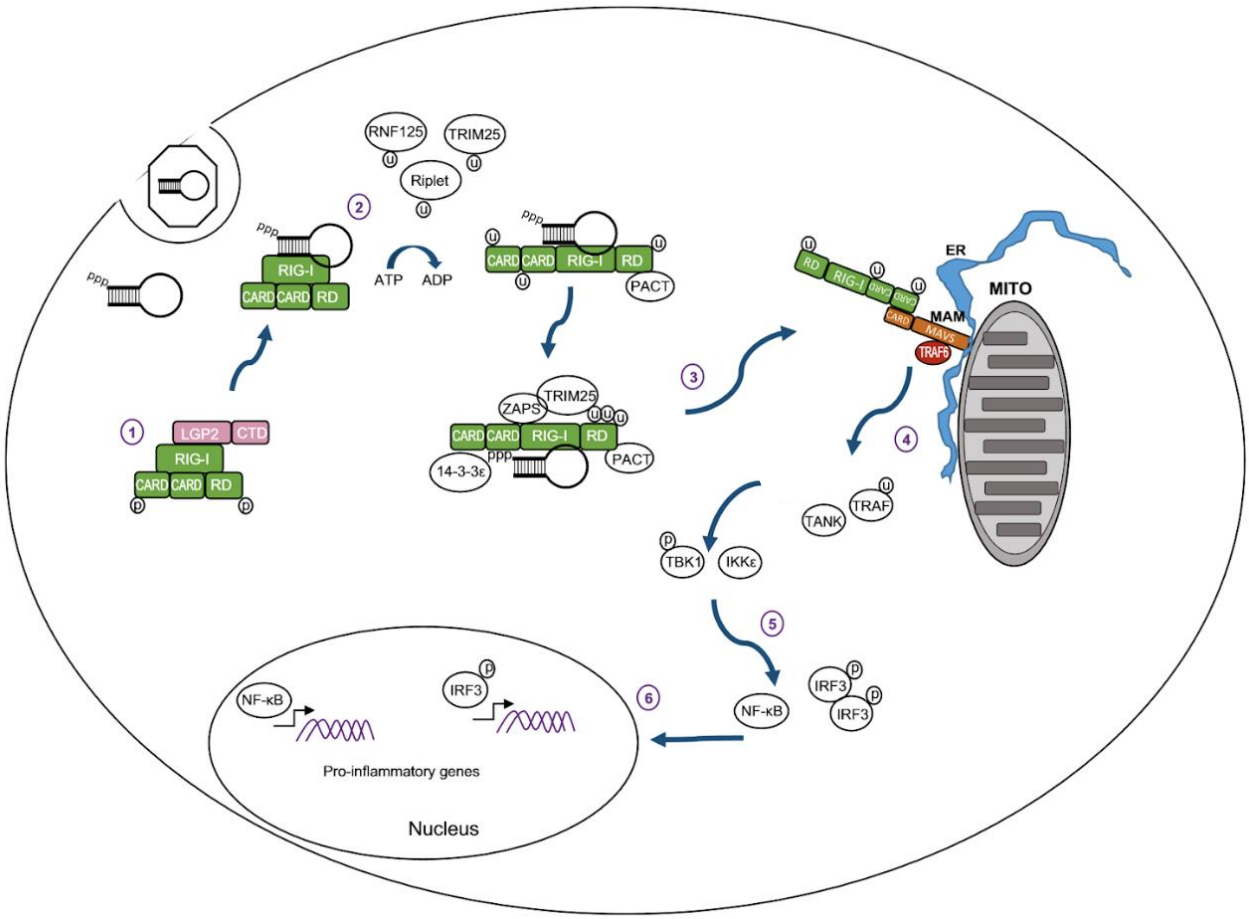

Figure 30. RIG-I signaling pathway. Antiviral response by recognition of viral RNA in the cytosol by RIG-I activates this pathway involving MAVS signalosome at mitochondria/ER contact sites , which leads to NFKB and IRF3 activation and consequently cytokine and IFN production. Adapted from (Kell & Gale, 2015)

In addition, mitochondria have a fundamental role in inflammasome activation. Indeed, upon infection some mitochondria-derived molecules like cardiolipin or mitochondrial DNA are released. The binding of these molecules and NLRP3 provokes the relocalization of NLRP3 from the cytosol to the mitochondria, where it activates the NLRP3 inflammasome. Finally, inflammasome activation leads to proinflammatory cytokines secretion (Q. Liu et al., 2018).

Innate immunity response impairment by influenza virus

Through evolution, viruses have developed several strategies to escape immunity. Upon influenza A infection, PB2 and PB1-F2 viral proteins have been described to target mitochondria and interact with MAVS to decrease IFN-β production (as described in B3 section). However, not only mitochondria are targeted by influenza viral proteins and other influenza proteins have been also described to interfere with the RIG-I pathway for blocking the immune response. Indeed, NS1 protein blocks the immune response at different stages: NS1 impedes the recognition of 5'-ppp influenza viral RNA by RIG-I receptor, inhibit RIG-I ubiquitination by TRIM25 and prevent activation and nuclear translocation of IRF-3, NF-κB and ATF-2 (Activating transcription factor 2) /c-Jun to evade cytokine and IFN production. NS1 also limits host cell gene expression by binding to CPSF30 (cleavage and polyadenylation specificity factor) and by interfering with the mRNA export machinery (Hale et al., 2010). Moreover, vRNP PB1, PB2 and PA proteins play a role in cap-snatching of host mRNAs causing host cell gene expression decrease thus IFN-β production. Finally, NP protein inhibits PKR (Protein kinase R), a host protein that blocks translation to limit influenza replication and also NP encapsulates free viral RNA in the cytosol to avoid RIG-I activation (Fig 31) (van der Sandt et al., 2012).

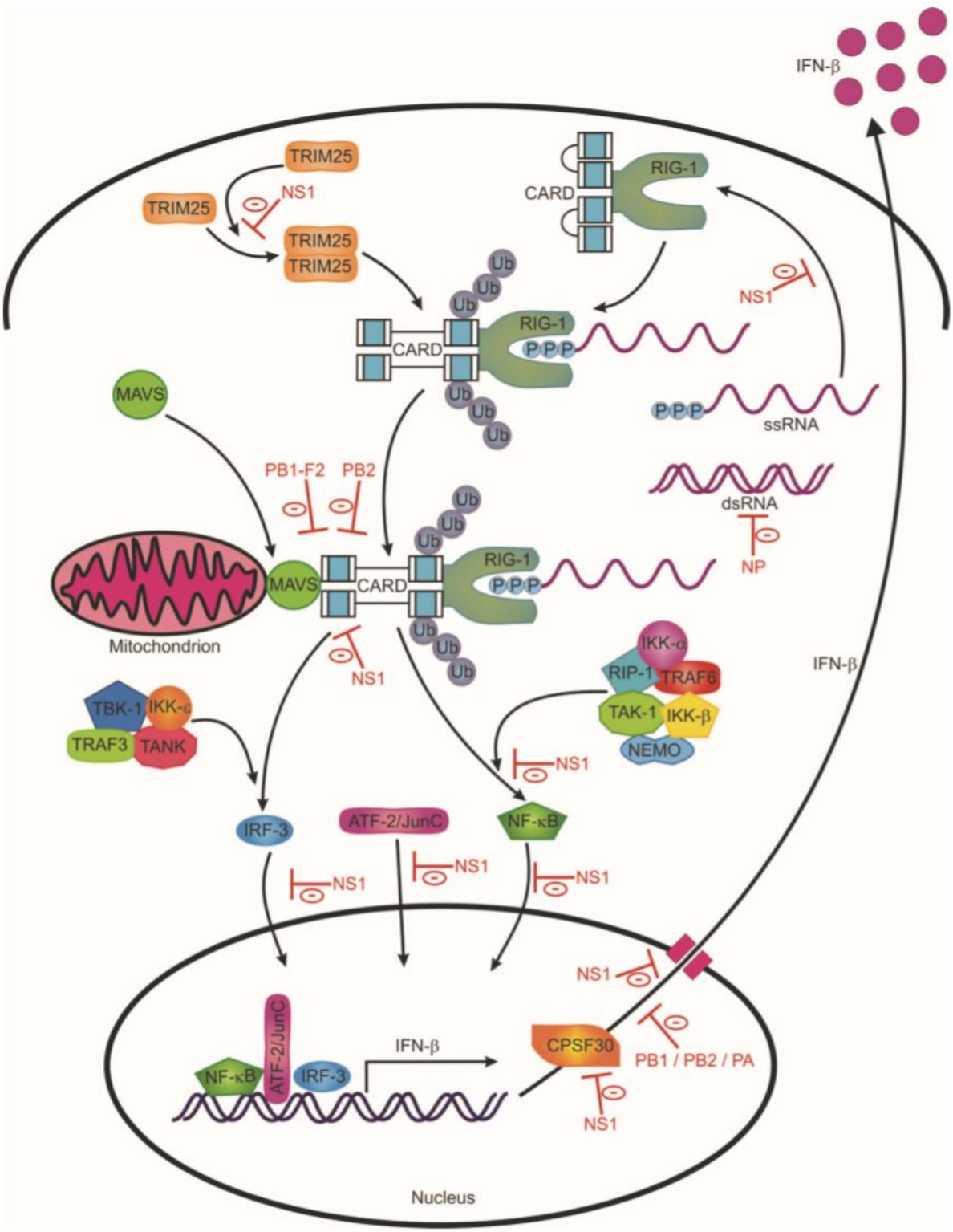

Figure 31. Inhibition of RIG-I signaling pathway by influenza A viruses. NS1, PB1, PB1-F2, PA and NP viral proteins inhibit RIG-I antiviral response at different stages in the pathway (van der Sandt et al., 2012).

RESULTS

The aim of the first paper “Mitochondrial morphodynamics alteration induced by influenza virus infection as new antiviral strategy” (submitted) was to perform a global study of endomembranes modifications upon influenza viral infection and to identify essential cellular host targets for virus replication. In addition, we explored the activity of a new host-directed antiviral molecule developed by Enyo Pharma.

To minimize cellular stress caused by trypsin treatment and serum deprivation normally used in influenza viral infection experiments, I first set up experimental conditions using complete media where I analyzed influenza virus replication properties.

Upon influenza viral infection, I confirmed two previously published phenotypes associated with H1N1 consequences on host cells: autophagy induction (via increase of LC3 puncta number) and Golgi fragmentation. While the study of late endosomes and endoplasmic reticulum did not reveal any significant evidence of membrane modifications, we reported much less early endosomes as well as massive mitochondrial network elongation. This mitochondrial phenotype was confirmed in A549 and MDCK cells infected by influenza A/H1N1, A/H3N2 and influenza B. Moreover, transfecting influenza viral RNA also led to a mitochondria elongation, suggesting that viral RNA is sufficient for altering mitochondrial morphology.

Moreover, electron microscopy analyses suggested that mitochondrial elongation in infected cells was promoted by mitochondria hyper-fusion and reveal a decrease of contact sites between ER and mitochondria. A decreased DRP1 recruitment and an increased stability of OPA1 at mitochondria finally suggest that influenza viral infection promotes a pro-fusion state in host cells.

Finally, the antiviral activity of a compound developed by Enyo Pharma (Mito-C) was tested. Mito-C treatment in influenza-infected cells reduced replication levels and reversed the viral-induced mitochondria hyper-fusion phenotype. Moreover, Mito-C was also shown to increase mitochondria-ER contact sites and to boost IFN production in a RIG-I dependent manner.

The aim of the second paper "Chemical targeting of NAF-1 protein reveals its function in mitochondrial morphodynamics" (currently in revision at EMBO Reports) was to understand how the modulation of mitochondria morphodynamics by Mito-C affects mitochondrial functions.

First, Mito-C was shown to rapidly induce mitochondria fragmentation in a reversible manner. The molecular study of the fusion and fission balance revealed that this fragmentation is DRP1 dependent and that it is maintained in time by soluble OPA1 accumulation.

Second, by captured compound mass spectrometry, MiNT was the first protein of the NEET family identified to be a target of Mito-C. In addition to MiNT, the NEET family is composed of mitoNEET and NAF-1. Interaction of Mito-C with all three NEET proteins has been validated in an *in vitro* iron-sulfur transfer assay.

Mito-C and NAF-1 has been shown to codistribute at the mitochondria and at the ER. Mito-C increase DRP1 recruitment to the mitochondria and moreover, NAF-1 partially co-localize with DRP1 at the contact sites. Interestingly, both Mito-C treatment and NAF-1 downregulation causes mitochondria fragmentation. Altogether, these results suggest that Mito-C and NAF-1 play a role in mitochondria fission in a DRP1 dependent manner at the interface between ER and mitochondria.

Finally, the antiviral effect of Mito-C was tested on Dengue virus (known to cause mitochondria elongation) and hepatitis B virus (known to cause mitochondria fragmentation). Mito-C reduced Dengue viral effects but didn't affect hepatitis B virus replication. Moreover, a reversion of mitochondria elongation in dengue-infected cells was observed, suggesting that targeting NAF-1 could be a specific therapeutic target to counteract viral replication in infectious diseases associated with mitochondrial elongation.

My contribution to these two papers was the following:

- Manuscript 1: I conceived the project, designed research, carried out the bulk of biochemistry, cell biology and virology experiments, organized the bulk of data, analyzed the data and wrote the manuscript.

- Manuscript 2: I conceived the project, contributed to biochemical and cell biology experiments, analyzed immunofluorescence experiments on infected cells, participated in electron microscopy experiments and participated in manuscript preparation and writing.

MANUSCRIPT 1

Mitochondrial morphodynamics alteration by influenza virus infection as new antiviral strategy

Mitochondrial morphodynamics alteration induced by influenza virus infection as a new antiviral strategy

Irene Pila-Castellanos[1,2*], Diana Molino[2*], Laetitia Lines[1], Laurent Chanteloup[1], Ivan Mikaelian[3], Laurène Meyniel-Schicklin[1], Patrice Codogno[2], Joe McKellar[4], Jacky Vonderscher[1], Olivier Moncorgé[4], Eric Meldrum[1], Caroline Goujon[4], Etienne Morel[2], Benoît de Chassey[1]

[1]ENYO-Pharma, Bioserra 1- Bâtiment 1 B, 60 Avenue Rockefeller, 69008, Lyon, France

[2]Institut Necker-Enfants Malades (INEM), INSERM U1151-CNRS UMR 8253, Université de Paris, 75015 Paris, France.

[3]Université de Lyon, Université Claude Bernard Lyon 1, INSERM 1052, CNRS 5286, Centre Léon Bérard, Centre de recherche en cancérologie de Lyon, 69373 Lyon, France.

[4]Institut de recherche en infectiologie à Montpellier (IRIM), UMR 9004 - CNRS, Université de Montpellier, 34090 Montpellier, France.

*equal authorship

Correspondence:

Etienne Morel etienne.morel@inserm.fr and Benoit de Chassey bdc@enyopharma.com

ABSTRACT

Influenza virus infections are major public health threats due to their high rates of morbidity and mortality. Upon influenza virus entry, host cells experience modifications of endomembranes, including those used for virus trafficking and replication. Here we report that influenza virus infection modifies mitochondrial morphodynamics by promoting mitochondria elongation and altering endoplasmic reticulum-mitochondria tethering in host cells. Virus induced mitochondria hyper-elongation was promoted by fission associated protein DRP1 relocalization to the cytosol, enhancing a pro-fusion status. We show that altering mitochondrial hyper-fusion with Mito-C, a novel pro-fission compound, not only restores mitochondrial morphodynamics and endoplasmic reticulum-mitochondria contact sites but also dramatically reduces influenza replication. Finally, we demonstrate that the observed Mito-C antiviral property is directly connected with the innate immunity signaling RIG-I complex at mitochondria. Our data highlight the importance of a functional interchange between mitochondrial morphodynamics and innate immunity machineries in the context of influenza viral infection.

INTRODUCTION

Viruses are obligate intracellular parasites that rely on the host cellular machinery to achieve their replication cycle and transmission. Efficient viral infections have evolved from strategies that hijack cell structures, pathways and mediators seeking to counteract these infections. This pro-viral balance sometimes results in dramatic intracellular endomembrane alterations (de Armas-Rillo et al., 2016; Miller and Krijnse-Locker, 2008). One striking example of viral infection impact on organelles is the plasticity of mitochondrial morphodynamics. Indeed, while some viruses like human Cytomegalovirus or Hepatitis B virus induce mitochondrial fission (Combs et al., 2019; Kim et al., 2013), other viruses like Dengue or Sendai trigger mitochondrial network elongation (Castanier, Garcin, Vazquez, & Arnoult, 2010; Chatel-Chaix et al., 2016). Mitochondrial antiviral signaling (MAVS) is an adaptor protein, localized at outer mitochondria membranes and at endoplasmic reticulum (ER)-mitochondria tethering interfaces, that makes the connection between mitochondria and innate immunity machinery (Horner et al., 2011). In this context, MAVS translates the detection of viral RNA by RIG-I Like Receptors (RLR) into an anti-viral type I interferon response (Kawai et al., 2005; Meylan et al., 2005; Seth et al., 2005; Xu et al., 2005). Interestingly, activation of RLR induces elongation of the mitochondrial network (Castanier, Garcin, Vazquez, & Arnoult, 2010; Chatel-Chaix et al., 2016) illustrating the functional interplay between mitochondrial morphodynamics regulation and the molecular control of innate immunity in host cells. Conversely, artificial elongation of mitochondria by depletion of DRP1, one major effector of the mitochondrial fission machinery, has been described to decrease the expression of interferon β in the context of Dengue virus infection (Chatel-Chaix et al., 2016).

Influenza virus genomic RNA is also sensed by mitochondrial RIG-I (Pichlmair et al., 2006). However, cell endomembranes alterations during the course of influenza virus infection have not been extensively explored. Briefly, influenza is a major cause of respiratory diseases and is responsible for the death of more than half million people worldwide each year (Iuliano et al., 2018). The current therapeutic arsenal associated with influenza is restricted to two viral targets, M2 ion channel and neuraminidase proteins, with the recent emergence of viral PB2 protein as a third viral target (Abraham et al., 2020). The main drawback associated with these direct-acting antiviral compounds is the rapid emergence of viral strains resistant to treatments an observation that underscore the importance of examining host directed strategies in the fight against Influenza virus infection (Hsu et al., 2012). One approach is to study the mechanisms by which the virus induces intracellular endomembrane alterations. In host cells, influenza infection is described to induce autophagy (Zhang et al., 2014) and fragmentation/dispersal of the Golgi apparatus (Yadav et al., 2016). Moreover, when addressed to the mitochondria, the viral protein PB1-F2 induces mitochondrial network fragmentation (Yoshizumi et al., 2014). Classical *in vitro* experimental settings used in influenza virus infection studies routinely include serum deprivation and are thus expected to artificially affect endomembranes network and function, a situation that could mask viral induced phenotypes. In this study, we analyzed the host cellular endomembranes morphodynamics alterations associated with influenza infection in optimized and stress reduced experimental conditions. We report for the first time the unexpected elongation of the mitochondrial network and perturbation of endoplasmic reticulum-mitochondria contact sites as a direct consequence of influenza virus infection and we demonstrate that influenza RNA, a RIG-I ligand, is sufficient to induce this phenotype. We show that influenza infection shifts the fusion/fission molecular machinery towards a fusion state, a situation that promotes the observed mitochondrial network elongation. Finally, we provide evidence that this elongated phenotype can be targeted in a RIG-I pathway dependent manner, with a pro-fission molecule to inhibit influenza virus replication.

RESULTS

Influenza virus infection induces mitochondria elongation and alters mitochondria-ER contact sites

Confocal fluorescence microscopy analyses of human alveolar epithelial A549 cells infected by H1N1 influenza A virus was performed to gain insights into subcellular organellar alterations possibly induced by influenza virus infection. In order to minimize additional cellular stress associated with infection, we set up a protocol with reduced cell exposure to trypsin and serum deprivation, conditions often associated with viral infection *in vitro*. Indeed, trypsin treatment profoundly modifies cellular morphology and distribution of viral components (**supplementary figure 1a**) and serum deprivation induces mitochondria and Golgi fragmentation (**supplementary figure 1b**). In our experimental design, cells were exposed to influenza virus for 1h in presence of trypsin in serum free medium before incubation in complete medium. The kinetics of trafficking and subcellular localizations of viral M2 and NP proteins were not modified in these conditions (**supplementary figure 1c, 1d and 1e**).

As expected, H1N1 influenza A infection induced accumulation of LC3-positive punctate staining in A549 cells (**supplementary figure 2a**), suggesting an already reported autophagy induction (Zhou et al., 2009) and staining with GM130, a Golgi marker, revealed fragmentation and dispersion of the Golgi apparatus (Yadav et al., 2016) (**supplementary figure 2b**). While the number and distribution of late endosomes (LAMP1 punctate staining) was not affected, EEA1 labeling revealed significantly less early endosomes following viral infection (**supplementary figure 2c and 2d**) and GFP-tagged Sec61β, used as a marker of ER morphology, remained similarly distributed in infected and uninfected cells (**supplementary figure 2e**) suggesting that no major ER morphology changes occur during H1N1 infection. Unexpectedly, while uninfected A549 cells exhibited globular mitochondria, H1N1 infection

clearly induced an elongated mitochondria phenotype as determined by TOMM20 immunofluorescence analysis (**figure 1a and 1b**).

Influenza viruses are sensed by different pattern-recognition receptors inside cells leading to activation of the innate immune system. The main cytosolic receptor is the RIG-I protein, which induces type I interferon production through the mitochondrial protein MAVS (Ishii et al., 2006; Meylan et al., 2005; Seth et al., 2005; Xu et al., 2005). Given the importance of MAVS in the regulation of the RIG-I pathway, we focused on the characterization of the mitochondria morphodynamics phenotype in H1N1 infected cells. Electron microscopy analysis confirmed a statistically significant increase of mitochondria length (**figure 1c and 1d**) thus excluding a potential accumulation of inter-mitochondrial junctions (Vernay et al., 2017). The mitochondrial elongation was detectable at 280 min post-infection and reached its maximum at 520 min, the latest time point measured of our time-lapse analysis (**figure 1e**). Mitochondria-ER contact sites membrane domains are proposed to mediate MAVS-dependent innate immune signaling (Horner et al., 2011). By a thorough analysis of electron microscopy pictures, we also provide evidence that mitochondrial elongation is associated with a significant reduction of contact sites number and density following infection (**figure 1f, 1g and 1h**). Overall, our analyses suggest that intracellular organelles are profoundly modified upon H1N1 virus infection with striking elongation of the mitochondrial network.

Interestingly, similar observation was made with influenza A H3N2 subtype and the more distant influenza B strain (IVB) suggesting that mitochondrial elongation is broadly associated with influenza viruses infection (**supplementary figure 3a**). Moreover, in addition to A549 cells, influenza A H1N1, H3N2 and influenza B viruses also elicited mitochondria elongation in MDCK renal epithelial cells (**supplementary figure 3b**) arguing for a general hallmark associated with influenza infections.

In the context of antiviral response studies, it has been reported that synthetic double stranded RNA poly I:C, known to bind and activate RIG-Like Receptors, also induces mitochondria elongation (Castanier et al., 2010). To test if H1N1 influenza A RNA is one of the viral elements responsible for this phenotype, we transfected A549 cells with a synthetic 87-mer 5'triphosphate hairpin RNA derived from the influenza A H1N1 genome. This hairpin RNA is known to be a RIG-I ligand that when introduced in cells triggers a potent interferon response (Hornung et al., 2006). In cells transfected with the influenza A RNA, the elongated mitochondrial phenotype observed in virus infected cells appeared 6h hours post-transfection and was concomitant with the detection of type I beta interferon production (**supplementary figure 4a, 4b, and 4c**). Accordingly, type I interferon secretion was maximal when the highest number of cells had elongated mitochondria (**supplementary figure 4a**). These data indicate that influenza A RNA is sufficient to induce mitochondria elongation in host cells.

To further investigate the regulation of the molecular machinery involved in mitochondria alteration promoted by viral infection, we examined subcellular localization and expression of DRP1 (Dynamin-1-like protein, also referred as DNM1L), the main protein involved in the mitochondrial fission machinery. Interestingly, we observed that viral infection induced an important mitochondria-to-cytosol relocalization of DRP1 (**figure 2a and 2b**), a phenomenon accompanied by a decrease in DRP1 protein total amount (**figure 2c and 2d**). Conversely, infection increased OPA1 signal at the mitochondria, suggesting a coalescence of the protein at this compartment, OPA1 being a key protein in mitochondrial fusion (Lee and Yoon, 2018) (**figure 2e and 2f**). Altogether, these data suggest that influenza viral infection shifts the mitochondria fusion/fission machinery towards a fusion state.

Drug designed mitochondria fragmentation inducer (Mito-C) inhibits influenza replication

In the context of H1N1 viral infection, we thought to evaluate whether the mitochondrial fusion phenotype we just described was required for influenza pathogenesis. We therefore investigated the effects of Mito-C, a molecule recently developed by ENYO Pharma and previously described to induce mitochondria fragmentation on virus replication (**Molino, Pila-Castellanos *et al;* manuscript under revision**). Our hypothesis was that Mito-C could counteract the effects of influenza virus infection on mitochondria fusion, restore a normal phenotype and inhibit influenza replication. First of all, cell viability assays demonstrated that Mito-C was not toxic on A549 cells (**supplementary figure 5**). To detect putative antiviral effect of Mito-C, A549 cells were then infected by H1N1 influenza A virus at a MOI (multiplicity of infection) of 0.1 and virus associated neuraminidase activity (NA) was quantified in the infected cells culture supernatant 2 days post-infection. Mito-C induced a dose-dependent inhibition of NA activity with an IC50 of ±50nM comparable to oseltamivir, the most efficient influenza antiviral compound known as Tamiflu©, also active in the low nanomolar range of concentration (**figure 3a**). This inhibitory effect was further validated in a plaque forming unit (PFU) assay which revealed that Mito-C exhibited a 10-fold inhibition of the virus titer at 2μM (**figure 3b and 3c**). Similarly, viral NP expression in western-blot analysis was shown to be dramatically decreased upon Mito-C treatment (**figure 3d and 3e**).

We next evaluated the mitochondria phenotype in influenza virus infected cells treated or not with Mito-C. Interestingly, while H1N1 infection promoted mitochondrial elongation as shown (**Figure 1a and 1c)**, the treatment with Mito-C reverted this phenotype as assessed by fluorescence (**figure 3f and 3g**) and electron microscopy analyses (**figure 3h and 3i**). At the sub-organelle level, we further show a restoration of mitochondria-ER contact sites integrity following Mito-C treatment in infectious conditions (**figure 3j, 3k and 3l**). Both the percentage of

mitochondria engaged in mitochondria-ER contact sites and the contact sites density were similar to uninfected conditions.

Mito-C potentiates innate immune response in infected cells in a RIG-I dependent manner

The increased number of mitochondria-ER contact sites induced by Mito-C suggests that this compound may activate the innate immune response associated with anti-viral response. Hence, we assessed the impact of the molecule on endogenous interferon λ1 and β expression by RT-qPCR since both cytokines are directly associated with anti-viral RIG-I pathway (Killip et al., 2015). Importantly, Mito-C had no effect upon either cytokine's expression in uninfected cells (**figure 4a and 4b**). As expected H1N1 viral infection enhanced IFNλ1 and IFNβ expression (**figure 4a and 4b**) and remarkably, the cytokine inductions were significantly enhanced when H1N1 infected cells were treated with Mito-C (**figure 4a and 4b**). These data are consistent with the observed inhibition of H1N1 virus replication by Mito-C (**figure 3**) and suggests that the anti-viral activity of Mito-C activity is dependent on the RIG-I pathway. Indeed, knockout of RIG-I by CRISPR/Cas9 technology (**figure 4c**) abrogated the antiviral activity of Mito-C as assessed by neuraminidase activity in treated and untreated infected cell supernatants (**figure 4d**). Overall, these data indicate that the antiviral activity of Mito-C relies on mitochondrial RIG-I pathway engagement and enhancement of interferon responses to influenza A RNA.

DISCUSSION

We provide here a landscape of cellular endomembrane modifications associated with influenza virus infection. Autophagy induction has been extensively described in the context of influenza infection (Zhang et al., 2014) and Golgi fragmentation is suspected to facilitate the intracellular trafficking of virions (Yadav et al., 2016). The reduction of the pool of early endosomes has never been reported following infection and further analysis is required to understand the functional impact of this phenotype for the virus and for its host.

Mitochondria elongation in H1N1 infected cells was unexpected as previous reports identified the full length form of the viral protein PB1-F2 as a pro-fission factor for mitochondria (Yoshizumi et al., 2014). The nature of the virus strain studied appears critical since approximately 11% of H1N1 and 96% of highly pathogenic H5N1 encode for full length PB1-F2. We demonstrate here that the experimental settings also profoundly affect the structure and dynamics of mitochondria. Serum starvation, systematically used in H1N1 related studies to allow multiple infection cycles, induces mitochondria fragmentation. Hence, we chose to reduce the cell exposure to this cellular stress and revealed that H1N1 viral infection induced mitochondrial network elongation.

Conflicting results have been reported about the functional consequences of mitochondria elongation in an infectious context. In the context of Sendai virus infection, elongation induced by DRP1 depletion enhances IFNβ expression (Castanier et al., 2010) while it is repressed in the context of Dengue virus infection (Chatel-Chaix et al., 2016). This apparent discrepancy can be reconciled by considering the number of ER-mitochondria contact sites: Sendai infection increases their number and Dengue virus disrupts them. Interestingly, ER-mitochondria contact sites are platforms for MAVS-dependent activation of innate immune response (Horner et al., 2011). Here, in agreement with what was previously described for Dengue, influenza virus

infection decreases the number of contact sites arguing for an acute and rapid limitation of innate immune response. The enhancement of interferon expression with Mito-C, a pro-fission factor that also restores the number of ER-mitochondria contact sites, supports the hypothesis that mitochondria elongation is detrimental to innate immunity.

Finally, the identification of influenza RNA as a sufficient viral element to induce mitochondria elongation is consistent with what has been reported previously with poly I:C (Castanier et al., 2010). This also supports the idea that any viral RNA, if not any RIG-I ligand, could be sufficient to induce mitochondria elongation. In this context, it seems that Mito-C antiviral capability relies on RIG-I engagement as a consequence of influenza infection for the pro-interferon activity that we report here. Indeed, no anti-viral activity is detectable in RIG-I knock-out cells. Together with its anti-Dengue virus activity, this finally suggests that Mito-C compound could have a broad-spectrum activity against viruses that are sensed by RIG-I and that induce mitochondria elongation (**Molino, Pila-Castellanos *et al;* manuscript under revision)**. In the current epidemic context, it is tempting to propose the repositioning of Mito-C against SARS-CoV-2, since SARS-coronavirus ORF9b protein was recently shown to induce mitochondrial network elongation and to inactivate RLR pathway by degrading MAVS signalosome (Shi et al., 2014). Further studies will be required to understand in detail the mechanisms by which influenza related viruses provoke alteration of mitochondria morphodynamics, but our study highlights the importance of the interconnection between innate immunity machinery regulation and mitochondria morphology in a viral context.

ACKNOWLEDGMENTS

We thank our team of colleagues at ENYO Pharma and at Institut Necker Enfants Malades for fruitful discussions and constant support. We also acknowledge the Institut Necker Enfants Malades and Necker campus associated facilities (SFR Necker INSERM US24, CNRS UMS 3633). This work was finally supported by institutional funding from INSERM, CNRS and University Paris-Descartes. We thank Dr. Nicolas Guyon-Gellin and Diane Sampson for critical reading of the manuscript. We also acknowledge the Centre Technologique des Microstructures (Université Claude Bernard, Lyon) and PLATIM (Plateau d'imagerie/microscopie, Lyon) platforms for imaging facilities.

AUTHOR CONTRIBUTIONS

I.P.C., D.M., E.Mo and B.d.C. conceived the project. I.P.C. designed research, carried out the bulk of biochemistry, cell biology and virology experiments, organized the bulk of data, analyzed the data and wrote the manuscript. D.M. designed part of the research, contributed to some of the biochemical and cell biology experiments, analyzed part of the data and participated in manuscript preparation. L.L. and L.C. contributed to cell biology and virology experiments. I.M. designed part of the research and analyzed part of the data. L.M.S. analyzed part of the data and wrote part of the manuscript. P.C. designed part of the research. J.M. performed live microscopy imaging experiments. O.M. performed live microscopy imaging experiments and generated RIG-I knock-out cell lines. J.V. designed part of the research. E.Me. designed part of the research and wrote the manuscript. C.G. designed part of the research and analyzed part of the data. E.Mo and B.d.C. co-supervised the study, designed research, analyzed the data and wrote the manuscript.

FIGURE LEGENDS

Figure 1. Influenza virus infection induces mitochondria elongation and alters ER-mitochondria contact sites

a, A549 cells infected with H1N1 influenza A virus at MOI 1 for 24h (or mock infected) were immunostained with anti-TOMM20 antibody (green), anti-NP antibody (red) and DAPI (blue); cropped areas show mitochondria morphology, elongated in infected condition. **b**, Quantification of elongated and globular mitochondria (TOMM20 signal) from single cells illustrated in (a) (N=150 cells from three independent experiments). **c**, Electron micrographs (EM) from A549 cells infected (or not) with influenza A H1N1 virus at MOI 1 for 24h; cropped areas show the mitochondria morphology, hyper-fused in the infected condition. **d**, Quantification of mitochondrial length in EM images from A549 cells illustrated in c (N=250 mitochondria, from three independent experiments). **e**, Mito-tracker time lapse video-microscopy on A549 cells infected with H1N1 virus from 120min to 520min post-infection; arrowheads show the formation of elongated mitochondria network. **f**, EM pictures from infected (or not) A549 cells with influenza A H1N1 virus at MOI 1 for 24h; arrowheads show mitochondria-ER contact sites. **g**, Quantification of mitochondria-ER contact sites in EM images from A549 cells illustrated in f (N=100 mitochondria, from three independent experiments). **h**, Quantification of mitochondria-ER contact sites density in EM images from A549 cells illustrated in f (N=100 mitochondria, from three independent experiments). All scale bars = 10µm, except in EM (1 µm). For evaluating significance of differences observed in b,d,g and h, a two-tailed Student's *t* test was used (*** indicates $p<0.0001$).

Figure 2. Influenza infection shifts the fusion/fission molecular machinery balance towards a fusion state.

a, A549 cells infected (or mock infected) with influenza A H1N1 virus at MOI 1 for 24h were immunostained with anti-TOMM20 antibody (green), anti-DRP1 antibody (red) and DAPI (blue); arrowheads indicate recruitment of DRP1 onto the mitochondrial surface (TOMM20). **b**, Quantification of DRP1 signal on TOMM20 positive structures from A549 cells illustrated in (a) (N=30 cells from three independent experiments). **c**, Representative western blot analysis of DRP1 in A549 cells infected (or not), with influenza A H1N1 virus at MOI 1 for 24h. **d**, Quantification of DRP1 western blots as showed in (c) (N=4). **e**, A549 cells infected (or not) with influenza A H1N1 virus at MOI 1 for 24h were immunostained with anti-TOMM20 antibody (green), anti-OPA1 antibody (red) and DAPI (blue); arrowheads indicate accumulation of OPA1 at the mitochondrial matrix (TOMM20). **f**, Quantification of OPA1 signal on TOMM20 positive structures from A549 cells illustrated in (e) (N=30 cells from three independent experiments). Scale bars = 10µm. For evaluating significance of differences observed in b, d and f, a two-tailed Student's *t* test was used (*** indicates $p<0.0001$).

Figure 3. Drug designed mitochondria fragmentation inducer (Mito-C) inhibits influenza replication

a, Determination of neuraminidase activity in the supernatant of A549 cells infected with influenza A H1N1 virus at MOI 0.1 for 48h, treated with Mito-C compound or oseltamivir at indicated concentrations (N=3). **b**, PFU assay in MDCK cells from A549 infected supernatants (MOI 0.1, 48h) treated with Mito-C or DMSO (vehicle) at indicated concentrations. **c**, Quantification of PFU illustrated in (b) (N=3). **d**, Western blot analysis of NP viral protein in A549

cells infected with H1N1 at MOI 0.1 for 48h, treated with Mito-C at 2µM or DMSO (vehicle). **e**, Quantification of NP western blot showed in (d) (N=3). **f**, A549 cells infected or not, with H1N1 at MOI 1 for 24h and treated with Mito-C at 2µM or DMSO were immunostained with anti-TOMM20 antibody (green) and DAPI (blue). **g**, Quantification of mitochondrial elongation (TOMM20 signal) from single cells illustrated in (f) (N=50 cells from three independent experiments). **h**, Electron micrographs (EM) from infected A549 cells with influenza A H1N1 virus at MOI 1 for 24h treated with Mito-C at 2µM or DMSO (vehicle); cropped areas show mitochondria morphology. **i**, Quantification of mitochondrial length in EM images from A549 cells illustrated in (h) (N=150). **j**, EM pictures from infected A549 cells with influenza A H1N1 at MOI 1 for 24h treated with Mito-C at 2µM or DMSO; arrowheads point at mitochondria-ER contact sites, increased upon Mito-C treatment. **k**, Quantification of mitochondria-ER contact sites number in EM images from A549 cells illustrated in (j) (N=250 mitochondria, from three independent experiments). **l**, Quantification of mitochondria-ER contact sites density in EM images from A549 cells illustrated in (j) (N=250 mitochondria, from three independent experiments). All scale bars = 10µm, except in EM (1µm). For evaluating significance of differences observed in c, e, g, i, k and l, two-tailed Student's *t* test was used (*** indicates $p<0.0001$).

Figure 4. Mito-C potentiates innate immune response in infected cells in a RIG-I dependent manner

a, RT-qPCR analysis of IFNλ1 mRNA from A549 cells infected (or mock infected) with H1N1 at MOI 1 for 24h and treated with Mito-C at 2µM or with DMSO (N=3). **b**, RT-qPCR analysis of IFNβ mRNA from A549 cells infected (or mock infected) with H1N1 at MOI 1 for 24h and treated with Mito-C at 2µM or with DMSO (N=3). **c**, Western blot analysis of RIG-I expression in two

independent A549 RIG-I$^{-/-}$cell lines with and without IFNα treatment (CRISPR/Cas9, guide #1 and guide #2) **d**, Determination of neuraminidase activity in the supernatant of A549 wild type and RIG-I$^{-/-}$ cells (guide #1 and guide #2), infected with H1N1 at MOI 1 for 24h, treated with Mito-C at 2µM or DMSO (N=3). For evaluating significance of differences observed in c, e, g, I, k and l two-tailed Student's *t* test was used (*** indicates $p<0.0001$, NS for non-significant).

Supplementary figure 1. Experimental set-up for viral infections

a, A549 cells infected with influenza H1N1 virus at MOI 1 for 24h without serum and treated with trypsin (or not) were immunostained with anti-NP antibody (green) and DAPI (blue). **b**, A549 cells cultured with serum (or not) for 24h were immunostained with anti-TOMM20 antibody (green), DAPI (blue, left panel) and anti-GM130 antibody (green) and DAPI (blue, right panel); cropped areas show mitochondria and Golgi morphology, modified upon serum starvation. **c**, A549 cells were infected with H1N1 virus at MOI 1 in serum-free medium supplemented with trypsin. After 1h, cells were washed and the medium was replaced (or not) with medium containing serum. Cells were immunostained after 6h, 14h and 24h post infection with anti-NP antibody (green), anti-M2 antibody (red) and DAPI (blue). **d**, Quantification of infected cells (NP signal) from single cells illustrated in (c). **e**, Quantification of infected cells (M2 signal) from single cells illustrated in (c). Scale bars = 10µm. For evaluating significance of differences observed in d and e two-tailed Student's *t* test was used (** indicates $p<0.001$, NS for non-significant).

Supplementary figure 2. Organellar alterations induced by influenza A H1N1 infection

a, A549 cells infected (or not) with H1N1 virus at MOI 1 for 24h were immunostained with anti-LC3 antibody (green) and DAPI (blue) and pictures were quantified for LC3 positive structures per cell (N=30 cells from three independent experiments). **b**, A549 cells infected (or not) with H1N1 virus at MOI 1 for 24h were immunostained with anti-GM130 antibody (green) and DAPI (blue) and pictures were quantified for fragmented Golgi from single cells (N=30 cells from three independent experiments). **c**, A549 cells infected (or not) with H1N1 virus at MOI 1 for 24h were immunostained with anti-LAMP1 antibody (green) and DAPI (blue) and pictures were quantified

for LAMP1 positive structures per cell (N=30 cells from three independent experiments). **d**, A549 cells infected (or not) with H1N1 virus at MOI 1 for 24h were immunostained with anti-EEA1 antibody (green) and DAPI (blue) and pictures were quantified for EEA1 positive structure per cell (N=30 cells from three independent experiments). **e**, A549-Sec61β-GFP stable cell line was infected (or not) with H1N1 virus at MOI 1 for 24h and immunostained with DAPI (blue); cropped areas show ER morphology (N=30 cells from three independent experiments). Scale bars = 10µm. For evaluating significance of differences observed in a, b, c and d, a two-tailed Student's *t* test was used (*** indicates $p<0.0001$, NS for non-significant).

Supplementary figure 3. Mitochondria elongation is not a unique signature of influenza A H1N1 viruses

a, A549 cells infected (or not) with influenza A H1N1, influenza A H3N2 or influenza B (IBV) viruses at MOI 1 for 24h were immunostained with anti-TOMM20 antibody (green), anti-NP antibody (red) and DAPI (blue) and pictures were quantified for mitochondrial elongation from single cells (N=50 cells from three independent experiments); cropped areas show mitochondria morphology. **b**, MDCK cells infected (or not) with influenza A H1N1, influenza A H3N2 or IBV viruses at MOI 1 for 24h were immunostained with anti-TOMM20 antibody (green), anti-NP antibody (red) and DAPI (blue) and pictures were quantified for mitochondrial elongation from single cells (N=50 cells from three independent experiments); cropped areas show mitochondria morphology. Scale bars = 10µm. For evaluating significance of differences observed in a and b two-tailed Student's *t* test was used (*** indicates $p<0.0001$; NS for non-significant).

Supplementary figure 4. Expression of H1N1 dsRNA is sufficient to induce mitochondria elongation

a, A549 cells were transfected (or not) with an 87-mer 5'triphosphate hairpin RNA synthesized from a sequence of influenza A H1N1 virus genome (dsRNA) for 3h, 6h and 24h and IFNβsecretion was measured in cell supernatant (N=3). **b**, A549 cells transfected (or not) with dsRNA for 24h were immunostained with anti-TOMM20 antibody (green) and DAPI (blue); cropped areas show mitochondria morphology, elongated in transfected condition (N=3). **c**, Quantification of elongated mitochondria illustrated in (b) at 3h, 6h and 24h (N=3). Scale bars = 10µm. For evaluating significance of differences observed in a and c, a two-tailed Student's *t* test was used (*** indicates $p<0.0001$; NS for non-significant).

Supplementary figure 5. Mito-C treatment does not induce cell death

a, A549 cells treated for 48h with increasing and indicated concentrations of Mito-C, DMSO (vehicle) or culture media without vehicle were stained with propidium iodide (PI) and analyzed by cytometry (N=3). **b**, Lactate dehydrogenase (LDH) enzyme release was measured in supernatants of A549 cells treated for 48h with increasing concentrations of Mito-C or DMSO (N=3). For evaluating significance of differences observed in a and b, a two-tailed Student's *t* test (NS for non-significant).

MATERIALS AND METHODS

Cell lines and viruses

Human lung adenocarcinoma (A549, ATCC) and Madin-Darby Canine Kidney (MDCK, ATCC) cell lines were grown in Dulbecco's modified Eagle's medium (DMEM, Gibco) supplemented with 10% heat-inactivated fetal bovine serum (FBS, Pan Biotech) and 50 IU/ml penicillin G, 50 mg/ml streptomycin (Gibco), at 37°C under 5% CO_2. A549-Sec61β-GFP stable cell line was obtained after plasmid transfection (Addgene, 15108) using Fugene HD transfection Reagent (Promega, #E2311) following the manufacturer's instructions. 48h after transfection, transfected cells were submitted to selection by geneticin treatment (Themo Fisher, #0131035) at 1400µg/ml for 10 days. For CRISPR–Cas9-mediated RIG-I (DDX58) gene disruption, A549 cells stably expressing Cas9 were generated as described before (Doyle et al., 2018). Briefly, Cas9-expressing A549 cells were transduced with control or RIG-I guide RNA expressing Lentiguide-Neo vectors and selected with G418 (1mg/ml) for at least 15 days. The guide RNA coding sequences used were as follows: g1-CTRL 5' -AGCACGTAATGTCCGTGGAT, g2-CTRL 5′ -CAATCGGCGACGTTTTAAAT, g1-RIG-I 5' -GGGTCTTCCGGATATAATCC, g2-RIG-I 5' – TTGCAGGCTGCGTCGCTGCT. RIG-I CRISPR-Cas9 gene disruption was confirmed by western-blotting following IFNα treatment (INTRON A; Merck Sharp & Dohme, 1,000 U/ml) for 24 h. Influenza A virus A/New Caledonia/2006 (H1N1) (clinical isolate), influenza A virus A/H3N2/ Wyoming/2002 and Influenza B virus B/Virginia/2009 (ATCC 3VR-1784) were propagated in MDCK cells.

Infection experiments and Mito-C treatment

Two different experimental designs were used to carry out influenza infection experiments. To perform multi-round infection, A549 cells were infected with influenza A H1N1 virus at a multiplicity of infection (MOI) of 0.1 in infection medium (DMEM serum-free medium supplemented with 50 IU/ml penicillin, 50 mg/ml streptomycin and 0.2 mg/ml TPCK-trypsin (Sigma, #4352157)). After 48h, supernatants were harvested to test neuraminidase activity (Munana test) and viral titer (PFU). Cells were harvested as well to test viral protein levels in western blot. To perform single-round infection, A549 or MDCK cells were infected with the indicated influenza virus at MOI of 1 in infection medium. After 1h, cells were washed and the medium was replaced with warm DMEM medium supplemented with 10% heat inactivated FBS and 50 IU/ml penicillin G, 50 mg/ml streptomycin. At indicated times, cells were lysed to carry out western blot assays or fixed in 4% PFA to perform immunofluorescence assays. When indicated, Mito-C was added to A549 cells at the same time as influenza virus at the indicated concentrations. As negative control, the same amount of DMSO was used.

Neuraminidase assay

A fluorometric assay was used to detect influenza virus neuraminidase activity. This viral enzyme is able to cleave the 2′-(4-Methylumbelliferyl)-α-D-N-acetylneuraminic acid sodium salt hydrate (Munana, Sigma, #M8639), generating a fluorescent product that can thus be quantified. In 96-black plate, 25µl of infection supernatants were added to 75µl of 20 mM Munana in PBS containing Ca^{2+} and Mg^{2+}. After 1h incubation at 37°C, the reaction was stopped by adding 100µl of glycine 0.1 M and ethanol 25%. Fluorescence was recorded using TECAN Spark 20M at wavelengths of 365nm for excitation and 450nm for emission. The R statistical

software was used to perform the dose-response analysis (drc package) and plot the dose-response data and the associated logistic regression (ggplot2 library).

Plaque forming unit assay (PFU)

PFU assays were used to titer viral stocks and to determinate titer of Mito-C antiviral effect in infected cells. Briefly, supernatants from these two experiments were serial diluted following 1:3 dilution factor in infection medium. 500µL of each virus dilution was added to a monolayer of MDCK cells in 6-well plates. Cells were incubated 90 min for viral uptake and then virus was washed off. A mix of 2% SeaKem agarose (Lonza, #50011) and 2xMEM (Gibco) supplemented with 0.4µg/ml TPCK trypsin (1:1) were added to each well. Plates were incubated for 72 h at 37°C, 5%CO_2. Cells were fixed in a 10% PFA solution and then stained with crystal violet solution (0.3% crystal violet, 10% ethanol in water) for 30min at room temperature and abundantly rinsed with distilled water. Infectious titers were calculated considering the corresponding dilution factor after PFU numeration.

Western blot analyses

Western blot (WB) analyses were performed with precast gradient gels 4-12% Bis-Tris (Invitrogen) and 3-8% Tris-Acetate (for DRP1 and OPA1 detection) using standard methods. Briefly, cells were washed twice with cold PBS and lysed on ice in NP-40 buffer (150 mM NaCl, 20mM Tris-HCl at pH8, 1mM EDTA, 1% NP-40) for 20min in the presence of the complete protease inhibitor cocktail (Roche). The soluble fraction was recovered after centrifugation at 13000g for 20min, then protein concentration was measured by the BCA

protein assay kit (Pierce) using bovine serum albumin (BSA) as a standard. Protein lysates were diluted in Laemmli SDS sample buffer (Thermo Fisher) before being incubated for 10 min at 95°C. After transfer, PVDF membranes were blocked in 5% milk/Tween 0.1% buffer for 1h and incubated with primary antibodies overnight at 4° in 5% BSA/TBS - Tween 0.1% buffer. After secondary HRP antibody staining, membranes were visualized using ECL western blotting substrate (Thermo Fisher) and a Pxi Imaging System (Syngene). Quantification of band intensity was carried out using Image J software.

Immunofluorescence and confocal microscopy

For immunofluorescence analysis (IF), cells were plated on 12-mm glass coverslips and fixed with 4% paraformaldehyde (Sigma) in PBS for 20 min at room temperature. After 3 washes of 10 min each in PBS, cells were blocked with fetal bovine serum (10%) in PBS for 30min. Incubation with primary antibodies was performed in permeabilization buffer (0.05% saponin in 10% FBS-PBS buffer). Coverslips were mounted on microscope slides using prolong diamond antifade mountant with DAPI (Thermo Fisher, #P36962). Images were obtained using a 63x/1.4 oil-immersion objective with Leica TCS SP5 confocal microscope, using a 405 nm diode laser line exciting DAPI, a 488 nm argon laser line exciting Alexa Fluor 488, a 561 nm diode laser line for Alexa Fluor 546 and laser He/Ne 633 nm for Alexa 647. Acquisitions were done in sequential mode and fluorescence acquired in separated channels.

Antibodies and dilutions

Primary antibodies used were the following: mouse anti-TOMM20 (BD Biosciences 612278, 1:1000 for IF); rabbit anti-TOMM20 (Abcam ab186734, 1:1000 for IF); mouse anti- DRP1(BD Biosciences 611112 , 1:500 for WB and IF); rabbit anti- OPA-1 (Cell signaling 67589, 1:500 for WB); mouse anti-GM130 (BD Biosciences 610823, 1:500 in IF); rabbit anti-LAMP1 (Abcam ab24170, 1:500 in IF); mouse anti-EEA1 (BD Biosciences 610456, 1:1000 in IF); rabbit anti-LC3 (MBL PM036, 1:1000 in IF); mouse anti beta-actin (Sigma A1978; 1:1000 for WB); rabbit anti-influenza A virus M2 protein (Abcam ab5416; 1:1000 for IF); mouse anti-influenza A virus nucleoprotein (Abcam ab128193, 1:1000 in IF and WB); mouse anti-influenza B virus nucleoprotein (Abcam ab20711, 1:1000 in IF); RIG-I (Covalab, 102466, 1:100 in WB). For secondary antibodies, we used for immunofluorescence an Alexa 488 conjugated donkey anti-mouse (Invitrogen #A21202, 1:800), Alexa 488 conjugated donkey anti-rabbit (Invitrogen #A21206, 1:800), Alexa 647 conjugated donkey anti-mouse (Invitrogen #A31571, 1:800), Alexa 647 conjugated donkey anti-rabbit (Invitrogen #A31573, 1:800). For western blotting we used Secondary HRP conjugate anti-rabbit IgG (GE Healthcare, 1:10000) and HRP conjugate anti-mouse IgG (Bio-Rad 1:10000).

Transmission electron microscopy

Cells were fixed for 1h at room temperature with 2% glutaraldehyde in 0.1µM sodium cacodylate buffer at pH7.4. Samples were then rinsed three times of 10min each in 0.1µM sodium cacodylate buffer and post-fixed with 1% osmium tetroxide in 0.1µM sodium cacodylate buffer for 30 min. Contrast was done in uranyl acetate 1% for 30min, then the samples were dehydrated in a graded series of ethanol ending with 100% ethanol. Samples were then

embedded in EPON. About 70nm sections were prepared with a Leica Ultracut 7 ultramicrotome. The sections were observed using a Philips CM120 electron microscope operating at 120 kV. Images were captured using a GATAN Orius 200 camera.

Live imaging microscopy

A549 cells were seeded in each compartment of Cellview cell culture dishes (4 compartments, glass bottom, Greiner). The following day, cells were infected with influenza A H1N1 virus at MOI of 1 in a final volume of serum-free DMEM of 250 µl. After 1h incubation at 37°C, the inoculum was removed and 500µl of live microscopy media (DMEM containing no phenol red supplemented with L-glutamine, pyruvate, 10% serum and antibiotics) containing MitoTracker Orange CM-H_2TMRos (ThermoFisher, dilution 1 :10 000) was added. Uninfected control cells were treated in the same way. Image acquisition was performed using a Nikon inverted microscope (EclipseTi2) coupled with a Dragonfly spinning disk unit (Andor, Oxford Instruments Company). An oil immersion objective (100X Plan Apo lambda, numerical aperture (NA) 1.45 0.13mm) was used. Acquisitions were performed every 5 minutes for 15h (3 fields per condition). A z step of 1µm was used for the z-stacks.

RNA extraction and qPCR analyses

RNA was extracted from A549 cells using RNeasy mini kit (Qiagen, 74106) according to the manufacturer's instructions. After DNA digestion with Ambion Turbo DNase (Thermo Fisher, "AM2238), 500ng of RNA were subjected to reverse transcription by using the High-Capacity RNA-to-cDNA kit (Thermo Fisher, "4387406). The obtained cDNA was then used for IFNβ and

IFNλ1 detection by qPCR with FastStart Universal SYBR green PCR master mix (Roche) using a Light Cycler 480 II (Roche). The following primers were used: IFNβ forward: CGCCGCATTGACCATCTA, IFNβ reverse: GACATTAGCCAGGAGGTTCTC, IFNλ1 forward: GCAGGTTCAAATCTCTGTCACC, IFNλ1 reverse: AAGACAGGAGAGCTGCAACTC.

dsRNA transfection and interferon measurement

A549 cells were transfected with 3p-hpRNA 5' triphosphate hairpin RNA, a 87-mer synthesized from a sequence of influenza A H1N1 virus (Invivogen, tlrl-hprna) using Lyovec reagent for transfection following the manufacturer's protocol (Invivogen, lyec-12). After 3h, 6h and 24h cells were fixed in PFA 4% for immunofluorescence assays and supernatants were harvested for interferon beta (IFNβ) quantification. IFNβ measurement was performed using verikine-HS human IFN beta serum ELISA Kit (PBL assay science, 41415-1) following manufacturer's instructions.

Toxicity assays

A549 cells were treated for 48h at indicated concentrations with Mito-C. As negative control, the same amount of DMSO was used. Two different tests were performed. First, cell death was quantified by a propidium iodide (PI) assay according to the manufacturer's protocol (Thermo Fisher, #P1304MP). Data were analyzed on a BD Accuri C6 Plus flow cytometer (BD Biosciences) and processed using BD Accuri C6 software (BD Biosciences). Second, levels of lactate dehydrogenase (LDH) in supernatants were quantified using the cytotoxicity detection kit

(Roche, #11644793001) following manufacturer's instructions. Absorbance was recorded using TECAN Spark 20M at wavelengths of 496nm.

Image analysis and statistics

Image analysis was performed using Image J, ICY and Zeiss ZEN softwares. For mounting representative images, background was reduced using brightness and contrast adjustments applied to the whole image. For analyzing the recruitment of DRP1 on mitochondria, a mask on the fluorescence in TOMM20 channel was used to define the region to measure the total intensity of the DRP1 signal in the DRP1 channel. For statistics of data we used GraphPad Prism software. After evaluation of mean, standard deviation and standard errors we evaluate data distributions using normality test: KS normality test, D'Agostino & Pearson omnibus normality test and Shapiro-Wilk normality test. Data where processed as normally distributed when at least 2 out of 3 tests resulted positive, otherwise they were processed as non-parametric distributions. Gaussian distributions were analyzed with the more appropriate t-test or ANOVA and non-Gaussian distributed sets of data were evaluated with the more appropriate non-parametric test, Mann-Whitney or ANOVA, as specified in figure legends.

REFERENCES

Abraham, G.M., Morton, J.B., and Saravolatz, L.D. (2020). Baloxavir: A Novel Antiviral Agent in the Treatment of Influenza. Clin. Infect. Dis.

de Armas-Rillo, L., Valera, M.-S., Marrero-Hernández, S., and Valenzuela-Fernández, A. (2016). Membrane dynamics associated with viral infection. Rev. Med. Virol. *26*, 146–160.

Castanier, C., Garcin, D., Vazquez, A., and Arnoult, D. (2010). Mitochondrial dynamics regulate the RIG-I-like receptor antiviral pathway. EMBO Rep. *11*, 133–138.

Chatel-Chaix, L., Cortese, M., Romero-Brey, I., Bender, S., Neufeldt, C.J., Fischl, W., Scaturro, P., Schieber, N., Schwab, Y., Fischer, B., et al. (2016). Dengue Virus Perturbs Mitochondrial Morphodynamics to Dampen Innate Immune Responses. Cell Host Microbe *20*, 342–356.

Combs, J.A., Norton, E.B., Saifudeen, Z.R., Bentrup, K.H.Z., Katakam, P. V, Morris, C.A., Myers, L., Kaur, A., Sullivan, D.E., and Zwezdaryk, K.J. (2019). Human Cytomegalovirus Alters Host Cell Mitochondrial Function during Acute Infection. J. Virol. *94*.

Doyle, T., Moncorgé, O., Bonaventure, B., Pollpeter, D., Lussignol, M., Tauziet, M., Apolonia, L., Catanese, M.T., Goujon, C., and Malim, M.H. (2018). The interferon-inducible isoform of NCOA7 inhibits endosome-mediated viral entry. Nat. Microbiol. *3*, 1369–1376.

Horner, S.M., Liu, H.M., Park, H.S., Briley, J., and Gale, M. (2011). Mitochondrial-associated endoplasmic reticulum membranes (MAM) form innate immune synapses and are targeted by hepatitis C virus. Proc. Natl. Acad. Sci. U. S. A. *108*, 14590–14595.

Hornung, V., Ellegast, J., Kim, S., Brzózka, K., Jung, A., Kato, H., Poeck, H., Akira, S., Conzelmann, K.K., Schlee, M., et al. (2006). 5′-Triphosphate RNA is the ligand for RIG-I. Science (80-.). *314*, 994–997.

Hsu, J., Santesso, N., Mustafa, R., Brozek, J., Chen, Y.L., Hopkins, J.P., Cheung, A., Hovhannisyan, G., Ivanova, L., Flottorp, S.A., et al. (2012). Antivirals for treatment of influenza: A systematic review and meta-analysis of observational studies. Ann. Intern. Med. *156*, 512–524.

Ishii, K.J., Coban, C., Kato, H., Takahashi, K., Torii, Y., Takeshita, F., Ludwig, H., Sutter, G., Suzuki, K., Hemmi, H., et al. (2006). A Toll-like receptor-independent antiviral response induced by double-stranded B-form DNA. Nat. Immunol. *7*, 40–48.

Iuliano, A.D., Roguski, K.M., Chang, H.H., Muscatello, D.J., Palekar, R., Tempia, S., Cohen, C., Gran, J.M., Schanzer, D., Cowling, B.J., et al. (2018). Estimates of global seasonal influenza-associated respiratory mortality: a modelling study. Lancet *391*, 1285–1300.

Kawai, T., Takahashi, K., Sato, S., Coban, C., Kumar, H., Kato, H., Ishii, K.J., Takeuchi, O., and Akira, S. (2005). IPS-1, an adaptor triggering RIG-I- and Mda5-mediated type I interferon induction. Nat. Immunol. *6*, 981–988.

Killip, M.J., Fodor, E., and Randall, R.E. (2015). Influenza virus activation of the interferon system. Virus Res. *209*, 11–22.

Kim, S.-J., Khan, M., Quan, J., Till, A., Subramani, S., and Siddiqui, A. (2013). Hepatitis B Virus Disrupts Mitochondrial Dynamics: Induces Fission and Mitophagy to Attenuate Apoptosis. PLoS Pathog. *9*, e1003722.

Lee, H., and Yoon, Y. (2018). Mitochondrial membrane dynamics—functional positioning of OPA1. Antioxidants *7*.

Meylan, E., Curran, J., Hofmann, K., Moradpour, D., Binder, M., Bartenschlager, R., and Tschopp, J. (2005). Cardif is an adaptor protein in the RIG-I antiviral pathway and is targeted by hepatitis C virus. Nature *437*, 1167–1172.

Miller, S., and Krijnse-Locker, J. (2008). Modification of intracellular membrane structures for virus replication. Nat. Rev. Microbiol. *6*, 363–374.

Pichlmair, A., Schulz, O., Tan, C.P., Näslund, T.I., Liljeström, P., Weber, F., and Reis e Sousa, C. (2006). RIG-I-mediated antiviral responses to single-stranded RNA bearing 5'-phosphates. Science *314*, 997–1001.

Seth, R.B., Sun, L., Ea, C.-K., and Chen, Z.J. (2005). Identification and characterization of MAVS, a mitochondrial antiviral signaling protein that activates NF-kappaB and IRF 3. Cell *122*, 669–682.

Shi, C.-S., Qi, H.-Y., Boularan, C., Huang, N.-N., Abu-Asab, M., Shelhamer, J.H., and Kehrl, J.H. (2014). SARS-coronavirus open reading frame-9b suppresses innate immunity by targeting mitochondria and the MAVS/TRAF3/TRAF6 signalosome. J. Immunol. *193*, 3080–3089.

Vernay, A., Marchetti, A., Sabra, A., Jauslin, T.N., Rosselin, M., Scherer, P.E., Demaurex, N., Orci, L., and Cosson, P. (2017). MitoNEET-dependent formation of intermitochondrial junctions. Proc. Natl. Acad. Sci. U. S. A. *114*, 8277–8282.

Xu, L.-G., Wang, Y.-Y., Han, K.-J., Li, L.-Y., Zhai, Z., and Shu, H.-B. (2005). VISA is an adapter protein required for virus-triggered IFN-beta signaling. Mol. Cell *19*, 727–740.

Yadav, V., Panganiban, A.T., Honer Zu Bentrup, K., and Voss, T.G. (2016). Influenza infection modulates vesicular trafficking and induces Golgi complex disruption. Virusdisease *27*, 357–368.

Yoshizumi, T., Ichinohe, T., Sasaki, O., Otera, H., Kawabata, S.I., Mihara, K., and Koshiba, T. (2014). Influenza a virus protein PB1-F2 translocates into mitochondria via Tom40 channels and impairs innate immunity. Nat. Commun. *5*, 6–10.

Zhang, R., Chi, X., Wang, S., Qi, B., Yu, X., and Chen, J.-L.L. (2014). The regulation of autophagy by influenza A virus. Biomed Res. Int. *2014*, 498083.

Zhou, Z., Jiang, X., Liu, D., Fan, Z., Hu, X., Yan, J., Wang, M., and Gao, G.F. (2009). Autophagy is involved in influenza A virus replication. Autophagy *5*, 321–328.

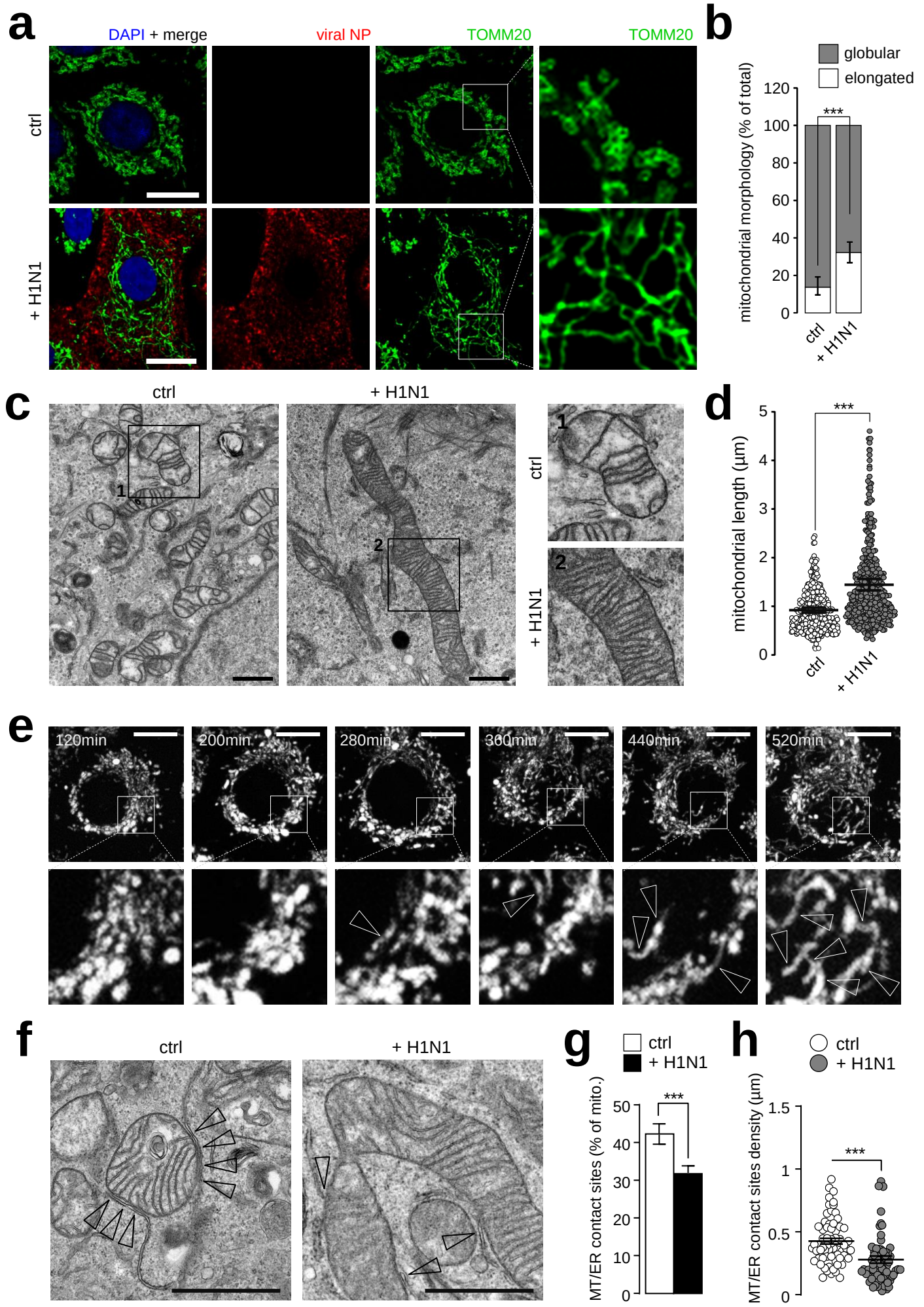
a
DAPI + merge
viral NP
TOMM20
TOMM20
ctrl
+ H1N1
b
globular
elongated
mitochondrial morphology (% of total)
120
100
80
60
40
20
0
***
ctrl
+ H1N1
c
ctrl
+ H1N1
1
2
ctrl
+ H1N1
d
mitochondrial length (µm)
5
4
3
2
1
0
***
ctrl
+ H1N1
e
120min
200min
280min
360min
440min
520min
f
ctrl
+ H1N1
g
ctrl
+ H1N1
MT/ER contact sites (% of mito.)
50
40
30
20
10
0
***
h
ctrl
+ H1N1
MT/ER contact sites density (µm)
1.5
1
0.5
0
***

Figure 1

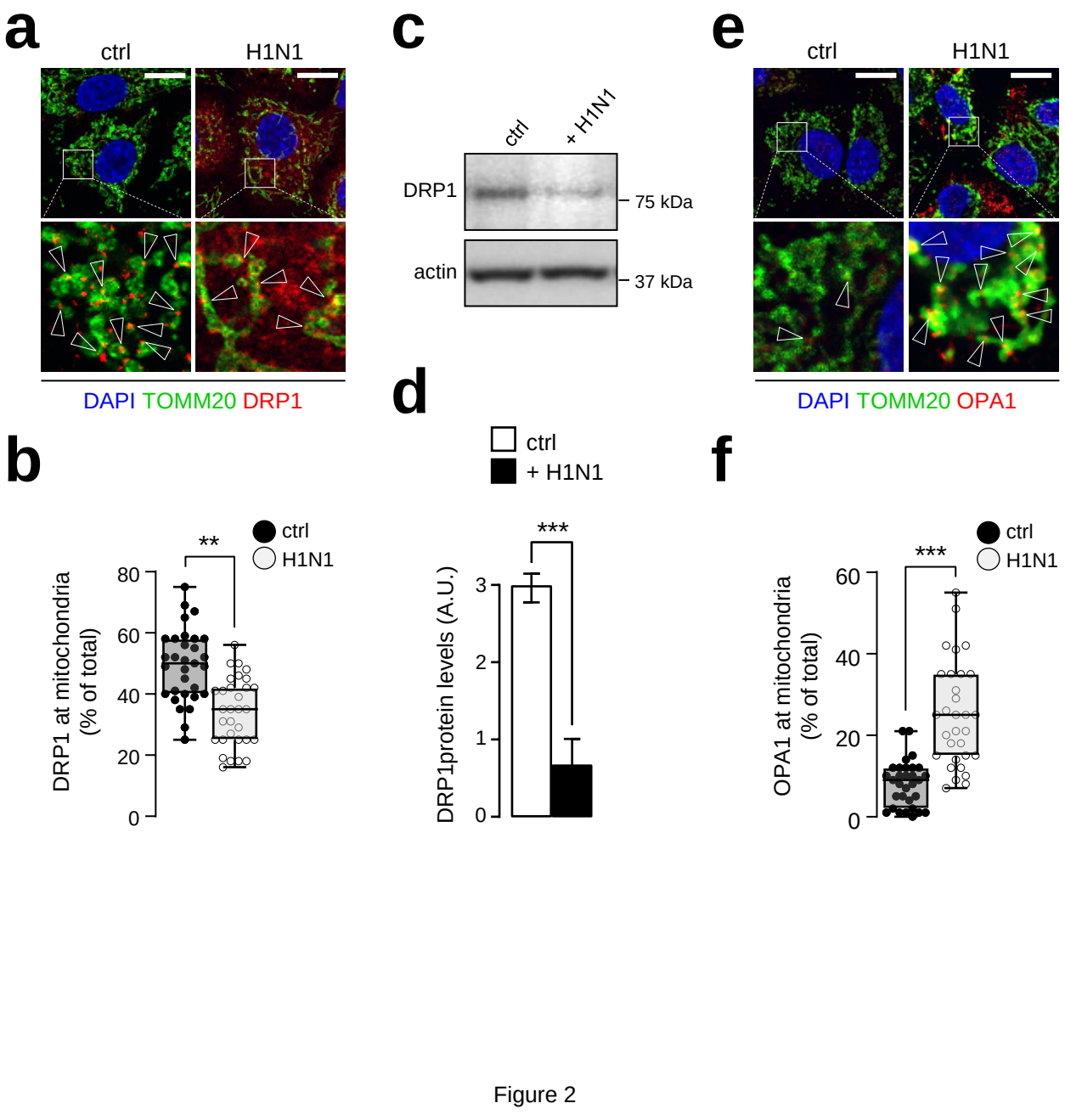
a
ctrl
H1N1
DAPI TOMM20 DRP1
c
ctrl
+ H1N1
DRP1
75 kDa
actin
37 kDa
e
ctrl
H1N1
DAPI TOMM20 OPA1
b
ctrl
H1N1
**
DRP1 at mitochondria (% of total)
0
20
40
60
80
d
ctrl
+ H1N1
***
DRP1protein levels (A.U.)
0
1
2
3
f
ctrl
H1N1
***
OPA1 at mitochondria (% of total)
0
20
40
60

Figure 2

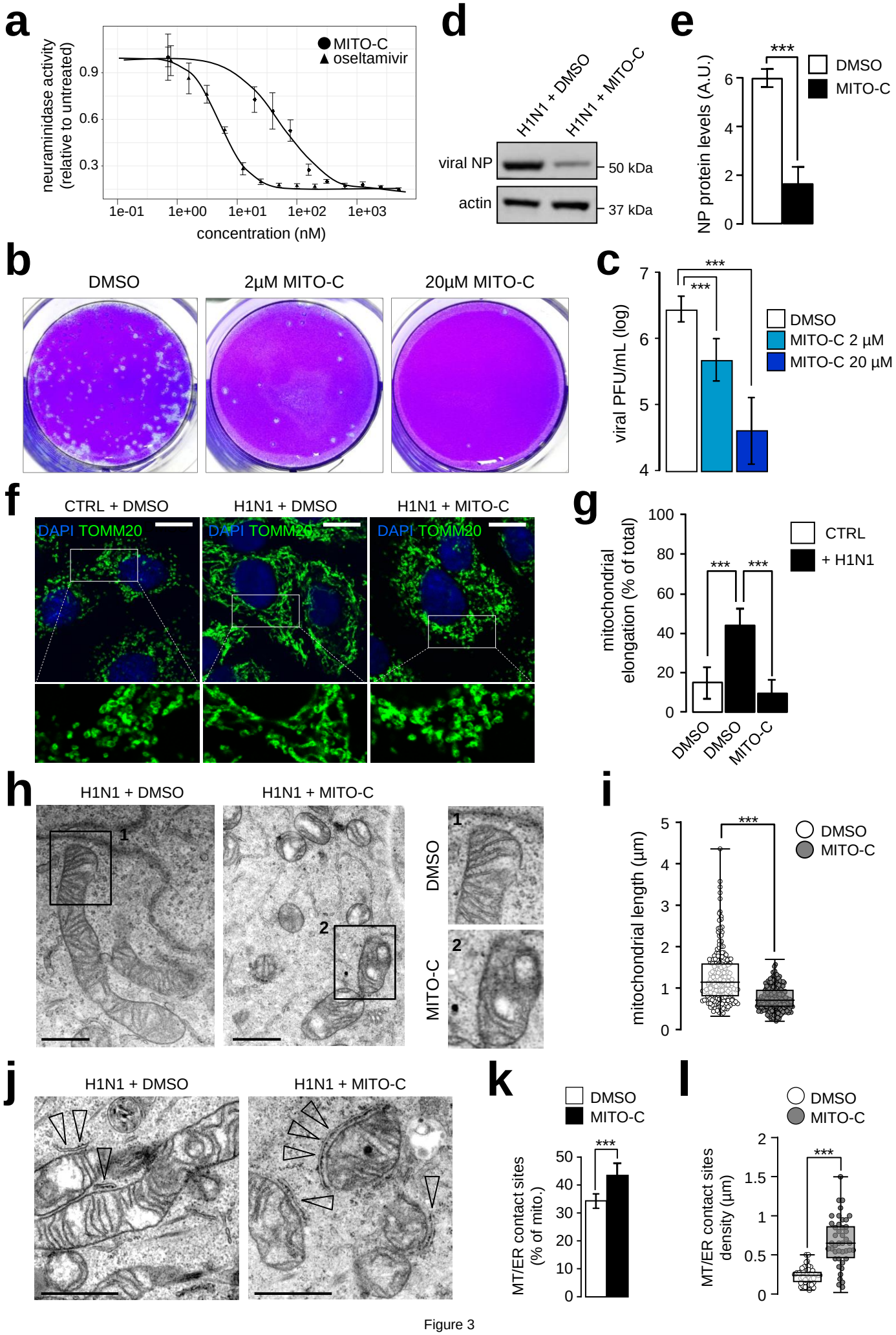
a
neuraminidase activity (relative to untreated)
0.9
0.6
0.3
MITO-C
oseltamivir
1e-01
1e+00
1e+01
1e+02
1e+03
concentration (nM)
d
H1N1 + DMSO
H1N1 + MITO-C
viral NP
50 kDa
actin
37 kDa
e
NP protein levels (A.U.)
***
DMSO
MITO-C
b
DMSO
2µM MITO-C
20µM MITO-C
c
viral PFU/mL (log)
***
***
DMSO
MITO-C 2 µM
MITO-C 20 µM
f
CTRL + DMSO
H1N1 + DMSO
H1N1 + MITO-C
DAPI TOMM20
g
mitochondrial elongation (% of total)
***
***
CTRL
+ H1N1
DMSO
DMSO
MITO-C
h
H1N1 + DMSO
H1N1 + MITO-C
1
2
DMSO
MITO-C
i
mitochondrial length (µm)
***
DMSO
MITO-C
j
H1N1 + DMSO
H1N1 + MITO-C
k
MT/ER contact sites (% of mito.)
***
DMSO
MITO-C
l
MT/ER contact sites density (µm)
***
DMSO
MITO-C

Figure 3

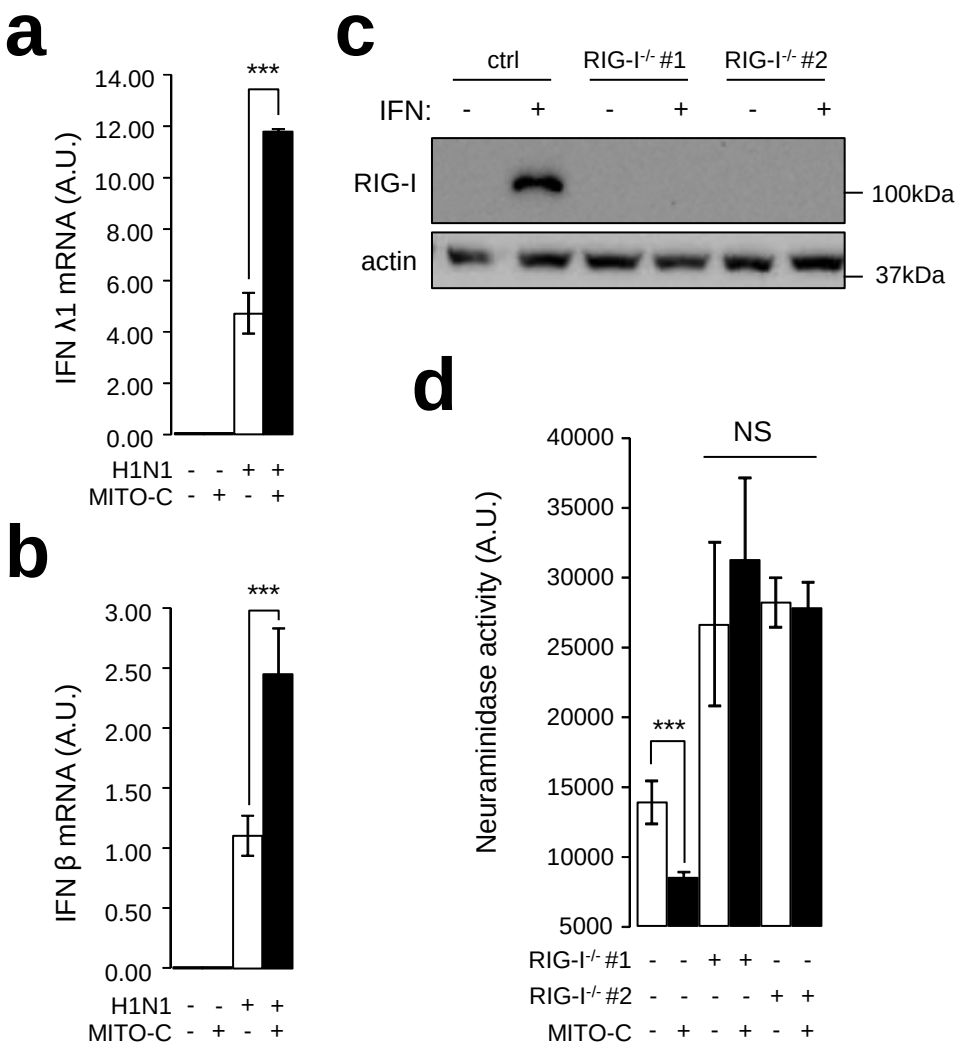
a
IFN λ1 mRNA (A.U.)
14.00
12.00
10.00
8.00
6.00
4.00
2.00
0.00
***
H1N1 - - + +
MITO-C - + - +
b
IFN β mRNA (A.U.)
3.00
2.50
2.00
1.50
1.00
0.50
0.00
***
H1N1 - - + +
MITO-C - + - +
c
ctrl
RIG-I-/- #1
RIG-I-/- #2
IFN: - + - + - +
RIG-I
actin
100kDa
37kDa
d
Neuraminidase activity (A.U.)
40000
35000
30000
25000
20000
15000
10000
5000
NS
***
RIG-I-/- #1 - - + + - -
RIG-I-/- #2 - - - - + +
MITO-C - + - + - +

Figure 4

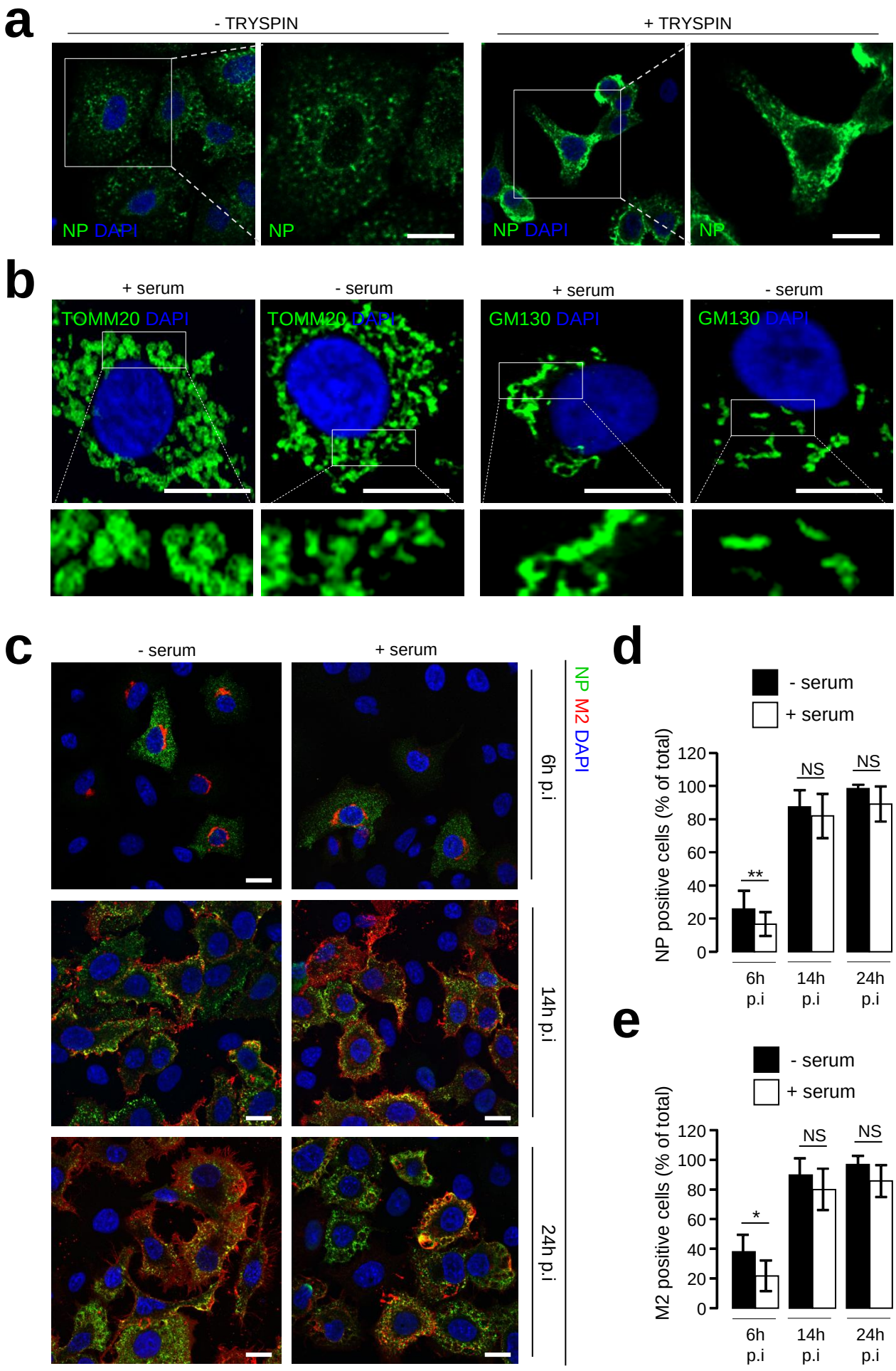

Supplementary Figure 1

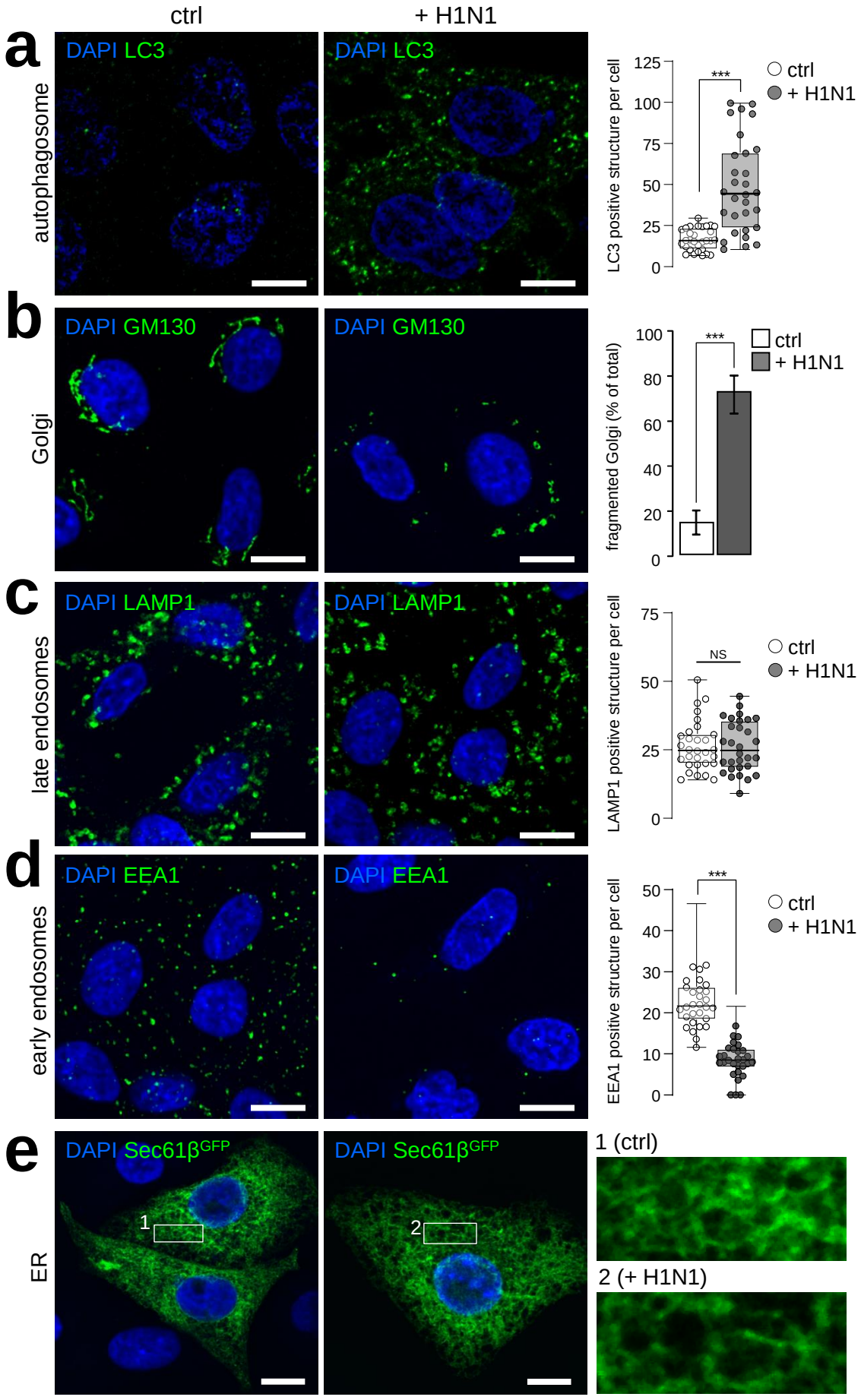

Supplementary Figure 2

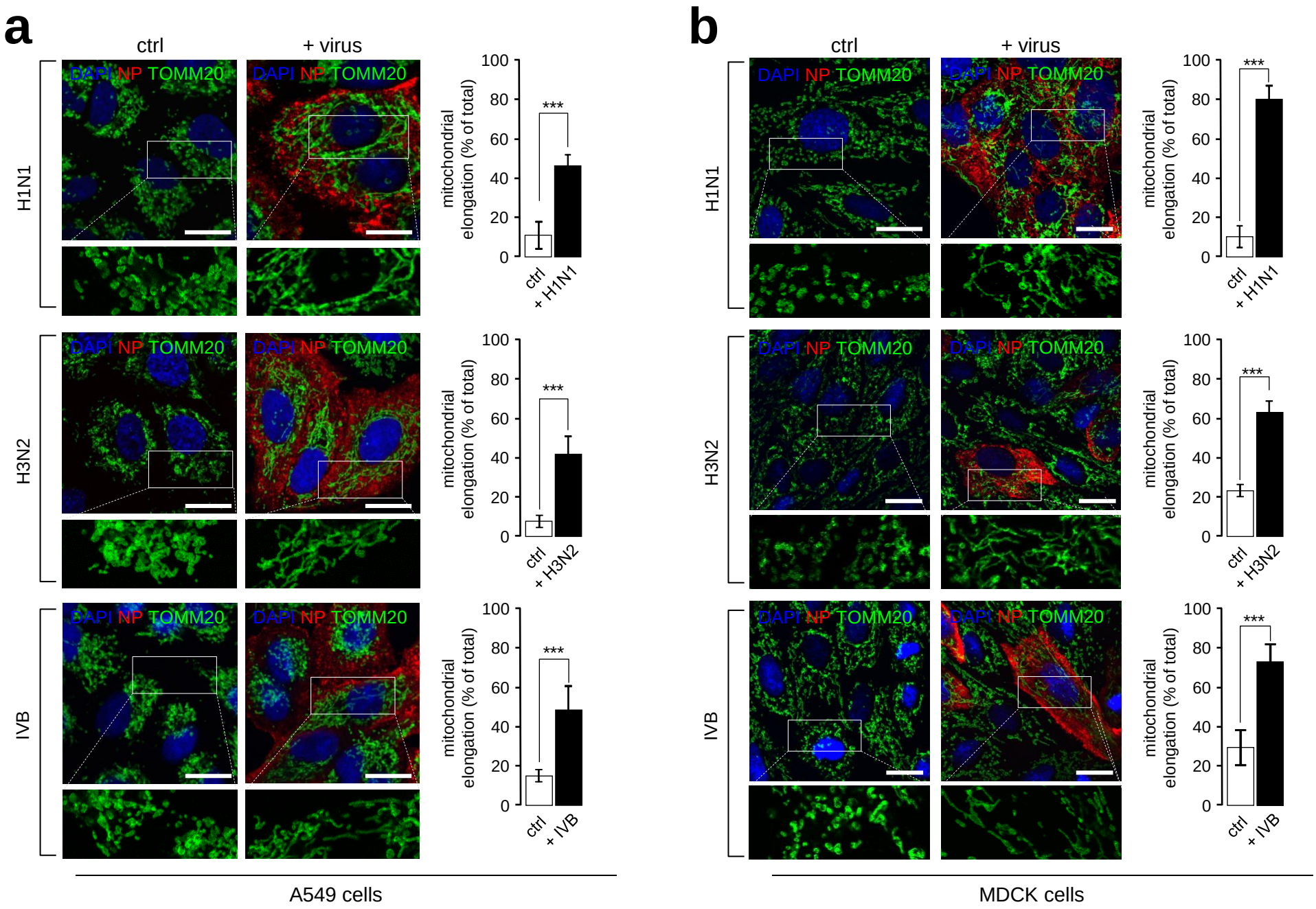

Supplementary Figure 3

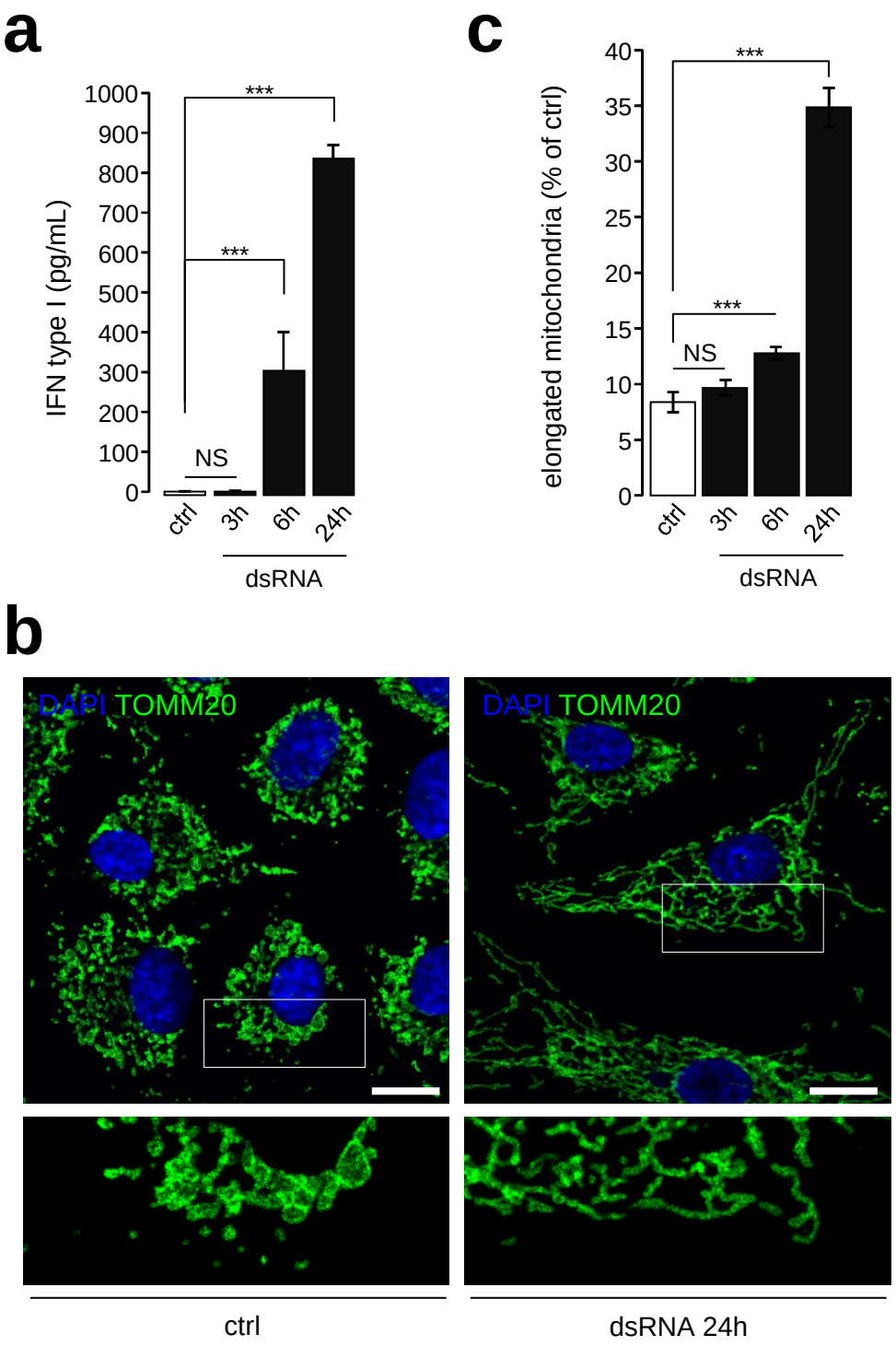

Supplementary Figure 4

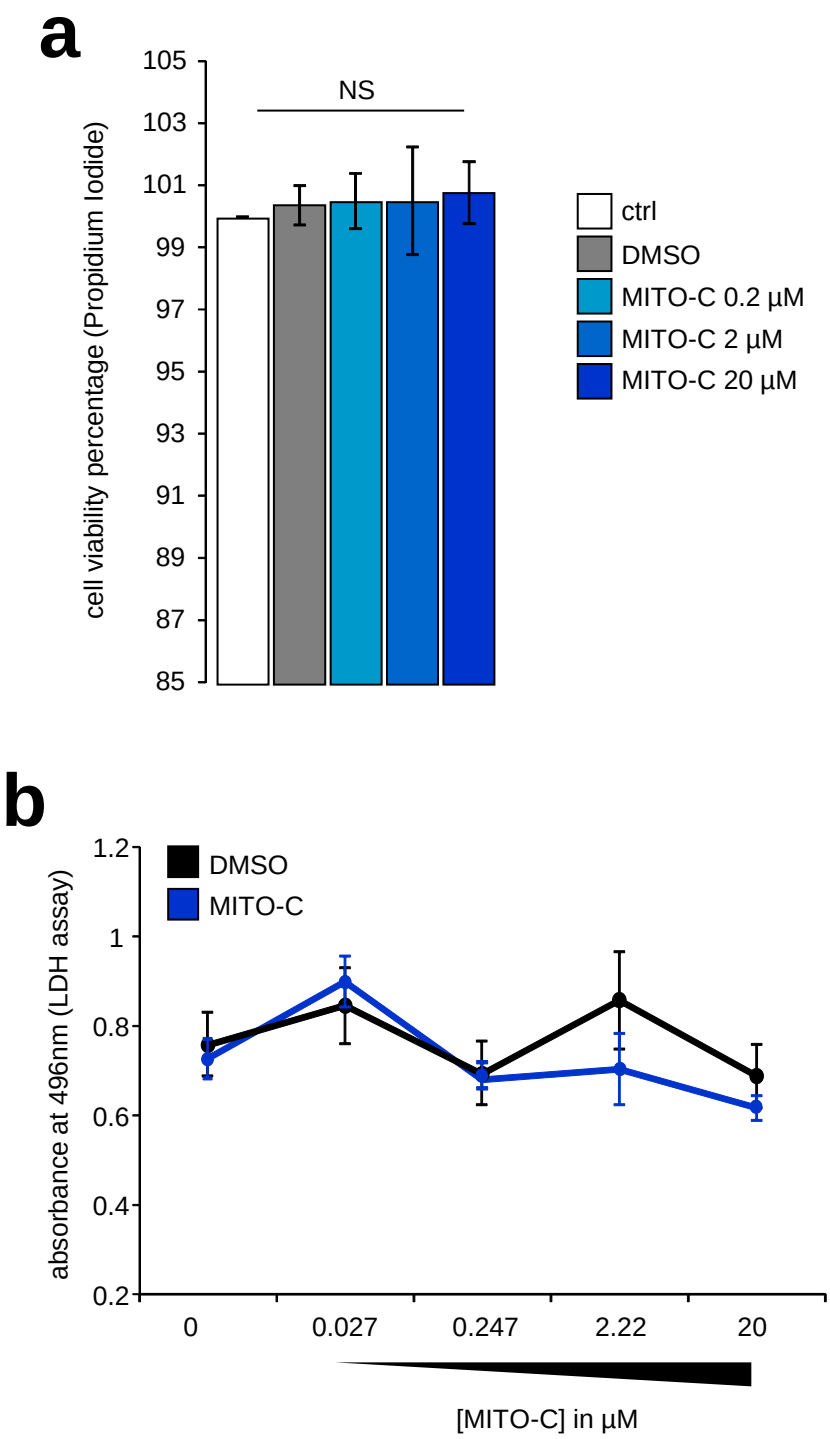

Supplementary Figure 5

MANUSCRIPT 2

Chemical targeting of NAF-1 protein reveals its function in mitochondrial morphodynamics

Chemical targeting of NEET proteins reveals their function in mitochondrial morphodynamics.

Diana Molino[1*], Irene Pila-Castellanos[1,2*], Henri-Baptiste Marjault[3], Leila Rochin[4], Ola Karmi[3], Yang-Sung Sohn[3], Laetitia Lines[2], Ahmed Hamaï[1], Stéphane Joly[2], Pauline Radreau[2], Jacky Vonderscher[2], Patrice Codogno[1], Francesca Giordano[4], Alessia Ruggieri[5], Peter Machin[2], Eric Meldrum[2], Rachel Nechushtai[3], Benoit de Chassey[2] and Etienne Morel[1]

[1]Institut Necker-Enfants Malades (INEM), INSERM U1151-CNRS UMR 8253, Université Paris Descartes-Sorbonne Paris Cité, 75014 Paris, France.
[2]ENYO-Pharma, Bâtiment Domilyon, 321 avenue Jean Jaurès, 69007 Lyon, France
[3]The Alexander Silberman Institute of Life Science, the Hebrew University of Jerusalem, Edmond J. Safra Campus at Givat Ram, Jerusalem 91904, Israel.
[4]Institute for Integrative Biology of the Cell (I2BC), CEA, CNRS, Paris-Sud University, Paris-Saclay University, Gif-sur-Yvette, Cedex 91198, France
[5]Department of Infectious Diseases, Molecular Virology, Centre for Integrative Infectious Disease Research (CIID), University of Heidelberg, Heidelberg, Germany
*equal authorship

Correspondence:
Benoit de Chassey bdc@enyopharma.com and Etienne Morel etienne.morel@inserm.fr

Abstract

Several human pathologies including neurological, cardiac, infectious, cancerous and metabolic diseases have been associated with altered mitochondria morphodynamics. Here we identify a small organic molecule, we named Mito-C, which is addressed to mitochondria and rapidly provokes mitochondrial network fragmentation. Biochemical analyses reveal that Mito-C is a member of a novel class of heterocyclic compounds that target the NEET protein family, previously reported to regulate mitochondrial iron and ROS homeostasis. One of the NEET proteins, NAF-1, is shown for the first time to be an important regulator of mitochondria morphodynamics by facilitating recruitment of DRP1 to the ER-mitochondria interface. Consistently with observation that certain viruses modulate mitochondrial morphogenesis as a necessary part of their replication cycle, Mito-C counteracts Dengue induced mitochondrial network hyperfusion and represses viral replication. The novel chemical class to which Mito-C belongs is of therapeutic relevance in pathologies where altered mitochondria dynamics is part of disease etiology and NAF-1 is highlighted as an important therapeutic target in antiviral research.

Introduction

Mitochondria are double membrane organelles essential for energy homeostasis in eukaryotes but also critical for regulating iron and calcium homeostasis, redox regulation, autophagy, innate immunity and cell death [1]. A broad range of diseases, including viral infections, have been associated with irregular mitochondria morphology and dynamics, highlighting the central role of mitochondrial network dynamics in the maintenance of cellular homeostasis [2]. Regulation of mitochondrial morphology is a consequence of a balance between fission and fusion events that maintain mitochondria number, size and shape [3]. This dynamic equilibrium enables adaptation to a wide range of stress situations. Moreover, mitochondria are physically bound to the endoplasmic reticulum (ER), via ER-Mitochondrial contact sites (ER-MTcs). ER-MTcs engage multiple proteins, from both ER and mitochondria and are involved in a wide range of cellular functions, including autophagosome biogenesis and mitochondrial fission. A critical regulator of the mitochondrial fission process is the cytosolic GTPase dynamin-related protein 1 (DRP1), which relocates to the mitochondrial surface to promote mitochondrial network fragmentation [4]. Interestingly, DRP1 recruitment to ER-MTcs defines the position of the mitochondrial division site [5], although how this directed recruitment occurs still remains unclear.

In addition to proteins involved in fission/fusion regulation, many other proteins of critical importance to cell function such as the respiratory chain, innate immunity, redox regulation and iron homeostasis are located on or in the mitochondria. Among these mitochondria-associated proteins are members of the NEET family which regulate iron and reactive oxygen species (ROS) homeostasis in the mitochondria [6–8]. There are three NEET proteins: MitoNEET, NAF-1 and MiNT and they are reported to localize at the mitochondria matrix (MiNT), the outer-mitochondrial membrane (MitoNEET and NAF-1) and the Endoplasmic Reticulum (NAF-1). Their unique ability to reversibly bind the redox active [2Fe-2S] cluster enables their function as iron-sulfur transfer proteins transferring [2Fe-2S] clusters out of the mitochondria [9,10]. MitoNEET has been associated with the regulation of oxidative phosphorylation in mitochondria [11] and deletion of its gene (*cisd1*) alters the integrity of inter-mitochondrial junctions [12]. In human, frame shift mutations in the *cisd2* gene encoding NAF-1 result in the autosomal recessive disorder Wolfram Syndrome Type 2 (WFS2), characterized at the cellular level by mitochondria dysfunctions, iron accumulation in mitochondria, increased autophagy and cell death. In contrast to MitoNEET and NAF-1, MiNT is less characterized. Recently the crystal structure of MiNT has been resolved and its contribution to tumorigenesis explored, especially in correlation with iron and ROS

homeostasis in cancer cells [13]. Despite the numerous studies connecting NEET proteins to different mitochondrial disorders, no functional connection has been made to infectious diseases.

Here we find that Mito-C, a compound not previously described, targets the NEET protein NAF-1, modifies mitochondrial morphology and dynamics and is able to counteract Dengue-induced mitochondria network hyperfusion and to strongly reduce Dengue virus replication. Furthermore, via pharmacological and genetic approaches we here also reveal the central role of NEET proteins in regulation of mitochondrial membrane dynamics via the ER-mitochondria associated fission machinery.

Results

We synthesized a novel small molecule, Mito-C (2-[(3,4-Dimethoxybenzoyl)amino]-6,6-dimethyl-5,7-dihydro-4H-benzothiophene-3-carboxylic acid, Fig1a) that was selected for its ability to affect the morphology of the mitochondrial network without adverse impact upon cell viability. The mitochondrial morphology modification was quantified using an unbiased image analysis method based on an immunofluorescence parameter termed skewness. This reflects the symmetry of the network as determined by the distribution of mitochondrial fluorescent staining in 2D space (FigS1a). In a dose dependent manner (0.2µM to 2µM, FigS1b and S1c), Mito-C rapidly induces mitochondrial network fragmentation (Fig1b and 1c), with no evidence of cell death following much longer treatment (24 hours) at concentrations up to 20µM (FigS2a and S2b). The Mito-C associated mitochondrial fragmentation observed after 15 minutes of treatment was reversible, with cells recovering normal mitochondria following wash out and overnight culture (FigS2c and S2d).

To determine the protein binding target of Mito-C we used a photo-affinity labeling based method (Capture Compound Mass Spectrometry) to identify the cellular target of Mito-C. Mito-C was synthesized with a photo-reactive function for covalent cross-linking to bound protein and a sorting function for isolation of bound protein and identification by mass spectrometric analysis [14]. This approach revealed interaction of the capture compound with the NEET protein MiNT. To examine the functional effect of Mito-C upon NEET proteins, possible effect upon the rate of release of the [2Fe-2S] cluster from each purified NEET protein was tested with or without Mito-C or an inactive analogue Mito-N (a structural analogue of Mito-C with no effect upon the morphology of the mitochondrial network). As shown in Fig1d (for NAF-1) and FigS3 (for MitoNEET and MiNT) the presence of Mito-C significantly enhanced the stability of NAF1, MitoNEET and MiNT for their bound [2Fe-2S] cluster thus in effect inhibiting their Fe/2Fe-2S transfer function. Such a functional test proved the physical binding of Mito-C to NEET proteins.

MiNT and MitoNEET have both been reported to localize exclusively to the mitochondrial matrix and outer membrane respectively [15]. However, NAF1 has been reported to localize to both the ER ([16] [15] and FigS4a), to the mitochondria-associated membranes [17] and MT outer membranes [18] and FigS4b). We now show that NAF-1 is localized at ER and ER-MT interface subdomains (FigS4c) using PTPIP51 as marker of ER-MTcs [19,20]. To strengthen the hypothesis that Mito-C elicits its effects in cells by modulating NEET protein function, a fluorescent-tagged version of Mito-C (^{fluo}Mito-C) was generated by linking the 7-nitrobenzofurazan green fluorescent tag on the para position of the right hand phenol ring (Fig 1a). Live microscopy imaging revealed that ^{fluo}Mito-C targets both mitochondria (MT) and

Endoplasmic Reticulum (ER) as illustrated by the colocalization between ^{fluo}Mito-C and the MT live probe mitotracker RedOx or the ER marker Sec61-RFP (FigS5a and FigS5b). The colocalization observed between the NAF1-RFP and ^{fluo}Mito-C further indicates that the NEET proteins and Mito-C are localized to the same cellular compartments (Fig1e). Altogether, our data indicate that Mito-C targets NEET proteins by inhibiting their [2Fe-2S] transfer function and initiates immediate and reversible MT network fragmentation.

To address whether the MT induced fragmentation correlates with impairment of the energetic capacity of MT, we measured the mitochondrial oxygen consumption rate (OCR) and the MT transmembrane potential following treatment with Mito-C (FigS6). No significant changes in MT respiration or membrane potential are observed in treatment between 15 minutes and 2h (FigS6a, S6b and S6c). Furthermore, no effect on MT mass was observed (FigS6d and S6e). These data reveal that the observed phenotypes are due to changes in mitochondria morphodynamics and suggest that the morphology and function of the MT network are not necessary coupled. To determine the contribution of NEET proteins to the observed effects of Mito-C, we analyzed the impact of siRNA-mediated knock down of each NEET protein transcript (Fig2a, 2b and 2c) on MT morphology (Fig2d). Reducing NAF-1 protein expression causes a significant increase in MT network symmetry, as measured by MT skewness while reducing MitoNEET or MiNT protein levels do not cause significant changes (Fig2e). To better assess the role of NAF-1 protein in MT morphodynamics we analyzed the MT network in cells stably expressing shRNA designed to reduce NAF-1 expression (Fig2f, g and h)). Electron microscopy analysis show an increase of MT fragmentation when NAF-1 protein is reduced, and this effect is rescued upon restoration of NAF-1 protein expression (Fig2f and 2h).

During mitochondrial fission, the dynamin related protein DRP1 is recruited to ER-MTcs to trigger the fission process [4,18], but the mechanisms that result in its enrichment and/or stability at the ER-MTcs remain poorly understood. Interestingly, NAF-1 colocalizes partially with DRP1 at ER-MTcs (Fig3a) and fluorescence image analysis shows that 15 minutes of Mito-C treatment leads to increased recruitment of DRP1 at mitochondrial surface (Fig 3b and 3c). This observation is confirmed by subcellular fractionation experiments (Fig 3d and 3e). Time course analysis of DRP1 expression following Mito-C treatment also showed an increase in total DRP1 protein (FigS7a and S7b), without any observed changes in phosphorylation at Serine 616 (DRP1^{S616}), (FigS7a and S7c) a post-translational modification known to promote mitochondrial fission during mitosis [21,22]. To assess whether the effects of Mito-C on mitochondrial morphology were directly connected to DRP1 mitochondrial recruitment and function, we co-expressed a dominant negative version of DRP1 (*drp1K38A)* and mCherry, to discriminate between transfected and non-transfected cells. Expression of

drp1K38A is known to inhibit mitochondria fission [4,23]. We observed that Mito-C treatment causes the expected fragmented MT phenotype in non-transfected cells (NT, Fig 3f), while this effect was inhibited by expression of *drp1K38A,* which rather resulted in a hyperfused mitochondrial network both in presence and absence of Mito-C (Fig 3f and 3g). These data demonstrate that Mito-C and NAF-1 regulate MT fission in a manner dependent on DRP1 recruitment at MT, presumably at ER-MT contact sites.

Further investigation of the Mito-C stimulated MT fragmentation phenotype examined the level of isoforms of the MT-associated membrane dynamics regulator OPA1 (optic atrophy 1 protein). Long forms of OPA1 (L-OPA1) are associated with fusion [24,25] while shorter forms (S-OPA1) are considered fission mediators [26]. Interestingly, Mito-C treatment induces a time dependent decrease in L-OPA1 and a concomitant accumulation of S-OPA1 further confirming Mito-C and thereby NAF-1 function shifts the mitochondrial dynamic equilibrium toward a fission state (Fig S7c and S7d).

To go further, we investigated the possible role for SAMM50, a protein which localizes to the mitochondrial outer membrane and at ER-MTcs [27] and has been reported to interact with DRP1, promote its recruitment at MT surface and induce DRP1-dependent mitochondrial fission through an unknown mechanism (Ott *et al.*, 2012; Jian *et al.*, 2018, Liu *et al.*, 2016; Jian *et al.*, 2018). Interestingly, we show that siRNA downregulation of SAMM50 (FigS8a and S8b) increases DRP1 protein levels (FigS8a and S8c) and results in fragmentation of mitochondrial network (FigS8d and S8e). These phenotypes are strikingly similar to those we observed for the knock down of NAF-1 (Fig2 and S7). Taken together, these data suggest that NAF1 is essential for DRP1 dependent MT-fission via regulation of the mobilization of DRP1 at the ER and mitochondria interface.

Several viruses are known to modulate mitochondrial morphogenesis to result in elongation as a necessary part of their replication cycle [30]. These include Dengue virus, HIV-1, Sendai virus and SARS coronavirus which have been shown to promote elongation of the MT network in infected cells [31–34]. The effects of Mito-C and reduced NAF-1 protein expression on MT morphodynamics motivated an investigation into the possible effect of Mito-C upon the replication of specific viruses. Interestingly, we show that Mito-C treatment significantly reduces Dengue viral titer by more than one log (Fig4a) and concomitantly inhibits Dengue virus induced MT hyperfusion (Fig4b), We obtained similar results with Mito-C treatment of cells infected with two related flaviviruses Zika and West Nile virus (Fig4c and d). Our results suggest that Mito-C treatment and inhibition of NAF-1 function, through effects of MT fission counteract replication of viruses reliant upon elongated MT morphogenesis for successful replication. Conversely, hepatitis B virus (HBV) is described to induce

mitochondrial fragmentation [35]. Interestingly, treatment with Mito-C failed to impair HBV replication cycle, as indicated by the quantification of the surface antigen (HBsAg) and relaxed circular DNA (rcDNA) in the supernatant from infected cells (FigS9) thus providing a clue on the specificity of Mito-C anti-viral properties, based on mitochondrial morphodynamics phenotypes. Altogether, our data suggest that Mito-C is an anti-viral compound specific against viruses that enhance mitochondrial fusion as a necessary part of their replication cycle.

Discussion

Here we report a novel small molecule (Mito-C) that targets the [2Fe-2S] lability/cluster transfer function of the three NEET proteins. Mito-C stimulates rapid and reversible mitochondrial fragmentation and the importance of the NEET protein NAF-1 for this effect is demonstrated by reduction of its expression recapitulating the fragmented mitochondrial phenotype. NAF-1 colocalizes with DRP1 at the ER-MTcs and the effect of Mito-C is dependent upon DRP-1 recruitment to the surface of mitochondria. Mito-C also stimulates MT fragmentation concomitant with accumulation of S-OPA1 a cleavage product of the fusion mediator OPA1 known to mediate MT fission. The therapeutic relevance of these observations is illustrated by the effect of Mito-C against replication of viruses reliant upon altered MT morphogenesis for successful replication.

Our present data suggest that beside intracellular iron levels modulation, NAF-1 protein can participate in the regulation of DRP1 recruitment to ER/ MT interface. If and how NAF-1 [2Fe-2S] cluster lability/ transfer at the ER-MT contact sites regulates mitochondrial morphogenesis remains to be elucidated. However, it is interesting to note that NEET proteins have been associated to different pathological conditions in which MT morphology as well as ER-MT contact site alterations appear to be a frequent signature: metabolic disorders, neurological, cancer [36–39] and now infections.

Interestingly enough, NAF-1 has also been shown to physically interact with Beclin1, a key protein of the class III PI3Kinase required for autophagosome biogenesis [40]. Autophagosomes have been proposed to form at the ER-MTcs [41] and several pathological conditions, including infections activate the autophagic pathway [33,34]. Here we highlight a function of NAF-1 at the sites of MT fission machinery recruitment suggesting that NAF-1 may participate in different processes reliant upon ER-MTcs machinery.

A role for mitochondrial morphodynamics, as well as MT-ER interface regulation, in viral replication and/or host response is highlighted here by the actions of Mito-C upon Dengue virus replication, while the lack of efficacy against HBV doesn’t preclude the activity against a diverse array of viruses, and the observed inability of the virus to stimulate mitochondrial network elongation in treated cells. Eliciting an anti-viral effect by targeting human NEET proteins opens important new perspectives in antiviral research.

Our study points to the ER-MTcs as regions of intracellular communication integrating stress conditions such as viral infection and highlights NAF-1 as an important therapeutic target in diseases where altered mitochondria dynamics is implicated in disease etiology. The novel chemical class to which Mito-C belongs may prove a powerful tool to modulate mitochondrial dynamics in such pathological situations.

Acknowledgements

We thank Dr Rappaport, Dr Arnoult, Dr Schmidt-Chanasit and Dr Mikaelian for kindly sharing reagents and advices with us. We thank as well our team of colleagues at ENYO Pharma and at INEM for fruitful discussions and constant support. We also acknowledge the INEM associated imaging, metabolic platform and FACS facilities (SFR Necker INSERM US24, CNRS UMS 3633). We warmly thanks Ivan Nemazanyy at INEM for its help with designing and performing the Seahorse© essays. F.G and L.R. were supported by ANR Jeune Chercheur (ANR0015TD), ATIP-Avenir Program. The present work has benefited from Imagerie-Gif core facility supported by l'Agence Nationale de la Recherche (ANR-11-EQPX-0029, ANR-10-INBS-04, ANR-11-IDEX-0003-02). Work in A.R.'s laboratory was funded by the Deutsche Forschungsgemeinschaft (DFG, German Research Foundation) - Projektnummer 240245660 – SFB 1129 TP13. RN acknowledges BSF (Binational Science Foundation (BSF) Grant No. 2015831. This work was finally supported by institutional funding from INSERM, CNRS and University Paris-Descartes and grants from ANR (ANR-17-CE14-0030-02 and ANR-17-CE13-0015-003), to P.C. and E.Mo.

Author contributions:

D.M., I.P.C., B.d.C., and E.Mo. conceived the project. D.M. designed, carried out the bulk of biochemical and cell biology experiments, organized the bulk of data, made statistical analyses and wrote the manuscript. I.P.C. contributes to some of the biochemical and cell biology experiments, analyzed immunofluorescence experiments on infected cells, participated in electron microscopy experiments and participated in manuscript preparation. H.B.M. performed electron microscopy and iron-sulfur clusters release experiments. L.R. performed some of the contact sites related experiments. O.K. and Y,-S, S generated and characterized stable shCisd2/NAF-1 cell lines. A.H. helped out for cytometry experiments and analyses. L.L. performed iron-sulfur clusters release experiments. P.R. and S.J. performed HBV experiments. A.R. performed Dengue, Zika and West Nile viruses infection experiments and edited the manuscript. J.V. designed part of the research. P.C., F.G., E.Me., P.M. and R.N. designed part of the research and wrote the manuscript. B.d.C and E.Mo. co-supervised the study, designed research and wrote the manuscript.

Figures Legends

Figure 1: Mito-C, a new chemical compound targeting NEETs proteins, induces mitochondrial network fragmentation

a, The structure of Mito-C **b**, HeLa cells were treated with DMSO or 2µM Mito-C for 15 min and immunostained with anti-TOMM20 (green) antibody and DAPI; cropped areas show the mitochondria symmetry changes. **c**, quantification of skewness of the TOMM20 signal from single cells (n=100). **d**, profile of [2Fe–2S] cluster release from purified recombinant NAF-1 was determined in untreated control or in presence of Mito-C and it's inactive closely related analogue MITO-N by monitoring absorbance at 458 nm as a function of time. **e**, time lapse video-microscopy on HeLa cells transfected with NAF-1-mRFP (red) and treated with ^{fluo}Mito-C (green). The distance/intensity fluorescence quantification graph illustrates the codistribution of ^{fluo}Mito-C and NAF-1-mRFP. All scale bars = 10µm. For evaluating significance of differences observed in c, t-test was used (*** indicates $p<0.0001$); for differences observed in e one-way Anova followed by Dunn's post-test was used (*** indicates $p<0.0001$).

Figure 2: Knocking down NEETs causes mitochondrial fragmentation

a, western blot analysis of MitoNEET expression in HeLa cells transfected with *CISD1* siRNA; Bar Chart (right panel) shows replicate quantifications (n=3) of MitoNEET expression. **b**, western blot analysis of NAF-1 expression in HeLa cells transfected with *CISD2* siRNA ; graph (right panel) shows the replicates quantifications (n=3) of NAF-1 expression. **c**, q-PCR analysis of *CISD3* mRNA levels from HeLa cells transfected with siRNA targeting CISD3 (n=9). **d**, HeLa cells transfected with siRNA to reduce expression of MitoNEET (*CISD1*), NAF-1 (*CISD2*) or MiNT (*CISD3*) and immunostained with anti TOMM20 antibody. **e**, Single cell skewness quantification from images as shown in d, (n =125-130 cells). **f**, Electron microscopy pictures from 150 cells in transfected as described in g. **g**, Western blot analysis of *NAF-1* expression in cells stably transfected with control shRNA, shRNA targeting reduction of NAF-1 protein expression, or shRNA targeting reduction of NAF-1 protein expression complemented with plasmid derived expression of NAF-1; western blot quantification of NAF-1 is shown on the accompanying bar chart (n=3). **h**, Quantification of mitochondrial length in EM images from cells transfected as described in g. (n=260-270)). To evaluate significant differences observed in a, b, c, and g a t-test was used (for a ** indicates $p<0.001$; for b * p is 0.045; c ** p is 0.005); for differences observed in e and f one way

Anova followed by Bonferroni's post-test was used (*** indicates p<0.0001); in i one way Anova followed by Dunn's post-test was used (*** indicates p<0.0001). Immunofluorescence scale bars = 10µm. Scale bars from EM analyses = 0.5 µm.

Figure 3: Mito-C causes DRP1 dependent mitochondrial fission

a, HeLa cells were transfected with NAF-1-GFP plasmid (green) and immunostained with antibodies to PTIP51 (ER-MT contact site marker, blue) and DRP1 (red); three color merged image is shown in the far-right panel with arrowheads indicating the white triple colocalization domains. **b**, HeLa cells treated or not, with 2µM Mito-C for 15 min where immunostained with anti-TOMM20 (red) and anti-DRP1 (green); arrowheads in the far-right panel indicate recruitment of DRP1 onto the mitochondrial surface (TOMM20). **c**, Quantification of DRP1 signal on TOMM20 positive structures (n=45). **d**, Western blot analysis of DRP1 and TOMM20 protein in cytosolic and mitochondrial fractions treated or not, with 2µM Mito-C as indicated. **e**, Quantification of western blots showed in d and expressed as a distribution of DRP1 in the cytosolic and mitochondrial fractions (n=5) **f**, HeLa cells were transfected with DRP1K38A mutant and mCherry and treated or not, with Mito-C (T for transfected, NT for not transfected). **g**, quantification of the mitochondrial phenotypes observed in f (30-35 images each with an average of 15-20 cells from triplicate independent experiments were analyzed). To evaluate significant differences observed in c, Mann Whitney was used (** p is 0.003); To evaluate statistical differences shown in g, a one-way Anova test was used (*** indicates p<0.0001). All scale bars = 10µm.

Figure 4 Mito-C counteracts flaviviruses replications

a, c, d, HuH7 cells were treated with Mito-C at the indicated concentrations and infected with Dengue (a), West Nile (c) and Zika (d) viruses. Infectious titers are presented as % of control in Mito-C concentration of 2 and 10 µM conditions, upon 72 h of viral infection (n=3). **b**, HuH7 cells were treated with Mito-C, infected with Dengue virus and fixed after 72h of infection. Cells were then immunostained for endogenous TOMM20 (green channel) and viral Dengue NS5 protein (Red). Cropped areas illustrate the mitochondrial morphology in described conditions. To evaluate significance of differences observed in a, c and d, two-way Anova followed by Bonferroni's post-test was used. NS, for non-significant, in a ** indicate p=0.006 and *** p= 0.0003, in c ** for p=0.009, in d * for p=0.025. Scale bars = 10µm.

Figure S1 Signal skewness as a measure of mitochondrial symmetry

a, schematic view of spatial pixels distribution and skewness quantification: the higher distribution symmetry corresponds to the higher skewness value. **b**, HeLa cells were treated with increasing concentrations of Mito-C for 15 minutes, fixed and immunostained for TOMM20 and analyzed by light microscopy to evaluate skewness. **c**, quantification of signal skewness informs acquisitions illustrated in b, (n=45-50). To evaluate significance of differences observed in c, one-way Anova followed by Bonferroni's post-test was used (NS for non-significant, *** for $p<0.0001$). Scale bar = 10 µm.

Figure S2: Mito-C treatment is reversible and does not induce cell death

a, b, HeLa cells treated for 24h with increasing concentrations of Mito-C were stained with propidium iodide (PI) and annexin V and analyzed by cytometry. **c**, HeLa cells were treated with DMSO or 2 µM Mito-C for 15min, with 2 µM Mito-C for 15min than washed-out overnight, treatments were blocked by fixation and mitochondria visualized by immunostaining with anti-TOMM20. **d**, quantification of mitochondrial skewness following treatment or treatment followed by removal of compound as illustrated in c (n=120-140, where n are cells). To evaluate significance of differences in b we used t-test, NS for non-significant. In d one-way Anova was used (NS for non-significant, ** indicates $p<0.001$ and ***$p<0.0001$). Scale bar =10 µm.

Figure S3: Mito-C localizes to both mitochondria and Endoplasmic Reticulum

a, HeLa cells were treated with ^{fluo}Mito-C (green), incubated with Mitotracker Redox (red) and analyzed by live microscopy. **b**, HeLa cells were transfected with Sec61βRFP (as ER marker), treated with ^{fluo}Mito-C (green), and analyzed by live microscopy Scale bar are 10 µm.

Figure S4: Mito-C impacts Fe-S clusters release from MitoNEET and MiNT proteins

a and **b**, profile of [2Fe–2S] clusters release from purified recombinant MitoNEET and MiNT were determined in in presence or absence of Mito-C and Mito-N (an inactive form of Mito-C) via monitoring their absorbance at 458 nm as a function of time. For differences observed in both a and b one-way Anova followed by Dunn's post-test was used (*** indicates $p<0.0001$).

Figure S5: NAF-1 localizes to the ER-MT contact sites

a, HeLa cells were transfected with Sec61βRFP (ER marker, red) and NAF-1-GFP (green), fixed and analyzed by confocal microscopy. **b**, HeLa cells were transfected with NAF-1-GFP (green), fixed, immunostained with TOMM20 antibody (red) and analyzed by confocal microscopy. **c**, HeLa cells were transfected with Sec61βRFP (ER marker, red), and NAF-1GFP (green), fixed, immunostained for PTIP51 (ER-MT contact sites marker, blue) and analyzed by confocal microscopy. Scale bars = 10 µm.

Figure S6: Mitochondrial mass, membrane potential and oxygen consumption rate of Mito-C treated cells

a, oxygen consumption rate (OCR) of cells treated with Mito-C 2, 10 and 20 µM were measured by Seahorse© technique. Measurements start before starting the treatment, arrow indicates the Mito-C injection. **b**, to evaluate the mitochondrial potential, cells were treated with Mito-C for 24hrs at the indicated range of concentrations and stained with Mitotracker Redox and analyzed by cytometry. **c**, to evaluate the mitochondrial potential, cells were treated with Mito-C at 2µM over a time course and then stained with Mitotracker Redox and analyzed by cytometry. **d**, To evaluate the total mitochondrial mass over a time course of treatment, HeLa cells were treated with DMSO or Mito-C at 2µM for the time duration indicated, stained with Mitotracker green and analyzed by cytometry. **e**, To evaluate the total mitochondrial mass at a fixed time point following treatment with an increasing range of concentrations of Mito-C cells were treated with DMSO or Mito-C for 24hrs at concentration indicated, stained with Mitotracker green and analyzed by cytometry

Figure S7: Expression of DRP1 and OPA1 during Mito-C treatment

a, Western blot analysis of DRP1 and ^{phospho616}DRP1 expression in total extracts from cells treated with 2µM Mito-C for the times indicated. **b, c**, Quantifications by Western blot with anti-DRP1 and anti-^{phospho616}DRP1 (n=5). **d**, Western blot analysis of OPA1 expression in total extracts from cells treated with 2µM Mito-C during time course indicated; long and short isoforms are indicated. **e,f**, Quantification of Western blot for long and short isoforms of OPA1 shown in d. To evaluate significance of differences observed in b,c,e and f we used a one-way Anova followed by Dunn's post-test in a and Bonferroni's post-test in c, e and f (ns for non-significant *p<0.01, (**p<0.001***p<0.0001).

Figure S8: Knock down of SAMM50 induces mitochondria fragmentation

a, Western blot analysis of SAMM50 and DRP1 protein in total extracts from cells transfected with siRNA for SAMM50 ER-MT associated protein (siSAMM50) or with control siRNA (siCTRL). **b** and **c**, Western blot quantification for SAMM50 and DRP1 as shown in a (n=5). **d**, HeLa cells were transfected with siRNA for SAMM50 ER-MT associated protein (siSAMM50) or with control siRNA (siCTRL), fixed and immunostained with anti-SAMM50 (red) and mitotracker (green). Scale bar = 10µm. **e**, quantification of mitochondrial phenotype. For each image the % of cells displaying a fragmented or filamentous (indicated as normal) phenotype is shown. Data were generated from analysis 30 images containing 15-30 cells each. To evaluate significance of differences observed in b and c we used an unpaired t-test, in b ** p is 0.001, in c ** p is 0.008. In e one-way Anova followed by Dunn's post-test was used (***p<0.0001).

Figure S9: absence of MITO-C effect on Hepatitis B virus replication

a, Relative secretion of HBsAg (from Hepatitis B virus (HBV)) in dHepaRG cells treated post-infection with 10 µM of Mito-C or the FXR agonist GW4064. **b**, Relative secretion of HBV viral DNA in dHepaRG cells treated post-infection with 10 µM of Mito-C or GW4064 and quantified by quantitative PCR.

Materials and Methods

Cell culture, transfection and treatment with molecules

HeLa cells (ATCC) were grown in Minimum Essential Medium (MEM, Gibco), supplemented with GlutaMAX and 10% FCS at 37°C and 5% CO_2. Huh7 cell were maintained in Dulbeccos's modified Eagle´s medium (DMEM) supplemented with 2 mM L-glutamine, 1x non-essential amino acids, 100 U/ml penicillin, 100 µg/ml streptomycin (all from GIBCO, Life Technologies) and 10% fetal calf serum (Capricorn). INS-1E-cells were grown in RPMI 1640 with 11.1 mmol/L D-glucose supplemented with 10% heat-inactivated fetal bovine serum, 100 U/mL penicillin, 100 g/mL streptomycin, 10 mmol/L HEPES, 2 mmol/L L-glutamine, 1 mmol/L sodium pyruvate, and 50 mol/L mercapto-ethanol. INS-1E-knockdown cell lines were generated as described previously [42] and maintained in the same medium as control cells with Puromycin (1g/mL). Human HepaRG cells were grown in William's E Medium supplemented with 50 IU/mL penicillin, 50 µg/mL streptomycin, 2 mM l-glutamine, 5 µg/mL insulin, 25 µg/mL hydrocortisone hemisuccinate, and 10% FCS at 37°C and 5% CO_2. Plasmid transfection in HeLa cells were performed using FuGENE® HD Transfection Reagent (Promega, E2311) following the manufacturer's instructions. Analyses were performed 24 h after transfection. Constructs used include NAF-1-GFP and NAF-1-RFP which were generated by cloning the ORF sequence NM_001008388.4(CISD2) into pcDNA3.1(+)-C-eGFP and pmCherry-N1 Vector by GeneScript; the dominant mutant K38A DRP1 was a gift from D. Arnoult (INSERM UMR-S 1014, Hôpital Paul Brousse, Villejuif, France); Sec61β-RFP was a kind gift from T. Rapoport (Harvard University, Cambridge, MA, USA). siRNA transfections were performed using Lipofectamine RNAiMAX (Invitrogen, 12323563) following the manufacturer's guidelines. Analyses were performed 72 h after transfection. siRNAs used were: siCTRL (Qiagen, AllStars Negative Control siRNASI03650318); siCISD1 (Qiagen, SI04758194); siCISD2 (Qiagen, si04985855); siCISD3 (Qiagen, SI04758187); SAMM50 (Dharmacon, mix 1:1 J-017871-18 and J-017871-19); Non-targeting (Dharmacon, D-001810-10). Cells were treated with Mito-C, Mito-N and ^{fluo}Mito-C compounds at the indicated concentrations diluted directly in culture media, as negative control the same amount of DMSO was used.

Protein extracts, membrane fractionation and Western blot analyses

For total protein extracts, cells were washed twice with 1XPBS and then directly lysed on ice with 1X Laemmli buffer (60mM Tris-HCl pH=6.8, 2% SDS, 10% Glycerol, bromophenol blue, supplemented with fresh added 100mM DTT final), lysates were incubated for 10 min at

90°C. For mitochondrial and cytosolic fraction preparations, after treatment HeLa cells were washed twice and gently scraped in cold PBS. Cell pellets were recovered via centrifugation at 600g for 5 min. Cells were gently re-suspended in M buffer (440 mM mannitol, 140mM sucrose, 40mM HEPES, 1mM EDTA, 2mg/ml fatty acid free BSA and protease/phosphatase inhibitor cocktail) and placed on ice for 10 minutes. After homogenization with Dounce homogenizer (20 stroke), the lysate was centrifuged at 600g for 5min to pellet nuclei and recover the post nuclear supernatant (PNS). The PNS was than centrifuged at 7200 g for 15 min at 4°C to collect the mitochondrial enriched fraction and the supernatant (cytosolic fraction). For routine SDS-PAGE, precast gradient gels (4-20% Tris-Glycine, Invitrogen) were used and home-made 7.5% Tris-Glycine gels for OPA-1 detection. Separated proteins were transferred onto PVDF membranes. Membranes were blocked with BSA 3%/ TBS/0.1% tween for 1h and incubated with primary antibodies overnight at 4° in 2% BSA/TBS/0.1%tween. Immunoblot analysis was performed by chemiluminescence (Millipore) in a ChemiDoc MP Imaging System (Bio-Rad). Quantification of band intensities were carried using Image J software.

Immunofluorescence and confocal microscopy

For immunofluorescence analysis, cells were plated on 12-mm glass coverslips and fixed with 4% paraformaldehyde in PBS for 20 min at room temperature. After 3 washes of 20 min each in PBS, cells were blocked with fetal calf serum (10%) in PBS for 30 min. Incubation with primary antibodies was performed in permeabilization buffer (0.05% saponin in blocking buffer). Coverslips were mounted on microscope slides using home-made Mowiol mounting medium with or without DAPI. Images were obtained using a 63x oil-immersion objective with Leica TCS SP5 confocal microscope, using a 405 nm diode laser line exciting DAPI, a 488 nm argon laser line exciting Alexa Fluor 488, a 561 nm diode laser line for Alexa Fluor 546 and laser He/Ne 633 nm for Alexa 647. Acquisitions were done in sequential mode and fluorescence acquired in separated channels. For some experiments, optical sections were acquired with a 63x/1.4 Oil immersion objective using the LAS-X software and fluorescent pictures were collected with a PMTs GaAsP hybride camera (Hamamatsu).

Image analysis and statistics of data

Image analysis was performed using Image J software. For mounting representative images, background was reduced using brightness and contrast adjustments applied to the whole image. For obtaining skewness measurements a circle of 6µM diameter was drawn and moved near the nucleus of each cell, then skewness values were obtained from the set

measurement plugin option “skewness” of ImageJ software. For analyzing the recruitment of DRP1 on mitochondria, a mask on the fluorescence in TOMM20 channel was used to define the region to measure the total intensity of the DRP1 signal in the DRP1 channel. For statistics of data we used GraphPad Prism software. After evaluation of mean, standard deviation and standard errors we evaluate data distributions using normality test: KS normality test, D'Agostino & Pearson omnibus normality test and Shapiro-Wilk normality test. Data where processed as normally distributed when at least 2 out of 3 test resulted positive, otherwise they were processed as non-parametric distributions. Gaussian distributions were analyzed with the more appropriate t-test or Anova and non-Gaussian distributed sets of data were evaluated with the more appropriate non parametric test, Mann Whitney or ANOVA, as specified in figure legends.

Antibodies used and dilutions

The primary antibodies used are the following: mouse anti-TOMM20 (BD Biosciences 612278,1:1000 for WB, 1:400 for immunofluorescence); rabbit anti-MitoNEET (Proteintech 16006-1-AP, 1:3000); rabbit anti – NAF-1 (Proteintech 13318-1-AP, 1:3000); mouse anti-DRP1(BD Biosciences 611112 , 1:1000); rabbit anti- DRP1 P616 (Cell signaling 3455, 1:1000): rabbit anti-PTPIP51(Novus biological NBP1-84738, 1:1000 for WB, 1:200 for immunofluorescence); mouse anti- OPA-1 (BD Biosciences 612607, 1:1000); rabbit anti SAMM50 (Sigma HPA034537, 1:1000 for WB, 1:200 for immunofluorescence); mouse anti beta-actin (Abcam ab8226, 1:1000); rabbit anti-Dengue virus NS5 protein (GeneTex GTX124253, 1:1000). For secondary antibodies, we used for immunofluorescence an Alexa 488 conjugated donkey anti-mouse (Invitrogen A21202, 1:800), Alexa 488 conjugated donkey anti-rabbit (Invitrogen A21206, 1:800), Alexa 647 conjugated donkey anti-mouse (Invitrogen A31571, 1:800), Alexa 647 conjugated donkey anti-rabbit (Invitrogen A31573, 1:800). For western blotting we used Secondary HRP conjugate anti-rabbit IgG (GE Healthcare, 1:10000) and HRP conjugate anti-mouse IgG (Bio-Rad 1:10000).

RNA extraction and quantification

RNA was extracted from cells using NucleoSpin RNA kit (Macherey-Nagel, 740984.50) according to the manufacturer’s instructions. cDNA was made from 1 µg of RNA using M-MLV reverse transcriptase (Life Technologies, 28025013). Detection of MiNT transcript was performed by qPCR with iTAQ universal SYBR Green supermix (Applied biosystem) using

the following primers for 5′-GCAGGGAAAACCTACAGGTG – 3’ and 5′-TGAGTGGAGATAGGCCAGTG – 3’ (Eurofins) in a qTOWER machine (Analytik Jena).

Flow cytometry analyses

Cells were treated as indicated in each figure legend. After treatment, cell death was quantified using Annexin V-FITC/Propidium Iodide (PI) assay according to the manufacturer’s protocol (Annexin V-FITC Apoptosis Detection Kit II, 556570, BD PharmingenTM). For mitochondria analysis we used MitoTracker Red CMXRos (Thermo Fisher, M7512) and MitoTracker Green FM (Thermo Fisher, M7514). Data were analyzed by a LSRFortessaTM flow cytometer (BD Biosciences, San Jose, CA) and processed using Cell Quest software (BD Biosciences) and FlowJo software (FLOWJO, LLC).

Oxygen consumption rate and mitochondrial activity measurements

For measurements of mitochondria activity, Hela cells were seeded at a density of 6000/well in a XFe96 cell culture microplate. 16 hours later cells were balanced for 1h in un-buffered XF assay media (Agilent Technologies) supplemented with 2 mM Glutamine, 10 mM Glucose and 1 mM Sodium Pyruvate, than oxygen consumption rate were measured by Seahorse bio analyzer. Values were taken every 3 minutes and Mito-C was injected during the assay at reading time of 10 min (indicated by the arrow in the figure S6a) at the final concentrations of 2, 10 or 20 µM. The data were normalized to protein content measured in each well using BCA assay (Thermo Fisher Scientific) according to manufacturer’s instructions

Mito-C synthesis

Mito-C (2-[(3,4-Dimethoxybenzoyl)amino]-6,6-dimethyl-5,7-dihydro-4H-benzothiophene-3-carboxylic acid) was synthetized by Charles River company as following: a reaction vessel was charged 4,4-dimethylcyclohexanone (CAS: 4255-62-3, 5.00 g, 39.6 mmol), methyl cyanoacetate (CAS: 105-34-0, 3.8 ml, 43.6 mmol), diethylamine (CAS: 109-89-7, 2.0 ml, 19.8 mmol) and sulfur (CAS: 7704-34-9, 1.52 g, 47.5 mmol). The reaction was solvated in methanol (25 ml) and set to stir at RT. The reaction mixture was stirred at room temperature for 60 hours. The volatiles were removed under reduced pressure and the residue was purified by flash chromatography on silica gel (eluting with 0-20% EtOAc in isohexane) which afforded *methyl 2-amino-6,6-dimethyl-4,5,6,7- tetrahydrobenzo[b] thiophene-3-carboxylate* as a pale yellow solid (7.22 g, yield 76%). ^{1}H NMR ($CDCl_3$, 400MHz): δ = 5.92

(s, 2H), 3.79 (s, 3H), 2.69 (t, J=6.4 Hz, 2H), 2.27 (s, 2H), 1.48 (t, J=6.4 Hz, 2H), 0.98 (s, 6H). To a solution of methyl 2-amino-6,6-dimethyl-4,5,6,7-tetrahydrobenzo[b]thiophene-3-carboxylate (Preparation #1, 200 mg, 0.84 mmol) in DCM (5.0 ml) was added DIPEA (CAS: 7087-68-5, 220 µl, 1.25 mmol) and 3,4-dimethoxybenzoyl chloride (CAS: 3535-37-3, 120 µl, 1.00 mmol). The reaction mixture was stirred at RT overnight. The resulting mixture was diluted with DCM and water. The two phases were separated. The organic layer was passed through a phase separator and the solvent was removed under reduced pressure. The residue was dissolved in THF (4.0 ml) and MeOH (2.0 ml). To the solution was added LiOH aq. (CAS: 1310-66-3, 2.0M, 1.7 ml, 3.36 mmol). The reaction mixture was stirred at 50 ºC for 2 hours. The mixture was allowed to cool to RT and acidified with 1N aqueous HCl solution. The reaction mixture was then extracted with EtOAc. The organic phase was washed with brine and dried over Na_2SO_4. The solvent was removed under reduced pressure. Purification by RP-HPLC. RP-HPLC purification condition: Column XSELECT CSH Prep C18 19x250mm, 5µm. Mobile phase: MeCN in water (0.1% HCOOH), Flow rate: 20 ml/min; Wavelength: 210-260 nm DAD. Sample injected in DMSO (+ optional formic acid and water), 22 min non-linear gradient from 10% to 95% MeCN, centered around a specific focused gradient. ^{1}H NMR (DMSO-d_6, 400MHz): δ = 13.34 (br s, 1H), 12.36 (s, 1H), 7.49 - 7.45 (m, 2H), 7.18 (d, J=8.4 Hz, 1H), 3.86 (s, 3H), 3.85 (s, 3H), 2.75 (t, J=5.9 Hz, 2H), 2.42 (s, 2H), 1.50 (t, J=6.3 Hz, 2H), 0.98 (s, 6H). LC/MS (Table 1, Method A) R_t = 5.31 min; MS *m/z*: 390 $[M+H]^+$.Compounds were > 95% pure, reconstituted in 100% DMSO (Sigma) and diluted in cell culture medium for assays.

Flavivirus virus infection and estimation of virus titers upon Mito-C treatment

Dengue virus serotype 2 strain New Guinea C was produced as previously described and infectious titers determined by limiting dilution assay using Huh7 cells [43]. Zika virus strain MR766 was obtained from the European Virus Archive (EVAg, France). West Nile virus strain New-York99 was a kind gift of J. Schmidt-Chanasit (Hamburg, Germany). Zika and West Nile viruses were passaged once on C6/36 cells and stocks were prepared by virus amplification in VeroE6 cells. Virus stock titers were determined by plaque assay. In brief, VeroE6 cells were infected with serial dilutions of virus supernatants. Two hours post-infection inoculum was replaced by serum-free MEM medium (Gibco, Life Technologies) containing 1.5% carboxymethyl cellulose (Sigma Aldrich). At different days post infection (day 3 for West Nile virus, day 4 for Zika virus, day 8 for Dengue virus) cells were fixed by addition of formaldehyde to a final concentration of 5%. Cells were stained with crystal violet solution (1% crystal violet, 10% ethanol in H_2O) for 30 min at room temperature and rinsed extensively with H_2O. Infectious titers were calculated considering the corresponding dilution

factor. Huh7 cells ($1x10^5$) were infected with Dengue, Zika and West Nile viruses at a multiplicity of infection (MOI) of 0.1 $TCID_{50}$ or pfu per cell and simultaneously treated with 20 µM of mito-C for 48 h. Supernatants were harvested, filtered through 0.45 µM membrane and titrated by limiting dilution assay or plaque assay as described above. For immunofluorescence assays, Huh7 cells ($1x10^5$) were infected with Dengue virus at a MOI of 0.5 $TCID_{50}$ per cell and simultaneously treated with 20 µM of Mito-C for 72 h.

HBV infection and viral growth estimation under Mito-C or GW4064 treatment

Hepatitis B virus (HBV) inoculum was prepared from stably transfected HepG2.2.15 cell line as previously described [35]. HepaRG cell inoculation was performed with 100 genome-equivalent per cell in culture medium that contained 4%v/vPEG8000 (Sigma-Aldrich) for 24 h at 37°C. At day 2 post-infection, cultures were treated for 10 days with the following compounds Mito-C or GW4064 at indicated concentrations. HBs antigen (HBsAg) secreted into cell supernatants were quantified on the miniVIDAS apparatus using the VIDAS Ultra tests (Biomérieux, Marcy l'Etoile, France). Viral HBV DNA was extracted from cell supernatant using the QUIAAmp MinElute virus spin kit (Qiagen, Courtaboeuf, France) on a QIAcube apparatus (Qiagen). Extractions were carried out following the manufacturer's recommendations. Eluates were directly used for quantification of secreted viral DNA by quantitative PCR experiments using primers for rcHBV DNA: forward 5'-GGGGAGGAGATTAGGTTAAAGGTC-3', reverse 5'-CACAGCTTGGAGGCTTGAACAGTGG-3' and the QuantiFast SYBR green PCR kit (Qiagen) on a LightCycler 480 II (Roche Applied Science).

Transmission electron microscopy

Cells were fixed for 2h at room temperature with 2% glutaraldehyde in 0.1µM sodium cacodylate buffer at pH of 7.4. Samples were then rinsed three times of 10 min each in 0.1µM sodium cacodylate buffer and post-fixed with 1% osmium tetroxide in 0.1µM sodium cacodylate buffer for 30 min. Contrast was done in uranyl acetate 1% for 30 min, then the samples were dehydrated in a graded series of ethanol ending with 100% ethanol. Samples were then embedded in EPON. About 70 nm sections were prepared with a Leica Ultracut 7 ultramicrotome. The sections were observed using a Philips CM120 electron microscope operating at 120 kV. Images were captured using a GATAN Orius 200 camera.

Fe-S cluster transfer assay

The stability of NEET protein binding for its [2Fe–2S] cluster was determined from monitoring their characteristic absorbance at 458 nm as a function of time with ~66 µ*M* NAF-1 protein in 20 m*M* Tris–HCl pH 5.5, 100 m*M* NaCl on a Synergy 2 microplate reader (BioTek Instruments). NEET proteins were expressed and purified as previously described [44].

References

1. Galluzzi L, Kepp O, Kroemer G (2012) Mitochondria: master regulators of danger signalling. *Nat Rev Mol Cell Biol* **13**: 780–788.

2. Zemirli N, Morel E, Molino D (2018) Mitochondrial dynamics in basal and stressful conditions. *Int J Mol Sci* **19**:.

3. Tilokani L, Nagashima S, Paupe V, Prudent J (2018) Mitochondrial dynamics: overview of molecular mechanisms. *Essays Biochem* **62**: 341–360.

4. Smirnova E, Shurland DL, Ryazantsev SN, van der Bliek AM (1998) A human dynamin-related protein controls the distribution of mitochondria. *J Cell Biol* **143**: 351–358.

5. Friedman JR, Lackner LL, West M, DiBenedetto JR, Nunnari J, Voeltz GK (2011) ER Tubules Mark Sites of Mitochondrial Division. *Science (80-)* **334**: 358–362.

6. Tamir S, Paddock ML, Darash-Yahana-Baram M, Holt SH, Sohn YS, Agranat L, Michaeli D, Stofleth JT, Lipper CH, Morcos F, et al. (2015) Structure–function analysis of NEET proteins uncovers their role as key regulators of iron and ROS homeostasis in health and disease. *Biochim Biophys Acta - Mol Cell Res* **1853**: 1294–1315.

7. Mittler R, Darash-Yahana M, Sohn YS, Bai F, Song L, Cabantchik IZ, Jennings PA, Onuchic JN, Nechushtai R (2019) NEET Proteins: A New Link Between Iron Metabolism, Reactive Oxygen Species, and Cancer. *Antioxid Redox Signal* **30**: 1083–1095.

8. Karmi O, Marjault H-B, Pesce L, Carloni P, Onuchic JN, Jennings PA, Mittler R, Nechushtai R (2018) The unique fold and lability of the [2Fe-2S] clusters of NEET proteins mediate their key functions in health and disease. *J Biol Inorg Chem* **23**: 599–612.

9. Tamir S, Paddock ML, Darash-Yahana-Baram M, Holt SH, Sohn YS, Agranat L, Michaeli D, Stofleth JT, Lipper CH, Morcos F, et al. (2015) Structure-function analysis of NEET proteins uncovers their role as key regulators of iron and ROS homeostasis in health and disease. *Biochim Biophys Acta* **1853**: 1294–1315.

10. Mittler R, Darash-Yahana M, Sohn YS, Bai F, Song L, Cabantchik IZ, Jennings PA, Onuchic JN, Nechushtai R (2019) NEET Proteins: A New Link Between Iron Metabolism, Reactive Oxygen Species, and Cancer. *Antioxid Redox Signal* **30**: 1083–1095.

11. Wang Y, Landry AP, Ding H (2017) The mitochondrial outer membrane protein mitoNEET is a redox enzyme catalyzing electron transfer from $FMNH_2$ to oxygen or ubiquinone. *J Biol Chem* **292**: 10061–10067.

12. Vernay A, Marchetti A, Sabra A, Jauslin TN, Rosselin M, Scherer PE, Demaurex N, Orci L, Cosson P (2017) MitoNEET-dependent formation of intermitochondrial junctions. *Proc Natl Acad Sci U S A* **114**: 8277–8282.

13. Lipper CH, Karmi O, Sohn YS, Darash-Yahana M, Lammert H, Song L, Liu A, Mittler R, Nechushtai R, Onuchic JN, et al. (2018) Structure of the human monomeric NEET protein MiNT and its role in regulating iron and reactive oxygen species in cancer cells. *Proc Natl Acad Sci U S A* **115**: 272–277.

14. Köster H, Little DP, Luan P, Muller R, Siddiqi SM, Marappan S, Yip P (2007) Capture compound mass spectrometry: a technology for the investigation of small molecule protein interactions. *Assay Drug Dev Technol* **5**: 381–390.

15. Wiley SE, Murphy AN, Ross SA, van der Geer P, Dixon JE (2007) MitoNEET is an iron-containing outer mitochondrial membrane protein that regulates oxidative capacity. *Proc Natl Acad Sci U S A* **104**: 5318–5323.

16. Amr S, Heisey C, Zhang M, Xia X-J, Shows KH, Ajlouni K, Pandya A, Satin LS, El-Shanti H, Shiang R (2007) A homozygous mutation in a novel zinc-finger protein, ERIS, is responsible for Wolfram syndrome 2. *Am J Hum Genet* **81**: 673–683.

17. Wang C-H, Chen Y-F, Wu C-Y, Wu P-C, Huang Y-L, Kao C-H, Lin C-H, Kao L-S, Tsai T-F, Wei Y-H (2014) Cisd2 modulates the differentiation and functioning of adipocytes by regulating intracellular Ca2+ homeostasis. *Hum Mol Genet* **23**: 4770–4785.

18. Chen Y-F, Kao C-H, Chen Y-T, Wang C-H, Wu C-Y, Tsai C-Y, Liu F-C, Yang C-W, Wei Y-H, Hsu M-T, et al. (2009) Cisd2 deficiency drives premature aging and causes mitochondria-mediated defects in mice. *Genes Dev* **23**: 1183–1194.

19. Helle SCJ, Kanfer G, Kolar K, Lang A, Michel AH, Kornmann B (2013) Organization and function of membrane contact sites. *Biochim Biophys Acta* **1833**: 2526–2541.

20. Gomez-Suaga P, Paillusson S, Stoica R, Noble W, Hanger DP, Miller CCJ (2017) The ER-Mitochondria Tethering Complex VAPB-PTPIP51 Regulates Autophagy. *Curr Biol* **27**: 371–385.

21. Liesa M, Palacín M, Zorzano A (2009) Mitochondrial dynamics in mammalian health and disease. *Physiol Rev* **89**: 799–845.

22. Taguchi N, Ishihara N, Jofuku A, Oka T, Mihara K (2007) Mitotic phosphorylation of dynamin-related GTPase Drp1 participates in mitochondrial fission. *J Biol Chem* **282**: 11521–11529.

23. Zemirli N, Pourcelot M, Ambroise G, Hatchi E, Vazquez A, Arnoult D (2014) Mitochondrial hyperfusion promotes NF-κB activation via the mitochondrial E3 ligase MULAN. *FEBS J* **281**: 3095–3112.

24. MacVicar T, Langer T (2016) OPA1 processing in cell death and disease - the long and short of it. *J Cell Sci* **129**: 2297–2306.

25. Duvezin-Caubet S, Jagasia R, Wagener J, Hofmann S, Trifunovic A, Hansson A, Chomyn A, Bauer MF, Attardi G, Larsson N-G, et al. (2006) Proteolytic processing of OPA1 links mitochondrial dysfunction to alterations in mitochondrial morphology. *J Biol Chem* **281**: 37972–37979.

26. Anand R, Wai T, Baker MJ, Kladt N, Schauss AC, Rugarli E, Langer T (2014) The i-AAA protease YME1L and OMA1 cleave OPA1 to balance mitochondrial fusion and fission. *J Cell Biol* **204**: 919–929.

27. Flinner N, Ellenrieder L, Stiller SB, Becker T, Schleiff E, Mirus O (2013) Mdm10 is an ancient eukaryotic porin co-occurring with the ERMES complex. *Biochim Biophys Acta* **1833**: 3314–3325.

28. Liu S, Gao Y, Zhang C, Li H, Pan S, Wang X, Du S, Deng Z, Wang L, Song Z, et al. (2016) SAMM50 Affects Mitochondrial Morphology through the Association of Drp1 in Mammalian Cells. *FEBS Lett* **590**: 1313–1323.

29. Jian F, Chen D, Chen L, Yan C, Lu B, Zhu Y, Chen S, Shi A, Chan DC, Song Z (2018) Sam50 Regulates PINK1-Parkin-Mediated Mitophagy by Controlling PINK1 Stability and Mitochondrial Morphology. *Cell Rep* **23**: 2989–3005.

30. Moreno-Altamirano MMB, Kolstoe SE, Sánchez-García FJ (2019) Virus Control of Cell Metabolism for Replication and Evasion of Host Immune Responses. *Front Cell Infect Microbiol* **9**: 95.

31. Fields JA, Serger E, Campos S, Divakaruni AS, Kim C, Smith K, Trejo M, Adame A, Spencer B, Rockenstein E, et al. (2016) HIV alters neuronal mitochondrial fission/fusion in the brain during HIV-associated neurocognitive disorders. *Neurobiol Dis* **86**: 154–169.

32. Castanier C, Garcin D, Vazquez A, Arnoult D (2010) Mitochondrial dynamics regulate the RIG-I-like receptor antiviral pathway. *EMBO Rep* **11**: 133–138.

33. Chatel-Chaix L, Cortese M, Romero-Brey I, Bender S, Neufeldt CJ, Fischl W, Scaturro P, Schieber N, Schwab Y, Fischer B, et al. (2016) Dengue Virus Perturbs Mitochondrial Morphodynamics to Dampen Innate Immune Responses. *Cell Host Microbe* **20**: 342–356.

34. Shi C-S, Qi H-Y, Boularan C, Huang N-N, Abu-Asab M, Shelhamer JH, Kehrl JH (2014) SARS-coronavirus open reading frame-9b suppresses innate immunity by targeting mitochondria and the MAVS/TRAF3/TRAF6 signalosome. *J Immunol* **193**: 3080–3089.

35. Kim S-J, Khan M, Quan J, Till A, Subramani S, Siddiqui A (2013) Hepatitis B Virus Disrupts Mitochondrial Dynamics: Induces Fission and Mitophagy to Attenuate Apoptosis. *PLoS Pathog* **9**: e1003722.

36. Erpapazoglou Z, Mouton-Liger F, Corti O (2017) From dysfunctional endoplasmic reticulum-mitochondria coupling to neurodegeneration. *Neurochem Int* **109**: 171–183.

37. Tubbs E, Rieusset J (2017) Metabolic signaling functions of ER-mitochondria contact sites: role in metabolic diseases. *J Mol Endocrinol* **58**: R87–R106.

38. Naia L, Ferreira IL, Ferreiro E, Rego AC (2017) Mitochondrial Ca2+ handling in Huntington's and Alzheimer's diseases - Role of ER-mitochondria crosstalk. *Biochem Biophys Res Commun* **483**: 1069–1077.

39. Doghman-Bouguerra M, Lalli E (2019) ER-mitochondria interactions: Both strength and weakness within cancer cells. *Biochim Biophys acta Mol cell Res* **1866**: 650–662.

40. Chang NC, Nguyen M, Germain M, Shore GC (2010) Antagonism of Beclin 1-dependent autophagy by BCL-2 at the endoplasmic reticulum requires NAF-1. *EMBO J* **29**: 606–618.

41. Hamasaki M, Furuta N, Matsuda A, Nezu A, Yamamoto A, Fujita N, Oomori H, Noda T, Haraguchi T, Hiraoka Y, et al. (2013) Autophagosomes form at ER-mitochondria contact sites. *Nature* **495**: 389–393.

42. Sohn Y-S, Tamir S, Song L, Michaeli D, Matouk I, Conlan AR, Harir Y, Holt SH, Shulaev V, Paddock ML, et al. (2013) NAF-1 and mitoNEET are central to human breast cancer proliferation by maintaining mitochondrial homeostasis and promoting tumor growth. *Proc Natl Acad Sci* **110**: 14676–14681.

43. Roth H, Magg V, Uch F, Mutz P, Klein P, Haneke K, Lohmann V, Bartenschlager R, Fackler OT, Locker N, et al. (2017) Flavivirus Infection Uncouples Translation Suppression from Cellular Stress Responses. *MBio* **8**:.

44. Zuris JA, Harir Y, Conlan AR, Shvartsman M, Michaeli D, Tamir S, Paddock ML, Onuchic JN, Mittler R, Cabantchik ZI, et al. (2011) Facile transfer of [2Fe-2S] clusters from the diabetes drug target mitoNEET to an apo-acceptor protein. *Proc Natl Acad Sci* **108**: 13047–13052.

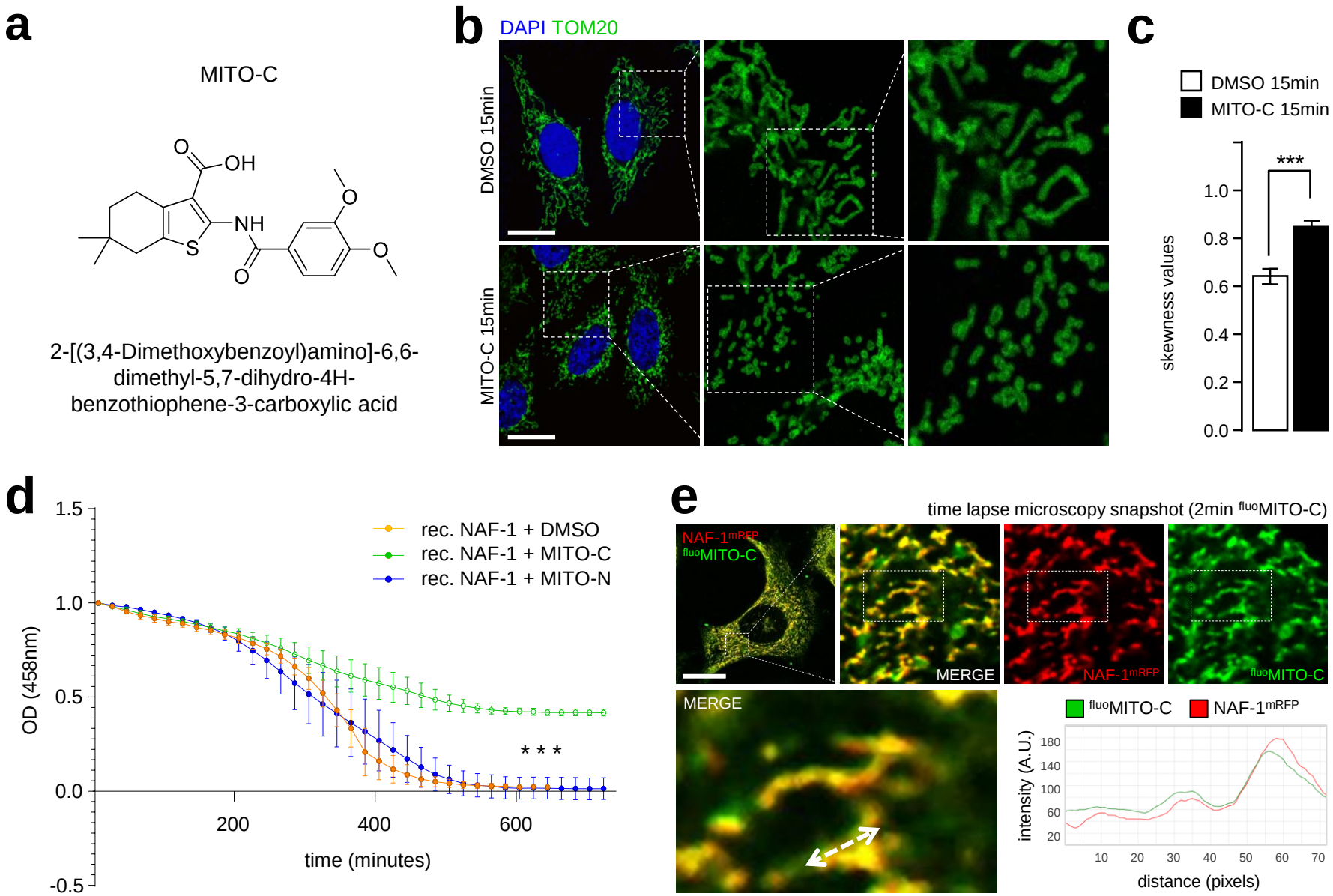
a
MITO-C
O
OH
NH
S
O
O
O
2-[(3,4-Dimethoxybenzoyl)amino]-6,6-dimethyl-5,7-dihydro-4H-benzothiophene-3-carboxylic acid
b
DAPI TOM20
DMSO 15min
MITO-C 15min
c
DMSO 15min
MITO-C 15min
***
skewness values
1.0
0.8
0.6
0.4
0.2
0.0
d
rec. NAF-1 + DMSO
rec. NAF-1 + MITO-C
rec. NAF-1 + MITO-N
OD (458nm)
1.5
1.0
0.5
0.0
-0.5
200
400
600
time (minutes)
* * *
e
time lapse microscopy snapshot (2min fluoMITO-C)
NAF-1mRFP
fluoMITO-C
MERGE
NAF-1mRFP
fluoMITO-C
MERGE
fluoMITO-C
NAF-1mRFP
intensity (A.U.)
180
140
100
60
20
10
20
30
40
50
60
70
distance (pixels)

Figure 1

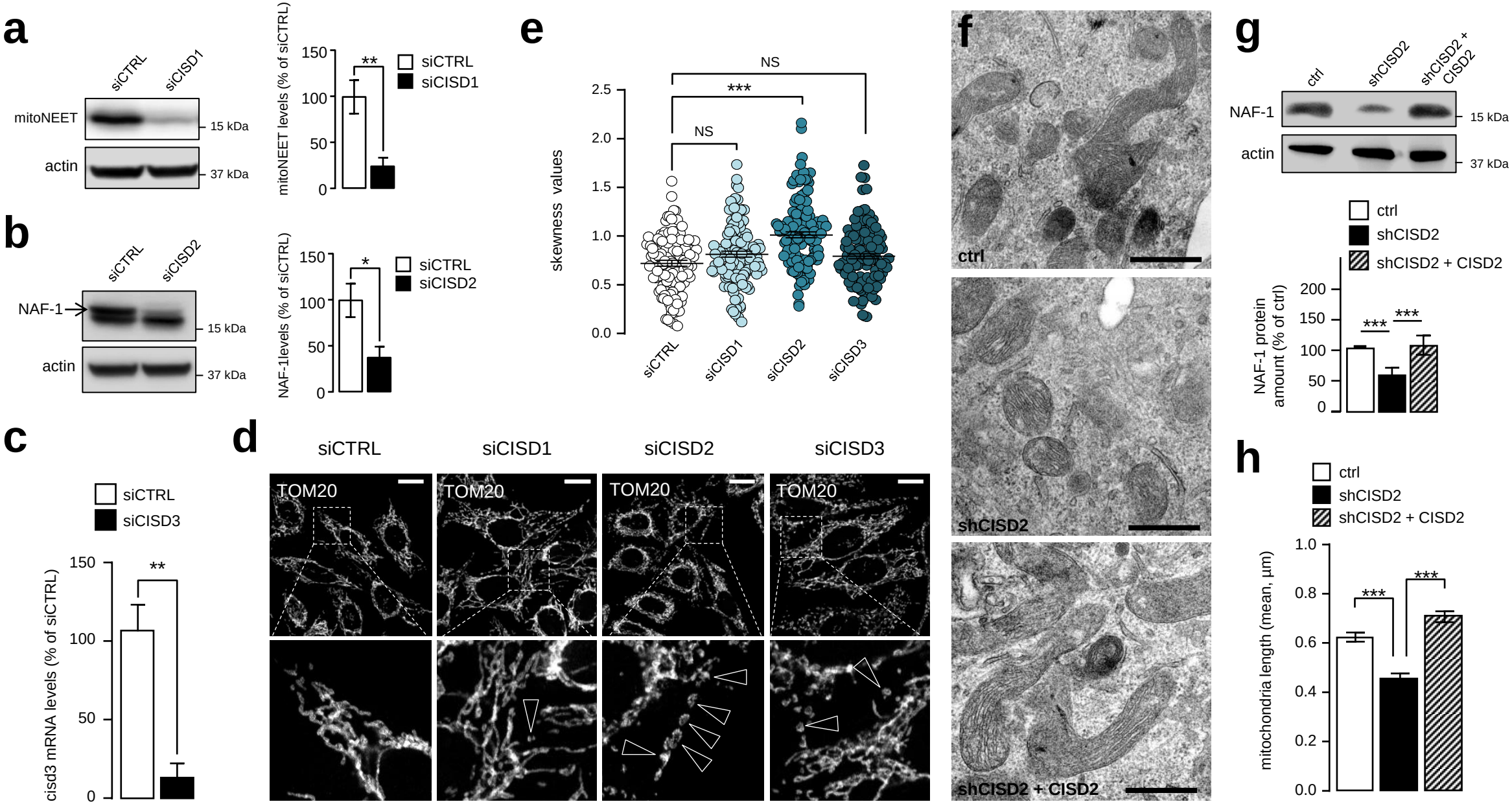
a
siCTRL
siCISD1
mitoNEET
15 kDa
actin
37 kDa
mitoNEET levels (% of siCTRL)
150
100
50
0
**
siCTRL
siCISD1
b
siCTRL
siCISD2
NAF-1
15 kDa
actin
37 kDa
NAF-1levels (% of siCTRL)
*
siCTRL
siCISD2
c
siCTRL
siCISD3
cisd3 mRNA levels (% of siCTRL)
**
d
siCTRL
siCISD1
siCISD2
siCISD3
TOM20
e
skewness values
2.5
2.0
1.5
1.0
0.5
0.0
NS
***
NS
siCTRL
siCISD1
siCISD2
siCISD3
f
ctrl
shCISD2
shCISD2 + CISD2
g
ctrl
shCISD2
shCISD2 + CISD2
NAF-1
15 kDa
actin
37 kDa
ctrl
shCISD2
shCISD2 + CISD2
NAF-1 protein amount (% of ctrl)
200
150
100
50
0
***
***
h
ctrl
shCISD2
shCISD2 + CISD2
mitochondria length (mean, µm)
1.0
0.8
0.6
0.4
0.2
0.0
***
***

Figure 2

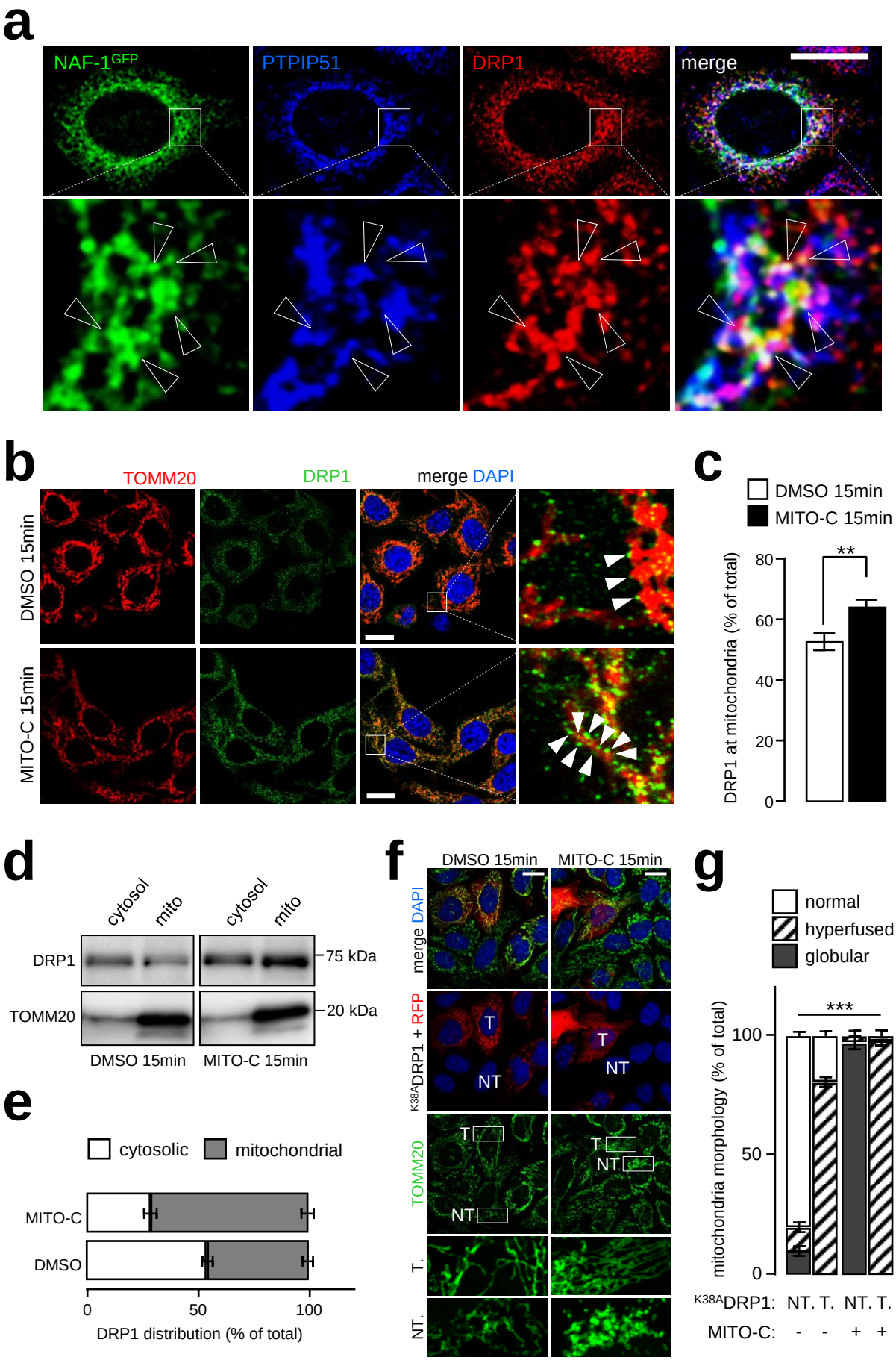
a
NAF-1GFP
PTPIP51
DRP1
merge
b
TOMM20
DRP1
merge DAPI
DMSO 15min
MITO-C 15min
c
DMSO 15min
MITO-C 15min
DRP1 at mitochondria (% of total)
80
60
40
20
0
**
d
cytosol
mito
cytosol
mito
DRP1
TOMM20
75 kDa
20 kDa
DMSO 15min
MITO-C 15min
e
cytosolic
mitochondrial
MITO-C
DMSO
0
50
100
DRP1 distribution (% of total)
f
DMSO 15min
MITO-C 15min
merge DAPI
K38ADRP1 + RFP
TOMM20
T.
NT.
T
NT
g
normal
hyperfused
globular
mitochondria morphology (% of total)
100
50
0
***
K38ADRP1: NT. T. NT. T.
MITO-C: - - + +

Figure 3

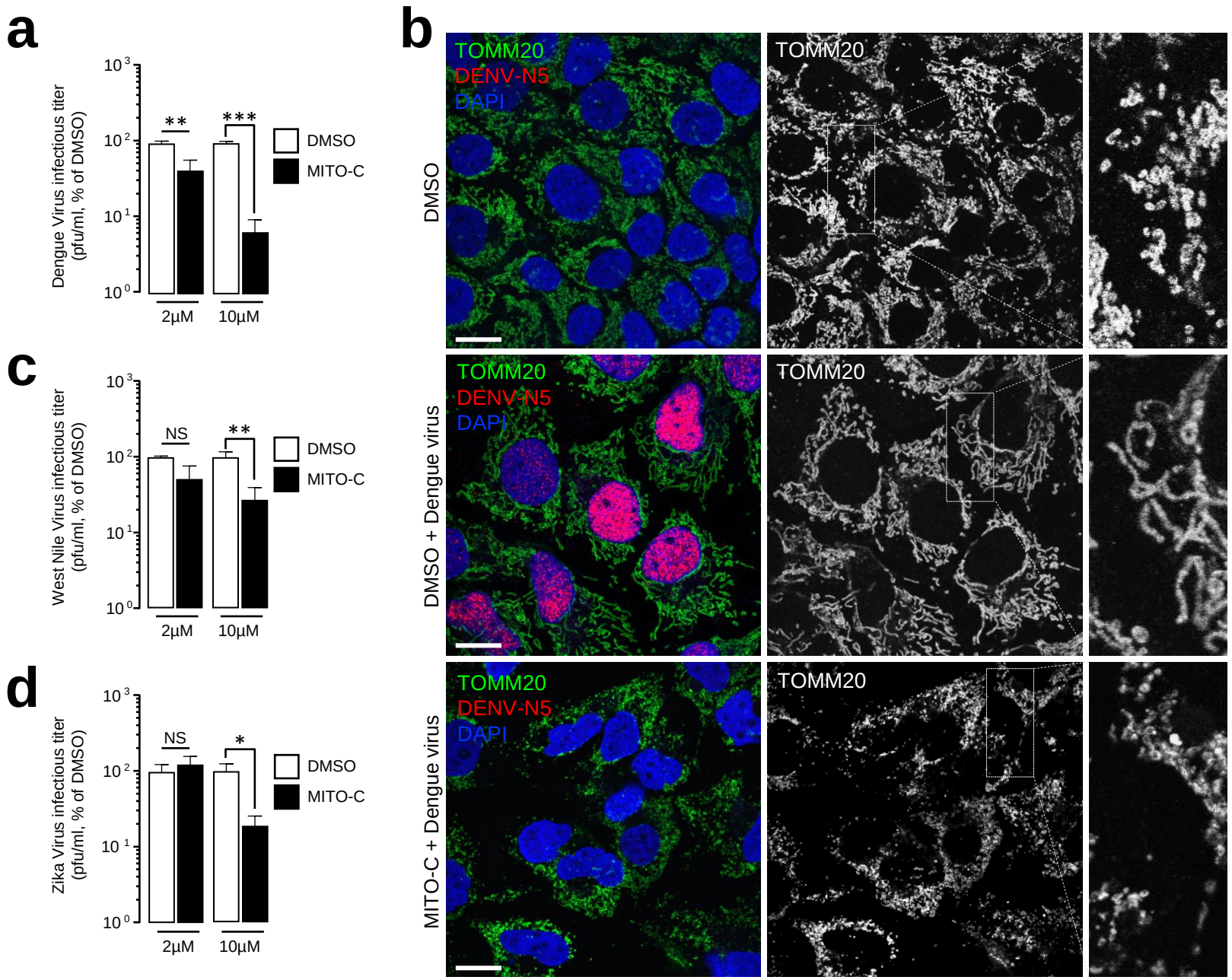
a
Dengue Virus infectious titer (pfu/ml, % of DMSO)
10^3
10^2
10^1
10^0
**
***
DMSO
MITO-C
2μM
10μM
b
DMSO
DMSO + Dengue virus
MITO-C + Dengue virus
TOMM20
DENV-N5
DAPI
TOMM20
c
West Nile Virus infectious titer (pfu/ml, % of DMSO)
NS
**
DMSO
MITO-C
2μM
10μM
d
Zika Virus infectious titer (pfu/ml, % of DMSO)
NS
*
DMSO
MITO-C
2μM
10μM

Figure 4

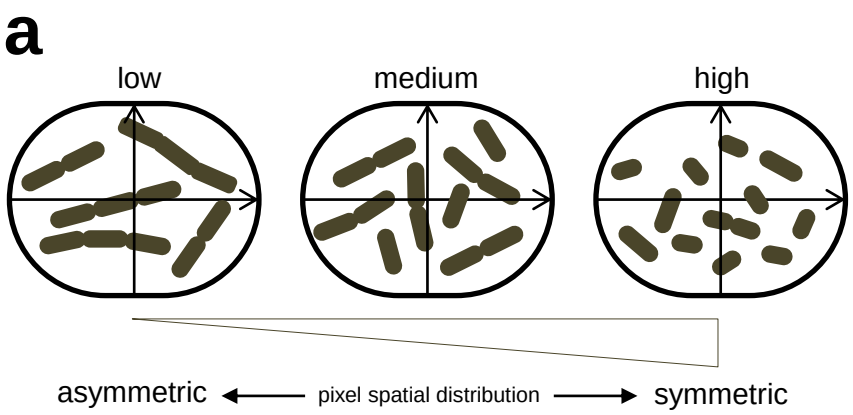
a
low
medium
high
asymmetric
pixel spatial distribution
symmetric

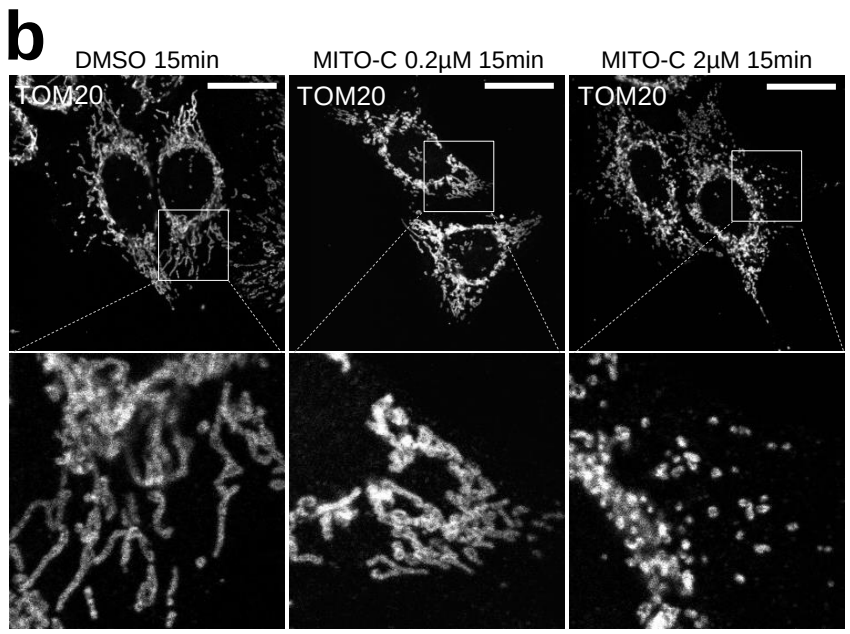
b
DMSO 15min
MITO-C 0.2µM 15min
MITO-C 2µM 15min
TOM20
TOM20
TOM20

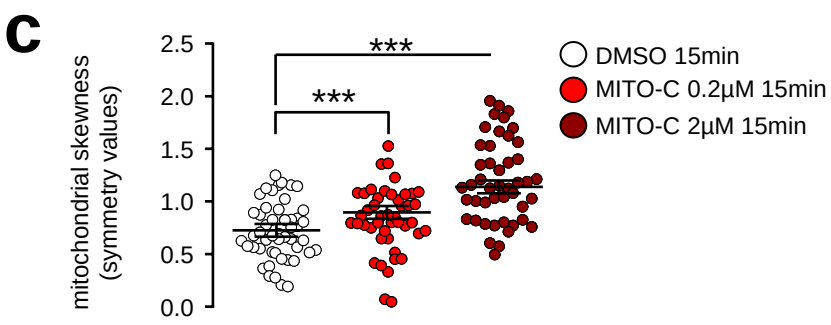
c
mitochondrial skewness
(symmetry values)
2.5
2.0
1.5
1.0
0.5
0.0
***
***
DMSO 15min
MITO-C 0.2µM 15min
MITO-C 2µM 15min

Figure S1

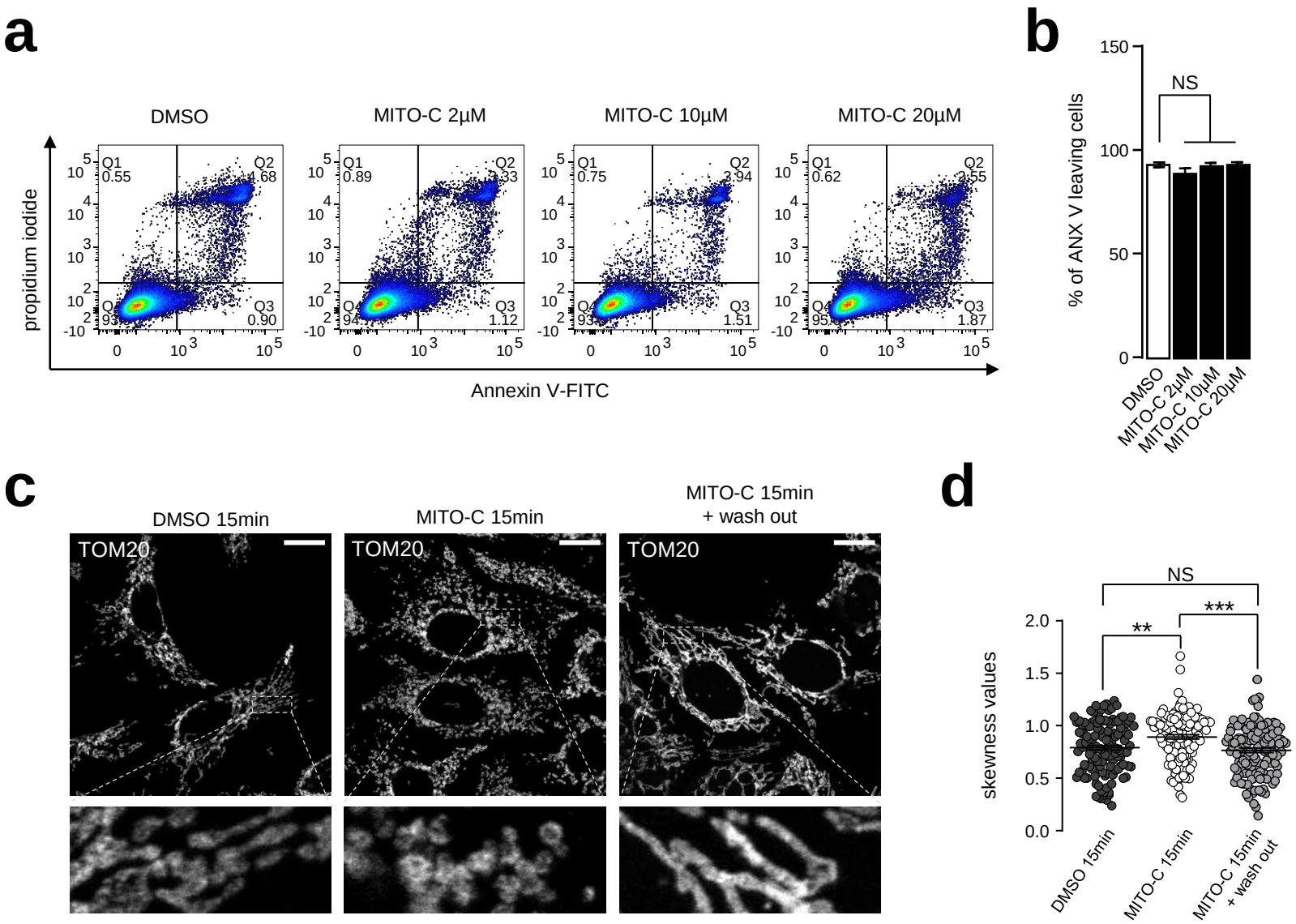
a
DMSO
MITO-C 2µM
MITO-C 10µM
MITO-C 20µM
propidium iodide
Annexin V-FITC
Q1 0.55
Q2 4.68
Q4 94.
Q3 0.90
Q1 0.89
Q2 3.33
Q4 94.
Q3 1.12
Q1 0.75
Q2 2.94
Q4 93.
Q3 1.51
Q1 0.62
Q2 2.55
Q4 95.
Q3 1.87
b
% of ANX V leaving cells
NS
DMSO
MITO-C 2µM
MITO-C 10µM
MITO-C 20µM
c
DMSO 15min
MITO-C 15min
MITO-C 15min
+ wash out
TOM20
d
skewness values
NS
**
***
DMSO 15min
MITO-C 15min
MITO-C 15min
+ wash out

Figure S2

a

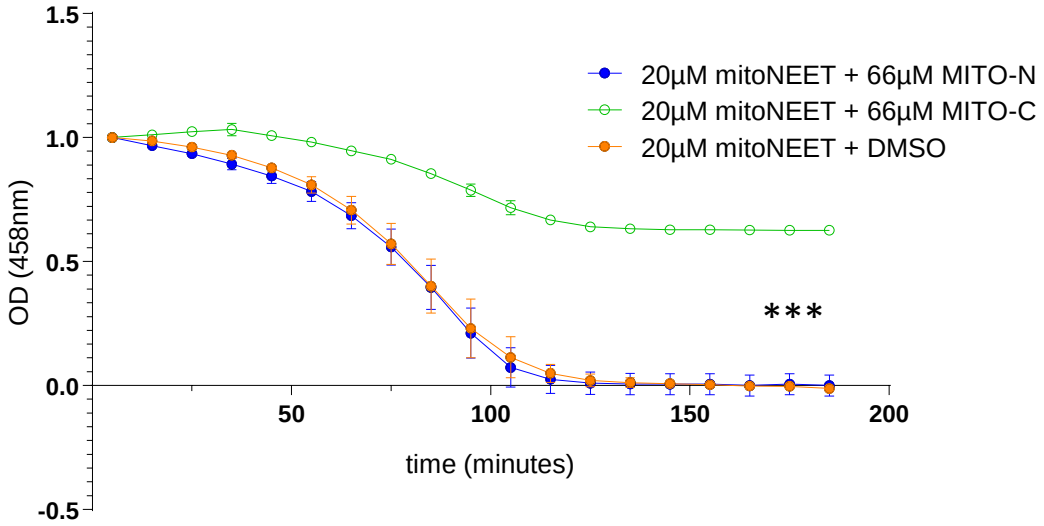
1.5
1.0
0.5
0.0
-0.5
OD (458nm)
50
100
150
200
time (minutes)
20µM mitoNEET + 66µM MITO-N
20µM mitoNEET + 66µM MITO-C
20µM mitoNEET + DMSO
***

b

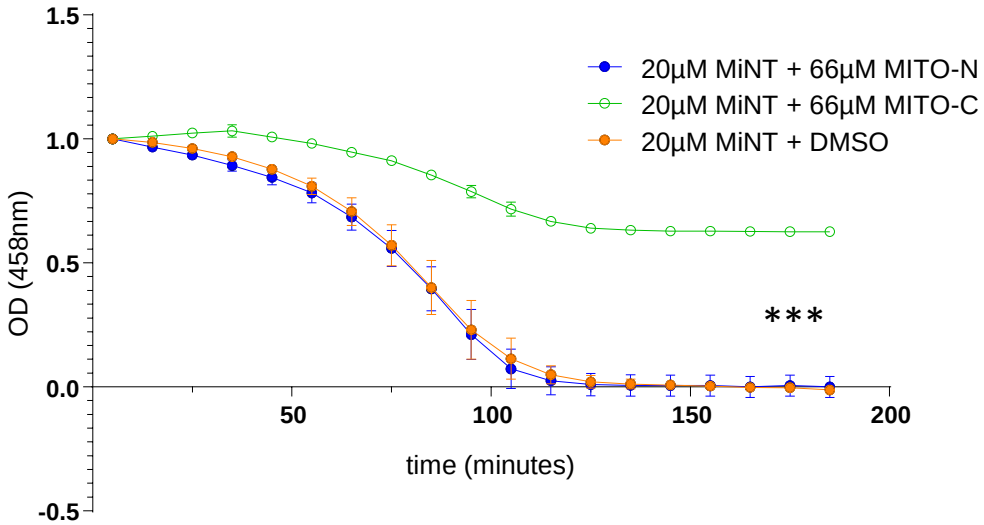
1.5
1.0
0.5
0.0
-0.5
OD (458nm)
50
100
150
200
time (minutes)
20µM MiNT + 66µM MITO-N
20µM MiNT + 66µM MITO-C
20µM MiNT + DMSO
***

Figure S3

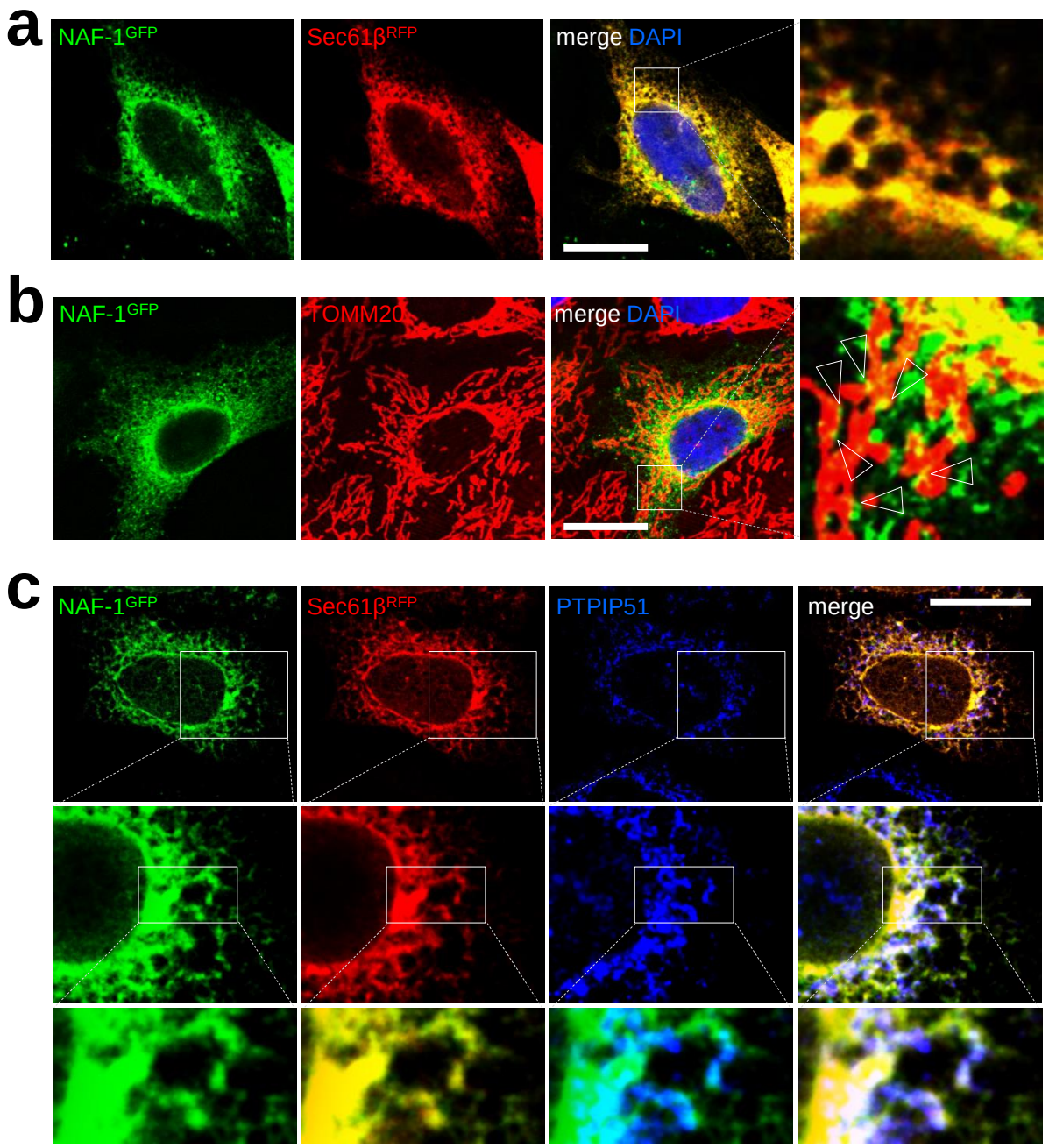
a
NAF-1GFP
Sec61βRFP
merge DAPI
b
NAF-1GFP
TOMM20
merge DAPI
c
NAF-1GFP
Sec61βRFP
PTPIP51
merge

Figure S4

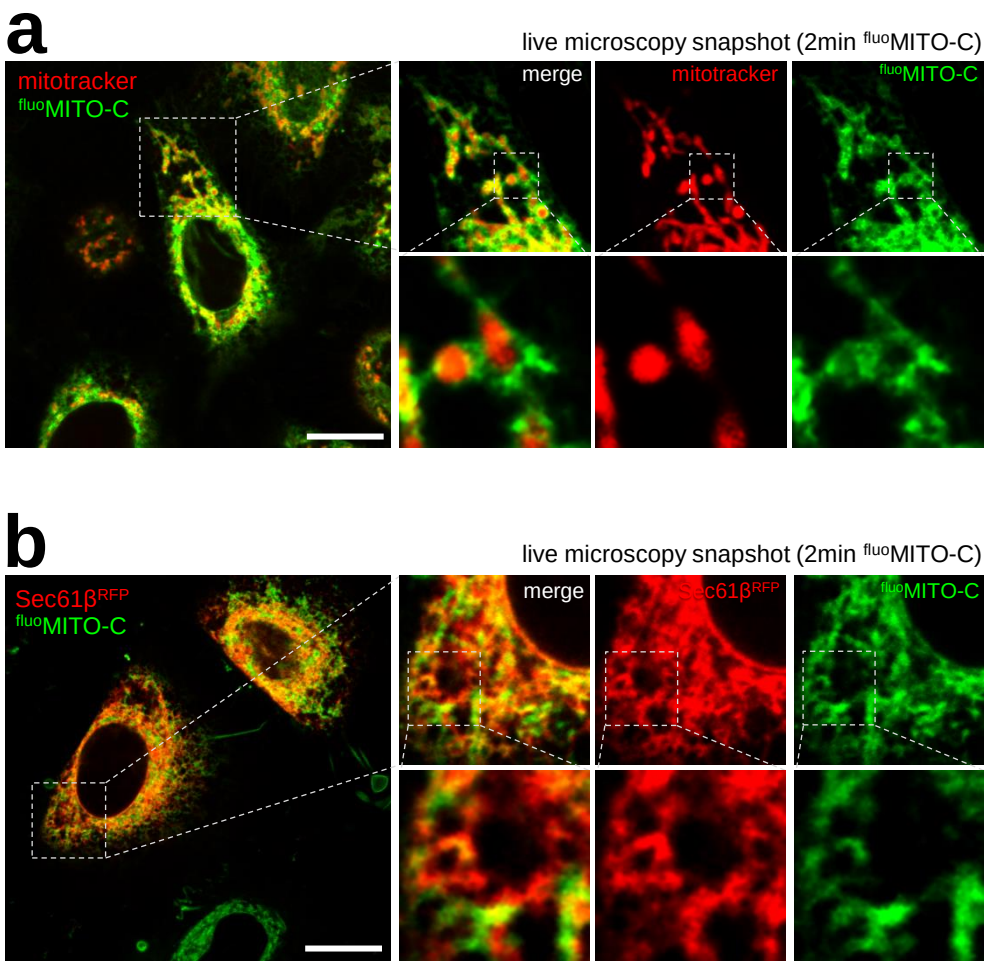
a
live microscopy snapshot (2min fluoMITO-C)
mitotracker
fluoMITO-C
merge
mitotracker
fluoMITO-C
b
live microscopy snapshot (2min fluoMITO-C)
Sec61βRFP
fluoMITO-C
merge
Sec61βRFP
fluoMITO-C

Figure S5

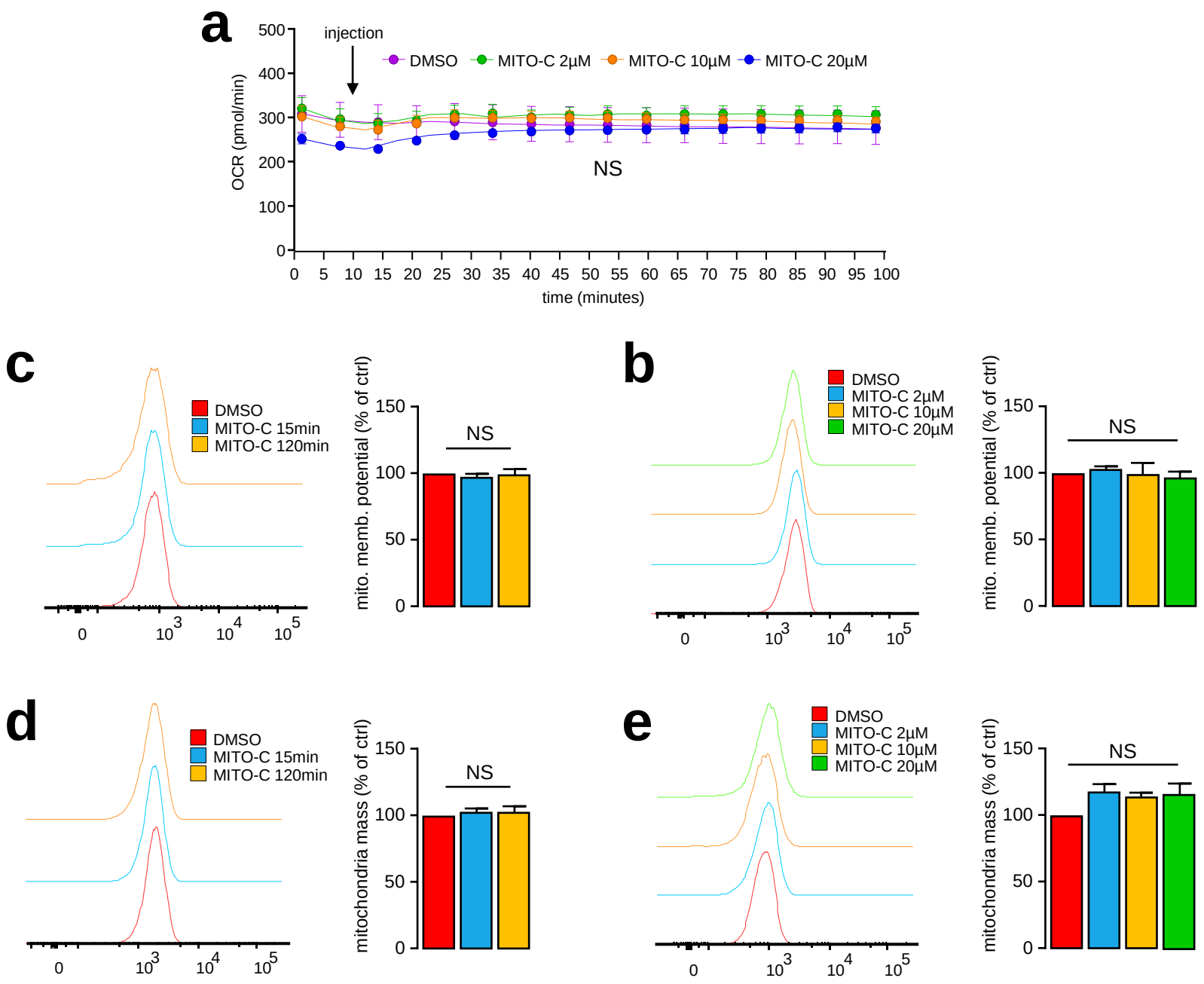
a
injection
DMSO
MITO-C 2µM
MITO-C 10µM
MITO-C 20µM
OCR (pmol/min)
NS
time (minutes)
c
DMSO
MITO-C 15min
MITO-C 120min
mito. memb. potential (% of ctrl)
NS
b
DMSO
MITO-C 2µM
MITO-C 10µM
MITO-C 20µM
mito. memb. potential (% of ctrl)
NS
d
DMSO
MITO-C 15min
MITO-C 120min
mitochondria mass (% of ctrl)
NS
e
DMSO
MITO-C 2µM
MITO-C 10µM
MITO-C 20µM
mitochondria mass (% of ctrl)
NS

Figure S6

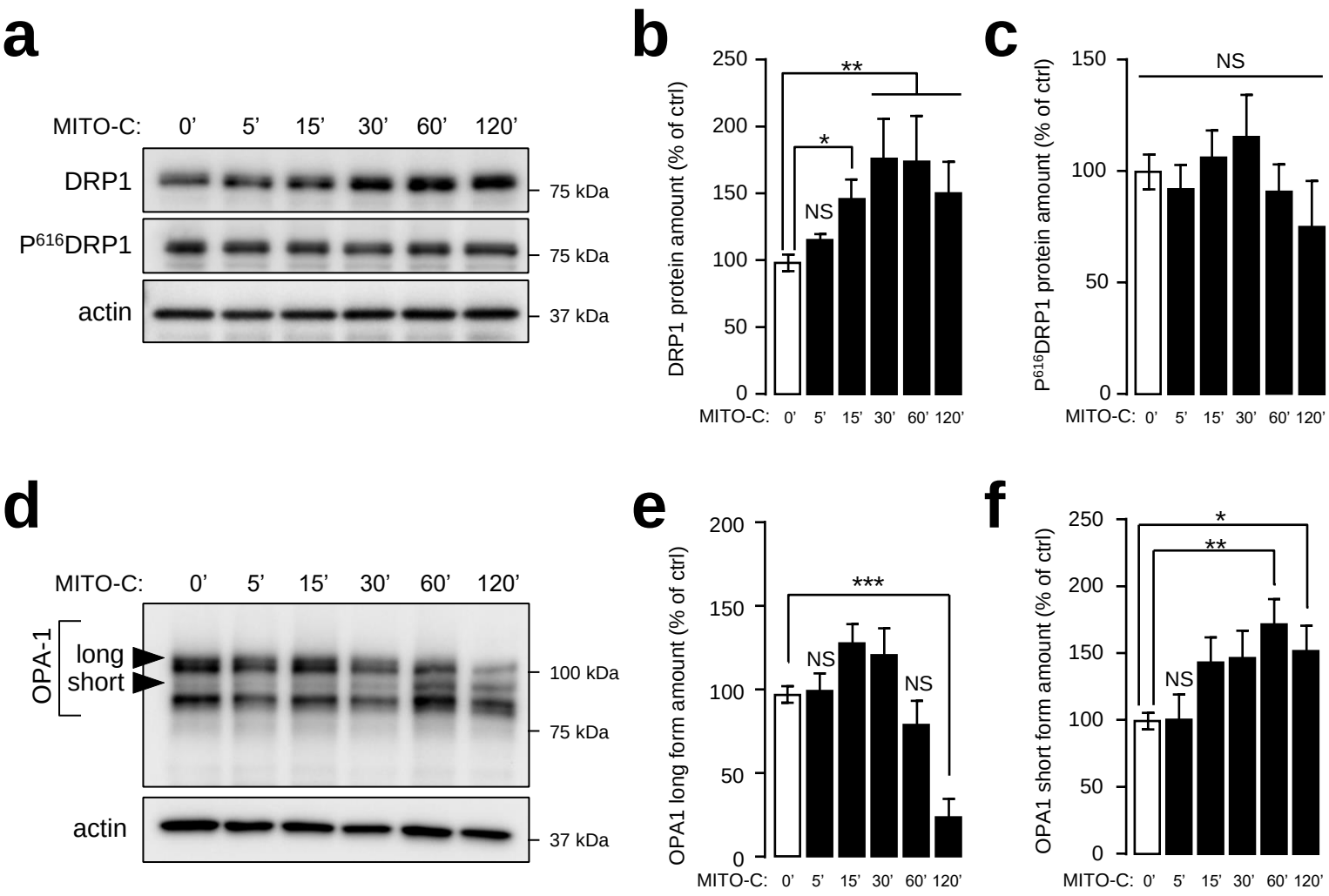
a
MITO-C: 0' 5' 15' 30' 60' 120'
DRP1
P616DRP1
actin
75 kDa
75 kDa
37 kDa
b
DRP1 protein amount (% of ctrl)
250
200
150
100
50
0
**
*
NS
MITO-C: 0' 5' 15' 30' 60' 120'
c
P616DRP1 protein amount (% of ctrl)
150
100
50
0
NS
MITO-C: 0' 5' 15' 30' 60' 120'
d
MITO-C: 0' 5' 15' 30' 60' 120'
OPA-1
long
short
actin
100 kDa
75 kDa
37 kDa
e
OPA1 long form amount (% of ctrl)
200
150
100
50
0
***
NS
NS
MITO-C: 0' 5' 15' 30' 60' 120'
f
OPA1 short form amount (% of ctrl)
250
200
150
100
50
0
*
**
NS
MITO-C: 0' 5' 15' 30' 60' 120'

Figure S7

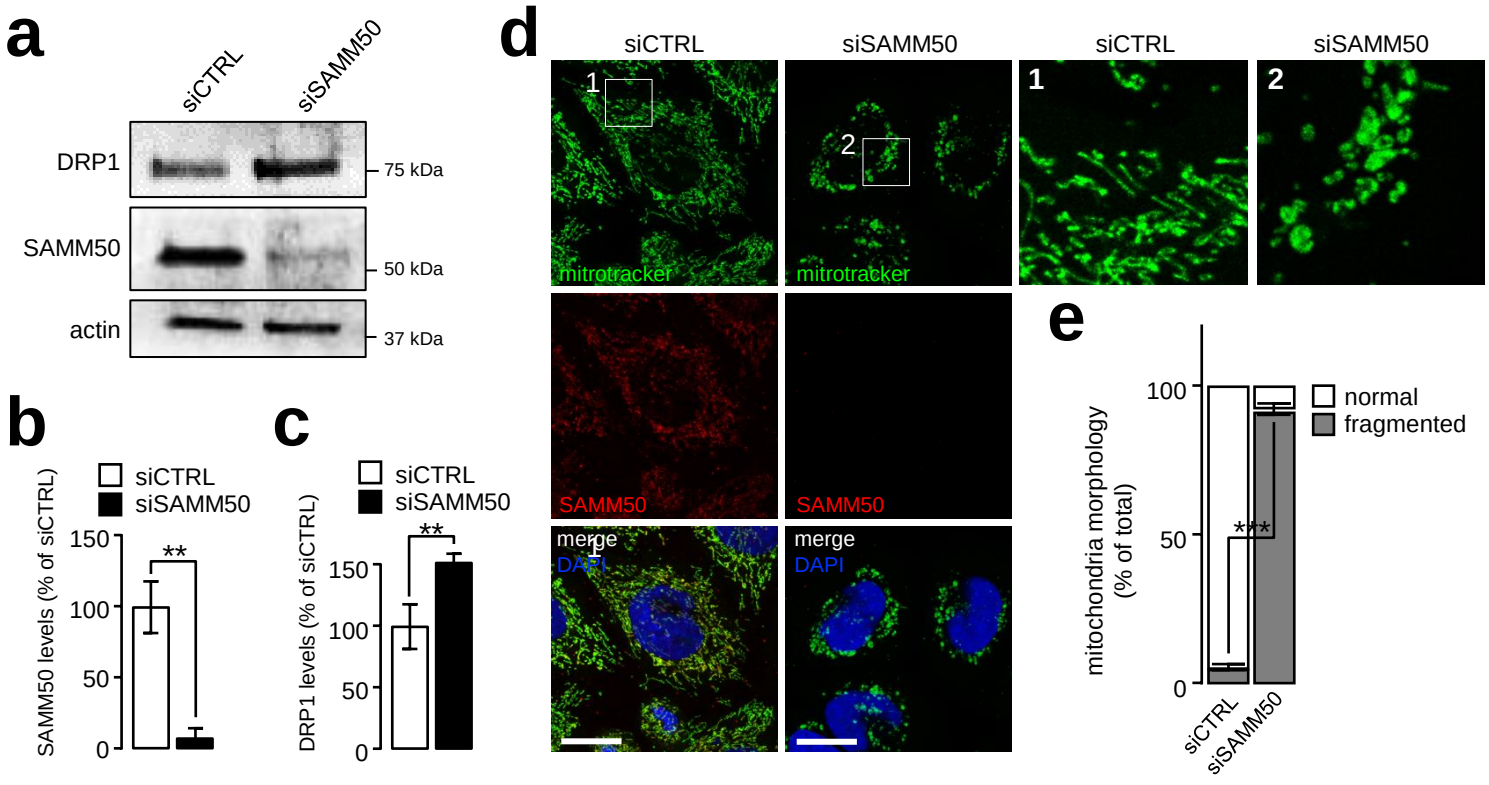
a
siCTRL
siSAMM50
DRP1
SAMM50
actin
75 kDa
50 kDa
37 kDa
b
siCTRL
siSAMM50
SAMM50 levels (% of siCTRL)
150
100
50
0
**
c
siCTRL
siSAMM50
DRP1 levels (% of siCTRL)
150
100
50
0
**
d
siCTRL
siSAMM50
siCTRL
siSAMM50
1
2
mitrotracker
SAMM50
merge
DAPI
e
mitochondria morphology (% of total)
100
50
0
***
normal
fragmented
siCTRL
siSAMM50

Figure S8

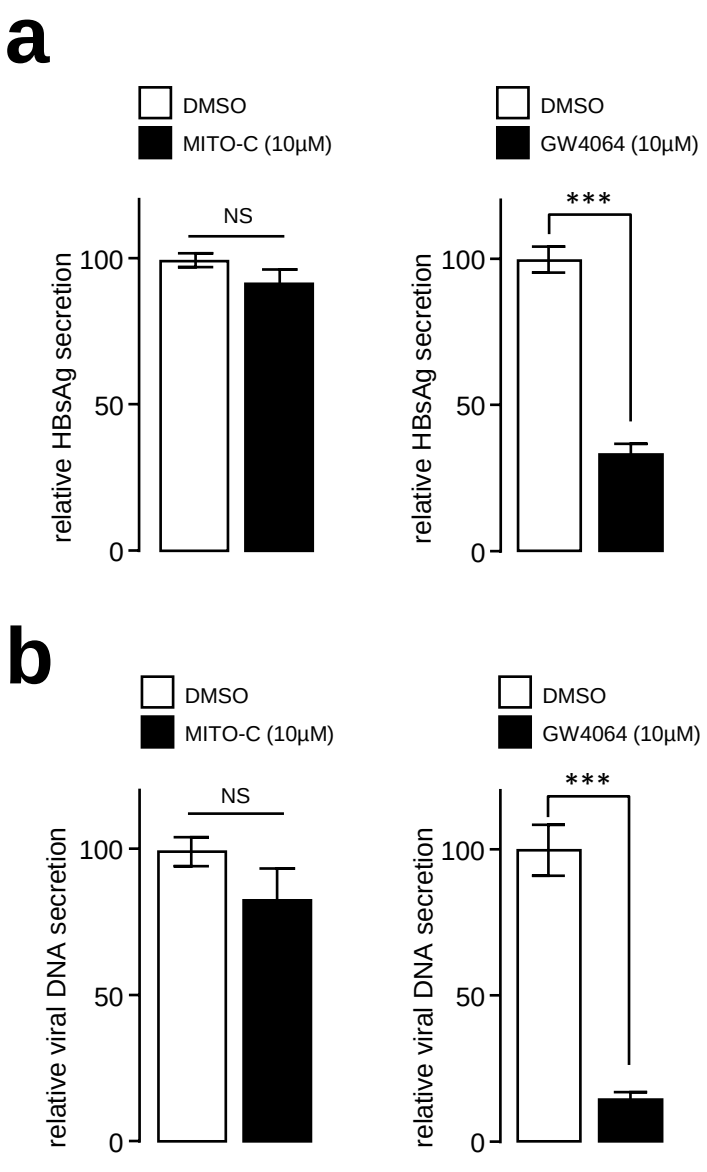
a
DMSO
MITO-C (10μM)
NS
relative HBsAg secretion
100
50
0
DMSO
GW4064 (10μM)
***
relative HBsAg secretion
100
50
0
b
DMSO
MITO-C (10μM)
NS
relative viral DNA secretion
100
50
0
DMSO
GW4064 (10μM)
***
relative viral DNA secretion
100
50
0

Figure S9

DISCUSSION

The goal of my PhD project was to investigate endomembranes alteration during influenza viral infection in host cells and to decipher whether the obtained results could help in the fine tuning of newly developed anti-viral strategies. This project thus mobilized cell biology and virology related experimental framework and unsuspectedly highlights the importance of considering mitochondrial network morphodynamics as a target to counteract influenza virus intracellular replication.

Experimental framework

First, the results obtained during my doctoral work highlighted the technical importance of choosing the optimal reduced-stress framework to carry up proper cell biology experiments in influenza viral infection context. Indeed, we showed that serum starvation and trypsin treatment, systematically used in H1N1 related studies to allow multiple infection cycles, can modify organelles morphology (and probably their function(s) as well). Most of influenza virus related studies focus on the specific tracking of a viral protein (eventually its interaction with a host protein) or into testing antiviral drugs and compounds in situations where the levels of influenza replication are monitored and analyzed. Surprisingly, a wide range study of all natural host cell type endomembranes status upon influenza infection has never been performed. Lack of information concerning a "global and dynamic" picture of how endomembranes are affected in influenza infection could thus lead to an experimental bias where it would be complicated to distinguish between a virus infection-caused phenotype or a phenotype where different stress factors can modify organelle(s) morphology and function.

Study of endomembranes modifications upon influenza infection and Mito-C treatment

Upon influenza infection in reduced-stress experimental set-up, we indeed show that several host cell endomembranes are modified (paper #1). We notably observed an increase of autophagosomal LC3 marker positive vesicles, Golgi fragmentation, a reduction of early endosomes number, a decrease of ER-mitochondria contact sites and a mitochondrial hyperfusion (Fig 32.A). While

autophagy and Golgi phenotypes have been reported previously, we report here for the first time a reduction of the early endosomes pool while late endosomes did not show significant difference. After attachment and internalization, the virus traffic through early endosomes (which maturates into late endosomes) via the endosomal pathway. At the late endosome, the V-ATPase-mediated pH acidification leads to fusion between the viral membrane and endosomal membrane to allow the release of viral RNPs to the cytoplasm (as described in section B2). Viral RNPs are released before fusing with lysosomes and experimenting total degradation. Interestingly, upon influenza infection, the interferon-inducible nuclear receptor co-activator 7 (NCOA7) has been described to interact with endo-lysosomal V-ATPase to increase endosomal acidification and acidic protease activity, finally resulting in virus degradation. These modifications impede viral and endosomal membranes fusion and consequently nuclear translocation of vRNP, thus inhibiting influenza infection (Doyle et al., 2018). These data suggest that the host antiviral response leads to accelerated early-to-late endosomal maturation to abrogate or diminish viral replication. This hypothesis could in part explain the reduction of early endosomal population that we observed, while the number of late endosomes is maintained to facilitate degradation of the endocytosed virus. Further investigation is thus required to understand the functional impact of these endosomal organelles modifications for viral infection and for the cell machinery.

We show that influenza virus entry in the host cell provokes mitochondrial network elongation (paper #1). Mito-C compound, developed by Enyo Pharma, is believed to target mitochondria and to provoke reversible mitochondria fragmentation in normal/uninfected cells (paper #2). Thus, influenza infection and Mito-C somehow present an opposed fusion/fission balance. While influenza infection promotes OPA1 increase at the mitochondria and DRP1 relocalization to the cytosol (pro-fusion state event), Mito-C favors DRP1 recruitment to the mitochondria and OPA1 cleavage (pro-fission state event). Furthermore, we report that Mito-C treatment on influenza infected cells leads to 1) influenza viral titer reduction, 2) inhibition of mitochondria hyperfusion, 3) increase number of ER-mitochondria contact sites and 4) enhanced interferon production in a RIG-I dependent manner (Fig 32.B).

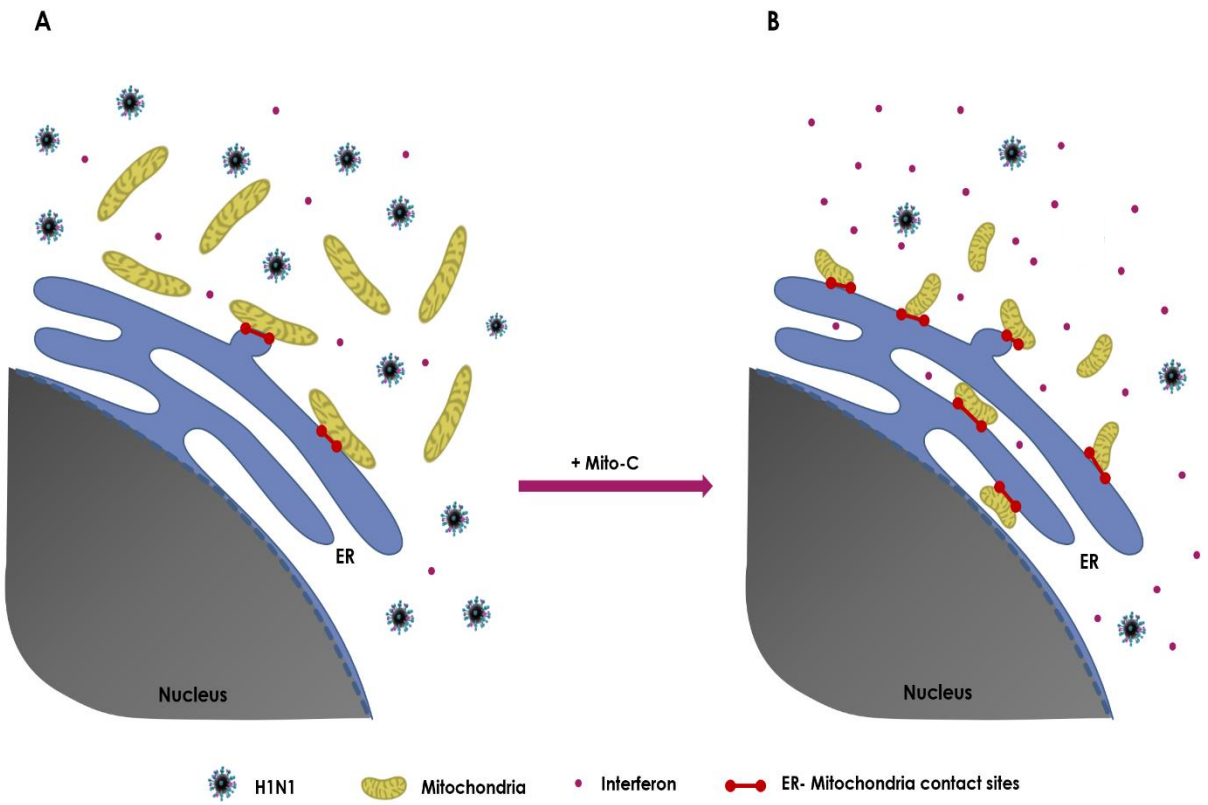

Figure 32. Proposed model 1. Mito-C treatment alleviates influenza infection by reverting mitochondria-induced hyperfusion, increasing ER-mitochondria contact sites and enhancing interferon response.

We also report that Mito-C targets mitochondrial NEET proteins (paper #2). Moreover, our data suggest a putative new function of NAF-1 as a regulator of mitochondria morphodynamics. Indeed, here we propose a model (Fig 33) where chemical perturbation of mitochondrial NAF-1 protein by Mito-C may first facilitate the rapid recruitment of DRP1 to the ER-mitochondria interface. In Mito-C treated cells situation, the ER-mitochondria contact sites are altered, resulting in mitochondria fission. Later, OPA-1 is cleaved and the accumulation of the short form of OPA-1 may maintain the pro-fission balance in time, as an adaptation to the situation.

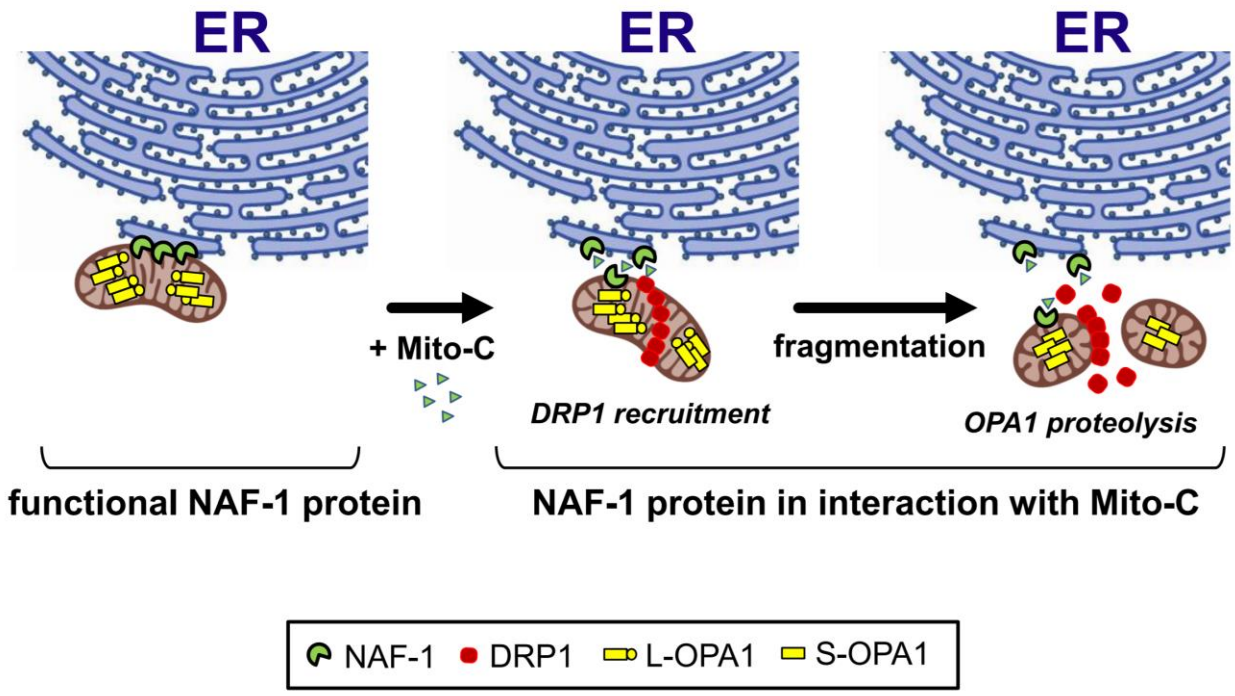

Figure 33. Proposed model 2. Mechanism of action of Mito-C in uninfected cells.

Finally, we show that Mito-C possesses also an antiviral activity against DENV (Dengue virus, also known to cause mitochondria elongation), suggesting that NAF-1/NEET protein(s) could be an important therapeutic target in antiviral research and in other pathologies where mitochondria dynamics are altered.

Mitochondrial elongation upon influenza infection and innate immunity

Mitochondria are known to be the power plant of the cell because of their role in respiration and energy production. Mitochondria also fulfill others important defense-related functions including apoptosis and innate immune response. For these reasons, this organelle represents a recurrent target for viruses during infection cycle, which goal is to inhibit innate immune response and manipulate the infected host cell for its own benefit (Castanier & Arnoult, 2011).

During influenza infection, viral RNA is detected by innate immunity RIG-I protein, which initiates signal transduction through MAVS activation at the mitochondria, resulting in interferon production and release (Jiang et al., 2012). Very interestingly, RIG-I activation promotes mitochondria network elongation. This mitochondrial morphology adjustment can be regulated by MAVS, which is suggested to promote mitochondria–ER contact sites and increase interferon production (Castanier, Garcin, Vazquez, & Arnoult, 2010). However, mitochondria elongation induced by DENV has been described to alleviate RIG-I dependent innate immunity response (Chatel-Chaix et al., 2016). In addition, our current results suggest that influenza infection reduces ER-mitochondria contact sites number and density and that Mito-C treatment restore the membrane tethering between ER and mitochondria, finally resulting in interferon production increase. In this context, our results suggest that the viral strategy may be oriented to target ER-mitochondria contact sites to impede interferon response. Thus, mitochondria elongation could be a consequence of virus induced ER-mitochondria contact sites disruption or even a failed tentative of host cells to increase interferon production.

Mitochondrial fragmentation upon influenza infection, innate immunity and apoptosis

Upon influenza viral infection, PB1-F2, an accessory protein of influenza A viruses, was shown to potentiate virulence upon infection. Indeed, viral PB1-F2 plays a role in pathogenesis by altering the host inflammatory and innate immune responses and by inducing cell death. Because there are multiple PB1-F2 sequence variants in influenza viruses, the virulence associated to PB1-F2 can differ depending on viral strains as well as host species (Kamal, Alymova, & York, 2018). As described in section B3, PB1-F2 has been previously reported to be addressed to the mitochondria and to behave as a pro-fission factor, resulting in mitochondria fragmentation (Yoshizumi et al., 2014). This targeting of PB1-F2 protein to mitochondria network may result in two specific consequences: 1) alteration of RIG-I-dependent innate immunity and 2) apoptosis cell death. Interestingly, PB1-F2 C-terminal portion can binds to MAVS protein, suppressing the RIG-I signaling pathway and thus inhibiting the induction and production of type I interferon. In addition, PB1-F2 accumulation in mitochondria leads to a reduction of mitochondrial membrane potential. Because mitochondrial-mediated innate immunity signaling is regulated in the mitochondrial

membrane and depends on the mitochondrial membrane potential, PB1-F2-mediated decrease of mitochondrial membrane potential impairs cellular innate immunity (Varga, Grant, Manicassamy, & Palese, 2012; Yoshizumi et al., 2014). Furthermore, the loss of mitochondrial membrane potential induced by PB1-F2 appears to enhance virus-associated cell death in a cell type-dependent manner (Gibbs, Malide, Hornung, Bennink, & Yewdell, 2003). Mitochondrial membrane potential decrease is enhanced by two factors: PB1-F2 possess a pore forming activity similar to the pore forming activity of pro-apoptotic Bcl-2 members and PB1-F2 interacts with VDAC, promoting permeability transition pore opening (Chanturiya et al., 2004; Zamarin, García-Sastre, Xiao, Wang, & Palese, 2005). It has been demonstrated that there is a link between fragmentation and apoptosis. When mitochondria become fragmented upon infection, the balance turn to apoptosis and mitophagy (Khan, Syed, Kim, & Siddiqui, 2015). Surprisingly, PB1-F2 low pathogenic viral variants (in absent C-terminal polypeptide) do not disturb mitochondrial functions. Altogether, these data suggest that mitochondrial fragmentation associated with influenza viral infection is due to some forms of PB1-F2 proteins and that its enhanced virulence could be associated to the shift to mitochondrial fragmentation and apoptosis processes associated with this mitochondrial phenotype. Our results show host mitochondrial elongation in PB1-F2 negative influenza viral strains conditions. This phenotype has not been associated with an increased apoptosis yet, but cell death should be explored in these new experimental conditions that we report.

Mitochondrial morphodynamics and metabolism upon influenza infection

Importantly, mitochondrial morphodynamics are also implicated in metabolism homeostasis. Several stress situations are associated with an increase of cellular energy demand, which is linked to a mitochondrial elongation and an increase of respiration coupled to ATP synthesis (Liesa & Shirihai, 2013). In some infectious contexts, when mitochondria becomes elongated, bioenergetics can be facilitated (Khan et al., 2015). Moreover, upon influenza infection, a massive consumption of ATP at the early stages of infection has been reported (Maruyama et al., 2018). Taken together, these results suggest that mitochondrial elongated network observed in our study is consistent with the fact that ATP production is necessary at early stages of infection. Indeed, the rapid ATP

production may be beneficial for both the cell (for interferon production, an anabolic process that requires energy) and for the virus (for synthesis of its own proteins using the cellular machinery).

Mitochondrial morphodynamics, metabolism and immunity upon Dengue infection

In other infectious contexts, mitochondria morphodynamics has been also explored. Indeed, during DENV viral infection, the viral non-structural proteins 4B and 3 (NS4B, NS3) interact with mitochondrial membranes and alters mitochondrial morphology inducing their elongation and increasing respiration (and consequently ATP production) (Barbier, Lang, Valois, Rothman, & Medin, 2017). This shift to mitochondria pro-fusion status is due to loss of activation of DRP1 and DRP1 mitochondrial relocalization. As a result, the integrity of ER-mitochondria contact sites are compromised, reducing the interface for innate immune signaling and the interferon response RIG-I-dependent to promote viral infection (Barbier et al., 2017; Chatel-Chaix et al., 2016). In the influenza infectious context, several viral influenza proteins have been described to impair immunity response as well. Particularly, PB2 and PB1-F2 have been shown to interact directly with mitochondrial membranes and MAVS protein to perturb immunity host cell response (described in section B3 and C5 and in the present discussion). In our study, we have reported that Mito-C compound has an antiviral effect in both DENV (paper #2) and influenza (paper #1) viruses by reversing the viral induced mitochondria elongation. On the contrary, Mito-C has no antiviral effect on HBV (hepatitis B virus, paper #2), a virus known to cause mitochondria fission and to enhance mitophagy to weaken virus-induced apoptosis and boost cell survival to enable viral persistence (Kim et al., 2013). Altogether, these data suggest that influenza and DENV viruses impair mitochondrial innate immunity using the same strategy acquired during their co-evolution with the host. Furthermore, we could extrapolate these data and consider Mito-C as a tool to treat and get a better understanding of viral biology from other viruses causing mitochondria elongation like the new emerging coronavirus SARS-Cov-2, since SARS9b protein of SARS-coronavirus has been described to induce mitochondrial network elongation (Shi et al., 2014).

NEET proteins and their possible implication in innate immunity

As described above, Mito-C, which target mitochondrial NEETs proteins, possess an acute antiviral effect by modifying ER-mitochondria contact sites and RIG-I pathway. These results point out a possible role of NEET proteins upon viral infection and associated innate immunity that needs to be further explored. Interestingly, a high-throughput screening study suggested that MiNT could interacts with MAVS and C1QBP proteins (Complement component 1 Q subcomponent-binding protein) (Floyd et al., 2016). Moreover, C1QBP have been described to interact with MAVS. Indeed, entry of viral RNA in the host cell trigger the translocation of C1QBP to the outer mitochondrial membrane and interact with MAVS, resulting in MAVS signaling inhibition and viral promotion (Xu, Xiao, Liu, Ren, & Gu, 2009). MiNT interaction with MAVS and C1QBP must be confirmed and their putative implication in mitochondrial innate immunity regulation deserves to be explored upon influenza infection context. Another NEET protein-protein interaction that may be implicated in morphodynamics and immunity is the reported crosstalk described between NAF-1 and Serca2b (sarcoendoplasmic reticulum Ca^{2+} ATPase 2). Indeed, authors reported that NAF-1 modulates Serca2b oxidation, resulting in ER Ca^{2+} uptake and intracellular Ca^{2+} homeostasis regulation (Shen et al., 2017). This Ca^{2+} transfer occurs notably at ER-mitochondria contact sites (Bravo-Sagua et al., 2017) and Ca^{2+} transport has been described to be implicated in mitochondria associated morphodynamics regulation (Zhao, Li, Wang, Yu, & Liu, 2015). Because Mito-C enhances immune response in viral infection and targets NAF-1 (which is localized at the ER and mitochondria interface), our data suggest that NAF-1 may play a role in immunity at ER-contact sites by notably regulating Ca^{2+}.

Iron role in viral infection and innate immunity

A recent study has revealed some new insights concerning the role of iron upon influenza infection. Indeed, ferric ammonium citrate (a non-transferrin binding iron form) has been shown to inhibit influenza, HIV (human immunodeficiency virus) and Zika infections by blocking endosomal viral release, inducing liposome aggregation and intracellular vesicle fusion, associated with iron-dependent cell death (Wang et al., 2018). Interestingly, HIV and Zika viruses have been described

to cause mitochondria elongation (Chatel-Chaix et al., 2016; Fields et al., 2016). Thus, iron can be as well considered as a therapeutic target to inhibit viral infections. Interestingly, iron accumulation can be reversed by the use of an iron chelator in NAF-1 deficient cells isolated from Wolfram syndrome 2 patients (described in section C3) (Danielpur et al., 2016). Because we have demonstrated that Mito-C stabilizes 2FE-2S clusters on the NEET proteins (paper #2), we could similarly hypothesize that its antiviral effect could be also related to the modulation of iron content at the mitochondria. Overall, iron cell levels and NEET proteins could act as immune-modulators and impact viral infection.

Influenza infection and NEET proteins role in autophagy

Our results and several published studies showed that autophagic pathway can be altered by influenza infection. While infected cells show an increase of LC3-II amount and an accelerated autophagic flux (Zhou et al., 2009), inhibition of autophagy significantly reduces influenza viral replication (Zhu et al., 2015). Interestingly, NAF-1 has been described to interact with Beclin1, a key protein PI3Kinase required for autophagosome biogenesis (Chang, Nguyen, Germain, & Shore, 2010). Moreover, autophagosomes formation take place at the ER- mitochondria contacts sites (Hamasaki et al., 2013). Overall, these results suggest that targeting NAF-1 may modify autophagy pathway and consequently influenza infection.

Concluding remarks

The work I developed during my PhD project brings new perspective in the understanding of innate immunity in viral infection context. Historically, innate immunity studies were performed at the molecular level by studying cellular and viral proteins, their interactions and signaling cascades. More recently, the study of host organelles such as mitochondria has allowed us to analyze the impact of their morphodynamics changes upon infection. Now, the study of dialog between endomembranes gives us new insights (and tools) in the field, indicating that innate immunity is constituted of several parallel processes that occur at different cellular levels: molecular, organellar

and also communication between organelles at a subcellular level. In conclusion, my doctoral project allowed highlighting the central role of mitochondrial morphodynamics and ER-mitochondria contact sites regulation in innate immune response to influenza viral replication. We propose Mito-C compound as a new putative antiviral molecule and a powerful tool to help understanding the underlying viral strategy. Moreover, targeting human NEET/CISDs proteins, and understanding their function in viral infection, opens important new perspectives in antiviral research. Indeed, virus need host cellular machinery in order to ensure efficient replication. The high rate of mutation to adapt to current direct-acting antiviral compounds lead to the emergence of mutated viral strains, rapidly resistant to the existing treatments. As a recent example, the last anti-influenza direct-acting drug approved by FDA 18 months ago (baloxavir marboxil) already provokes apparition of influenza resistant strains. Our data suggest that a change in the rational about antiviral development strategy by targeting host proteins (instead of targeting viral proteins) in a reversible manner would allow to abrogate efficiently influenza virus(es) replication without resistant strain emergence, thus avoiding long-term inefficacy of current direct-targeting antiviral drugs.

REFERENCES

Ackerman, E. E., Alcorn, J. F., Hase, T., & Shoemaker, J. E. (2019). A dual controllability analysis of influenza virus-host protein-protein interaction networks for antiviral drug target discovery. *BMC Bioinformatics*, *20*(1). https://doi.org/10.1186/s12859-019-2917-z

Amr, S., Heisey, C., Zhang, M., Xia, X. J., Shows, K. H., Ajlouni, K., Pandya, A., Satin, L. S., El-Shanti, H., & Shiang, R. (2007). A homozygous mutation in a novel zinc-finger protein, ERIS, is responsible for Wolfram syndrome 2. *American Journal of Human Genetics*, *81*(4), 673–683. https://doi.org/10.1086/520961

Anand, R., Wai, T., Baker, M. J., Kladt, N., Schauss, A. C., Rugarli, E., & Langer, T. (2014). The i-AAA protease YME1L and OMA1 cleave OPA1 to balance mitochondrial fusion and fission. *Journal of Cell Biology*, *204*(6), 919–929. https://doi.org/10.1083/jcb.201308006

Anand, S. K., & Tikoo, S. K. (2013). Viruses as modulators of mitochondrial functions. *Advances in Virology*, *2013*. https://doi.org/10.1155/2013/738794

Aridor, M., & Hannan, L. A. (2000). *2000 Traffic Jam A Compendium of Human Diseases that.pdf*. 836–851.

Armstrong, J. S. (2006). Mitochondria: A target for cancer therapy. *British Journal of Pharmacology*, *147*(3), 239–248. https://doi.org/10.1038/sj.bjp.0706556

Asha, K., & Kumar, B. (2019). Emerging Influenza D Virus Threat: What We Know so Far! *Journal of Clinical Medicine*, *8*(2), 192. https://doi.org/10.3390/jcm8020192

Badham, M. D., & Rossman, J. S. (2016). Filamentous Influenza Viruses. In *Current Clinical Microbiology Reports* (Vol. 3, Issue 3, pp. 155–161). Springer. https://doi.org/10.1007/s40588-016-0041-7

Ban, T., Ishihara, T., Kohno, H., Saita, S., Ichimura, A., Maenaka, K., Oka, T., Mihara, K., & Ishihara, N. (2017). Molecular basis of selective mitochondrial fusion by heterotypic action between OPA1 and cardiolipin. *Nature Cell Biology*, *19*(7), 856–863. https://doi.org/10.1038/ncb3560

Barbier, V., Lang, D., Valois, S., Rothman, A. L., & Medin, C. L. (2017). Dengue virus induces mitochondrial elongation through impairment of Drp1-triggered mitochondrial fission. *Virology*, *500*(September 2016), 149–160. https://doi.org/10.1016/j.virol.2016.10.022

Bárcena, C., Mayoral, P., & Quirós, P. M. (2018). Mitohormesis, an Antiaging Paradigm. *International Review of Cell and Molecular Biology*, *340*, 35–77. https://doi.org/10.1016/bs.ircmb.2018.05.002

Barlan, K., Rossow, M. J., & Gelfand, V. I. (2013). The journey of the organelle: Teamwork and regulation in intracellular transport. *Current Opinion in Cell Biology*, *25*(4), 483–488. https://doi.org/10.1016/j.ceb.2013.02.018

Barlowe, C. K., & Miller, E. A. (2013). *Secretory Protein Biogenesis and Traffic in the Early Secretory Pathway*. https://doi.org/10.1534/genetics.112.142810

Barman, S., & Nayak, D. P. (2000). Analysis of the Transmembrane Domain of Influenza Virus Neuraminidase, a Type II Transmembrane Glycoprotein, for Apical Sorting and Raft Association. *Journal of Virology*, *74*(14), 6538–6545. https://doi.org/10.1128/jvi.74.14.6538-6545.2000

Barodia, S. K., Prabhakaran, K., Karunakaran, S., Mishra, V., & Tapias, V. (2019). Editorial: Mitochondria and Endoplasmic Reticulum Dysfunction in Parkinson's Disease. *Frontiers in Neuroscience*, *13*, 1171. https://doi.org/10.3389/fnins.2019.01171

Beale, R., Wise, H., Stuart, A., Ravenhill, B. J., Digard, P., & Randow, F. (2014). A LC3-interacting motif in the influenza A virus M2 protein is required to subvert autophagy and maintain virion stability. *Cell Host and Microbe*, *15*(2), 239–247. https://doi.org/10.1016/j.chom.2014.01.006

Benador, I. Y., Veliova, M., Mahdaviani, K., Petcherski, A., Wikstrom, J. D., Assali, E. A., Acín-Pérez, R., Shum, M., Oliveira, M. F., Cinti, S., Sztalryd, C., Barshop, W. D., Wohlschlegel, J. A., Corkey, B. E., Liesa, M., & Shirihai, O. S. (2018). Mitochondria Bound to Lipid Droplets Have Unique Bioenergetics, Composition, and Dynamics that Support Lipid Droplet Expansion. *Cell Metabolism*, *27*(4), 869-885.e6. https://doi.org/10.1016/j.cmet.2018.03.003

Béraud-Dufour, S., & Balch, W. (2002). A journey through the exocytic pathway. *Journal of Cell Science*, *115*(9), 1779–1780.

Bexiga, M. G., & Simpson, J. C. (2013). Human diseases associated with form and function of the Golgi complex. *International Journal of Molecular Sciences*, *14*(9), 18670–18681. https://doi.org/10.3390/ijms140918670

Biswas, A., Chakrabarti, A. K., & Dutta, S. (2019). Current challenges: from the path of "original antigenic sin" towards the development of universal flu vaccines. *International Reviews of Immunology*, *0*(0), 1–16. https://doi.org/10.1080/08830185.2019.1685990

Bock, F. J., & G Tait, S. W. (n.d.). Mitochondria as multifaceted regulators of cell death. *Nature Reviews Molecular Cell Biology*. https://doi.org/10.1038/s41580-019-0173-8

Boivin, S., Cusack, S., Ruigrok, R. W. H., & Hart, D. J. (2010). Influenza A virus polymerase: Structural insights into replication and host adaptation mechanisms. *Journal of Biological Chemistry*, *285*(37), 28411–28417. https://doi.org/10.1074/jbc.R110.117531

Boutant, M., Kulkarni, S. S., Joffraud, M., Ratajczak, J., Valera-Alberni, M., Combe, R., Zorzano, A., & Cantó, C. (2017). Mfn2 is critical for brown adipose tissue thermogenic function. *The EMBO Journal*, *36*(11), 1543–1558. https://doi.org/10.15252/embj.201694914

Bouvier, N. M., & Palese, P. (2008). The biology of influenza viruses. *Vaccine*, *26*(SUPPL. 4). https://doi.org/10.1016/j.vaccine.2008.07.039

Brandizzi, F., & Barlowe, C. (2013). Organization of the ER-Golgi interface for membrane traffic control. *Nature Reviews Molecular Cell Biology*, *14*(6), 382–392. https://doi.org/10.1038/nrm3588

Bravo-Sagua, R., Parra, V., López-Crisosto, C., Díaz, P., Quest, A. F. G., & Lavandero, S. (2017). Calcium transport and signaling in mitochondria. *Comprehensive Physiology*, *7*(2), 623–634. https://doi.org/10.1002/cphy.c160013

Braymer, J. J., & Lill, R. (2017). Iron–sulfur cluster biogenesis and trafficking in mitochondria. *Journal of Biological Chemistry*, *292*(31), 12754–12763. https://doi.org/10.1074/jbc.R117.787101

Buonagurio, D. A., Nakada, S., Fitch, W. M., & Palese, P. (1986). Epidemiology of influenza C virus in man: Multiple evolutionary lineages and low rate of change. *Virology*, *153*(1), 12–21. https://doi.org/10.1016/0042-6822(86)90003-6

Cadena, C., Ahmad, S., Xavier, A., Hou, F., Binder, M., & Hur, S. (2019). Ubiquitin-Dependent and-Independent Roles of E3 Ligase RIPLET in Innate Immunity The E3 ligase RIPLET activates RIG-I via dual ubiquitin-dependent and-independent mechanisms that together work to discriminate the length of dsRNA sensed by RIG-I. *Cell*, *177*. https://doi.org/10.1016/j.cell.2019.03.017

Carnell, G. W., Ferrara, F., Grehan, K., Thompson, C. P., & Temperton, N. J. (2015). Pseudotype-based neutralization assays for influenza: A systematic analysis. *Frontiers in Immunology*, *6*(MAR), 1–17. https://doi.org/10.3389/fimmu.2015.00161

Castanier, C., & Arnoult, D. (2011). Mitochondrial localization of viral proteins as a means to subvert host defense. *Biochimica et Biophysica Acta - Molecular Cell Research*, *1813*(4), 575–583. https://doi.org/10.1016/j.bbamcr.2010.08.009

Castanier, C., Garcin, D., Vazquez, A., & Arnoult, D. (2010). Mitochondrial dynamics regulate the RIG-I-like receptor antiviral pathway. *EMBO Reports*, *11*(2), 133–138. https://doi.org/10.1038/embor.2009.258

Chakrabarti, R., Ji, W. K., Stan, R. V., Sanz, J. de J., Ryan, T. A., & Higgs, H. N. (2018). INF2-mediated actin polymerization at the ER stimulates mitochondrial calcium uptake, inner membrane constriction, and division. *Journal of Cell Biology*, *217*(1), 251–268. https://doi.org/10.1083/jcb.201709111

Chandel, N. S. (2014). Mitochondria as signaling organelles. *BMC Biology*, *12*. https://doi.org/10.1186/1741-7007-12-34

Chang, N. C., Nguyen, M., Germain, M., & Shore, G. C. (2010). Antagonism of Beclin 1-dependent autophagy by BCL-2 at the endoplasmic reticulum requires NAF-1. *EMBO Journal*, *29*(3), 606–618. https://doi.org/10.1038/emboj.2009.369

Chanturiya, A. N., Basanez, G., Schubert, U., Henklein, P., Yewdell, J. W., & Zimmerberg, J. (2004). PB1-F2, an Influenza A Virus-Encoded Proapoptotic Mitochondrial Protein, Creates Variably Sized Pores in Planar Lipid Membranes. *Journal of Virology*, *78*(12), 6304–6312. https://doi.org/10.1128/jvi.78.12.6304-6312.2004

Chatel-Chaix, L., Cortese, M., Romero-Brey, I., Bender, S., Neufeldt, C. J., Fischl, W., Scaturro, P., Schieber, N., Schwab, Y., Fischer, B., Ruggieri, A., & Bartenschlager, R. (2016). Dengue Virus Perturbs Mitochondrial Morphodynamics to Dampen Innate Immune Responses. *Cell Host and Microbe*, *20*(3), 342–356. https://doi.org/10.1016/j.chom.2016.07.008

Chen, H., Detmer, S. A., Ewald, A. J., Griffin, E. E., Fraser, S. E., & Chan, D. C. (2003). Mitofusins Mfn1 and Mfn2 coordinately regulate mitochondrial fusion and are essential for embryonic development. *Journal of Cell Biology*, *160*(2), 189–200. https://doi.org/10.1083/jcb.200211046

Chen, Y. F., Kao, C. H., Chen, Y. T., Wang, C. H., Wu, C. Y., Tsai, C. Y., Liu, F. C., Yang, C. W., Wei, Y. H., Hsu, M. T., Tsai, S. F., & Tsai, T. F. (2009). Cisd2 deficiency drives premature aging and causes mitochondria-mediated defects in mice. *Genes and*

Development, *23*(10), 1183–1194. https://doi.org/10.1101/gad.1779509

Cheng, Z., Landry, A. P., Wang, Y., & Ding, H. (2017). Binding of nitric oxide in CDGSH-type [2Fe-2S] clusters of the human mitochondrial protein miner2. *Journal of Biological Chemistry*, *292*(8), 3146–3153. https://doi.org/10.1074/jbc.M116.766774

Chin, C. R., & Brass, A. L. (2013). A genome wide RNA interference screening method to identify host factors that modulate Influenza A virus replication. In *Methods* (Vol. 59, Issue 2, pp. 217–224). Methods. https://doi.org/10.1016/j.ymeth.2012.09.009

Chlanda, P., Schraidt, O., Kummer, S., Riches, J., Oberwinkler, H., Prinz, S., Kräusslich, H.-G., & Briggs, J. A. G. (2015). Structural Analysis of the Roles of Influenza A Virus Membrane-Associated Proteins in Assembly and Morphology. *Journal of Virology*, *89*(17), 8957–8966. https://doi.org/10.1128/jvi.00592-15

Cho, B., Cho, H. M., Jo, Y., Kim, H. D., Song, M., Moon, C., Kim, H., Kim, K., Sesaki, H., Rhyu, I. J., Kim, H., & Sun, W. (2017). ARTICLE Constriction of the mitochondrial inner compartment is a priming event for mitochondrial division. *Nature Communications*, *8*. https://doi.org/10.1038/ncomms15754

Chou, Y. ying, Heaton, N. S., Gao, Q., Palese, P., Singer, R., & Lionnet, T. (2013). Colocalization of Different Influenza Viral RNA Segments in the Cytoplasm before Viral Budding as Shown by Single-molecule Sensitivity FISH Analysis. *PLoS Pathogens*, *9*(5). https://doi.org/10.1371/journal.ppat.1003358

Cipolat, S., De Brito, O. M., Dal Zilio, B., & Scorrano, L. (2004). OPA1 requires mitofusin 1 to promote mitochondrial fusion. *Proceedings of the National Academy of Sciences of the United States of America*, *101*(45), 15927–15932. https://doi.org/10.1073/pnas.0407043101

Cohen, S., Valm, A. M., & Lippincott-Schwartz, J. (2018). Interacting organelles. In *Current Opinion in Cell Biology* (Vol. 53, pp. 84–91). Elsevier Ltd. https://doi.org/10.1016/j.ceb.2018.06.003

Coletti, P., Poletto, C., Turbelin, C., Blanchon, T., & Colizza, V. (2018). Shifting patterns of seasonal influenza epidemics. *Scientific Reports*, *8*(1), 1–12. https://doi.org/10.1038/s41598-018-30949-x

Collin, E. A., Sheng, Z., Lang, Y., Ma, W., Hause, B. M., & Li, F. (2015). Cocirculation of Two Distinct Genetic and Antigenic Lineages of Proposed Influenza D Virus in Cattle. *Journal of Virology*, *89*(2), 1036–1042. https://doi.org/10.1128/jvi.02718-14

Colman, P. M., Varghese, J. N., & Laver, W. G. (1983). Structure of the catalytic and antigenic sites in influenza virus neuraminidase. *Nature*, *303*(5912), 41–44. https://doi.org/10.1038/303041a0

Colombini, M. (2016). The VDAC channel: Molecular basis for selectivity. *Biochimica et Biophysica Acta - Molecular Cell Research*, *1863*(10), 2498–2502. https://doi.org/10.1016/j.bbamcr.2016.01.019

Compans, R. W., & Dimmock, N. J. (1969). An electron microscopic study of single-cycle infection of chick embryo fibroblasts by influenza virus. *Virology*, *39*(3), 499–515. https://doi.org/10.1016/0042-6822(69)90098-1

Couet, J., Belanger, M. M., Roussel, E., & Drolet, M. C. (2001). Cell biology of caveolae and caveolin. *Advanced Drug Delivery Reviews*, *49*(3), 223–235. https://doi.org/10.1016/s0169-409x(01)00139-9

Cros, J. F., & Palese, P. (2003). Trafficking of viral genomic RNA into and out of the nucleus: Influenza, Thogoto and Borna disease viruses. *Virus Research*, *95*(1–2), 3–12. https://doi.org/10.1016/S0168-1702(03)00159-X

Cross, K., Langley, W., Russell, R., Skehel, J., & Steinhauer, D. (2010). Composition and Functions of the Influenza Fusion Peptide. *Protein & Peptide Letters*, *16*(7), 766–778. https://doi.org/10.2174/092986609788681715

Csordás, G., Weaver, D., & Hajnóczky, G. (2018). Endoplasmic Reticulum-Mitochondrial Contactology: Structure and Signaling Functions. *Trends in Cell Biology*, *28*(7), 523–540. https://doi.org/10.1016/j.tcb.2018.02.009

Dadonaite, B., Gilbertson, B., Knight, M. L., Trifkovic, S., Rockman, S., Laederach, A., Brown, L. E., Fodor, E., & Bauer, D. L. V. (2019). The structure of the influenza A virus genome. *Nature Microbiology*, *4*(11), 1781–1789. https://doi.org/10.1038/s41564-019-0513-7

Dan Dunn, J., Alvarez, L. A. J., Zhang, X., & Soldati, T. (2015). Reactive oxygen species and mitochondria: A nexus of cellular homeostasis. In *Redox Biology* (Vol. 6, pp. 472–485). Elsevier B.V. https://doi.org/10.1016/j.redox.2015.09.005

Danielpur, L., Sohn, Y. S., Karmi, O., Fogel, C., Zinger, A., Abu-Libdeh, A., Israeli, T., Riahi, Y., Pappo, O., Birk, R., Zangen, D. H., Mittler, R., Cabantchik, Z. I., Cerasi, E., Nechushtai, R., & Leibowitz, G. (2016). GLP-1-RA corrects mitochondrial labile iron accumulation and improves β-cell function in type 2 wolfram syndrome. *Journal of Clinical Endocrinology*

and Metabolism, *101*(10), 3592–3599. https://doi.org/10.1210/jc.2016-2240

Das, A., Nag, S., Mason, A. B., & Barroso, M. M. (2016). Endosome-mitochondria interactions are modulated by iron release from transferrin. *The Journal of Cell Biology*, *214*(7), 831–845. https://doi.org/10.1083/jcb.201602069

De Brito, O. M., & Scorrano, L. (2008). Mitofusin 2 tethers endoplasmic reticulum to mitochondria. *Nature*, *456*(7222), 605–610. https://doi.org/10.1038/nature07534

de Chassey, B., Meyniel-Schicklin, L., Vonderscher, J., André, P., & Lotteau, V. (2014). Virus-host interactomics: New insights and opportunities for antiviral drug discovery. *Genome Medicine*, *6*(11), 1–14. https://doi.org/10.1186/s13073-014-0115-1

De Silva, D., Tu, Y. T., Amunts, A., Fontanesi, F., & Barrientos, A. (2015). Mitochondrial ribosome assembly in health and disease. *Cell Cycle*, *14*(14), 2226–2250. https://doi.org/10.1080/15384101.2015.1053672

De Vlugt, C., Sikora, D., & Pelchat, M. (2018). Insight into influenza: A virus cap-snatching. *Viruses*, *10*(11). https://doi.org/10.3390/v10110641

de Wit, E., & Fouchier, R. A. M. (2008). Emerging influenza. *Journal of Clinical Virology*, *41*(1), 1–6. https://doi.org/10.1016/j.jcv.2007.10.017

Dias, A., Bouvier, D., Crépin, T., McCarthy, A. A., Hart, D. J., Baudin, F., Cusack, S., & Ruigrok, R. W. H. (2009). The cap-snatching endonuclease of influenza virus polymerase resides in the PA subunit. *Nature*, *458*(7240), 914–918. https://doi.org/10.1038/nature07745

Dobrovolny, H. M., & Beauchemin, C. A. A. (2017). Modelling the emergence of influenza drug resistance: The roles of surface proteins, the immune response and antiviral mechanisms. *PLoS ONE*, *12*(7), 1–26. https://doi.org/10.1371/journal.pone.0180582

Dolman, N. J., Gerasimenko, J. V., Gerasimenko, O. V., Voronina, S. G., Petersen, O. H., & Tepikin, A. V. (2005). Stable Golgi-mitochondria complexes and formation of Golgi Ca2+ gradients in pancreatic acinar cells. *Journal of Biological Chemistry*, *280*(16), 15794–15799. https://doi.org/10.1074/jbc.M412694200

Dowdle, W. R., Davenport, F. M., Fukumi, H., Schild, G. C., Tumova, B., Webster, R. G., & Zakstelskaja, L. Y. (1975). Orthomyxoviridae. *Intervirology*, *5*(5), 245–251. https://doi.org/10.1159/000149921

Doyle, T., Moncorgé, O., Bonaventure, B., Pollpeter, D., Lussignol, M., Tauziet, M., Apolonia, L., Catanese, M. T., Goujon, C., & Malim, M. H. (2018). The interferon-inducible isoform of NCOA7 inhibits endosome-mediated viral entry. In *Nature Microbiology* (Vol. 3, Issue 12, pp. 1369–1376). Nature Publishing Group. https://doi.org/10.1038/s41564-018-0273-9

Du, X., King, A. A., Woods, R. J., & Pascual, M. (2017). Evolution-informed forecasting of seasonal influenza A (H3N2). *Science Translational Medicine*, *9*(413). https://doi.org/10.1126/scitranslmed.aan5325

Dudek, J. (2017). Role of cardiolipin in mitochondrial signaling pathways. *Frontiers in Cell and Developmental Biology*, *5*(SEP), 1–17. https://doi.org/10.3389/fcell.2017.00090

Dudev, T., Grauffel, C., & Lim, C. (2016). Influence of the Selectivity Filter Properties on Proton Selectivity in the Influenza A M2 Channel. *Journal of the American Chemical Society*, *138*(39), 13038–13047. https://doi.org/10.1021/jacs.6b08041

Edinger, T. O., Pohl, M. O., & Stertz, S. (2014). Entry of influenza A virus: Host factors and antiviral targets. *Journal of General Virology*, *95*(PART 2), 263–277. https://doi.org/10.1099/vir.0.059477-0

Ehses, S., Raschke, I., Mancuso, G., Bernacchia, A., Geimer, S., Tondera, D., Martinou, J. C., Westermann, B., Rugarli, E. I., & Langer, T. (2009). Regulation of OPA1 processing and mitochondrial fusion by m-AAA protease isoenzymes and OMA1. *Journal of Cell Biology*, *187*(7), 1023–1036. https://doi.org/10.1083/jcb.200906084

Elbaz-Alon, Y., Rosenfeld-Gur, E., Shinder, V., Futerman, A. H., Geiger, T., & Schuldiner, M. (2014). A dynamic interface between vacuoles and mitochondria in yeast. *Developmental Cell*, *30*(1), 95–102. https://doi.org/10.1016/j.devcel.2014.06.007

English, A. R., & Voeltz, G. K. (2013). Interconnections with Other Organelles. *Cold Spring Harbor Perspectives in Biology*, 1–16. https://doi.org/10.1101/cshperspect.a013227

Farhan, H., & Rabouille, C. (2011). Signalling to and from the secretory pathway (Journal of Cell Science 124, 171-180). *Journal of Cell Science*, *124*(4), 669. https://doi.org/10.1242/jcs.086991

Feng, G., Liu, B., Hou, T., Wang, X., & Cheng, H. (2017). Mitochondrial Flashes: Elemental Signaling Events in Eukaryotic Cells. *Handbook of Experimental Pharmacology*, *240*, 403–422. https://doi.org/10.1007/164_2016_129

Fenouille, N., Nascimbeni, A. C., Botti-Millet, J., Dupont, N., Morel, E., & Codogno, P. (2017). To be or not to be cell autonomous? Autophagy says both. *Essays in Biochemistry*, *61*(6), 649–661. https://doi.org/10.1042/EBC20170025

Ferecatu, I., Canal, F., Fabbri, L., Mazure, N. M., Bouton, C., & Golinelli-Cohen, M. P. (2018). Dysfunction in the mitochondrial Fe-S assembly machinery leads to formation of the chemoresistant truncated VDAC1 isoform without HIF-1α activation. *PLoS ONE*, *13*(3), 1–21. https://doi.org/10.1371/journal.pone.0194782

Fessler, E., Eckl, E.-M., Schmitt, S., Alves Mancilla, I., Meyer-Bender, M. F., Hanf, M., Philippou-Massier, J., Krebs, S., Zischka, H., & Jae, L. T. (2076). A pathway coordinated by DELE1 relays mitochondrial stress to the cytosol. *Nature*, *579*, 433. https://doi.org/10.1038/s41586-020-2076-4

Fields, J. A., Serger, E., Campos, S., Divakaruni, A. S., Kim, C., Smith, K., Trejo, M., Adame, A., Spencer, B., Rockenstein, E., Murphy, A. N., Ellis, R. J., Letendre, S., Grant, I., & Masliah, E. (2016). HIV alters neuronal mitochondrial fission/fusion in the brain during HIV-associated neurocognitive disorders. *Neurobiology of Disease*, *86*, 154–169. https://doi.org/10.1016/j.nbd.2015.11.015

Floyd, B. J., Wilkerson, E. M., Veling, M. T., Minogue, C. E., Xia, C., Beebe, E. T., Wrobel, R. L., Cho, H., Kremer, L. S., Alston, C. L., Gromek, K. A., Dolan, B. K., Ulbrich, A., Stefely, J. A., Bohl, S. L., Werner, K. M., Jochem, A., Westphall, M. S., Rensvold, J. W., … Conceived, D. J. P. (2016). Mitochondrial protein interaction mapping identifies new regulators of respiratory chain function of the project and its design HHS Public Access. *Mol Cell*, *63*(4), 621–632. https://doi.org/10.1016/j.molcel.2016.06.033

Francy, C. A., Clinton, R. W., Fröhlich, C., Murphy, C., & Mears, J. A. (2017). Cryo-EM Studies of Drp1 Reveal Cardiolipin Interactions that Activate the Helical Oligomer. *Scientific Reports*, *7*(1), 1–12. https://doi.org/10.1038/s41598-017-11008-3

Frank, S., Gaume, B., Bergmann-Leitner, E. S., Leitner, W. W., Robert, E. G., Catez, F., Smith, C. L., & Youle, R. J. (2001). The Role of Dynamin-Related Protein 1, a Mediator of Mitochondrial Fission, in Apoptosis. *Developmental Cell*, *1*(4), 515–525. https://doi.org/10.1016/S1534-5807(01)00055-7

Friedman, J. R., Lackner, L. L., West, M., DiBenedetto, J. R., Nunnari, J., & Voeltz, G. K. (2011). ER tubules mark sites of mitochondrial division. *Science*, *334*(6054), 358–362. https://doi.org/10.1126/science.1207385

Friedman, J. R., & Nunnari, J. (2014). Mitochondrial form and function. *Nature*, *505*(7483), 335–343. https://doi.org/10.1038/nature12985

Frohman, M. A. (2015). Role of mitochondrial lipids in guiding fission and fusion NIH Public Access. *J Mol Med (Berl)*, *93*(3), 263–269. https://doi.org/10.1007/s00109-014-1237-z

Fujii, Y., Goto, H., Watanabe, T., Yoshida, T., & Kawaoka, Y. (2003). Selective incorporation of influenza virus RNA segments into virions. *Proceedings of the National Academy of Sciences of the United States of America*, *100*(4), 2002–2007. https://doi.org/10.1073/pnas.0437772100

Fung, H. Y. J., Fu, S. C., & Chook, Y. M. (2017). Nuclear export receptor CRM1 recognizes diverse conformations in nuclear export signals. *ELife*, *6*, 1–13. https://doi.org/10.7554/eLife.23961

Gagescu, R., Gruenberg, J., & Smythe, E. (2000). Membrane Dynamics in Endocytosis: Structure–Function Relationship 1 Atomic Resolution of the Clathrin-Based Machinery. *Traffic Munksgaard International Publishers Traffic Report*, *1*, 84–88.

Gannagé, M., Dormann, D., Albrecht, R., Dengjel, J., Torossi, T., Rämer, P. C., Lee, M., Strowig, T., Arrey, F., Conenello, G., Pypaert, M., Andersen, J., García-Sastre, A., & Münz, C. (2009). Matrix Protein 2 of Influenza A Virus Blocks Autophagosome Fusion with Lysosomes. *Cell Host and Microbe*, *6*(4), 367–380. https://doi.org/10.1016/j.chom.2009.09.005

Gao, Q., Chou, Y.-Y., Doganay, S., Vafabakhsh, R., Ha, T., & Palese, P. (2012). The Influenza A Virus PB2, PA, NP, and M Segments Play a Pivotal Role during Genome Packaging. *Journal of Virology*, *86*(13), 7043–7051. https://doi.org/10.1128/jvi.00662-12

Gatta, A. T., & Levine, T. P. (2017). Piecing Together the Patchwork of Contact Sites. *Trends in Cell Biology*, *27*(3), 214–229. https://doi.org/10.1016/j.tcb.2016.08.010

Geldenhuys, W. J., Benkovic, S. A., Lin, L., Yonutas, H. M., Crish, S. D., Sullivan, P. G., Darvesh, A. S., Brown, C. M., & Richardson, J. R. (2017). MitoNEET (CISD1) Knockout Mice Show Signs of Striatal Mitochondrial Dysfunction and a Parkinson's Disease Phenotype. *ACS Chemical Neuroscience*, *8*(12), 2759–2765.

https://doi.org/10.1021/acschemneuro.7b00287

Geldenhuys, W. J., Skolik, R., Konkle, M. E., Menze, M. A., Long, T. E., & Robart, A. R. (2019). Binding of thiazolidinediones to the endoplasmic reticulum protein nutrient-deprivation autophagy factor-1. *Bioorganic and Medicinal Chemistry Letters*, *29*(7), 901–904. https://doi.org/10.1016/j.bmcl.2019.01.041

Ghebrehewet, S., Macpherson, P., & Ho, A. (2016). Influenza. *BMJ (Online)*, *355*(December), 1–10. https://doi.org/10.1136/bmj.i6258

Gibbs, J. S., Malide, D., Hornung, F., Bennink, J. R., & Yewdell, J. W. (2003). *PB1F2 targets mitochondrial membranevia Helix(J Virol 2003 JS Gibbs).pdf*. *77*(13), 7214–7224. https://doi.org/10.1128/JVI.77.13.7214

Giese, S., Bolte, H., & Schwemmle, M. (2016). The feat of packaging eight unique genome segments. *Viruses*, *8*(6), 1–11. https://doi.org/10.3390/v8060165

Girard, M. P., Tam, J. S., Assossou, O. M., & Kieny, M. P. (2010). The 2009 A (H1N1) influenza virus pandemic: A review. *Vaccine*, *28*(31), 4895–4902. https://doi.org/10.1016/j.vaccine.2010.05.031

Gomez-Suaga, P., Paillusson, S., Stoica, R., Noble, W., Hanger, D. P., & Miller, C. C. J. (2017). The ER-Mitochondria Tethering Complex VAPB-PTPIP51 Regulates Autophagy. *Current Biology*, *27*(3), 371–385. https://doi.org/10.1016/j.cub.2016.12.038

Granatiero, V., De Stefani, D., & Rizzuto, R. (2017). Mitochondrial calcium handling in physiology and disease. In *Advances in Experimental Medicine and Biology* (Vol. 982, pp. 25–47). Springer New York LLC. https://doi.org/10.1007/978-3-319-55330-6_2

Grant, E. J., Chen, L., Quiñones-Parra, S., Pang, K., Kedzierska, K., & Chen, W. (2014). T-cell immunity to influenza a viruses. *Critical Reviews in Immunology*, *34*(1), 15–39. https://doi.org/10.1615/CritRevImmunol.2013010019

Gu, R. X., Liu, L. A., & Wei, D. Q. (2013). Structural and energetic analysis of drug inhibition of the influenza A M2 proton channel. *Trends in Pharmacological Sciences*, *34*(10), 571–580. https://doi.org/10.1016/j.tips.2013.08.003

Guo, X., Aviles, G., Liu, Y., Tian, R., Unger, B. A., Lin, Y.-H. T., Wiita, A. P., Xu, K., Correia, M. A., & Kampmann, M. (2078). Mitochondrial stress is relayed to the cytosol by an OMA1-DELE1-HRI pathway. *Nature*, *579*. https://doi.org/10.1038/s41586-020-2078-2

Haasbach, E., Müller, C., Ehrhardt, C., Schreiber, A., Pleschka, S., Ludwig, S., & Planz, O. (2017). The MEK-inhibitor CI-1040 displays a broad anti-influenza virus activity in vitro and provides a prolonged treatment window compared to standard of care in vivo. *Antiviral Research*. https://doi.org/10.1016/j.antiviral.2017.03.024

Hailey, D. W., Rambold, A. S., Satpute-Krishnan, P., Mitra, K., Sougrat, R., Kim, P. K., & Lippincott-Schwartz, J. (2010). Mitochondria Supply Membranes for Autophagosome Biogenesis during Starvation. *Cell*, *141*(4), 656–667. https://doi.org/10.1016/j.cell.2010.04.009

Hale, B. G., Albrecht, R. A., & García-Sastre, A. (2010). Innate immune evasion strategies of influenza viruses. In *Future Microbiology* (Vol. 5, Issue 1, pp. 23–41). https://doi.org/10.2217/fmb.09.108

Hamasaki, M, Furuta, N., Matsuda, A., Nezu, A., Yamamoto, A., Fujita, N., Oomori, H., Noda, T., Haraguchi, T., Hiraoka, Y., Amano, A., & Yoshimori, T. (2013). Autophagosomes form at ER-mitochondria contact sites. *Nature*, *495*(7441), 389–393.

Hamasaki, Maho, Furuta, N., Matsuda, A., Nezu, A., Yamamoto, A., Fujita, N., Oomori, H., Noda, T., Haraguchi, T., Hiraoka, Y., Amano, A., & Yoshimori, T. (2013). Autophagosomes form at ER-mitochondria contact sites. *Nature*, *495*(7441), 389–393. https://doi.org/10.1038/nature11910

Han, J., Perez, J. T., Chen, C., Li, Y., Benitez, A., Kandasamy, M., Lee, Y., Andrade, J., tenOever, B., & Manicassamy, B. (2018). Genome-wide CRISPR/Cas9 Screen Identifies Host Factors Essential for Influenza Virus Replication. *Cell Reports*, *23*(2), 596–607. https://doi.org/10.1016/j.celrep.2018.03.045

Hariri, H., Ugrankar, R., Liu, Y., & Henne, W. M. (2016). Inter-organelle ER-endolysosomal contact sites in metabolism and disease across evolution. *Communicative and Integrative Biology*, *9*(3). https://doi.org/10.1080/19420889.2016.1156278

Hatch, A. L., Ji, W. K., Merrill, R. A., Strack, S., & Higgs, H. N. (2016). Actin flaments as dynamic reservoirs for Drp1 recruitment. *Molecular Biology of the Cell*, *27*(20), 3109–3121. https://doi.org/10.1091/mbc.E16-03-0193

Hause, B. M., Ducatez, M., Collin, E. A., Ran, Z., Liu, R., Sheng, Z., Armien, A., Kaplan, B., Chakravarty, S., Hoppe, A. D., Webby, R. J., Simonson, R. R., & Li, F. (2013). Isolation of a Novel Swine Influenza Virus from Oklahoma in 2011 Which Is Distantly Related to

Human Influenza C Viruses. *PLoS Pathogens*, *9*(2). https://doi.org/10.1371/journal.ppat.1003176

Helenius, A. (1992). Unpacking the incoming influenza virus. *Cell*, *69*(4), 577–578. https://doi.org/10.1016/0092-8674(92)90219-3

Helle, S. C. J., Kanfer, G., Kolar, K., Lang, A., Michel, A. H., & Kornmann, B. (2013). Organization and function of membrane contact sites. *Biochimica et Biophysica Acta - Molecular Cell Research*, *1833*(11), 2526–2541. https://doi.org/10.1016/j.bbamcr.2013.01.028

Herrmann, J. M., & Riemer, J. (2010). The intermembrane space of mitochondria. *Antioxidants and Redox Signaling*, *13*(9), 1341–1358. https://doi.org/10.1089/ars.2009.3063

Hilsch, M., Goldenbogen, B., Sieben, C., Höfer, C. T., Rabe, J. P., Klipp, E., Herrmann, A., & Chiantia, S. (2014). Influenza a matrix protein m1 multimerizes upon binding to lipid membranes. *Biophysical Journal*, *107*(4), 912–923. https://doi.org/10.1016/j.bpj.2014.06.042

Holt, S. H., Darash-Yahana, M., Sohn, Y. S., Song, L., Karmi, O., Tamir, S., Michaeli, D., Luo, Y., Paddock, M. L., Jennings, P. A., Onuchic, J. N., Azad, R. K., Pikarsky, E., Cabantchik, I. Z., Nechushtai, R., & Mittler, R. (2016). Activation of apoptosis in NAF-1-deficient human epithelial breast cancer cells. *Journal of Cell Science*, *129*(1), 155–165. https://doi.org/10.1242/jcs.178293

Holzerova, E., Danhauser, K., Haack, T. B., Kremer, L. S., Melcher, M., Ingold, I., Kobayashi, S., Terrile, C., Wolf, P., Rg Schaper, J., Mayatepek, E., Baertling, F., Pedro, J., Angeli, F., Conrad, M., Strom, T. M., Meitinger, T., Prokisch, H., & Distelmaier, F. (n.d.). *Human thioredoxin 2 deficiency impairs mitochondrial redox homeostasis and causes early-onset neurodegeneration*. https://doi.org/10.1093/brain/awv350

Homma, M., Ohyama, S., & Katagiri, S. (1982). Age distribution of the antibody to type C influenza virus. *Microbiology and Immunology*, *26*(7), 639–642. https://doi.org/10.1111/mim.1982.26.7.639

Honda, A., Ueda, K., Nagata, K., & Ishihama, A. (1988). RNA polymerase of influenza virus: Role of NP in RNA chain elongation. *Journal of Biochemistry*, *104*(6), 1021–1026. https://doi.org/10.1093/oxfordjournals.jbchem.a122569

Hönscher, C., Mari, M., Auffarth, K., Bohnert, M., Griffith, J., Geerts, W., van der Laan, M., Cabrera, M., Reggiori, F., & Ungermann, C. (2014). Cellular metabolism regulates contact sites between vacuoles and mitochondria. *Developmental Cell*, *30*(1), 86–94. https://doi.org/10.1016/j.devcel.2014.06.006

Horner, S. M., Liu, H. M., Park, H. S., Briley, J., & Gale, M. (2011). Mitochondrial-associated endoplasmic reticulum membranes (MAM) form innate immune synapses and are targeted by hepatitis C virus. *Proceedings of the National Academy of Sciences of the United States of America*, *108*(35), 14590–14595. https://doi.org/10.1073/pnas.1110133108

Humphreys, M. (2018). The influenza of 1918: Evolutionary perspectives in a historical context. *Evolution, Medicine and Public Health*, *2018*(1), 219–229. https://doi.org/10.1093/emph/eoy024

Huotari, J., & Helenius, A. (2011). Endosome maturation. *EMBO Journal*, *30*(17), 3481–3500. https://doi.org/10.1038/emboj.2011.286

Hurst, S., Hoek, J., & Sheu, S.-S. (2017). Mitochondrial Ca2+ and regulation of the permeability transition pore. *Journal of Bioenergetics and Biomembranes*, *49*(1), 27–47. https://doi.org/10.1007/s10863-016-9672-x

Inupakutika, M. A., Sengupta, S., Nechushtai, R., Jennings, P. A., Onuchic, J. N., Azad, R. K., Padilla, P., & Mittler, R. (2017). Phylogenetic analysis of eukaryotic NEET proteins uncovers a link between a key gene duplication event and the evolution of vertebrates. *Scientific Reports*, *7*(February), 1–10. https://doi.org/10.1038/srep42571

Ishihara, N., Fujita, Y., Oka, T., & Mihara, K. (2006). Regulation of mitochondrial morphology through proteolytic cleavage of OPA1. *EMBO Journal*, *25*(13), 2966–2977. https://doi.org/10.1038/sj.emboj.7601184

Iuliano, A. D., Roguski, K. M., Chang, H. H., Muscatello, D. J., Palekar, R., Tempia, S., Cohen, C., Gran, J. M., Schanzer, D., Cowling, B. J., Wu, P., Kyncl, J., Ang, L. W., Park, M., Redlberger-Fritz, M., Yu, H., Espenhain, L., Krishnan, A., Emukule, G., … Mustaquim, D. (2018). Estimates of global seasonal influenza-associated respiratory mortality: a modelling study. *The Lancet*, *391*(10127), 1285–1300. https://doi.org/10.1016/S0140-6736(17)33293-2

Ivanov, A. I. (2014). Pharmacological inhibitors of exocytosis and endocytosis: novel bullets for old targets. *Methods in Molecular Biology (Clifton, N.J.)*, *1174*, 3–18. https://doi.org/10.1007/978-1-4939-0944-5_1

Jian, F., Chen, D., Chen, L., Yan, C., Lu, B., Zhu, Y., Chen, S., Shi, A., Chan, D. C., & Song, Z. (2018). Sam50 Regulates PINK1-Parkin-Mediated Mitophagy by Controlling PINK1 Stability and Mitochondrial Morphology. *Cell Reports*, *23*(10), 2989–3005. https://doi.org/10.1016/j.celrep.2018.05.015

Jiang, F., Ramanathan, A., Miller, M. T., Tang, G.-Q., Gale, M., Patel, S. S., & Marcotrigiano, J. (n.d.). *Structural Basis of RNA Recognition and Activation by Innate Immune Receptor RIG-I*. https://doi.org/10.1038/nature10537

Jorgensen, P., Mereckiene, J., Cotter, S., Johansen, K., Tsolova, S., & Brown, C. (2018). How close are countries of the WHO European Region to achieving the goal of vaccinating 75% of key risk groups against influenza? Results from national surveys on seasonal influenza vaccination programmes, 2008/2009 to 2014/2015. *Vaccine*, *36*(4), 442–452. https://doi.org/10.1016/j.vaccine.2017.12.019

Jutel, A., & Banister, E. (2013). "I was pretty sure I had the 'flu": Qualitative description of confirmed-influenza symptoms. *Social Science and Medicine*, *99*, 49–55. https://doi.org/10.1016/j.socscimed.2013.10.011

Kamal, R. P., Alymova, I. V., & York, I. A. (2018). Evolution and virulence of influenza A virus protein PB1-F2. In *International Journal of Molecular Sciences* (Vol. 19, Issue 1). MDPI AG. https://doi.org/10.3390/ijms19010096

Kamerkar, S. C., Kraus, F., Sharpe, A. J., Pucadyil, T. J., & Ryan, M. T. (2018). Dynamin-related protein 1 has membrane constricting and severing abilities sufficient for mitochondrial and peroxisomal fission. *Nature Communications*, *9*(1). https://doi.org/10.1038/s41467-018-07543-w

Karlas, A., Machuy, N., Shin, Y., Pleissner, K.-P., Artarini, A., Heuer, D., Becker, D., Khalil, H., Ogilvie, L. A., Hess, S., Mäurer, A. P., Müller, E., Wolff, T., Rudel, T., & Meyer, T. F. (2010). Genome-wide RNAi screen identifies human host factors crucial for influenza virus replication. *Nature*, *463*(7282), 818–822. https://doi.org/10.1038/nature08760

Karmi, O., Marjault, H. B., Pesce, L., Carloni, P., Onuchic, J. N., Jennings, P. A., Mittler, R., & Nechushtai, R. (2018). The unique fold and lability of the [2Fe-2S] clusters of NEET proteins mediate their key functions in health and disease. *Journal of Biological Inorganic Chemistry*, *23*(4), 599–612. https://doi.org/10.1007/s00775-018-1538-8

Kell, A. M., & Gale, M. (2015). RIG-I in RNA virus recognition. *Virology*, *479–480*, 110–121. https://doi.org/10.1016/j.virol.2015.02.017

Kerry, P. S., Willsher, N., & Fodor, E. (2008). A cluster of conserved basic amino acids near the C-terminus of the PB1 subunit of the influenza virus RNA polymerase is involved in the regulation of viral transcription. *Virology*, *373*(1), 202–210. https://doi.org/10.1016/j.virol.2007.11.030

Khan, M., Syed, G. H., Kim, S. J., & Siddiqui, A. (2015). Mitochondrial dynamics and viral infections: A close nexus. In *Biochimica et Biophysica Acta - Molecular Cell Research* (Vol. 1853, Issue 10, pp. 2822–2833). Elsevier. https://doi.org/10.1016/j.bbamcr.2014.12.040

Kim, H., Webster, R. G., & Webby, R. J. (2018). Influenza Virus: Dealing with a Drifting and Shifting Pathogen. *Viral Immunology*, *31*(2), 174–183. https://doi.org/10.1089/vim.2017.0141

Kim, S. J., Khan, M., Quan, J., Till, A., Subramani, S., & Siddiqui, A. (2013). Hepatitis B Virus Disrupts Mitochondrial Dynamics: Induces Fission and Mitophagy to Attenuate Apoptosis. *PLoS Pathogens*, *9*(12), 1–12. https://doi.org/10.1371/journal.ppat.1003722

King, N. (2007). Amino Acids and the Mitochondria. In *Mitochondria* (pp. 151–166). Springer New York. https://doi.org/10.1007/978-0-387-69945-5_6

Klein, O., Roded, A., Hirschberg, K., Fukuda, M., Galli, S. J., & Sagi-Eisenberg, R. (2018). Imaging fitc-dextran as a reporter for regulated exocytosis. *Journal of Visualized Experiments*, *2018*(136), 1–10. https://doi.org/10.3791/57936

Kormuth, K. A., Lin, K., Qian, Z., Myerburg, M. M., Marr, L. C., & Lakdawala, S. S. (2019). Environmental Persistence of Influenza Viruses Is Dependent upon Virus Type and Host Origin. *MSphere*, *4*(4), 1–14. https://doi.org/10.1128/msphere.00552-19

Koshiba, T. (2013). Mitochondrial-mediated antiviral immunity. *Biochimica et Biophysica Acta - Molecular Cell Research*, *1833*(1), 225–232. https://doi.org/10.1016/j.bbamcr.2012.03.005

Krammer, F. (2016). Novel universal influenza virus vaccine approaches. *Current Opinion in Virology*, *17*, 95–103. https://doi.org/10.1016/j.coviro.2016.02.002

Kumar, B., Asha, K., Khanna, M., Ronsard, L., Meseko, C. A., & Sanicas, M. (2018). The emerging influenza virus threat: status and new prospects for its therapy and control. *Archives of Virology*, *163*(4), 831–844. https://doi.org/10.1007/s00705-018-3708-y

Kusminski, C., Holland, W., & Sun, K. (2012). MitoNEET, a key regulator of mitochondrial function and lipid homeostasis. *Nature …*, *250*(2), 192–205. https://doi.org/10.1002/cne.902500206

Kwak, S. H., Park, K. S., Lee, K. U., & Lee, H. K. (2010). Mitochondrial metabolism and diabetes. In *Journal of Diabetes Investigation* (Vol. 1, Issue 5, pp. 161–169). Wiley-Blackwell. https://doi.org/10.1111/j.2040-1124.2010.00047.x

Lackner, L. L. (2019). The Expanding and Unexpected Functions of Mitochondria Contact Sites. *Trends in Cell Biology*, *29*(7), 580–590. https://doi.org/10.1016/j.tcb.2019.02.009

Lahiri, S., Chao, J. T., Tavassoli, S., Wong, A. K. O., Choudhary, V., Young, B. P., Loewen, C. J. R., & Prinz, W. A. (2014). A Conserved Endoplasmic Reticulum Membrane Protein Complex (EMC) Facilitates Phospholipid Transfer from the ER to Mitochondria. *PLoS Biology*, *12*(10). https://doi.org/10.1371/journal.pbio.1001969

Lai, S., Qin, Y., Cowling, B. J., Ren, X., Wardrop, N. A., Gilbert, M., Tsang, T. K., Wu, P., Feng, L., Jiang, H., Peng, Z., Zheng, J., Liao, Q., Li, S., Horby, P. W., Farrar, J. J., Gao, G. F., Tatem, A. J., & Yu, H. (2016). Global epidemiology of avian influenza A H5N1 virus infection in humans, 1997-2015: a systematic review of individual case data. *The Lancet. Infectious Diseases*, *16*(7), e108–e118. https://doi.org/10.1016/S1473-3099(16)00153-5

Lakadamyali, M., Rust, M. J., & Zhuang, X. (2004). Endocytosis of influenza viruses. In *Microbes and Infection* (Vol. 6, Issue 10, pp. 929–936). Elsevier Masson SAS. https://doi.org/10.1016/j.micinf.2004.05.002

Lakdawala, S. S., Fodor, E., & Subbarao, K. (2016). Moving On Out: Transport and Packaging of Influenza Viral RNA into Virions. *Annual Review of Virology*, *3*(1), 411–427. https://doi.org/10.1146/annurev-virology-110615-042345

Lakdawala, S. S., Wu, Y., Wawrzusin, P., Kabat, J., Broadbent, A. J., Lamirande, E. W., Fodor, E., Altan-Bonnet, N., Shroff, H., & Subbarao, K. (2014). Influenza A Virus Assembly Intermediates Fuse in the Cytoplasm. *PLoS Pathogens*, *10*(3). https://doi.org/10.1371/journal.ppat.1003971

Langat, P., Raghwani, J., Dudas, G., Bowden, T. A., Edwards, S., Gall, A., Bedford, T., Rambaut, A., Daniels, R. S., Russell, C. A., Pybus, O. G., McCauley, J., Kellam, P., & Watson, S. J. (2017). Genome-wide evolutionary dynamics of influenza B viruses on a global scale. *PLoS Pathogens*, *13*(12), e1006749.

https://doi.org/10.1371/journal.ppat.1006749

Le Roy, C., & Wrana, J. L. (2005). Clathrin- and non-clathrin-mediated endocytic regulation of cell signalling. *Nature Reviews Molecular Cell Biology*, *6*(2), 112–126. https://doi.org/10.1038/nrm1571

Lee, C. M., Weight, A. K., Haldar, J., Wang, L., Klibanov, A. M., & Chen, J. (2012). Polymer-attached zanamivir inhibits synergistically both early and late stages of influenza virus infection. *Proceedings of the National Academy of Sciences of the United States of America*, *109*(50), 20385–20390. https://doi.org/10.1073/pnas.1219155109

Lee, H., & Yoon, Y. (2018). Mitochondrial membrane dynamics—functional positioning of OPA1. *Antioxidants*, *7*(12). https://doi.org/10.3390/antiox7120186

Lee, J. E., Westrate, L. M., Wu, H., Page, C., & Voeltz, G. K. (2017). *Mitochondrial Division*. *540*(7631), 139–143. https://doi.org/10.1038/nature20555.Multiple

Leneva, I. A., Falynskova, I. N., Makhmudova, N. R., Poromov, A. A., Yatsyshina, S. B., & Maleev, V. V. (2019). Umifenovir susceptibility monitoring and characterization of influenza viruses isolated during ARBITR clinical study. *Journal of Medical Virology*, *91*(4), 588–597. https://doi.org/10.1002/jmv.25358

Leung, H. S. Y., Li, O. T. W., Chan, R. W. Y., Chan, M. C. W., Nicholls, J. M., & Poon, L. L. M. (2012). Entry of Influenza A Virus with a 2,6-Linked Sialic Acid Binding Preference Requires Host Fibronectin. *Journal of Virology*, *86*(19), 10704–10713. https://doi.org/10.1128/jvi.01166-12

Li, X., & Palese, P. (1994). Characterization of the polyadenylation signal of influenza virus RNA. *Journal of Virology*, *68*(2), 1245–1249. https://doi.org/10.1128/jvi.68.2.1245-1249.1994

Liesa, M., Palacín, M., & Zorzano, A. (2009). Mitochondrial dynamics in mammalian health and disease. *Physiological Reviews*, *89*(3), 799–845. https://doi.org/10.1152/physrev.00030.2008

Liesa, M., & Shirihai, O. S. (2013). Mitochondrial dynamics in the regulation of nutrient utilization and energy expenditure. *Cell Metabolism*, *17*(4), 491–506. https://doi.org/10.1016/j.cmet.2013.03.002

Linster, M., Schrauwen, E. J. A., van der Vliet, S., Burke, D. F., Lexmond, P., Bestebroer, T. M., Smith, D. J., Herfst, S., Koel, B. F., & Fouchier, R. A. M. (2019). The Molecular Basis for Antigenic Drift of Human A/H2N2 Influenza Viruses. *Journal of Virology*, *93*(8).

https://doi.org/10.1128/jvi.01907-18

Lipper, C. H., Karmi, O., Sohn, Y. S., Darash-Yahana, M., Lammert, H., Song, L., Liu, A., Mittler, R., Nechushtai, R., Onuchic, J. N., & Jennings, P. A. (2017). Structure of the human monomeric NEET protein MiNT and its role in regulating iron and reactive oxygen species in cancer cells. *Proceedings of the National Academy of Sciences of the United States of America*, *115*(2), 272–277. https://doi.org/10.1073/pnas.1715842115

Liu, Q., Zhang, D., Hu, D., Zhou, X., & Zhou, Y. (2018). The role of mitochondria in NLRP3 inflammasome activation. In *Molecular Immunology* (Vol. 103, pp. 115–124). Elsevier Ltd. https://doi.org/10.1016/j.molimm.2018.09.010

Liu, S., Gao, Y., Zhang, C., Li, H., Pan, S., Wang, X., Du, S., Deng, Z., Wang, L., Song, Z., & Chen, S. (2016). SAMM50 Affects Mitochondrial Morphology through the Association of Drp1 in Mammalian Cells. *FEBS Letters*, *590*(9), 1313–1323. https://doi.org/10.1002/1873-3468.12170

Long, J. C. D., & Fodor, E. (2016). The PB2 Subunit of the Influenza A Virus RNA Polymerase Is Imported into the Mitochondrial Matrix. *Journal of Virology*, *90*(19), 8729–8738. https://doi.org/10.1128/jvi.01384-16

Lowen, A. C. (2017). Constraints, Drivers, and Implications of Influenza A Virus Reassortment. *Annual Review of Virology*, *4*(1), 105–121. https://doi.org/10.1146/annurev-virology-101416-041726

Lowen, A. C., Mubareka, S., Steel, J., & Palese, P. (2007). Influenza virus transmission is dependent on relative humidity and temperature. *PLoS Pathogens*, *3*(10), 1470–1476. https://doi.org/10.1371/journal.ppat.0030151

Luo, D., Ding, S. C., Vela, A., Kohlway, A., Lindenbach, B. D., & Pyle, A. M. (2011). *Structural insights into RNA recognition by RIG-I*.

M., K., T.H., N., W.S., B., & K., K. (2016). Knowns and unknowns of influenza B viruses. *Future Microbiology*, *11*(1), 119–135. http://www.embase.com/search/results?subaction=viewrecord&from=export&id=L607483021%5Cnhttp://dx.doi.org/10.2217/fmb.15.120%5Cnhttp://sfx.metabib.ch/sfx_locater?sid=EMBASE&issn=17460921&id=doi:10.2217/fmb.15.120&atitle=Knowns+and+unknowns+of+influenza+B+v

Marí, M., Morales, A., Colell, A., García-Ruiz, C., & Ferná Ndez-Checa, J. C. (n.d.). *Mitochondrial Glutathione, a Key Survival Antioxidant*.

Mårtensson, C. U., Doan, K. N., & Becker, T. (2017). Effects of lipids on mitochondrial functions. *Biochimica et Biophysica Acta - Molecular and Cell Biology of Lipids*, *1862*(1), 102–113. https://doi.org/10.1016/j.bbalip.2016.06.015

Martin, K., & Helenius, A. (1992). Transport of incoming influenza virus nucleocapsids into the nucleus. *Trends in Cell Biology*, *2*(1), 8. https://doi.org/10.1016/0962-8924(92)90130-f

Maruyama, H., Kimura, T., Liu, H., Ohtsuki, S., Miyake, Y., Isogai, M., Arai, F., & Honda, A. (2018). Influenza virus replication raises the temperature of cells. *Virus Research*, *257*, 94–101. https://doi.org/10.1016/j.virusres.2018.09.011

Matrosovich, M. N., Matrosovich, T. Y., Gray, T., Roberts, N. A., & Klenk, H. D. (2004). Human and avian influenza viruses target different cell types in cultures of human airway epithelium. *Proceedings of the National Academy of Sciences of the United States of America*, *101*(13), 4620–4624. https://doi.org/10.1073/pnas.0308001101

Matsuzaki, Y., Sugawara, K., Furuse, Y., Shimotai, Y., Hongo, S., Oshitani, H., Mizuta, K., & Nishimura, H. (2016). Genetic Lineage and Reassortment of Influenza C Viruses Circulating between 1947 and 2014. *Journal of Virology*, *90*(18), 8251–8265. https://doi.org/10.1128/jvi.00969-16

Mayor, S., & Pagano, R. E. (2007). Pathways of clathrin-independent endocytosis. *Nature Reviews Molecular Cell Biology*, *8*(8), 603–612. https://doi.org/10.1038/nrm2216

Mayr, J. A. (2014). Lipid metabolism in mitochondrial membranes. *Journal of Inherited Metabolic Disease*, *38*(1), 137–144. https://doi.org/10.1007/s10545-014-9748-x

Mclaughlin, M. M., Skoglund, E. W., & Ison, M. G. (2015). Peramivir: An intravenous neuraminidase inhibitor. *Expert Opinion on Pharmacotherapy*, *16*(12), 1889–1900. https://doi.org/10.1517/14656566.2015.1066336

Medlock, A. E., Shiferaw, M. T., Marcero, J. R., Vashisht, A. A., Wohlschlegel, J. A., Phillips, J. D., & Dailey, H. A. (2015). Identification of the mitochondrial heme metabolism complex. *PLoS ONE*, *10*(8), 1–20. https://doi.org/10.1371/journal.pone.0135896

Mejia, E. M., & Hatch, G. M. (2016). Mitochondrial phospholipids: role in mitochondrial function. *Journal of Bioenergetics and Biomembranes*, *48*(2), 99–112. https://doi.org/10.1007/s10863-015-9601-4

Memorandum, W. H. O. (1980). A revision of the system of nomenclature for influenza viruses: a WHO memorandum. *Bulletin of the World Health Organization*, *58*(4), 585–591.

Milane, L., Trivedi, M., Singh, A., Talekar, M., & Amiji, M. (2015). Mitochondrial biology, targets, and drug delivery. In *Journal of Controlled Release* (Vol. 207). Elsevier B.V. https://doi.org/10.1016/j.jconrel.2015.03.036

Miriyala, S., Holley, A. K., & St Clair, D. K. (2011). *Mitochondrial Superoxide Dismutase-Signals of Distinction*.

Mittler, R., Darash-Yahana, M., Sohn, Y. S., Bai, F., Song, L., Cabantchik, I. Z., Jennings, P. A., Onuchic, J. N., & Nechushtai, R. (2019). NEET Proteins: A new link between iron metabolism, reactive oxygen species, and cancer. *Antioxidants and Redox Signaling*, *30*(8), 1083–1095. https://doi.org/10.1089/ars.2018.7502

Molino, D., Zemirli, N., Codogno, P., & Morel, E. (2017). The Journey of the Autophagosome through Mammalian Cell Organelles and Membranes. *Journal of Molecular Biology*, *429*(4), 497–514. https://doi.org/10.1016/j.jmb.2016.12.013

Monto, A. S., Gravenstein, S., Elliott, M., Colopy, M., & Schweinle, J. (2000). Clinical signs and symptoms predicting influenza infection. *Archives of Internal Medicine*, *160*(21), 3243–3247. https://doi.org/10.1001/archinte.160.21.3243

Moore, A. S., & Holzbaur, E. L. F. (2018). Mitochondrial-cytoskeletal interactions: dynamic associations that facilitate network function and remodeling. *Current Opinion in Physiology*, *3*, 94–100. https://doi.org/10.1016/j.cophys.2018.03.003

Mor, A., White, A., Zhang, K., Thompson, M., Esparza, M., Muñoz-Moreno, R., Koide, K., Lynch, K. W., García-Sastre, A., & Fontoura, B. M. A. (2016). Influenza virus mRNA trafficking through host nuclear speckles. *Nature Microbiology*, *1*(7). https://doi.org/10.1038/nmicrobiol.2016.69

Morel, E., Mehrpour, M., Botti, J., Dupont, N., Hamaï, A., Nascimbeni, A. C., & Codogno, P. (2017). Autophagy: A Druggable Process. *Annual Review of Pharmacology and Toxicology*, *57*(1), 375–398. https://doi.org/10.1146/annurev-pharmtox-010716-104936

Mousavi, S. A., Malerød, L., Berg, T., & Kjeken, R. (2004). Clathrin-dependent endocytosis. In *Biochemical Journal* (Vol. 377, Issue 1, pp. 1–16). Portland Press Ltd. https://doi.org/10.1042/BJ20031000

Müller, K. H., Kakkola, L., Nagaraj, A. S., Cheltsov, A. V., Anastasina, M., & Kainov, D. E. (2012). Emerging cellular targets for influenza antiviral agents. In *Trends in Pharmacological Sciences* (Vol. 33, Issue 2, pp. 89–99). https://doi.org/10.1016/j.tips.2011.10.004

Münk, C., Sommer, A. F. R., & König, R. (2011). Systems-Biology Approaches to Discover Anti-Viral Effectors of the Human Innate Immune Response. *Viruses*, *3*, 1112–1130. https://doi.org/10.3390/v3071112

Münz, C. (2014). Influenza a virus lures autophagic protein LC3 to budding sites. *Cell Host and Microbe*, *15*(2), 130–131. https://doi.org/10.1016/j.chom.2014.01.014

Naviaux, R. K. (2014). Metabolic features of the cell danger response. *Mitochondrion*, *16*, 7–17. https://doi.org/10.1016/j.mito.2013.08.006

Nayak, D. P., Hui, E. K. W., & Barman, S. (2004). Assembly and budding of influenza virus. *Virus Research*, *106*(2 SPEC.ISS.), 147–165. https://doi.org/10.1016/j.virusres.2004.08.012

Neirynck, S., Deroo, T., Saelens, X., Vanlandschoot, P., Jou, W. M., & Fiers, W. (1999). A universal influenza A vaccine based on the extracellular domain of the M2 protein. *Nature Medicine*, *5*(10), 1157–1163. https://doi.org/10.1038/13484

Nielson, J. R., & Rutter, J. P. (2018). Lipid-mediated signals that regulate mitochondrial biology. *Journal of Biological Chemistry*, *293*(20), 7517–7521. https://doi.org/10.1074/jbc.R117.001655

Nobusawa, E., & Sato, K. (2006). Comparison of the Mutation Rates of Human Influenza A and B Viruses. *Journal of Virology*, *80*(7), 3675–3678. https://doi.org/10.1128/jvi.80.7.3675-3678.2006

Noda, T. (2012). Native morphology of influenza virions. *Frontiers in Microbiology*, *2*(JAN), 1–5. https://doi.org/10.3389/fmicb.2011.00269

Noton, S. L., Simpson-Holley, M., Medcalf, E., Wise, H. M., Hutchinson, E. C., McCauley, J. W., & Digard, P. (2009). Studies of an Influenza A Virus Temperature-Sensitive Mutant Identify a Late Role for NP in the Formation of Infectious Virions. *Journal of Virology*, *83*(2), 562–571. https://doi.org/10.1128/jvi.01424-08

Nunnari, J., & Suomalainen, A. (2012). Mitochondria: In sickness and in health. In *Cell* (Vol. 148, Issue 6, pp. 1145–1159). https://doi.org/10.1016/j.cell.2012.02.035

O'Hanlon, R., & Shaw, M. L. (2019). Baloxavir marboxil: the new influenza drug on the market. *Current Opinion in Virology*, *35*(Table 1), 14–18. https://doi.org/10.1016/j.coviro.2019.01.006

Olayioye, M. A., Noll, B., & Hausser, A. (2019). Spatiotemporal Control of Intracellular Membrane Trafficking by Rho GTPases. *Cells*, *8*(12), 1478. https://doi.org/10.3390/cells8121478

Olichon, A., Baricault, L., Gas, N., Guillou, E., Valette, A., Belenguer, P., & Lenaers, G. (2003). Loss of OPA1 perturbates the mitochondrial inner membrane structure and integrity, leading to cytochrome c release and apoptosis. *Journal of Biological Chemistry*, *278*(10), 7743–7746. https://doi.org/10.1074/jbc.C200677200

Otera, H., & Mihara, K. (2011). Molecular mechanisms and physiologic functions of mitochondrial dynamics. *Journal of Biochemistry*, *149*(3), 241–251. https://doi.org/10.1093/jb/mvr002

Pakos-Zebrucka, K., Koryga, I., Mnich, K., Ljujic, M., Samali, A., & Gorman, A. M. (2016). The integrated stress response. *EMBO Reports*, *17*(10), 1374–1395. https://doi.org/10.15252/embr.201642195

Panthu, B., Terrier, O., Carron, C., Traversier, A., Corbin, A., Balvay, L., Lina, B., Rosa-Calatrava, M., & Ohlmann, T. (2017). The NS1 Protein from Influenza Virus Stimulates Translation Initiation by Enhancing Ribosome Recruitment to mRNAs. *Journal of Molecular Biology*, *429*(21), 3334–3352. https://doi.org/10.1016/j.jmb.2017.04.007

Paterson, D., & Fodor, E. (2012). Emerging Roles for the Influenza A Virus Nuclear Export Protein (NEP). *PLoS Pathogens*, *8*(12). https://doi.org/10.1371/journal.ppat.1003019

Paterson, R. G., Takeda, M., Ohigashi, Y., Pinto, L. H., & Lamb, R. A. (2003). Influenza B virus BM2 protein is an oligomeric integral membrane protein expressed at the cell surface. *Virology*, *306*(1), 7–17. https://doi.org/10.1016/S0042-6822(02)00083-1

Paul, B. T., Manz, D. H., Torti, F. M., & Torti, S. V. (2017). Mitochondria and Iron: current questions. In *Expert Review of Hematology* (Vol. 10, Issue 1, pp. 65–79). Taylor and Francis Ltd. https://doi.org/10.1080/17474086.2016.1268047

Peter, A. T. J., Herrmann, B., Antunes, D., Rapaport, D., Dimmer, K. S., & Kornmann, B. (2017). Vps13-Mcp1 interact at vacuole-mitochondria interfaces and bypass ER-mitochondria contact sites. *Journal of Cell Biology*, *216*(10), 3219–3229.

https://doi.org/10.1083/jcb.201610055

Pinto, L. H., Holsinger, L. J., & Lamb, R. A. (1992). Influenza virus M2 protein has ion channel activity. *Cell*, *69*(3), 517–528. https://doi.org/10.1016/0092-8674(92)90452-I

Pinto, L. H., & Lamb, R. A. (2006). The M2 proton channels of influenza A and B viruses. *Journal of Biological Chemistry*, *281*(14), 8997–9000. https://doi.org/10.1074/jbc.R500020200

Pizzorno, A., Terrier, O., de Lamballerie, C. N., Julien, T., Padey, B., Traversier, A., Roche, M., Hamelin, M. E., Rhéaume, C., Croze, S., Escuret, V., Poissy, J., Lina, B., Legras-Lachuer, C., Textoris, J., Boivin, G., & Rosa-Calatrava, M. (2019). Repurposing of drugs as novel influenza inhibitors from clinical gene expression infection signatures. *Frontiers in Immunology*, *10*(JAN). https://doi.org/10.3389/fimmu.2019.00060

Pleschka, S., Wolff, T., Ehrhardt, C., Hobom, G., Planz, O., Rapp, U. R., & Ludwig, S. (2001). Influenza virus propagation is impaired by inhibition of the Raf/MEK/ERK signalling cascade. *Nature Cell Biology*, *3*(3), 301–305. https://doi.org/10.1038/35060098

Plotch, S. J., Tomasz, J., & Krug, R. M. (1978). Absence of detectable capping and methylating enzymes in influenza virions. *Journal of Virology*, *28*(1), 75–83. http://www.ncbi.nlm.nih.gov/pubmed/702657

Porcelli, A. M., Ghelli, A., Zanna, C., Pinton, P., Rizzuto, R., & Rugolo, M. (2005). pH difference across the outer mitochondrial membrane measured with a green fluorescent protein mutant. *Biochemical and Biophysical Research Communications*, *326*(4), 799–804. https://doi.org/10.1016/j.bbrc.2004.11.105

Prasai, K. (2017). Regulation of mitochondrial structure and function by protein import: A current review. In *Pathophysiology* (Vol. 24, Issue 3). Elsevier Ireland Ltd. https://doi.org/10.1016/j.pathophys.2017.03.001

Ramsay, L. C., Buchan, S. A., Stirling, R. G., Cowling, B. J., Feng, S., Kwong, J. C., & Warshawsky, B. F. (2019). The impact of repeated vaccination on influenza vaccine effectiveness: A systematic review and meta-analysis. *BMC Medicine*, *17*(1), 1–16. https://doi.org/10.1186/s12916-018-1239-8

Rapaport, D. (2002). Biogenesis of the mitochondrial TOM complex. *Trends in Biochemical Sciences*, *27*(4), 191–197. https://doi.org/10.1016/S0968-0004(02)02065-0

Reggiori, F., & Ungermann, C. (2017). Autophagosome Maturation and Fusion. In *Journal of Molecular Biology*. https://doi.org/10.1016/j.jmb.2017.01.002

Reina, J., & Reina, N. (2017). [Favipiravir, a new concept of antiviral drug against influenza viruses]. *Revista Espanola de Quimioterapia : Publicacion Oficial de La Sociedad Espanola de Quimioterapia*, *30*(2), 79–83. http://www.ncbi.nlm.nih.gov/pubmed/28176519

Rieusset, J. (2018). The role of endoplasmic reticulum-mitochondria contact sites in the control of glucose homeostasis: An update. *Cell Death and Disease*, *9*(3), 1–12. https://doi.org/10.1038/s41419-018-0416-1

Rios, R. M., & Bornens, M. (2003). The Golgi apparatus at the cell centre. *Current Opinion in Cell Biology*, *15*(1), 60–66. https://doi.org/10.1016/S0955-0674(02)00013-3

Roger, A. J., Muñoz-Gómez, S. A., & Kamikawa, R. (2017). The Origin and Diversification of Mitochondria. *Current Biology*, *27*(21), R1177–R1192. https://doi.org/10.1016/j.cub.2017.09.015

Rohini, K., Ramanathan, K., & Shanthi, V. (2019). Multi-Dimensional Screening Strategy for Drug Repurposing with Statistical Framework—A New Road to Influenza Drug discovery. *Cell Biochemistry and Biophysics*, *77*(4), 319–333. https://doi.org/10.1007/s12013-019-00887-0

Rossignol, J. F., Frazia, S. La, Chiappa, L., Ciucci, A., & Santoro, M. G. (2009). *Thiazolides, a New Class of Anti-influenza Molecules Targeting Viral Hemagglutinin at the Post-translational Level* * □ *S*. https://doi.org/10.1074/jbc.M109.029470

Rossman, J. S., Jing, X., Leser, G. P., Balannik, V., Pinto, L. H., & Lamb, R. A. (2010). Influenza Virus M2 Ion Channel Protein Is Necessary for Filamentous Virion Formation. *Journal of Virology*, *84*(10), 5078–5088. https://doi.org/10.1128/jvi.00119-10

Rossman, Jeremy S., & Lamb, R. A. (2011). Influenza virus assembly and budding. In *Virology* (Vol. 411, Issue 2, pp. 229–236). https://doi.org/10.1016/j.virol.2010.12.003

Rota, P. A., Wallis, T. R., Harmon, M. W., Rota, J. S., Kendal, A. P., & Nerome, K. (1990). Cocirculation of two distinct evolutionary lineages of influenza type B virus since 1983. *Virology*, *175*(1), 59–68. https://doi.org/10.1016/0042-6822(90)90186-U

Samji, T. (2009). Influenza A: Understanding the viral life cycle. *Yale Journal of Biology and Medicine*, *82*(4), 153–159.

Santel, A., & Fuller, M. T. (2001). Control of mitochondrial morphology by a human mitofusin. *Journal of Cell Science*, *114*(5), 867–874.

Sautto, G. A., Kirchenbaum, G. A., & Ross, T. M. (2018). Towards a universal influenza vaccine: Different approaches for one goal. *Virology Journal*, *15*(1), 1–12. https://doi.org/10.1186/s12985-017-0918-y

Scheuch, G., Canisius, S., Nocker, K., Hofmann, T., Naumann, R., Pleschka, S., Ludwig, S., Welte, T., & Planz, O. (2018). Targeting intracellular signaling as an antiviral strategy: aerosolized LASAG for the treatment of influenza in hospitalized patients. *Emerging Microbes & Infections*, *7*(1), 21. https://doi.org/10.1038/s41426-018-0023-3

Schild, G. C., Newman, R. W., Webster, R. G., Major, D., & Hinshaw, V. S. (1980). Antigenic analysis of influenza a virus surface antigens: Considerations for the nomenclature of influenza virus. *Comparative Immunology, Microbiology and Infectious Diseases*, *3*(1–2), 5–18. https://doi.org/10.1016/0147-9571(80)90034-X

Schnell, J. R., & Chou, J. J. (2008). Structure and mechanism of the M2 proton channel of influenza A virus. *Nature*, *451*(7178), 591–595. https://doi.org/10.1038/nature06531

Schuldiner, M., & Weissman, J. S. (2013). The contribution of systematic approaches to characterizing the proteins and functions of the endoplasmic reticulum. *Cold Spring Harbor Perspectives in Biology*, *5*(3), 1–14. https://doi.org/10.1101/cshperspect.a013284

Scott, C. C., Vacca, F., & Gruenberg, J. (2014). Endosome maturation, transport and functions. *Seminars in Cell and Developmental Biology*, *31*, 2–10. https://doi.org/10.1016/j.semcdb.2014.03.034

Sebastian, R., Diaz, M.-E., Ayala, G., Letinic, K., Moncho-Bogani, J., & Toomre, D. (n.d.). Spatio-temporal analysis of constitutive exocytosis in epithelial cells. *IEEE/ACM Transactions on Computational Biology and Bioinformatics*, *3*(1), 17–32. https://doi.org/10.1109/TCBB.2006.11

Shai, N., Yifrach, E., Van Roermund, C. W. T., Cohen, N., Bibi, C., Ijlst, L., Cavellini, L., Meurisse, J., Schuster, R., Zada, L., Mari, M. C., Reggiori, F. M., Hughes, A. L., Escobar-Henriques, M., Cohen, M. M., Waterham, H. R., Wanders, R. J. A., Schuldiner, M., & Zalckvar, E. (2018). Systematic mapping of contact sites reveals tethers and a function for the peroxisome-mitochondria contact. *Nature Communications*, *9*(1). https://doi.org/10.1038/s41467-018-03957-8

Shao, W., Li, X., Goraya, M. U., Wang, S., & Chen, J. L. (2017). Evolution of influenza a virus by mutation and re-assortment. *International Journal of Molecular Sciences*, *18*(8). https://doi.org/10.3390/ijms18081650

Shen, Z.-Q., Chen, Y.-F., Chen, J.-R., Jou, Y.-S., Wu, P.-C., Kao, C.-H., Wang, C.-H., Huang, Y.-L., Chen, C.-F., Huang, T.-S., Shyu, Y.-C., Tsai, S.-F., Kao, L.-S., & Tsai, T.-F. (2017). CISD2 Haploinsufficiency Disrupts Calcium Homeostasis, Causes Nonalcoholic Fatty Liver Disease, and Promotes Hepatocellular Carcinoma. *Cell Reports*, *21*(8), 2198–2211. https://doi.org/10.1016/j.celrep.2017.10.099

Shi, C.-S., Qi, H.-Y., Boularan, C., Huang, N.-N., Abu-Asab, M., Shelhamer, J. H., & Kehrl, J. H. (2014). SARS-Coronavirus Open Reading Frame-9b Suppresses Innate Immunity by Targeting Mitochondria and the MAVS/TRAF3/TRAF6 Signalosome. *The Journal of Immunology*, *193*(6), 3080–3089. https://doi.org/10.4049/jimmunol.1303196

Shin, J. S., Ku, K. B., Jang, Y., Yoon, Y. S., Shin, D., Kwon, O. S., Go, Y. Y., Kim, S. S., Bae, M. A., & Kim, M. (2017). Comparison of anti-influenza virus activity and pharmacokinetics of oseltamivir free base and oseltamivir phosphate. *Journal of Microbiology*, *55*(12), 979–983. https://doi.org/10.1007/s12275-017-7371-x

Shtykova, E. V., Baratova, L. A., Fedorova, N. V., Radyukhin, V. A., Ksenofontov, A. L., Volkov, V. V., Shishkov, A. V., Dolgov, A. A., Shilova, L. A., Batishchev, O. V., Jeffries, C. M., & Svergun, D. I. (2013). Structural analysis of influenza a virus matrix protein M1 and Its self-assemblies at low pH. *PLoS ONE*, *8*(12), 1–10. https://doi.org/10.1371/journal.pone.0082431

Sieczkarski, S. B., & Whittaker, G. R. (2002). Influenza Virus Can Enter and Infect Cells in the Absence of Clathrin-Mediated Endocytosis. *Journal of Virology*, *76*(20), 10455–10464. https://doi.org/10.1128/jvi.76.20.10455-10464.2002

Signes, A., & Fernandez-Vizarra, E. (2018). Assembly of mammalian oxidative phosphorylation complexes I–V and supercomplexes. In *Essays in Biochemistry* (Vol. 62, Issue 3, pp. 255–270). Portland Press Ltd. https://doi.org/10.1042/EBC20170098

Sivitz, W. I., & Yorek, M. A. (2010). Mitochondrial dysfunction in diabetes: From molecular mechanisms to functional significance and therapeutic opportunities. *Antioxidants and Redox Signaling*, *12*(4), 537–577. https://doi.org/10.1089/ars.2009.2531

Skehel, J. J., & Wiley, D. C. (2000). Receptor Binding and Membrane Fusion in Virus Entry: The Influenza Hemagglutinin. *Annual Review of Biochemistry*, *69*(1), 531–569. https://doi.org/10.1146/annurev.biochem.69.1.531

Smirnova, E., Griparic, L., Shurland, D.-L., & Van Der Bliek, A. M. (2001). Drp1 Is Required for Mitochondrial Division in Mammalian Cells. *Molecular Biology of the Cell*, *12*(August), 2245–2256. https://www.ncbi.nlm.nih.gov/pmc/articles/PMC58592/pdf/mk0801002245.pdf

Smirnova, E., Shurland, D. L., Ryazantsev, S. N., & Van Der Bliek, A. M. (1998). A human dynamin-related protein controls the distribution of mitochondria. *Journal of Cell Biology*, *143*(2), 351–358. https://doi.org/10.1083/jcb.143.2.351

Smorodintsev, A. A., Golubev, D. B., & Luzjanina, T. Y. (1982). Principles of rational classification and nomenclature of human influenza A viruses. *Bollettino Dell'Istituto Sieroterapico Milanese*, *61*(3), 202–209. http://www.ncbi.nlm.nih.gov/pubmed/6927250

Song, Z., Ghochani, M., McCaffery, J. M., Frey, T. G., & Chan, D. C. (2009). Mitofusins and OPA1 mediate sequential steps in mitochondrial membrane fusion. *Molecular Biology of the Cell*, *20*(15), 3525–3532. https://doi.org/10.1091/mbc.E09-03-0252

Spinelli, J. B., & Haigis, M. C. (2018). The multifaceted contributions of mitochondria to cellular metabolism. In *Nature Cell Biology* (Vol. 20, Issue 7, pp. 745–754). Nature Publishing Group. https://doi.org/10.1038/s41556-018-0124-1

Stegmann, T. (2000). Membrane fusion mechanisms: The influenza hemagglutinin paradigm and its implications for intracellular fusion. *Traffic*, *1*(8), 598–604. https://doi.org/10.1034/j.1600-0854.2000.010803.x

Stöhr, K. (2002). Reflection & Reaction Influenza — WHO cares. *The Lancet, Infectious Diseases*, *2*(September), 7424–7424.

Stubbs, T. M., & Te Velthuis, A. J. W. (2014). The RNA-dependent RNA polymerase of the influenza A virus. In *Future Virology* (Vol. 9, Issue 9, pp. 863–876). Future Medicine Ltd. https://doi.org/10.2217/fvl.14.66

Su, B., Wurtzer, S., Rameix-Welti, M. A., Dwyer, D., van der Werf, S., Naffakh, N., Clavel, F., & Labrosse, B. (2009). Enhancement of the influenza a hemagglutinin (HA)-mediated cell-cell fusion and virus entry by the viral neuraminidase (NA). *PLoS ONE*, *4*(12). https://doi.org/10.1371/journal.pone.0008495

Su, S., Fu, X., Li, G., Kerlin, F., & Veit, M. (2017). Novel Influenza D virus: Epidemiology, pathology, evolution and biological characteristics. *Virulence*, *8*(8), 1580–1591. https://doi.org/10.1080/21505594.2017.1365216

Swerdlow, R. H. (2018). Mitochondria and Mitochondrial Cascades in Alzheimer's Disease. *Journal of Alzheimer's Disease*, *62*(3), 1403–1416. https://doi.org/10.3233/JAD-170585

Szul, T., & Sztul, E. (2011). COPII and COPI traffic at the ER-Golgi interface. *Physiology*, *26*(5), 348–364. https://doi.org/10.1152/physiol.00017.2011

Tait, S. W. G., & Green, D. R. (2013). Mitochondrial regulation of cell death. *Cold Spring Harbor Perspectives in Biology*, *5*(9). https://doi.org/10.1101/cshperspect.a008706

Takeda, M., Leser, G. P., Russell, C. J., & Lamb, R. A. (2003). Influenza virus hemagglutinin concentrates in lipid raft microdomains for efficient viral fusion. *Proceedings of the National Academy of Sciences of the United States of America*, *100*(25), 14610–14617. https://doi.org/10.1073/pnas.2235620100

Tamir, S., Paddock, M. L., Darash-Yahana-Baram, M., Holt, S. H., Sohn, Y. S., Agranat, L., Michaeli, D., Stofleth, J. T., Lipper, C. H., Morcos, F., Cabantchik, I. Z., Onuchic, J. N., Jennings, P. A., Mittler, R., & Nechushtai, R. (2015). Structure-function analysis of NEET proteins uncovers their role as key regulators of iron and ROS homeostasis in health and disease. *Biochimica et Biophysica Acta - Molecular Cell Research*, *1853*(6), 1294–1315. https://doi.org/10.1016/j.bbamcr.2014.10.014

Taubenberger, J. K., & Kash, J. C. (2010). Influenza virus evolution, host adaptation, and pandemic formation. In *Cell Host and Microbe* (Vol. 7, Issue 6, pp. 440–451). Cell Press. https://doi.org/10.1016/j.chom.2010.05.009

Te Velthuis, A. J. W., & Fodor, E. (2016). Influenza virus RNA polymerase: Insights into the mechanisms of viral RNA synthesis. *Nature Reviews Microbiology*, *14*(8), 479–493. https://doi.org/10.1038/nrmicro.2016.87

Teodoro, J. S., Palmeira, C. M., & Rolo, A. P. (2018). Mitochondrial membrane potential (ΔΨ) fluctuations associated with the metabolic states of mitochondria. In *Methods in Molecular Biology* (Vol. 1782, pp. 109–119). Humana Press Inc. https://doi.org/10.1007/978-1-4939-7831-1_6

Thorn, P., Zorec, R., Rettig, J., & Keating, D. J. (2016). Exocytosis in non-neuronal cells. *Journal of Neurochemistry*, 849–859. https://doi.org/10.1111/jnc.13602

Tilokani, L., Nagashima, S., Paupe, V., & Prudent, J. (2018). Mitochondrial dynamics: Overview of molecular mechanisms. *Essays in Biochemistry*, *62*(3), 341–360. https://doi.org/10.1042/EBC20170104

Treanor, J. (2004). Influenza Vaccine - Outmaneuvering Antigenic Shift and Drift. *New England Journal of Medicine*, *350*(3), 218–220. https://doi.org/10.1056/NEJMp038238

Tremblay, B. P., & Haynes, C. M. (2020). Mitochondrial distress call moves to the cytosol to trigger a response to stress. *Nature*, *579*(7799), 348–349. https://doi.org/10.1038/d41586-020-00552-0

Tubbs, E., & Rieusset, J. (2017). Metabolic signaling functions of ER–mitochondria contact sites: Role in metabolic diseases. *Journal of Molecular Endocrinology*, *58*(2), R87–R106. https://doi.org/10.1530/JME-16-0189

Valleron, A. J., Cori, A., Valtat, S., Meurisse, S., Carrat, F., & Boëlle, P. Y. (2010). Transmissibility and geographic spread of the 1889 influenza pandemic. *Proceedings of the National Academy of Sciences of the United States of America*, *107*(19), 8778–8781. https://doi.org/10.1073/pnas.1000886107

Valm, A. M., Cohen, S., Legant, W. R., Melunis, J., Hershberg, U., Wait, E., Cohen, A. R., Davidson, M. W., Betzig, E., & Lippincott-Schwartz, J. (2017). Applying systems-level spectral imaging and analysis to reveal the organelle interactome. *Nature*, *546*(7656), 162–167. https://doi.org/10.1038/nature22369

Van Der Bliek, A. M., Sedensky, M. M., & Morgan, P. G. (2017). Cell biology of the mitochondrion. *Genetics*, *207*(3), 843–871. https://doi.org/10.1534/genetics.117.300262

van der Laan, M., Horvath, S. E., & Pfanner, N. (2016). Mitochondrial contact site and cristae organizing system. *Current Opinion in Cell Biology*, *41*, 33–42. https://doi.org/10.1016/j.ceb.2016.03.013

van der Sandt, C. E., Kreijtz, J. H. C. M., & Rimmelzwaan, G. F. (2012). Evasion of influenza A viruses from innate and adaptive immune responses. *Viruses*, *4*(9), 1438–1476. https://doi.org/10.3390/v4091438

Varga, Z. T., Grant, A., Manicassamy, B., & Palese, P. (2012). Influenza Virus Protein PB1-F2 Inhibits the Induction of Type I Interferon by Binding to MAVS and Decreasing Mitochondrial Membrane Potential. *Journal of Virology*, *86*(16), 8359–8366. https://doi.org/10.1128/jvi.01122-12

Vasin, A. V., Temkina, O. A., Egorov, V. V., Klotchenko, S. A., Plotnikova, M. A., & Kiselev, O. I. (2014). Molecular mechanisms enhancing the proteome of influenza A viruses: An overview of recently discovered proteins. *Virus Research*, *185*, 53–63. https://doi.org/10.1016/j.virusres.2014.03.015

Vemula, S. V., Sayedahmed, E. E., Sambhara, S., & Mittal, S. K. (2017). Vaccine approaches conferring cross-protection against influenza viruses. *Expert Review of Vaccines*, *16*(11), 1141–1154. https://doi.org/10.1080/14760584.2017.1379396

Vernay, A., Marchetti, A., Sabra, A., Jauslin, T. N., Rosselin, M., Scherer, P. E., Demaurex, N., Orci, L., & Cosson, P. (2017). MitoNEET-dependent formation of intermitochondrial junctions. *Proceedings of the National Academy of Sciences of the United States of America*, *114*(31), 8277–8282. https://doi.org/10.1073/pnas.1706643114

Viboud, C., Grais, R. F., Lafont, B. A. P., Miller, M. A., & Simonsen, L. (2005). Multinational Impact of the 1968 Hong Kong Influenza Pandemic: Evidence for a Smoldering Pandemic. *The Journal of Infectious Diseases*, *192*(2), 233–248. https://doi.org/10.1086/431150

Visher, E., Whitefield, S. E., McCrone, J. T., Fitzsimmons, W., & Lauring, A. S. (2016). The Mutational Robustness of Influenza A Virus. *PLoS Pathogens*, *12*(8), 1–25. https://doi.org/10.1371/journal.ppat.1005856

Wang, C. H., Chen, Y. F., Wu, C. Y., Wu, P. C., Huang, Y. L., Kao, C. H., Lin, C. H., Kao, L. Sen, Tsai, T. F., & Wei, Y. H. (2014). Cisd2 modulates the differentiation and functioning of adipocytes by regulating intracellular Ca 2+ homeostasis. *Human Molecular Genetics*, *23*(18), 4770–4785. https://doi.org/10.1093/hmg/ddu193

Wang, Hong, Sreenevasan, U., Hu, H., Saladino, A., Polster, B. M., Lund, L. M., Gong, D. W., Stanley, W. C., & Sztalryd, C. (2011). Perilipin 5, a lipid droplet-associated protein, provides physical and metabolic linkage to mitochondria. *Journal of Lipid Research*, *52*(12), 2159–2168. https://doi.org/10.1194/jlr.M017939

Wang, Hongbin, Li, Z., Niu, J., Xu, Y., Ma, L., Lu, A., Wang, X., Qian, Z., Huang, Z., Jin, X., Leng, Q., Wang, J., Zhong, J., Sun, B., & Meng, G. (2018). Antiviral effects of ferric ammonium citrate. *Cell Discovery*, *4*(1). https://doi.org/10.1038/s41421-018-0013-6

Wang, L. (2016). Mitochondrial purine and pyrimidine metabolism and beyond. In *Nucleosides, Nucleotides and Nucleic Acids* (Vol. 35, Issues 10–12, pp. 578–594). Taylor and Francis Inc. https://doi.org/10.1080/15257770.2015.1125001

Wang, M., & Veit, M. (2016). Hemagglutinin-esterase-fusion (HEF) protein of influenza C virus. *Protein and Cell*, *7*(1), 28–45. https://doi.org/10.1007/s13238-015-0193-x

Wang, Y., Landry, A. P., & Ding, H. (2017). The mitochondrial outer membrane protein mitoNEET is a redox enzyme catalyzing electron transfer from FMNH2 to oxygen or ubiquinone. *Journal of Biological Chemistry*, *292*(24), 10061–10067. https://doi.org/10.1074/jbc.M117.789800

Wen, F., Bedford, T., & Cobey, S. (2016). Explaining the geographical origins of seasonal influenza A (H3N2). *Proceedings of the Royal Society B: Biological Sciences*, *283*(1838). https://doi.org/10.1098/rspb.2016.1312

Westermann, B. (2010). Mitochondrial fusion and fission in cell life and death. *Nature Reviews Molecular Cell Biology*, *11*(12), 872–884. https://doi.org/10.1038/nrm3013

Westermann, B. (2015). The mitochondria-plasma membrane contact site. *Current Opinion in Cell Biology*, *35*, 1–6. https://doi.org/10.1016/j.ceb.2015.03.001

Wharton, S. A., Belshe, R. B., Skehel, J. J., & Hay, A. J. (1994). Role of virion M2 protein in influenza virus uncoating: Specific reduction in the rate of membrane fusion between virus and liposomes by amantadine. *Journal of General Virology*, *75*(4), 945–948. https://doi.org/10.1099/0022-1317-75-4-945

Whitley, B. N., Engelhart, E. A., & Hoppins, S. (2019). Mitochondrial dynamics and their potential as a therapeutic target. *Mitochondrion*, *49*(June), 269–283. https://doi.org/10.1016/j.mito.2019.06.002

Wiley, S. E., Paddock, M. L., Abresch, E. C., Gross, L., Van Der Geer, P., Nechushtai, R., Murphy, A. N., Jennings, P. A., & Dixon, J. E. (2007). The outer mitochondrial membrane protein mitoNEET contains a novel redox-active 2Fe-2S cluster. *Journal of Biological Chemistry*, *282*(33), 23745–23749. https://doi.org/10.1074/jbc.C700107200

Wilson, I. A., Skehel, J. J., & Wiley, D. C. (1981). Structure of the haemagglutinin membrane glyco˚ resolution. Nature, protein of influenza virus at 3. *A*, *289*, 366–373.

Wohlgemuth, N., Lane, A. P., & Pekosz, A. (2018). Influenza A Virus M2 Protein Apical Targeting Is Required for Efficient Virus Replication. *Journal of Virology*, *92*(22). https://doi.org/10.1128/jvi.01425-18

Wong, Y. C., Ysselstein, D., & Krainc, D. (2018). Mitochondria-lysosome contacts regulate mitochondrial fission via RAB7 GTP hydrolysis. *Nature*, *554*(7692), 382–386. https://doi.org/10.1038/nature25486

Wozniak, R. W. (2014). *Host Cell Factors Necessary for Influenza A Infection : Meta-Analysis of Genome Host Cell Factors Necessary for Influenza A Infection : Meta-Analysis of Genome Wide Studies*. *November 2012*. https://doi.org/10.6084/m9.figshare.1248958

Wu, M. J., Chen, Y. S., Kim, M. R., Chang, C. C., Gampala, S., Zhang, Y., Wang, Y., Chang, C. Y., Yang, J. Y., & Chang, C. J. (2019). Epithelial-Mesenchymal Transition Directs Stem Cell Polarity via Regulation of Mitofusin. *Cell Metabolism*, *29*(4), 993-1002.e6. https://doi.org/10.1016/j.cmet.2018.11.004

Xiong, J. (2018). Fatty Acid Oxidation in Cell Fate Determination. In *Trends in Biochemical Sciences* (Vol. 43, Issue 11, pp. 854–857). Elsevier Ltd. https://doi.org/10.1016/j.tibs.2018.04.006

Xu, L., Xiao, N., Liu, F., Ren, H., & Gu, J. (2009). Inhibition of RIG-I and MDA5-dependent antiviralm response by gC1qR at mitochondria. *Proceedings of the National Academy of Sciences of the United States of America*, *106*(5), 1530–1535. https://doi.org/10.1073/pnas.0811029106

Yadav, V., Panganiban, A. T., Honer Zu Bentrup, K., & Voss, T. G. (2016). Influenza infection modulates vesicular trafficking and induces Golgi complex disruption. *VirusDisease*, *27*(4), 357–368. https://doi.org/10.1007/s13337-016-0347-3

Yang, J., Liu, S., Du, L., & Jiang, S. (2016). A new role of neuraminidase (NA) in the influenza virus life cycle: implication for developing NA inhibitors with novel mechanism of action. *Reviews in Medical Virology*, *26*(4), 242–250. https://doi.org/10.1002/rmv.1879

Yoon, S. W., Webby, R. J., & Webster, R. G. (2014). Evolution and ecology of influenza a viruses. *Current Topics in Microbiology and Immunology*, *385*, 359–375. https://doi.org/10.1007/82_2014_396

Yoshizumi, T., Ichinohe, T., Sasaki, O., Otera, H., Kawabata, S. I., Mihara, K., & Koshiba, T. (2014). Influenza a virus protein PB1-F2 translocates into mitochondria via Tom40 channels and impairs innate immunity. *Nature Communications*, *5*, 6–10. https://doi.org/10.1038/ncomms5713

Youle, R. J., & Van Der Bliek, A. M. (2012). Good for Discussion: Mitochondrial Fission, Fusion, and Stress HHS Public Access. *Science*, *337*(6098), 1062–1065. https://doi.org/10.1126/science.1219855

Yun, J., & Finkel, T. (2014). Mitohormesis. *Cell Metabolism*, *19*(5), 757–766. https://doi.org/10.1016/j.cmet.2014.01.011

Zamarin, D., García-Sastre, A., Xiao, X., Wang, R., & Palese, P. (2005). Influenza virus PB1-F2 protein induces cell death through mitochondrial ANT3 and VDAC1. *PLoS Pathogens*, *1*(1), e4. https://doi.org/10.1371/journal.ppat.0010004

Zemirli, N., Morel, E., & Molino, D. (2018). Mitochondrial dynamics in basal and stressful conditions. *International Journal of Molecular Sciences*, *19*(2), 1–19. https://doi.org/10.3390/ijms19020564

Zhang, R., Chi, X., Wang, S., Qi, B., Yu, X., & Chen, J. L. (2014). The regulation of autophagy by influenza A virus. *BioMed Research International*, *2014*. https://doi.org/10.1155/2014/498083

Zhang, Y., & Whittaker, G. R. (2014). Influenza entry pathways in polarized MDCK cells. *Biochemical and Biophysical Research Communications*, *450*(1), 234–239. https://doi.org/10.1016/j.bbrc.2014.05.095

Zhao, L., Li, S., Wang, S., Yu, N., & Liu, J. (2015). The effect of mitochondrial calcium uniporter on mitochondrial fission in hippocampus cells ischemia/reperfusion injury. *Biochemical and Biophysical Research Communications*, *461*(3), 537–542. https://doi.org/10.1016/j.bbrc.2015.04.066

Zhirnov, O. P., & Klenk, H. D. (2013). Influenza A Virus Proteins NS1 and Hemagglutinin Along with M2 Are Involved in Stimulation of Autophagy in Infected Cells. *Journal of Virology*, *87*(24), 13107–13114. https://doi.org/10.1128/jvi.02148-13

Zhou, Z., Jiang, X., Liu, D., Fan, Z., Hu, X., Yan, J., Wang, M., & Gao, G. F. (2009). Autophagy is involved in influenza A virus replication. *Autophagy*, *5*(3), 321–328. https://doi.org/10.4161/auto.5.3.7406

Zhu, H. Y., Han, L., Shi, X. L., Wang, B. L., Huang, H., Wang, X., Chen, D. F., Ju, D. W., & Feng, M. Q. (2015). Baicalin inhibits autophagy induced by influenza A virus H3N2. *Antiviral Research*, *113*, 62–70. https://doi.org/10.1016/j.antiviral.2014.11.003

Zorov, D. B., Juhaszova, M., & Sollott, S. J. (2014). Mitochondrial reactive oxygen species (ROS) and ROS-induced ROS release. *Physiological Reviews, 94*(3), 909–950. https://doi.org/10.1152/physrev.00026.2013

Zulkefli, K. L., Houghton, F. J., Gosavi, P., & Gleeson, P. A. (2019). A role for Rab11 in the homeostasis of the endosome-lysosomal pathway. *Experimental Cell Research, 380*(1), 55–68. https://doi.org/10.1016/j.yexcr.2019.04.010

Zuris, J. A., Harir, Y., Conlan, A. R., Shvartsman, M., Michaeli, D., Tamir, S., Paddock, M. L., Onuchic, J. N., Mittler, R., Cabantchik, Z. I., Jennings, P. A., & Nechushtai, R. (2011). Facile transfer of [2Fe-2S] clusters from the diabetes drug target mitoNEET to an apo-acceptor protein. *Proceedings of the National Academy of Sciences of the United States of America*, *108*(32), 13047–13052. https://doi.org/10.1073/pnas.1109986108